Spatio-temporal modelling of civil violence:
Four frameworks for obtaining policy-relevant insights

Peter Baudains

A dissertation submitted in partial fulfillment

of the requirements for the degree of

Doctor of Philosophy

of the

University College London.

UCL Department of Mathematics

University College London

February 9, 2015

I, Peter Baudains, confirm that the work presented in this thesis is my own. Where information has been derived from other sources, I confirm that this has been indicated in the thesis.

Abstract

Mathematical modelling of civil violence can be accomplished in different ways. In this thesis, four modelling frameworks are investigated, each of which leads to different insights into the spatio-temporal properties of civil violence. These frameworks vary with respect to the extent in which empirical data is used in generating model assumptions, and the extent in which simplifying assumptions distance the model from the real world. An overarching objective is to compare the insights and underlying assumptions of each framework, and to consider how they might be consolidated to aid policy decision-making.

Within each framework, novel contributions both to the mathematical modelling of social systems, and to the theoretical understanding of civil violence are made. First, a novel data-driven approach for analysing local patterns of geographic diffusion in event data is presented, and applied to offences associated with the 2011 London riots. Second, by considering the decision-making of individuals, thereby taking an agent-based perspective, and using existing theory to construct model assumptions, a parametric statistical model of discrete choice is derived that more closely inspects the targets chosen by rioters, and how these choices might have changed over time. The application of this model to the policy domain is explored by considering police deployment strategies. Third, focusing on the interaction between two adversaries, and employing stochastic point process models, a series of multivariate and nonlinear Hawkes processes are proposed and used to explore spatio-temporal dependency during the Naxal insurgency in India. Fourth, a novel spatially-explicit differential equation-based model of conflict escalation between two adversaries is derived. A bifurcation is identified that results from the spatial disaggregation of the model. Implications for the interpretation of the model in the real world and potential applications are discussed.

Publications

Some of the work in this thesis has been described in the following publications:

Baudains, P., Braithwaite, A., and Johnson, S.D. 2013. Spatial patterns in the 2011 London riots. *Policing: A Journal of Policy and Practice*, 7(1):21-31.

Baudains, P., Johnson, S.D. and Braithwaite, A. 2013. Geographic patterns of diffusion in the 2011 London riots. *Applied Geography*, 45:211-219.

Baudains, P., Braithwaite, A., and Johnson, S.D. 2013. Target choice during extreme events: A discrete spatial choice model of the 2011 London riots. *Criminology*, 51(2):251-286.

In addition, the following manuscripts are in preparation:

Baudains, P., Belur, J., Braithwaite, A., Johnson, S.D. and Marchione, E. (In Preparation). Location, escalation, reciprocation: Multivariate point process modelling of the Naxal insurgency.

Baudains, P., Fry, H.M., Davies, T.P., Wilson, A.G. and Bishop, S.R. (In Preparation). A dynamic spatial model of conflict escalation.

Acknowledgements

I would like to thank my supervisor Steven Bishop for providing me with the opportunity to undertake this thesis and for the support he has given me throughout. I would like to acknowledge the academic support provided by Shane Johnson, Hannah Fry, Alex Braithwaite and Alan Wilson, and thank them for many illuminating and inspiring conversations during my studies. I would also like to thank the Metropolitan Police Service and Jyoti Belur for providing data. Finally, I would like to thank my wife, Sarah, without whom this thesis would not have been completed.

Contents

1 Introduction **19**

1.1 Motivation 20

1.2 Problem definition 24

1.3 Research objectives 25

1.4 Case studies 26

1.4.1 The 2011 London riots 26

1.4.2 The Naxal insurgency 27

1.4.3 Similarities between rioting and insurgency 28

1.5 Advances to knowledge 29

1.6 Thesis outline 31

2 Modelling methodology **35**

2.1 Introduction 36

2.2 Exploratory space-time data-driven modelling 36

2.2.1 Spatial autocorrelation 36

2.2.2 Tests for spatio-temporal interaction 38

2.2.3 Quantifying change in spatial event data 39

2.3 Spatio-temporal statistical modelling 43

2.3.1 Covariates of civil violence 44

2.3.2 Individual decision-making during civil violence 48

2.3.3 Predictive models 50

2.4 Spatially-explicit mechanistic modelling 51

2.4.1 Agent-based models 52

2.4.2 Differential equations 56

2.5 Discussion 63

3 Spatio-temporal patterns of rioting 67

3.1 Introduction 68

3.2 Data aggregation 69

3.3 Spatial randomness and autocorrelation 71

3.3.1 A measure of dispersion 72

3.3.2 A measure of autocorrelation 73

3.3.3 Simulating a random process 74

3.3.4 Testing for CSR in the 2011 London riots 76

3.4 Spatio-temporal interaction 81

3.5 Analysing local patterns of geographic diffusion 86

3.5.1 Proposed mechanisms for riot diffusion patterns 89

3.5.2 Simulating spatio-temporal independence with binary event data 96

3.5.3 Results 103

3.5.4 Conclusions 107

3.6 Discussion 109

4 Target choice during rioting 113

4.1 Introduction 114

4.2 A model of target choice in the 2011 London riots 115

4.2.1 A random utility model of discrete choice 118

4.2.2 Modelling the observed utility for rioter target choice 123

4.2.3 Parameter estimation 140

4.3 Simulating the 2011 London riots: Towards a policy tool 159

4.3.1 Microsimulation of target choice 159

4.3.2 Comparison of the model with empirical data 163

4.3.3 The model as a component in a policy tool 168

4.4 Discussion 174

5 Point process modelling of two adversaries 179

5.1 Introduction 180

5.2 The Naxal insurgency and police response in Andhra Pradesh 182

5.3 Hypotheses for a model of the Naxal conflict . . . 185
5.4 Point process models of the Naxal conflict . . . 192
5.4.1 Model 1: The Poisson process . . . 194
5.4.2 Models 2 and 3: Self-exciting Hawkes processes . . . 195
5.4.3 Model 4: Mutually-exciting Hawkes processes . . . 200
5.4.4 Model 5: Spatial Hawkes processes . . . 201
5.4.5 Model 6: Nonlinear spatial Hawkes processes . . . 202
5.5 Parameter estimation . . . 203
5.5.1 Likelihood for nonlinear multivariate Hawkes processes . . . 203
5.5.2 Parametric bootstrapping of confidence intervals . . . 208
5.5.3 Results . . . 212
5.6 Model evaluation . . . 218
5.6.1 Residual analysis . . . 218
5.6.2 Out of sample predictive performance . . . 222
5.7 Discussion . . . 225

6 Deterministic modelling of conflict 231
6.1 Introduction . . . 232
6.2 The Richardson model . . . 234
6.2.1 Nodes . . . 238
6.2.2 Foci . . . 240
6.2.3 Saddles . . . 241
6.2.4 Richardson policy options . . . 242
6.3 Spatial disaggregation of the Richardson model . . . 244
6.3.1 A PDE disaggregation of the competitive Lotka-Volterra system 245
6.3.2 A PDE disaggregation of the Richardson model . . . 247
6.3.3 An entropy-maximising spatial interaction disaggregation . . . 249
6.4 Nonlinear dynamical systems analysis . . . 257
6.4.1 A three-dimensional scenario . . . 259
6.4.2 A four-dimensional scenario . . . 265
6.4.3 Eight-dimensional scenarios . . . 278
6.4.4 A randomly-generated large N-dimensional model . . . 285

6.5 Discussion 290

7 Conclusion **293**

7.1 Comparison of modelling frameworks 294

7.2 Topics for further research 302

7.3 Concluding remarks 306

List of Figures

1.1 Potential insight and plausibility of different model frameworks 23

2.1 The change in the sum of defence budgets against the sum of defence budgets for four nations during the four years prior to the First World War 59

3.1 A map of the 2011 London riots 77
3.2 The empirical cumulative distribution of counts of offences across output areas that contained at least one offence 78
3.3 Two regular spatial grids over the same portion of London's Output Area geography 79
3.4 The neighbourhood of a focal spatial unit under queen contiguity 80
3.5 Results of the test for CSR 82
3.6 Results of the Knox test 86
3.7 Geographic patterns of diffusion 89
3.8 Police officers and offences 97
3.9 Network visualisation of the London riot data 99
3.10 Results for the first half of the data 105
3.11 Results for the second half of the data 106

4.1 Histogram of the distance between residential location and offence location 133
4.2 Age distribution of offenders 135
4.3 R^2 values for each of the different models tested 148
4.4 Exponentiated parameter estimates of the discrete choice model for $\delta t = 24$ without spillover effects 152

4.5 Exponentiated parameter estimates of the discrete choice model for $\delta t = 24$ with spillover effects . . . 153
4.6 Rioter counts for the 30 most targeted LSOAs according to the empirical data . . . 164
4.7 Rioter counts for the 30 most targeted LSOAs according to the average of the simulations . . . 166
4.8 Ratio of count to rank for each LSOA for both the empirical data and the simulation . . . 167
4.9 The simulated deployment utility for each LSOA in Greater London . . 171
4.10 The empirical deployment utility for each LSOA in Greater London . . 172

5.1 A choropleth map of Andhra Pradesh and Telangana showing the spatial distribution of event data . . . 186
5.2 The time series of the event data for each district in Telangana and Andhra Pradesh . . . 187
5.3 An example of a Hawkes process with events occurring at t_1, t_2 and t_3 . 199
5.4 A Q-Q plot to compare the Poisson process with the process obtained from the residual analysis . . . 221
5.5 Receiver operating characteristic (ROC) curves for: i) out of sample prediction of Naxal and police events using Model 6; ii) in-sample prediction of Naxal and police events using Model 6; and iii) an indiscriminate model that randomly assigns events to each day with a certain probability. . . . 226
5.6 Precision recall curves for the out of sample classifier of Model 6 (solid line) and an indiscriminate model that assigns new observations to be positive with probability τ (dashed line) . . . 227

6.1 The trace-determinant diagram for linear planar systems . . . 238
6.2 The dynamics around the equilibrium value of the Richardson model in equation 6.6 for different parameter values . . . 239
6.3 Unilateral policy options available to nation i . . . 243
6.4 A plot of $\dot{r}$ against r for the one-dimensional system in equation 6.36 . . 263
6.5 The value of r_+, as given in equation 6.39, for different values of β . . . 266

6.6 Selected solution curves of the linear system in equation 6.52 for $\rho < \bar{\rho}$ and for $\rho > \bar{\rho}$ 271
6.7 The bifurcation point $\bar{\rho}$ plotted against β according to equation 6.60 . . 272
6.8 The phase portrait of the system in equation 6.63 for two different values of ρ 274
6.9 Equilibria of the system in equation 6.64, denoted by r_e, for varying values of ρ 276
6.10 The stability of the equilibrium at the origin of the rs-plane for $\rho_1 \in [0.5, 1)$ and $\rho_2 \in [0.5, 1)$ and for $\beta = 0.5$, $\beta = 1$, and $\beta = 2$ 277
6.11 A scenario corresponding to the distance metric as defined in equation 6.67 279
6.12 The sum of the two solution curves in each zone for the spatial arrangement of zones as shown in Figure 6.11, for two different sets of parameter values 281
6.13 A scenario corresponding to the distance metric as defined in equation 6.68 282
6.14 The sum of the two solution curves in each zone for the spatial arrangement of zones as defined in equation 6.68, for two different parameter values 284
6.15 The equilibrium of the system with a) $\rho = 0.8$ and b) $\rho = 0.9$ 287
6.16 The value of $F(\rho)$, given in equation 6.72 for different values of ρ, for the scenario depicted in Figure 6.15 289
6.17 Normal form of the supercritical pitchfork bifurcation (left hand side) and its perturbation (right hand side) 292

7.1 Potential insight and plausibility of different modelling frameworks . . 301

List of Tables

4.1 The distribution of different crime types over the five days of rioting . . 125

4.2 The variables used to estimate the observed utility of each target 141

4.3 The number of offences and the number of LSOAs affected by day of rioting 146

4.4 Weighted R^2 values 148

4.5 Parameter estimates and their associated confidence intervals for the test of unobserved heterogeneity 151

5.1 Parameter estimates for each of the six models described in Section 5.4 213

5.2 Bootstrapped 95% confidence intervals of each parameter obtained with Model 6 214

Chapter 1

Introduction

1.1 Motivation

To motivate this thesis, a series of questions are first addressed.

Why model?

Modelling is widespread in a number of domains. The application of models to society has begun to deliver insights into, for instance, global pandemic spreading (Colizza et al., 2007), urban planning (Wilson, 2000; Batty, 2013), and the functioning of economies (Farmer and Foley, 2009). In particular, the application of models to society is beginning to deliver policy-relevant insights that can be used to better structure our society and its response to different events (Ball, 2012).

The idea that models can provide policy recommendations is in some sense obvious: the construction of a model is one of the most common ways by which human beings have come to make decisions. As Epstein (2008) describes, "anyone who ventures a projection, or imagines how a social dynamic—an epidemic, war, or migration—would unfold is running *some* model". Effective decision-making requires projections for a range of choices that might be made, and not just for the decision that is made. Moreover, better projections should lead to better decisions.

As Epstein goes on to explain, explicit models—which can be written down in a comprehensive (and ideally standardised) way—are preferable over implicit models – mental projections that cannot be reproduced and tested in accordance with the scientific method. The advantages of an explicit model over an implicit one is that the model can be reduced to a set of statements or assumptions that describe exactly how the model behaves over the range of scenarios to be considered. Moreover, the model should be entirely and exactly reproducible from this set of assumptions so that its implications, and any policy decisions that are made on its basis, can be questioned and challenged by others.

Besides providing a more scientific means by which the impact of policy interventions might be envisaged, there are a number of other benefits associated with the use of explicit models. For instance, if it is possible to specify a mechanism by which a particular phenomenon is thought to arise, then an explicit model can enable the evaluation of whether that mechanism provides a plausible explanation, thereby providing a test of associated theories from which that mechanism stems.

From an inductive perspective, models can help to distinguish between statistical noise and meaningful signals in empirical data, and might consequently suggest new theories and research by exposing or clarifying particular patterns or processes. Deductive modelling also requires sophisticated techniques to account for uncertainty or to incorporate potential influences on the mechanisms of interest. This has led to models being objects of scientific enquiry in their own right.

This thesis is motivated by the use of models in a policy setting. In particular, the extent to which different models afford policy insights is investigated. Conclusions are sought that lead to an improved understanding as to how theory and empirical data combine to generate model-based policy insights. This is achieved by contrasting the studies of four very different types of model, each applied to a particular problem regarding the spatio-temporal distribution of civil violence.

Why use different frameworks to build models?

There are different ways to build a model. Different models may employ different analytical techniques or have different underlying assumptions that subtly influence the range of insights that might be obtained. In this thesis, the term "model framework" is used to refer to a modelling method that uses a particular analytical approach. There is no widely agreed upon framework for developing models of social systems. Each approach can appear to offer a range of advantages and disadvantages over other approaches. In addition, there are many different frameworks that might be used for any given problem, and different frameworks may be favoured depending on a range of criteria including, for example, the academic discipline with which the modeller is most familiar. There have been few attempts at consolidating or contrasting different modelling frameworks in the study of civil violence.

In this thesis, to distinguish between different frameworks, models will be compared with respect to two facets: the extent to which empirical data is used in the construction of model assumptions, and the extent to which these assumptions are representative of the real-world phenomenon under consideration. Models that incorporate a large amount of empirical data, and which have few basic assumptions are likely to provide plausible accounts of the phenomenon of interest. However, the extent to which sophisticated insights might be obtained (for example, with regards to understanding

potential mechanisms or predicting future events) is likely to be limited. In particular, prediction with data-driven approaches that are informed by observations relies on the sample data containing sufficient information to enable extrapolation. In contrast, mechanistic approaches, in which a proposed mechanism generates model outputs that are thought to be responsible for the empirical data, are likely to be further removed from the real-world, but more likely to be able to account for qualitative changes in the underlying data generating process.

Figure 1.1 summarises the trade-off between potential insight and plausibility for a range of modelling frameworks that have been applied to study civil violence. The different modelling frameworks are placed along a spectrum, broadly defined by the ratio given by the number of model assumptions that remove the model from the real world, to the amount of data incorporated into the development of those model assumptions. The two curves represent the extent to which insight and plausibility typically change as this ratio varies, and as different modelling frameworks are employed.

Why model civil violence?

Outbreaks of civil violence, whether stemming from civil wars, insurgencies, rioting, or other forms of unrest, continues to dominate news reports around the globe. The onset and evolution of civil violence is traditionally discussed using anecdotal perspectives, rather than by employing explicit models to seek out underlying mechanisms or patterns that might be exploited from a policy perspective. However, there has been a recent dramatic increase in the quantity and quality of explicit models detailing various aspects of civil violence. This is partly due to increased data availability, which is crucial for modelling as it enables the development of models that are empirically consistent, and partly due to an increased range of sophisticated modelling techniques. Our understanding of civil violence can be improved though such models. This may in turn improve the way in which interventions are planned. Some have even suggested that by using modern modelling techniques to investigate problems of crime, war and terrorism, the number of fatalities associated with such events can ultimately be reduced (Helbing et al., 2015).

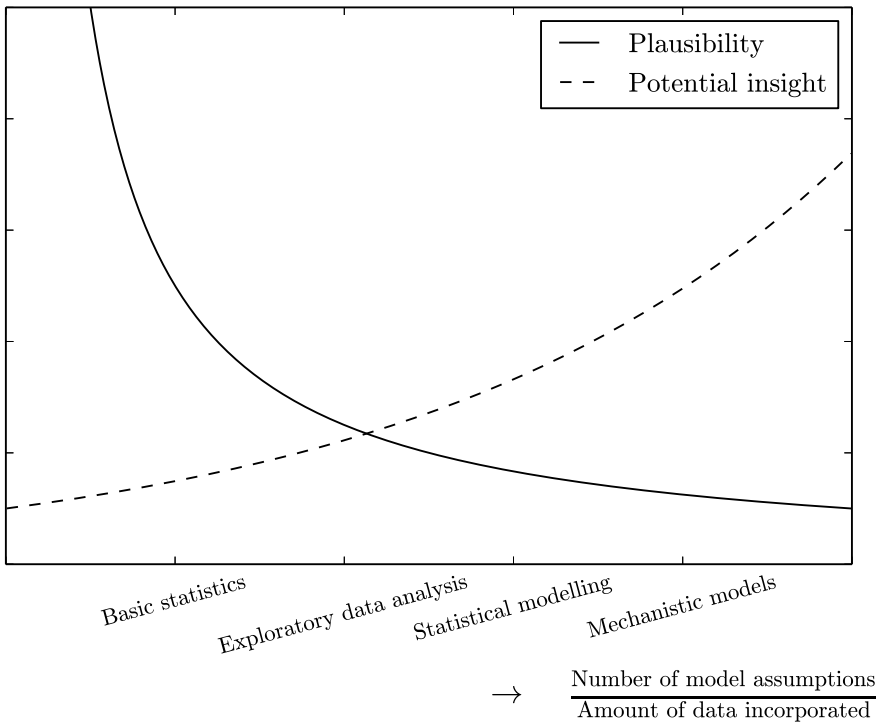

Figure 1.1: **Potential insight and plausibility of different model frameworks.** The frameworks considered in this thesis are placed along a spectrum broadly defined by a ratio given by the number of model assumptions that serve to remove each approach from the real world, to the extent to which empirical data forms part of the model development.

Why model civil violence in space and time?

Civil violence tends not to occur uniformly in space and time. Many existing models, however, do not explicitly account for spatially-varying and temporally-varying factors, which have been shown to lead to dramatically improved models (Weidmann and Ward, 2010).

Significant implications arise from using a model to design policy that does not account for appropriate spatial and temporal influences. For example, a model might predict the onset of civil violence in a particular country at a particular time but if it does not account for the duration over which this violence is expected to occur, or even whether it is a significant change in what has occurred previously, then policy interventions may be misguided. Additionally, for targeted interventions, policy-makers might be more concerned with determining the specific geographic location of the predicted violence, rather than the more aggregated spatial region of the country in which it is likely to occur.

Modelling the spatial and temporal influences of civil violence is also interesting from a mathematical perspective. There are a number of ways of incorporating spatio-temporal dependencies in exploratory, statistical and mechanistic models, many of which are considered in this thesis. Different methods to incorporate space and time are likely to influence the model in different ways. The approach taken to handle space and time in such models is itself an important research challenge.

1.2 Problem definition

Existing literature on civil violence tends to distinguish between violence stemming from civil wars and insurgencies, and violence that occurs during times of peace, such as civil unrest or rioting. Kalyvas (1999), for example, describes how “war structures choices and selects actors in fundamentally different ways than peace – even violent peace”. However, as Guichaoua (2010) argues, there is often not a clear distinction between these two types of violence as “in many situations, coercive powers are ambiguously distributed between state and non-state actors, resulting in ‘neither war nor peace’ forms of social order, conducive to sudden outbursts of collective violence”.

From a modelling perspective, very similar model frameworks have been applied to civil war, insurgencies, civil violence, riots, and even different types of crime, and

have been shown to lead to important insights regardless of the particular phenomenon studied. Although, that is not to say that theories regarding the occurrence of a particular type of violence cannot be incorporated, but, instead, that the underlying structure of the models employed for these different phenomena are often very similar. Since the overarching objective of this thesis is methodological, a strict definition of civil violence is not enforced. The empirical problem to be considered is the occurrence of events associated with a more general concept of civil violence, which incorporates events that occur as a result of insurgent warfare, civil unrest and rioting.

There have been a number of models applied to civil violence, some of which explicitly incorporate spatio-temporal influences and interdependence between events. Such studies encompass a range of different model frameworks. There have been few attempts to consider the implications of adopting one framework over another, particularly with regards to the range of insights that might be afforded in a policy setting. In particular, it has been previously argued that the choice of model framework too often depends on a researcher's familiarity and experience with a small range of analytical techniques (Schrodt, 2014). This thesis sets out to address this gap in the literature by providing a comparative exposition of different model frameworks that are capable of incorporating spatio-temporal influences and event interdependency in different ways. In addition, this thesis considers whether existing models are appropriate for exploring spatio-temporal influences and event interdependency during civil violence, and, where appropriate, introduces new models.

1.3 Research objectives

This thesis contributes to the mathematical modelling of civil violence by developing and analysing several spatio-temporal models that account for event interdependency across the spectrum of modelling frameworks introduced in Figure 1.1. The overarching objective is to contrast these modelling frameworks and determine their suitability for providing insights that might be utilised in a policy setting. After reviewing the range of frameworks that have been used to study such phenomena previously, four frameworks are explored in greater detail, by constructing novel models and applying them to case studies of civil violence. Specifically, for each of these frameworks, it is considered:

1. Whether the framework is appropriate for modelling civil violence in space and time, and, if not, methods are provided for disaggregating existing models;

2. What insights can be obtained concerning one of the two case studies investigated in this thesis;

3. How these insights might be used within a policy setting.

The four frameworks that are explored can be summarised as exploratory data-driven modelling; parametric statistical models of individual choice; stochastic models of point processes; and deterministic differential equations.

1.4 Case studies

Two case studies are employed in this thesis: the 2011 London riots and the Naxal insurgency. These case studies are chosen because they both exhibit interesting spatial and temporal variation, yet do so over different scales. Models that are able to be used over multiple scales are generally desirable since complex social systems, such as those studied in this thesis, can have different influences acting on different scales, many of which may be important to incorporate. In what follows, the two case studies are briefly described.

1.4.1 The 2011 London riots

Between the 6th and 10th August 2011, riots occurred at numerous locations across the UK. Violence initially broke out after a peaceful protest by family, friends, and members of the community of Mark Duggan, who was shot and killed by police officers in Tottenham, North London on the 4th August. On the 6th August, riots broke out in neighbouring communities. For five nights, the riots continued, initially throughout the capital and subsequently throughout the country. After the initial disturbances, the unrest on subsequent nights grew in intensity, before large numbers of police were deployed across the capital and in other cities, leading to a restoration of order. In London, it is estimated that there was in excess of $\pounds 200$ million of damage to public and private property; over two hundred injuries to police; and two deaths (Riots Communities and Victims Panel, 2011). Over 4,000 arrests were made in London alone (Metropolitan Police Service, 2012), many of which were identified via CCTV footage in the days following the disorder.

Predominantly, the riots took place in the highly populated areas of London, Birmingham and Manchester. However, even within these cities, and particularly in London, civil unrest occurred in some areas but not in others. Several geographically distinct areas, such as Hackney, Brixton, and Croydon, experienced large-scale violence, looting, and arson; whereas some of the areas in between—including Central London, Shepherd's Bush, and Leyton—experienced comparatively few events.

The first locations to experience rioting were around the Tottenham area in North London. Over the next days, riots occurred South London, before also occurring in other UK cities. This gave the impression that the riots were spreading geographically, and many commented how the onset of rioting in one location was imitated by others in different locations, implying some form of dependency between the events (Gross, 2011). This apparent dependency implies that standard modelling techniques assuming event independence are likely to be inappropriate, and the interactions between events forms a subject of enquiry in its own right.

There are many policy questions directly relevant to the 2011 UK riots. For example, studies have sought to identify the underlying sociological causes of the rioting (Solomos, 2011), and have examined whether the criminal justice response was appropriate (Bell et al., 2014). The policy question considered in this thesis is concerned with the spatial and temporal dependency of the riots, particularly with regards to event interdependency. In addition, it is considered how and why targets were chosen in London and, in particular, how police officers may have been optimally allocated across the city in order to have prevented damage to property, public space and people's livelihoods that occurred as a result of the riots.

1.4.2 The Naxal insurgency

The Naxal movement, whose name is taken from the small village of Naxalbari in West Bengal, where a peasant revolt took place in 1967, are a left-wing extremist group who have engaged in numerous attacks against civilians and the state in recent decades. Grievances of the Naxal movement initially stemmed from economic inequality and rural agricultural workers' inaccessibility to land ownership (Ahuja and Ganguly, 2007). After being quashed by the Indian government in the 1970s through the use of police and paramilitary forces (Basu, 2011), several factions of the Naxal movement were

formed, many of which had militant groups who engaged in insurgency against the state. In the early 2000s, various Naxal groups merged to form both militant (the People's Liberation Guerrilla Army) and political groups (the Communist Party of India). Insurgent violence continues to present day, but, in recent years, tends to be restricted within localised regions in Eastern and North Eastern India.

The states of Andhra Pradesh and Telangana, the latter of which was formed in 2014 when Andhra Pradesh bifurcated, experienced high levels of violence during the 2000s. Police periodically adopted various counter-insurgency measures in an attempt to quell the insurgency, including the formation of an aggressive paramilitary group called the Greyhounds. On numerous occasions, the police were drawn into armed conflict with the insurgents, resulting in both Naxal and police loss of life. Police counter-insurgent measures in Andhra Pradesh have been claimed to be effective in reducing levels of violence, despite limited quantitative studies (Sahni, 2007).

Policy questions associated with the Naxal insurgency apply equally here as they do to many other outbreaks of insurgent violence around the world. As well as being interested in the underlying mechanisms causing individuals to commit violence, policy-makers might also be interested in understanding the spatial extent of the violence, whether there is any evidence for spreading of the violence, and determining what might be the best counterinsurgency strategy to adopt.

1.4.3 Similarities between rioting and insurgency

The two case studies share a number of similarities but also some crucial differences. First, events associated with both rioting and insurgency have previously been shown to exhibit striking spatial, temporal and even spatio-temporal heterogeneity, suggesting that important processes play out in both space and time. Second, such patterning of events is likely to be constrained by the decision-making of the perpetrators and the environment in which they act. In the case of rioting, offenders may choose certain times to offend, and targets at which to commit their offences due to, for example, ongoing rioting at that same location. Insurgents may be constrained by transport costs or their desire to inflict damage on targets that are perceived to be particularly valuable. Third, the occurrence of events associated with both rioting and insurgency is likely to depend crucially on the interaction between, in the case of the former, rioters and police, and,

in the case of the latter, insurgents and counterinsurgents. This interaction, however, may be different in each of these cases. In the case of rioting, offenders who are motivated purely by the benefit associated with acquisitive crime, such as looting, might seek to avoid interactions with police in order to minimise the probability of arrest. Insurgents, however, may be more likely to target counterinsurgents as they represent a direct link to the state with which they are in conflict. These characterisations, however, are not necessarily dichotomous: there may feasibly be scenarios during which police are purposefully targeted during rioting, for example when the rioters have a grievance they want to make known to the state, and there may also be instances during which insurgents target civilian areas that are unlikely to contain any counterinsurgent agents.

As a result of these similarities, the two case studies are both explored using the models presented in this thesis. The detail in the available data associated with each case study enables the investigation of different processes that might be at play in each scenario and largely determines the type of model framework that can be applied. For the London riots, offence data is available at a fine spatial and temporal scale, enabling the consideration of local environmental factors and local event interdependency during rioting. In the case of the Naxal insurgency, a distinction can be made between insurgent actions and counterinsurgent activity, which enables this interaction to be more closely examined.

1.5 Advances to knowledge

There are several contributions in this thesis that advance the state of the art in spatio-temporal modelling of civil violence. Perhaps the main contribution is the consolidated presentation of a wide variety of model frameworks, all of which, it is argued, have a role to play in contributing to real-world insights and subsequent policy decision-making. A comparative study of these frameworks contributes in a novel way to existing literature. Within each modelling method and application presented, however, there are more specific contributions that advance existing knowledge. In what follows, these contributions are summarised.

In Chapter 3, which investigates data-driven frameworks for the analysis of spatio-temporal event data, a non-parametric Monte Carlo method for investigating local spatial-temporal patterns of diffusion is presented, which, to the knowledge of the au-

thor, has not been previously employed in this fashion. This method improves existing approaches by overcoming limitations associated with the assumption of uniform spatial and temporal randomness in binary Monte-Carlo models of event data. It enables improved understanding into event interdependency during phenomena that exhibit significant spatial and temporal clustering, such as rioting. The method is applied to the 2011 London riots to generate insights into event dependency, and a discussion into the possible mechanisms that might generate such patterns serves as a theoretical contribution to the literature.

In Chapter 4, a discrete spatial choice model of rioter target choice is used to investigate the targets selected by individuals during the 2011 London riots. To the knowledge of the author, such an approach has not previously been used in the context of rioting. The formulation of the model enables assessment of a number of extant theories regarding the behaviour of individuals during offending and instances of collective violence. The model presented incorporates interdependency between events by including a dynamic time-lagged variable tracking the number of events that occur in each area. Spatial spillover effects are also accounted for by including a range of spatially-lagged variables. A theoretical contribution is the evaluation of proposed theories, which have previously sought to explain offender behaviour, by assessing the ability for variables in the model associated with those theories to account for variance in the empirical data. The discrete spatial choice model is then incorporated into a novel microsimulation, which, it is argued, might be used within a policy setting to determine effective police deployment strategies.

Point process models have been widely used to model event interdependency in civil violence and other types of security and conflict phenomena. In Chapter 5, a range of multivariate point process models of conflict between two adversaries are developed, which enable quantification and estimation of spatial and temporal dependencies in event data. A contribution to the modelling literature is the derivation of a plurality of multivariate models that are designed to test a series of hypotheses concerning various characteristics of the violence. Two of the proposed models are also nonlinear, leading to an adapted estimation procedure to account for complications that arise due to nonlinearity, something that, to the knowledge of the author, has not been performed in previous literature. Rigorous analysis of the resulting models, including the estimation

of confidence intervals for the parameter estimates, a residual analysis, and a test of one of the model's out of sample predictive power is another significant contribution, serving as a best practice guide for reporting the success of future modelling efforts (prior studies do not typically report on all three of these aspects).

Finally, in Chapter 6, using the modelling framework of deterministic differential equations, a novel spatial disaggregation of a widely-cited model of conflict is derived and its use in obtaining insights into civil violence is discussed. A non-linear dynamical systems analysis combined with computational approaches for analysing the dynamics of a high-dimensional version of the system leads to several mathematical insights.

The models developed are discussed throughout with regards to the specific policy-relevant insights they afford. In Chapter 7, a more in-depth discussion of their comparison is presented. This discussion may be of most interest to those developing models for the purposes of policy and contains various reflections of the author.

1.6 Thesis outline

This thesis proceeds as follows. Chapter 2 describes the different model frameworks that have been used to model spatio-temporal influences in civil violence. Previous studies that employ each type of framework are reviewed. The discussion serves to motivate the advances associated within each framework that are presented throughout the thesis.

In Chapter 3, the first of the case studies, the 2011 London riots, is investigated with respect to a variety of space-time exploratory techniques. After performing several analyses with existing approaches, it is concluded that further insights can be obtained with a novel method for analysing the local patterns of diffusion in event data. This method is described, before the results associated with data from the London riots are presented and discussed. It is argued that the dynamic patterns observed during the riots were influenced by three principal mechanisms: a contagion effect enhanced by both new and old media; the environment and urban form within which the riots took place; and the interaction between rioters and police.

In Chapter 4, the decision-making of rioters is considered with respect to two of these explanations: contagion, whereby the presence of rioters at a particular location increases the likelihood of further rioting at that area, and the influence of the environ-

ment, whereby particular features of a location, such as retail centres, can influence the likelihood of rioting occurring. Building on theoretical perspectives of crowds, crime patterns and social disorganisation, a random utility discrete spatial choice model is proposed that incorporates the role of co-offending, and is applied to the riots in London. The results are presented and the ability for these theories to explain offender behaviour during rioting is discussed. Considering next the interaction between rioters and police, Chapter 4 concludes by incorporating the discrete spatial choice model into a microsimulation of police deployment. The suitability for the model to be used in a policy-making environment is discussed.

Chapter 5 investigates the interaction between two adversaries in space and time which, due to a lack of data on police activities, can not be performed with the 2011 London riots. A series of multivariate point process models are derived in the context of insurgent violence between police and Naxals in the Indian states of Andhra Pradesh and Telangana. These models are calibrated on data associated with this conflict, and a series of tests for model goodness of fit are presented, including an out of sample test on the predictive power of one of the models.

Chapter 6 begins by providing an overview of the Richardson model of conflict escalation, which comprises of a system of coupled ordinary differential equations. The model provides insights into the logical conclusions of a simple set of assumptions, without the requirement for an extensive amount of empirical data. It is argued that this model is well-suited to a more general process of conflict between two adversaries. The chapter addresses one of the weaknesses of the Richardson model—its lack of explicit dependence on space—by deriving a spatial model using an entropy maximising approach to disaggregating the effect of conflict escalation in space. This subsequent model is then analysed from a non-linear dynamical systems perspective, both analytically using low-dimensional systems, and computationally with high-dimensional systems. Insights into the spatial dependency of conflict escalation between adversaries are obtained and discussed.

In the conclusion of Chapter 7, the range of modelling frameworks presented in this thesis is consolidated in a comparative exposition. The focus here is on how the modelling frameworks and their range of possible insights might be used to aid policy decision-making. Extensions to the work presented in this thesis are considered before

concluding remarks are made.

Chapter 2

Modelling methodology

2.1 Introduction

A wide range of frameworks have been used to model civil violence. The insights afforded by these can be very diverse. The choice of framework employed in many studies is likely to depend on the questions that motivate the study, data availability, and the experiences of the modeller. In this chapter, previous models used to obtain insights into civil violence are discussed. This discussion is loosely based upon (and progresses along) the spectrum of models introduced in Figure 1.1 of Chapter 1. A range of exploratory data-driven, statistical and mechanistic modelling frameworks are described and models associated with each type of framework are reviewed. This wide range of literature serves to highlight the disparate approaches taken by many scholars to model civil violence, and to emphasise the types of insights that each framework affords. Additionally, the discussion serves to provide background to the approaches taken in the chapters that follow.

2.2 Exploratory space-time data-driven modelling

Exploratory techniques refer to a class of model frameworks that are used to illuminate and analyse important features of a dataset. They require few modelling assumptions, so that a researcher has few preconceptions as to what the analysis might reveal. Exploratory techniques may lead to significant insights in themselves but may also suggest further analyses, indicate hypotheses to be tested, and hint at assumptions that might reasonably form the basis of more sophisticated models.

Analysing event data in space and time is particularly suited to exploratory techniques, since they can provide quantitative assessment of the level of spatial and spatio-temporal dependency in the data. In what follows, a series of exploratory approaches that have been used to analyse the spatio-temporal dependency in civil violence event data are discussed, together with the insights that each approach affords. These three approaches consider, respectively, spatial autocorrelation, spatio-temporal interaction, and more intricate techniques that aim to quantify changes in spatial data.

2.2.1 Spatial autocorrelation

Spatial autocorrelation refers to the tendency for events to occur nearby to one another in geographic space. The detection of spatial autocorrelation is often used as a first

step in exploratory analysis of spatial data, and requires the rejection of a null model in which events occur randomly in space. Spatial statistics are employed to capture the geographic dependency of the empirical data, and are compared against statistics that would be obtained under the null model. Null model statistics can either be obtained analytically, by considering the probability distribution of event occurrence under the null model, or via Monte-Carlo simulation, in which a large number of realisations of the null model are generated using pseudo-random number generators and an empirical distribution of the spatial statistic is obtained (Besag and Diggle, 1977).

There are many spatial statistics that can be employed, the suitability of which can depend on the characteristics of the available empirical event data. For event data on civil violence, for instance, the data might be aggregated into spatial areas, and the frequency of event occurrence in each of those areas reported. In this case, area-level statistics such as Moran's I (Moran, 1950) or Geary's C (Geary, 1954), the latter of which is more sensitive to local variations, may be employed to detect autocorrelation. These two statistics are applied globally, incorporating the entire study region. If the detection of local spatial autocorrelation is required, for example, for the detection of hotspots of activity, then the G_i and G_i^* statistics of Getis and Ord (1992) or local variants of Moran's I or Geary's C (Anselin, 1995) might be employed. If, on the other hand, the data is available in point form, with accurate locations specified for each event, then a point pattern analysis may be used to detect spatial autocorrelation. The calculation of Ripley's K function (described in Dixon (2002)) or the spatial scan statistic of Kulldorff (1997) are two methods for the detection of spatial clustering in point patterns.

Explanations of spatial autocorrelation in event data take one of two perspectives. First, spatial autocorrelation may be a result of event occurrence being dependent on a confounding variable that varies in space and which is not captured by simple null models of spatial randomness. For example, events associated with civil violence are likely to vary with population density, which is highly heterogeneous in geographic space. As a result of this dependency, events will occur more closely to each other in space than under a null model of complete spatial randomness, in which population density is not controlled for, and spatial autocorrelation is subsequently observed. There are many examples of potential confounding variables including the distance from government

strongholds (Raleigh and Hegre, 2009); terrain (Do and Iyer, 2010); road accessibility (Zhukov, 2012); and communication links between areas (Myers, 2000). Identification of spatial autocorrelation can serve to stimulate the search for possible confounding variables and corresponding explanations that might be explored using more sophisticated models.

The second perspective used to explain spatial autocorrelation supposes that the occurrence of an event can directly impact the likelihood of a further event occurring. If this effect diminishes with geographic distance, so that a future event, should it occur as a result of an initial event, is more likely to occur near to the initial event than farther away from it, then spatial autocorrelation will be observed. There are many scenarios for which it can be argued this mechanism arises during civil violence. In the next section, spatio-temporal interaction of event data is described, which considers temporal influences in addition to the analysis of spatial data. In particular, tests for spatio-temporal interaction are often employed to determine whether spatial autocorrelation in a given dataset is a result of static confounding variables, or whether it also has some dynamic properties, which may be brought about by event interdependency.

2.2.2 Tests for spatio-temporal interaction

Temporal autocorrelation refers to the tendency for events to occur nearby to one another in time, and, similarly to spatial autocorrelation can arise as a result of event interdependency or by confounding variables that also vary in time. Spatio-temporal interaction is a stricter property of event data than both spatial and temporal autocorrelation and can be used to discount the influence of confounding variables that vary in space but not in time and confounding variables that vary in time but not in space. It refers to events that occur more closely to each other in both space and time than would be expected given the spatial and temporal distributions of the data. The presence of spatio-temporal interaction suggests that spatially-varying dynamic mechanisms are more likely to be responsible for the production of events than static or spatially homogeneous explanations.

There are a variety of techniques for the detection of spatio-temporal interaction in event data. The Knox test, described in Knox (1964a), compares the distances in both space and time between pairs of events by allocating each pair to a spatio-temporal

window of pre-specified resolution. The resulting categorisation of pairs of events over spatio-temporal windows of different resolutions can be compared against either the analytical expectation of a particular process (such as a Poisson process) or a Monte Carlo simulation, in which event times are randomly permuted over the locations in the empirical data. The Knox test was initially applied in an epidemiology setting (Knox, 1964b) but has since been applied to a wide range of problems in crime and security including burglary (Townsley et al., 2003; Johnson and Bowers, 2004); other types of urban crime (Grubesic and Mack, 2008); piracy (Marchione and Johnson, 2013); and insurgency and counterinsurgency in Iraq (Townsley et al., 2008; Johnson and Braithwaite, 2009; Braithwaite and Johnson, 2012).

The Mantel test (Mantel, 1967) provides a single measure of an empirical dataset without requiring the specification of space-time windows, which consequently alleviates potential edge effects in the data. Johnson and Bowers (2004), who use both the Mantel and the Knox test to investigate residential burglary, argue that the Knox test can potentially be more insightful as a range of spatio-temporal windows may be chosen and the clustering within each of them can be compared. Other tests for detecting spatio-temporal interaction include extensions to a spatio-temporal setting of Ripley's K-function for point processes (Diggle et al., 1995) and the k-nearest neighbour test of Jacquez (1996), used to detect the spatio-temporal signatures of different crime types in Grubesic and Mack (2008).

One of the main advantages of tests for spatio-temporal interaction is that few modelling assumptions are required to obtain relatively powerful insights into event data. Specifically, since such tests provide a relatively straightforward way to control for spatial and temporal variation, these effects can be largely neglected. The presence or not of spatio-temporal interaction can discount a range of mechanisms thought to have been responsible for the generation of event data.

2.2.3 Quantifying change in spatial event data

The timings and locations at which spatio-temporal interaction of event data arises, and its duration and geographic extent, have recently been of interest in a number of studies. Many of the tools used in analysing such effects are exploratory in nature, as they again require few modelling assumptions, which are typically informed by aggre-

gating statistics from the empirical data. The insights obtained by local perspectives of spatio-temporal interaction can be much more beneficial in a policy setting than the identification of global spatio-temporal interaction. The early identification of the local spreading of a disease or violence, for example, can lead to targeted vaccination or policing strategies that help to minimise its adverse impact and possible spreading.

One example of a more local and dynamic spatio-temporal exploratory technique is Kulldorff's space-time permutation scan statistic (Kulldorff, 2001; Kulldorff et al., 2005), which can be used to detect the emergence of hotspots of activity. This statistic and its associated Monte-Carlo method for assessing statistical significance has been shown to be robust for different spatial resolutions (Jones and Kulldorff, 2012) and under incomplete and inaccurate data (Malizia, 2013). Examples of its use in relation to civil violence event data can be found in O'Loughlin et al. (2010a), O'Loughlin et al. (2010b) and O'Loughlin and Witmer (2010). The method deploys moving cylindrical space-time windows of varying spatial and temporal resolution over the study area and compares the counts of events with what would be expected under a null hypothesis (e.g. of spatial and temporal homogeneity). The statistic is given by the maximum over all deployed cylinders of the generalised likelihood ratio, a function that compares the counts of empirical events both inside and outside the space-time window with the counts that would be expected under a null hypothesis. Since the method is applied locally in space and time, it can be used to detect the emergence of hotspots of activity.

A number of other studies have considered change in event patterns at a local level by, for each spatial region j, calculating the tuple

$$\left(X_j, \sum_l W_{jl} X_l \right), \tag{2.1}$$

where the variable X_j is a variable of interest, taken in previous studies to be a standardised count of events, or a binary indicator of event occurrence, in spatial region j, and W_{jl} is a row standardised matrix of spatial weights with zero diagonal. For a suitable definition of the spatial weights matrix, X_j provides information about event occurrence in spatial region j, and $Y_j = \sum_l W_{jl} X_l$ provides information about event occurrence in those areas nearby to region j. In Anselin (1995), using a standardised count of events, a comparison of X_j and Y_j is used to detect statistically significant areas of local autocorrelation of African conflict. Furthermore, the quadrant in which the

point (X_j, Y_j) lies in the plane indicates whether higher than average event occurrence is near in geographic space to other higher than average counts, whether low counts cluster near to other low counts, or whether there is negative autocorrelation and low counts are near to high counts. The variable Z_j is specified, which can take one of four values for each spatial region j. If there is a high number of events in both the focal region j and its neighbouring regions, then $Z_j = HH$. Conversely, if there are a low number of events in both j and its neighbouring regions, then $Z_j = LL$. If there is negative spatial autocorrelation, and a high count of events in the focal region is near to low counts, then $Z_j = HL$. $Z_j = LH$ is defined analogously. Thus, Z_j provides a simple indication of the local spatial autocorrelation near to spatial region j.

Cohen and Tita (1999) extend the local indicators of spatial association described in Anselin (1995) to consider temporal effects. By choosing an appropriate temporal partition of the empirical data, the authors calculate

$$\left(X_j(t_k), \sum_l W_{jl} X_l(t_k) \right), \tag{2.2}$$

for some time step t_k where the variables $X_j(t_k)$ and $Y_j(t_k) = \sum_l W_{jl} X_l(t_k)$ are as in equation 2.1 but specific to the time interval t_k. By determining the quadrant within which this tuple lies on the plane for different areas j and times t_k, the local characteristics of spatial autocorrelation in the event data at each time interval can be visualised and, moreover, categorised.

Defining $Z_j(t_k)$ analogously, and considering the change in $Z_j(t_k)$ over different time intervals leads to insights into to how the local spatial dependency in the event data changes. The transition $Z_j(t_k) \rightarrow Z_j(t_{k+1})$, which can take one of 16 possible values (e.g. $HH \rightarrow HH$, $HL \rightarrow LH$, etc.), can be interpreted as different dynamic processes in the event data. The transition $HL \rightarrow LH$, for example, corresponds to the relocation of events in the focal region to neighbouring regions. Similarly, $HL \rightarrow HH$ corresponds to escalation of event occurrence from a focal region to neighbouring regions. The identification of these patterns in event data can lead to a better appreciation of the range of mechanisms that might be at play. In many cases, the counts of each type of diffusion are compared against the counts that would be expected under a null hypothesis of event independence, which can be computed using a Monte Carlo simulation.

Using this framework, Cohen and Tita (1999) identify the presence of the geographic diffusion of homicide occurrence in Chicago; Hsueh et al. (2012) explore the different types of geographic diffusion in cases of Dengue fever in Taiwan; and LaFree et al. (2012) consider whether a change in strategy of the Spanish terrorism organisation ETA coincided with a change in the nature of the spatial diffusion of event occurrence.

Two further studies—Rey et al. (2011), who investigate burglary events in Arizona, and Schutte and Weidmann (2011), who investigate conflict events during the civil wars in Bosnia, Kosovo, Burundi and Rwanda—employ binary measures of event occurrence in each spatial region, known as join counts, rather than using standardised counts as described in Anselin (1995). That is, the variables $X_j(t_k)$ and $Y_j(t_k)$ determine whether at least one event occurred in, respectively, spatial region j or nearby regions at time t_k. Then, the transitions of the variable $Z_j(t_k) = (X_j(t_k), Y_j(t_k))$ are considered. This approach is particularly well-suited to relatively rare events in space and time and it alleviates the need for modification of the event data, for example by normalising. In this case, no choice is required regarding how to normalise event counts, a choice which may have a significant influence on the resulting analysis. To explain, if event counts are normalised at each time step, then an area with an apparent high level of events at one time step may appear to become an area with low intensity due to the onset of events elsewhere and not due to any change in the original area. Conversely, if the count of events are normalised across all time intervals considered in the analysis, then the identification of high intensity locations is sensitive to variation in the overall intensity of events.

Importantly, the frameworks described in this section are all exploratory. The null models against which some of the statistics described are compared against can often be easily specified using Monte Carlo modelling. These models are constructed with minimal assumptions regarding the underlying mechanisms in the generation of the event data. One example of a Monte-Carlo model that can be generated is complete spatio-temporal randomness, in which events are equally likely to occur within any spatial region and at any point in time over the entire study area. Simulations are used to generate the same number of events as in the empirical data under this assumption. Often a more appropriate model when considering spatio-temporal interaction is given by a Monte Carlo simulation that preserves both the spatial and temporal distribution

of the event data but loses any spatio-temporal dependence by randomly permuting the times associated with each event. This model enables a comparison of the data against a scenario with no spatio-temporal interaction and is useful for considering the effects of event interdependency.

2.3 Spatio-temporal statistical modelling

A statistical model specifies how a dependent variable is related to one or more explanatory variables. In contrast to exploratory approaches, statistical modelling requires assumptions as to how the system behaves and how some sample data is generated. Observations from a dataset are assumed to be generated by a probability distribution, the form of which is defined by the model. For parametric modelling, the model is specified up to a vector of parameters, denoted by $\boldsymbol{\beta}$. The task is then to select the value $\boldsymbol{\beta} = \hat{\boldsymbol{\beta}}$ so that the model is the one that would have most likely generated the sample data observed. Hypothesis testing can then be used to determine whether the relationship between dependent and explanatory variables specified by the model is appropriate, or whether another relationship should be considered.

Importantly, statistical modelling of civil violence event data can be used to test whether a proposed variable helps to explain the occurrence of events. The causal effect from an explanatory variable is justified by using theory to argue that a particular mechanism is responsible for the observation. Moreover, statistical modelling often forms the backbone of arguments that a particular mechanism is indeed responsible for the occurrence of events.

In classical statistical modelling, such as linear regression, the observation data is required to be independent. When the dependent variable in the model is the count or occurrence of events that are themselves suspected to be interdependent, this assumption is violated. Spatio-temporal approaches to statistical modelling have been developed in which independence across observations is not required. Such approaches are well-suited to event data occurring on relatively fine spatial and temporal scales.

In what follows, previous literature employing statistical models to obtain insights into civil violence event data from a spatio-temporal perspective is reviewed. This review is split into three sections. The first considers studies that employ data detailing the characteristics of the locations at which conflict is anticipated to occur, in order to

determine whether some of those variables covary with conflict occurrence, and may plausibly be incorporated into a explanation of the mechanism by which that conflict arises. The second section takes an individual perspective, and reviews literature that has employed statistical models at an individual level to investigate the choices made by those who engage in civil violence. Finally, statistical models that have been used to make predictions of event occurrence are considered, and their success in doing so is discussed.

2.3.1 Covariates of civil violence

The use of regression models in studies of civil violence as well as other types of conflict is widespread. Regression models can be employed to highlight statistical relationships between a number of variables. Taking the dependent variable of interest to be the onset or occurrence of civil violence within some space-time window, and taking the resolution of that space-time window, the units of analysis, to be the country-year, many studies have used regression models to highlight how the likelihood of conflict occurring in a country is related to structural variables such as GDP per capita, the presence of natural resources, and the type of government in power.

Two of the most widely-cited recent studies of civil conflict, Fearon and Laitin (2003) and Collier and Hoeffler (2004), use country-year logistic regression models populated with a range of explanatory variables. They argue that, in contrast to more traditional explanations of civil conflict such as relative deprivation (Gurr, 1970), variables that capture favourable conditions for a successful insurgency, such as state weakness, large populations and political instability, are often better at explaining civil conflict than variables designed at capturing grievances within a population, such as ethnic and religious fractionalisation, and economic inequality. In particular, variables designed at capturing grievances within a population are shown to add little explanatory power over the variables that capture the opportunity for insurgency. Although both models incorporate a temporal lag within each country, intended to capture some of the unobserved heterogeneity and to alleviate omitted variable bias, neither of the models incorporate spatial variables to account for spatial dependency.

Although stimulating a large number of subsequent models on civil conflict, the models of Fearon and Laitin (2003) and Collier and Hoeffler (2004) have often been

critiqued with respect to two key limitations: the lack of explicit spatial dependency, and the inappropriate use of country-years as the units of analysis.

Considering first the issue of spatial dependency, it has long been argued that, due to the presence of spatio-temporal clustering of conflict at the country-year level, the geographic context of a country appears have a significant influence on its internal functioning (Richardson, 1960b; Most and Starr, 1980; Starr and Most, 1983). As a consequence, a range of regression models that explicitly account for spatial dependency have been proposed. Two frameworks are the spatial autoregressive model and the spatially lagged error model. When an active spatial process is presumed to be present, such as the geographic contagion of conflict, the spatial autoregressive model is preferred (Beck et al., 2006); however, this model often requires sophisticated estimation techniques (Ward and Gleditsch, 2002).

Spatial regression models have been proposed that test a wide range of hypotheses concerning the types of spatial processes at play during civil violence. For example, exploring mechanisms responsible for the observed clustering of conflict, Salehyan and Gleditsch (2006) provide evidence for the association of this effect with the flow of refugees between countries; Buhaug and Gleditsch (2008) show that, by controlling for a wide range of dyadic variables, the importance of proximity to conflict is reduced, but neighbourhood contexts of conflict are still important, and that ethnic ties are a significant determinant in conflict clustering; and Braithwaite (2010) explores how a state's capacity to counter potential threats from civil conflict influences the likelihood of conflict spreading between neighbours. The latter of these employs a spatio-temporal lagged dependent variable predictor, rather than a pure spatial lag, so that the dependent variables at each point in time can be treated as independent from the explanatory variables.

Using country-years as a unit of analysis for many conflicts and, indeed, other types of civil violence is, in many cases, considered to be inappropriate. The spatial and temporal distribution of factors that influence the occurrence and onset of civil violence are likely to be highly heterogeneous. The violence may also only affect a small area of the country. In recent years, data on conflict and civil violence, as well as potential structural variables, have become available at much finer spatial and temporal resolutions. As a consequence, a number of recent studies have explored the

local factors that appear to influence the onset of civil violence and conflict around the world.

The study of rioting in US cities during the urban race riots of the 1960s is an early example of regression models being employed for the analysis of subnational factors associated with the onset of civil violence. In a series of studies, Spilerman (1970, 1971, 1976) argues that the occurrence of rioting was most positively associated with the proportion of non-white population in a given city. In fact, this variable was shown to absorb the effect of many of the other variables tested, which were chosen in accordance with sociological theory. More recently, Myers (1997) repeats the analysis by Spilerman, using modern event history techniques, to model the time until event occurrence, accounting for censored observations (i.e. accounting for events that do not occur in the dataset, rather than just ignoring them). While confirming the importance of non-white population size in US cities, measures of ethnic competition and geographic diffusion of riots were also shown to provide significant explanatory power. Myers (2000, 2010) more closely considers the role of geographic diffusion of rioting and shows that the effect of rioting did indeed spread spatially, but these effects were relatively short-lived. Furthermore, the spreading of rioting was found to be heterogeneous, with locations better served by mass media networks more likely to experience future violence.

With recent availability of worldwide data on subnational civil violence, the analyses of Fearon and Laitin (2003) and Collier and Hoeffler (2004) have been repeated at various levels of spatial and temporal resolution, and, in some cases, have been refuted. Using a fine spatial grid, Cederman et al. (2011) show that grievances stemming from inequalities and fractionalisation across different ethnic and social groups can indeed have a significant influence on the onset of violence. Local economic measures have also been shown to lead to an improved understanding of conflict onset over country-level indicators (Østby et al., 2009; Hegre et al., 2009; Buhaug et al., 2011; Vadlamannati, 2011).

Employing finer units of analysis than country-years means that the observed data and dependent variable is more susceptible to errors brought about by spatial dependency. As a consequence, these analyses typically control for spatial spillover effects, whereby the risk of conflict is potentially influenced by ongoing conflict in neighbour-

ing regions, using a spatial lag in either the dependent or explanatory variable(s). In addition, many studies also control for unobserved heterogeneity within each spatial unit via a temporal lag term. Some disaggregated studies of civil violence, however, have more explicitly considered spatial and temporal dependencies by making the spatially and temporally explicit terms the principal variables of interest. Weidmann and Ward (2010), for example, demonstrate how the inclusion of spatial and temporal terms in a logistic regression model of conflict occurrence during the civil war in Bosnia greatly improves the predictive ability of the model.

Focusing on other geographic aspects of conflict, Buhaug and Gates (2002) use the geographic area of a conflict and the distance of that conflict from the capital as the dependent variable in their regression model and show that, as well as being closely related, the land area, adjacency of international borders and the presence of natural resources can influence the size of the area affected by the conflict, whilst the distance from the capital is additionally dependent on the nature of the rebellion. Buhaug and Rød (2006) extend this analysis by showing how separatist conflicts in Africa are more likely to occur near to international borders and in remote and disadvantaged regions, whilst governmental conflicts are more likely to occur in urban areas and close to diamond fields.

A number of studies in civil conflict have also used event history approaches to determine the most likely areas to experience conflict based on the attributes of each location. Raleigh and Hegre (2009), for example, use a Cox Proportional Hazards model (Cox, 1972) to show that conflict is more likely to occur in locations with locally clustered populations far from capital cities and near to international borders. In addition, Buhuag et al. (2009) show that such separatist conflicts, which are located far from capital cities, can last substantially longer, but that the relative strength of rebel groups can drastically shorten conflicts. Holtermann (2015) employs an event history analysis of insurgent conflict in Nepal and shows how conflict dependency on covariates can change throughout the duration of the conflict and that, as a consequence, regression models with time-varying parameters, which are possible to construct using event history approaches, can lead to improved models.

Finally, a number of studies have pointed out that spatially dependent terms in regression models can have a number of different interpretations. Instead of purely

geographical distances, they may capture some form of generalised cost associated with a particular mechanism by which conflict is thought to spread. To explain, Beck et al. (2006), for example, use a measure of trade between nations, rather than purely geographic distance, in a model of the spread of democracy. In this way, they attempt to capture the underlying mechanism for the observed spatial dependency, rather than just relying on a geographic proxy. Similarly, Zhukov (2012) argues that the operations of insurgent and government forces during civil violence is likely to be constrained by infrastructure networks, and shows that by incorporating road networks into a distance metric via the spatially dependent variables, regression models can be vastly improved.

2.3.2 Individual decision-making during civil violence

Disaggregating from the country level, studies of violence during civil conflicts have often considered the perspective of groups that are bounded by either their proximity to one another or by their ethnic or socio-economic ties (Østby, 2008; Cederman et al., 2011). Additionally, various studies concerned with terrorism and insurgencies have considered the perspective of the terrorist or insurgent group committing attacks by incorporating independent variables such as terrorist group size, level of training and the age of the group in regression models (Clauset and Gleditsch, 2012; Asal et al., 2015; Holtermann, 2015). Despite these advances, there have been calls for the study of civil violence to be applied at yet lower levels of disaggregation, and to consider the decision-making of individuals, and how their decision-making results in the spatio-temporal signatures observed (Wilkinson, 2009).

In existing literature on civil violence, although an individual perspective is often formulated and discussed, empirical tests tend to rely on data aggregated at a higher level than the individual, particularly with regards to the spatio-temporal patterns of events. As an example, Kocher et al. (2011) and Lyall (2009) discuss the range of strategies available to civilians in the face indiscriminate violence by counterinsurgents. They test the theory that civilians are more likely to support the insurgents if they observe higher levels of indiscriminate violence. Using spatial techniques to test this theory at the village level, rather than at individual levels, they reach opposite conclusions using two distinct case studies of violence – aerial bombardment during the Vietnam War, and Russian artillery fire in Chechnya.

A small number of studies concerning collective violence and rioting have considered individual decision-making, largely with regards to the choice of target (Abudu et al., 1972; Berk and Aldrich, 1972; Rosenfeld, 1997; Auyero and Moran, 2007; Martin et al., 2009). The spatio-temporal influences during rioting have, however, not been adequately accounted for in statistical models of individual decision-making.

In contrast, the literature on criminology has long been concerned with how offender behaviour, and possible influences on that behaviour, shapes the resulting spatio-temporal distribution of event data. This is partly because individual level data on offenders and the crimes they commit is readily available for use in statistical models. There have been a large number of statistical models applied at the individual level with mechanisms inspired by a range of criminological theory. Some of the most prominent theories with regards to the spatio-temporal distribution of crime come from Environmental Criminology (Brantingham and Brantingham, 1981), which explicitly considers how individuals make decisions to offend based on the situations and surroundings in which they find themselves. One of Environmental Criminology's most prominent contributions, the routine activity approach (Cohen and Felson, 1979), supposes that crime occurs at the convergence in space and time of a motivated offender, a suitable target, and in the absence of a capable guardian. Crime pattern theory (Brantingham and Brantingham, 1993) then considers how the implications of the routine activity approach leads to the emergence of spatio-temporal concentrations of crime. As a result, using these theoretical perspectives, many studies have investigated the factors that influence the decision-making of individuals who commit offences (see Wortley and Mazerolle (2008) for an overview).

A recent common method for doing so is by employing spatial discrete choice models, which are suitable for situations in which an actor is faced with a choice in which each option has associated with it characteristics that are quantitatively distinguishable. The choice of location at which to commit a crime is one example where discrete choice models may be employed, although careful consideration of spatial and temporal influences is required. In this case, estimation of discrete choice models using empirical data can highlight the relative importance of the characteristics of an area in influencing the choice that is made. This approach has been applied to offender target choice for residential burglary (Bernasco and Nieuwbeerta, 2005; Clare et al.,

2009), street robbery (Bernasco and Block, 2009; Bernasco, 2010b; Bernasco et al., 2013), theft from motor vehicle (Johnson and Summers, 2015), and comparisons have been made over different types of crime (Bernasco, 2010a) and over different locations (Townsley et al., 2015).

2.3.3 Predictive models

Statistical models with a large number of independent variables can be criticised for placing too much emphasis on the outcomes of regression analyses that highlight covariates, and not enough emphasis on the causal mechanisms responsible for the generation of the empirical data (Schrodt, 2014). Some authors have argued that the focus of such studies should shift from identifying variables that covary, and which therefore might relate to a plausible mechanism that generates the data, to identifying the principal variables that improve our ability to predict unobserved or out of sample events. For example, Ward et al. (2010) show that the majority of variables included in the studies of Fearon and Laitin (2003) and Collier and Hoeffler (2004) amount to little improvement in the ability for the models to predict the onset of events, beyond what is included in just two predictors: the population of a country, and its GDP. Furthermore, they show that models containing a large number of statistically significant variables (with respect to the regression analysis) can even perform worse than simple baseline models containing just one of either population or GDP.

A number of predictive frameworks have been developed that attempt to identify variables that enable some form of prediction of civil conflict. In some cases, a wide range of independent covariates are incorporated and their predictive capability directly assessed (Hegre et al., 2013). However, as Ward et al. (2010) argue, the identification of a relatively small number of variables that have the most predictive power can also provide valuable insights and useful predictions (Ward and Gleditsch, 2002; Goldstone et al., 2010; Weidmann and Ward, 2010).

Another predictive modelling framework that has been employed to investigate civil violence stems from the theory of point processes. Point process models can be used to predict the timings and locations of different types of events. Although a wide range of structural variables can be incorporated into the model, many recent examples have included just the information on events that have happened in the past as predictor

variables. This approach can be particularly successful in using the temporal clustering present in much event data to model the increased likelihood of observing further events after the occurrence of a prior event. For example, Holden (1986) uses so-called Hawkes processes, which account for such excitation in the rate at which events occur, to determine whether a contagion effect can be observed in the frequency of aircraft hijackings in the US between 1968 and 1972. More recently, Hawkes processes have also been employed to model the timings of events associated with gang rivalries (Egesdal et al., 2010) and civilian deaths during the Iraq war (Lewis et al., 2011). Extensions of this same model have also been used to consider the timings of terrorist attacks in Southeast Asia (Porter and White, 2012; White et al., 2013). Short et al. (2014) propose a multivariate point process model to account for possible interaction effects arising from the behaviours of different gangs. Spatio-temporal models of point processes, in which the locations as well as the timings of future events are modelled have been used to model burglary (Mohler et al., 2011; Mohler, 2014) and insurgent warfare (Zammit-Mangion et al., 2012). In addition, these final studies demonstrate how point process models can be successfully used to improve prediction of event occurrence in space and time.

2.4 Spatially-explicit mechanistic modelling

Mechanistic modelling is distinct from the range of exploratory techniques and statistical approaches discussed so far. The principal reason for this is that mechanistic models do not necessarily require extensive amounts of empirical data in order to obtain insights. Instead, models are proposed by specifying theorised relationships between variables, which are directly incorporated into a model from which outputs can be obtained. The outputs of the model can then be assessed for their plausibility, and compared against what may have been empirically observed. If the outputs of the model are in agreement with observation, then there is support for the hypothesis that the proposed mechanism is indeed the process that is responsible for generating the empirical data. However, agreement between model outputs and empirical data does not mean that the proposed mechanism is actually responsible, rather, that it must merely be retained as a candidate explanation until either refuted and discounted, or further supported through the collection of data and subsequent analyses.

One of the main advantages of mechanistic models is that they can be used to consider what the impact might be on changes to the system or scenario being modelled. These changes may reflect sudden structural changes to the underlying mechanisms of the model, or may simply reflect a gradual change brought about by varying a parameter. The ability for mechanistic models to account for such changes makes them particularly useful in policy environments, where the potential impact of a policy decision and an understanding of its knock-on effects are often sought by decision-makers.

In what follows, two types of mechanistic model frameworks are discussed with respect to civil violence. The first, agent-based modelling, is a computational simulation technique that models each component in a system and its interactions with other components as a distinct and autonomous process. Next, the use of differential equations, which typically take a more aggregate perspective than agent-based models is considered.

2.4.1 Agent-based models

Agent-based models (ABMs) are simulations that represent each entity in a system as an independent and autonomous agent (Epstein and Axtell, 1996; Gilbert, 2007). An ABM consists of a set of rules that describe how the entities behave and, crucially, how they interact with other entities. Agent-based modelling is a framework well-suited to model complex systems: systems in which interactions between entities, for example between individuals, can produce emergent, or unexpected phenomena (Newman, 2011). Regularities in the spatio-temporal patterns associated with civil violence is an example of one such emergent phenomenon and ABMs can be constructed that attempt to replicate such patterns. Overcoming limitations associated with a lack of data at appropriate resolutions, ABMs have been employed as a means of understanding how different forms of individual behaviour might aggregate to system-wide outputs that may be empirically observed.

In many early applications of agent-based modelling, the behaviours proposed for the agents were somewhat simple, and the models were used largely to demonstrate that unanticipated emergent phenomena can be the result of individual autonomous adherence to simple rules. For example, in the model of neighbourhood segregation by Schelling (1971), agents' slight preference for similar neighbours can result in com-

plete neighbourhood segregation. The emphasis of this model was not to successfully replicate real-world individual behaviours, but to demonstrate that simple rules, when combined into a system with many interacting components, can produce unexpected results. The translation of this finding into the real-world provides support for the argument that observed segregation in urban areas is the result of inherent system properties, rather than any systematic prejudices in the population.

In another early example, Granovetter (1978) formulates a model of riot participation in which individuals can either choose to join a riot, or choose not to join, depending on the size of the riot and their perceived probability of being arrested. Each individual has associated to them a threshold that indicates the likelihood that they will join the riot given the number of rioters already engaged in the disorder. Thus, a safety in numbers effect is emphasised, with rioters who are more risk averse requiring a larger riot before they participate themselves. This model demonstrates how even with a range of risk averse people, it is possible for a cascading effect to result in widespread rioting. Furthermore, the model demonstrates sensitive dependence on initial conditions. Widespread rioting or a peaceful system state can depend on the presence of so-called 'instigators' to start the rioting, those with little to no risk aversion. Instigators enable others who are slightly risk averse to join who, in turn, enable even more risk averse individuals to participate.

Epstein (2002) presents an ABM of civil violence, which again incorporates relatively simplistic individual behaviours in order to capture interesting or unexpected dynamics at the overall system level. In this model, agents have heterogeneous levels of grievance and risk aversion, both of which influence the likelihood that any given agent engages in violence and becomes 'active' via a threshold model similar to the one employed in Granovetter (1978). The model also contains police agents which arrest active agents, who are then jailed before returning to the system in a passive state. The agents are free to move randomly on a simplified lattice and change their state based on their local environment. The model is explored in a variety of scenarios, including the occurrence of decentralised rebellion and ethnic violence, and results are interpreted in the context of the real-world. Given the wide range of empirical studies that investigate the causes of civil violence, Epstein's model of individual behaviour is certainly overly simplistic; however, Epstein argues that since the model exhibits outbursts and conta-

gion reminiscent of real-world rebellions, the model can be valuable in understanding how simple local behaviours can aggregate to global outcomes.

As the use of agent-based modelling has become more widespread, the range of behaviours available to agents have become increasingly complex, and more in line with extant theories of individual behaviour. There are a number of ABMs that, for example, employ criminological theory and robust empirical observations—such as the phenomenon of repeat victimisation in residential burglary in which houses who have recently been burgled are most likely to experience further burglary—to model a system containing offenders, opportunities to offend, and police response (Short et al., 2008; Johnson, 2008; Malleson et al., 2010; Bosse and Gerritsen, 2010; Birks et al., 2012) (see also Johnson and Groff (2014)).

In the case of civil violence, there have been several studies that extend the model of Epstein (2002), attempting to incorporate more realistic mechanisms into each agent's individual decision-making, their interactions, and the environment in which the model is simulated. For example, Fonoberova et al. (2012) explore a range of agent risk propensity functions that extend on Epstein's implicit linear relationship between the likelihood of engaging in violence and the ratio of police to rioters. The authors explore the effect of lattice size on the modelled police and crime numbers in comparison to empirical data. Torrens and McDaniel (2013) also extend the Epstein model by incorporating more realistic spatial information and agent decision-making when studying the onset of rioting.

Taking the perspective that insights can be obtained from simple models, Bennett (2008) proposes an ABM of an insurgency in which civilians can choose to commit attacks if their level of anger at the state or counterinsurgents exceeds their level of fear. Bennett uses this model to explore the tradeoff between effectiveness and accuracy of counterinsurgent forces. Although emphasising that the model is simplistic and therefore cannot capture a wide range of behaviours that have been observed in the literature, the model generates policy-level considerations for counterinsurgent forces, such as the comparative advantages of being highly accurate with counterinsurgent measures during the early stages of an insurgency.

As well as incorporating theories regarding individual behaviour, there is an increasing trend for ABMs of social systems to explicitly consider how the environment

in which the agents move impacts their decision-making and their interactions (Torrens and McDaniel, 2013; Heppenstall et al., 2012). A number of sophisticated ABMs with empirically driven modelling and validation procedures have explored the role of individual migration and the resulting spatial distributions of ethnic groups in the occurrence of violent events (Lim et al., 2007; Bhavnani and Choi, 2012; Weidmann and Salehyan, 2013; Bhavnani et al., 2014; Rutherford et al., 2014). By constructing models of specific examples of civil violence, and by calibrating outputs so that they are empirical consistent, as these studies do, the policy relevance of such models becomes immediately apparent. Bhavnani et al. (2014), for example, use their model of segregation and violence in Jerusalem to explore a number of counterfactuals that result from different policy decisions.

While agent-based modelling began as a conceptual tool to consider emergence in hypothetical and largely simplified systems, another simulation technique, microsimulation, began with the explicit aim of being data-driven and empirical. Microsimulation aims to overcome the ecological fallacy—which refers to problems brought about by assuming that characteristics of individuals within a given population can be assumed to be equal to the averaged statistics of that population—by modelling individuals using data from a population that includes those individuals. This requires a model that describes the variance within a population, and which therefore disaggregates the population statistics over each individual. Many of these models are typically based on the calculation of conditional probabilities for the underlying population, and are often explicitly spatial (Ballas et al., 2005). Such models simulate probabilities for the unknown attributes of an individual based on what is known about them (e.g. where they live, and what are the overall characteristics of the location in which they live). The aim is to construct realistic representation of the population that matches the overall statistics for a particular area.

The two model frameworks referred to as agent-based modelling and microsimulation are becoming indistinguishable: data-driven and explicitly spatial ABMs have begun to incorporate statistics of underlying populations to investigate the interactions of individuals (Heppenstall et al., 2012), whilst dynamic microsimulation models are becoming versatile enough to incorporate the changing behaviours of individuals and are therefore capable of exploring the emergent behaviour of populations (Birkin and

Wu, 2012).

With regards to such simulations of civil violence, on the one hand, some ABMs can be criticised for being overly simplistic and not incorporating extant theories regarding human behaviour; however, on the other, some models may appear to be overly complicated, with modelling decisions taken without proper justification. As a research tool, agent-based models have also been criticised as they can be difficult to reproduce and write code in a standardised way. More recently, empirical agent-based modelling, in which model outputs are compared against real-world data, has been demonstrated as a valuable tool in studying individual behaviours, and how these behaviours result in aggregate observed outcomes during civil violence. The development of agent-based models is becoming more established as a research tool (Grimm et al., 2010), and it is a method that looks set to play an increasing role in future research.

2.4.2 Differential equations

Models composed of differential equations (DEs) have also been widely used to obtain insights into social systems. In contrast to ABMs, in which the interest is often on individuals, the dependent variable in a DE-based model of a social system is often taken to be some attribute associated with a group of individuals. DE-based models are therefore typically used for more aggregated scenarios than ABMs (although, there are exceptions: DE-based models are employed with individual perspectives in Liebovitch et al. (2008) and Curtis and Smith (2008) and agent-based models are employed with aggregated perspectives in Cederman (2003)).

There are many examples of DE-based models being applied to study civil violence in a modern setting. Classical models, however, are typically concerned with the actions of two or more adversaries during more conventional forms of conflict or warfare. More recently, some of these have been adapted to consider modern conflicts, including civil violence and insurgencies. For this reason, attention is initially given to models of conventional conflict that have more recently been adapted and applied to civil violence.

In many cases, the dependent variable of a DE conflict model is taken to be the number of individuals on each side of a conflict. In an early example, Lanchester (1916) uses DEs to model different types of attritional warfare between two adversaries. He

considers how new technologies, such as the introduction of aircraft, might change military strategy. He does this by proposing two models: one in which the rate of loss of each adversary is proportional to the size of their opponent, representing aimed firepower, and one in which the loss of each adversary is proportional to the product of the size of their opponent and the size of themselves, corresponding to unaimed fire. In the case of aimed fire, the model suggests that a better advantage comes from having a larger army, rather than training the army to be more effective. For unaimed fire, the benefit associated with being more effective is equivalent to a benefit brought about by a numerical advantage, suggesting that effective training is likely to be just as successful as recruitment during warfare.

There have been a number of studies that follow Lanchester in modelling the change in the size of adversaries with DEs. Deitchman (1962), for example, proposes a Lanchester-type model of Guerrilla warfare. This model is further developed in Intriligator and Brito (1988), who incorporate a predator-prey framework to examine the impact of civilians, and in Kress and MacKay (2014), who generalise the model to account for military intelligence as well as diminishing numbers of insurgents. Atkinson et al. (2011) also use Lanchester-type models to investigate insurgent warfare, in which they compare a DE model to a number of modern conflicts.

Another class of DE-based models stems from the work of Richardson (1960a) on the actions of nations during the lead up to war. In this case, the dependent variable is not the size of each adversary but the level of military spending. The key assumption in Richardson's model is that the extent of a nation's military defences, denoted by p, reacts to the military defences of their adversary, given by q, at a rate proportional to q. The adversary behaves similarly and reacts to the defence p. This reciprocal action-reaction process can result in an escalating arms race between two adversaries. A nation may react to the military defences of its rival both as a defensive measure, in order to provide protection from the threat posed by their opponent, as well as an aggressive measure, to exert threat over their opponent.

Richardson believed this process on its own was not enough to model how arms races might evolve and so included two more factors which influenced the military defences of a nation: its own level of expenditure, which was hypothesised would diminish the change in defences as measured by the model, and also exogenous effects,

which were termed ‘grievances’. The model was first presented as a two-dimensional linear system of ordinary differential equations given by

$$\begin{aligned} \frac{dp}{dt} = \dot{p} &= -\sigma_1 p + \rho_1 q + \epsilon_1 \\ \frac{dq}{dt} = \dot{q} &= \ \rho_2 p - \sigma_2 q + \epsilon_2, \end{aligned} \tag{2.3}$$

where σ_1 and σ_2 are parameters that specify the strength of inhibition from each nation’s own expenditure on the model, ρ_1 and ρ_2 are parameters that specify the strength of interaction between adversaries, and ϵ_1 and ϵ_2 are parameters that specify the external grievances of each adversary.

Measuring the ‘defence’ of a nation—the dependent variable considered in this model—is difficult to achieve empirically. Richardson initially operationalised the dependent variables p and q by considering military expenditures of two adversaries. However, there are complications encountered by defining the variable in this way, as some have pointed out (Brauer, 2002). Richardson’s primary objective was to demonstrate how modelling simple interactions can shed light on the resolution of conflict, and was not necessarily on the quantification of military defences. As a result, he also allowed the possibility for negative values of p and q. Although difficult to comprehend in terms of military expenditure, it was argued that negative values might correspond to some measure of cooperation between the two nations, which might, for example, be measured via trade.

In the first application of the model in equation 2.3, Richardson (1960a) shows how the increase in military expenditure of four nations—Russia, Germany, France and Austria-Hungary—on two sides of a conflict in the years prior to the First World War very closely follows a pattern that would have been predicted by the model. A figure from Richardson (1960a) is reproduced in Figure 2.1 that shows the straight line expected from the model, against the data Richardson gathers for the years shown. The equation for the straight line is obtained by summing the two equations in 2.3 and assuming that both sides of the conflict react to their own defences and the defences of their opponent at the same rate, so that $\sigma_1 = \sigma_2$ and $\rho_1 = \rho_2$.

Perhaps as a consequence of the very close fit between the model and the small dataset in Figure 2.1, Richardson’s arms race model has been applied to various scenarios around the world which have been considered to exhibit ‘arms race’-type behaviour.

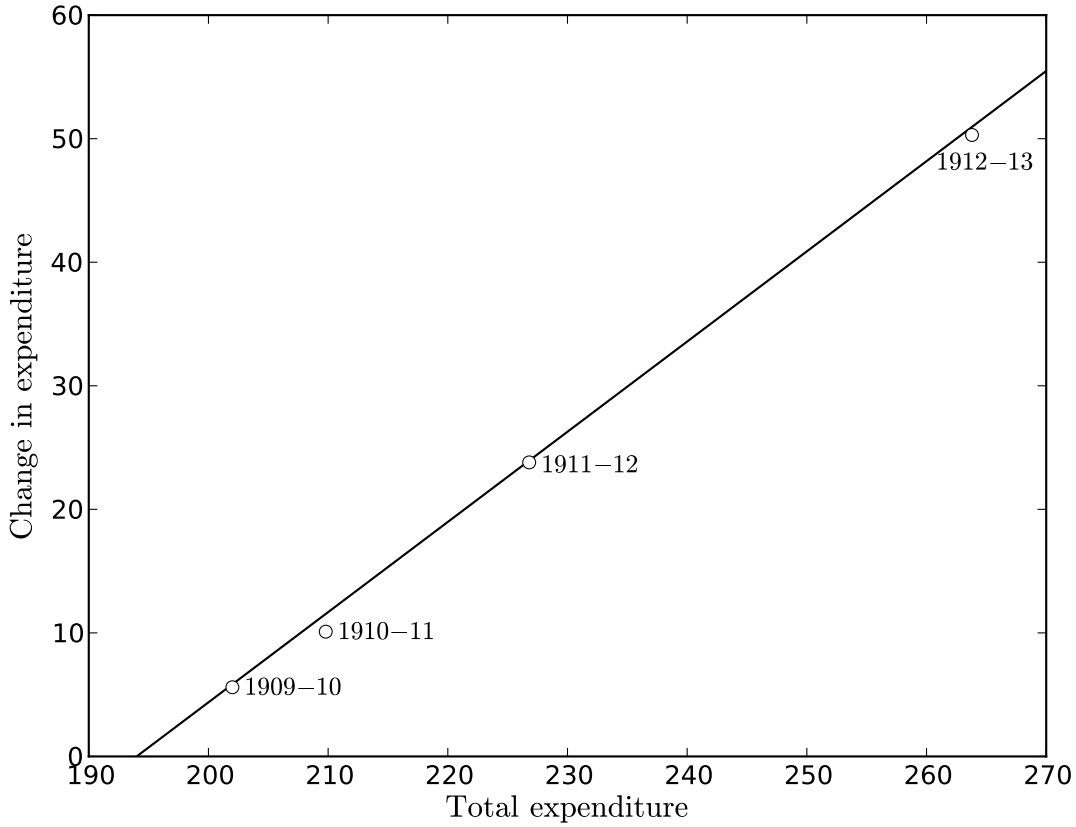

Figure 2.1: **The change in the sum of defence budgets against the sum of defence budgets for four nations during the four years prior to the First World War.** The four nations are Russia, Germany, France and Austria-Hungary and the values plotted represent the sum of defence budgets over these nations. Defence expenditure data was gathered from various sources by Richardson, and the line represents the best fit of what would be expected from the model in equation 6.1, assuming that $\sigma_1 = \sigma_2 = \sigma$ and $\rho_1 = \rho_2 = \rho$. This figure is reproduced from Richardson (1960a). The gradient is given by $\rho - \sigma$ and is estimated by Richardson to be 0.73. An ordinary least squares regression produces the same output.

In many of these cases, however, when using modern estimation techniques with large datasets, the model has been unable to reproduce the empirical data to such a close extent. In fact, much of the time, the model prediction is found to be a poor fit to the data. Dunne and Smith (2007) give an overview of some of the econometric applications of Richardson's arms race model. They discuss the mixed results when the model is applied to the India-Pakistan arms race from 1960. In particular, using purely temporal vector autoregression methods, they apply the Richardson model to arms expenditure data for India and Pakistan for the period between 1960 and 2003. They find that, for some time periods, action-reaction type dynamics present in the Richardson model can be observed in empirical data; however, for other time periods, no such consistencies can be found.

Brauer (2002) reviews applications of the model to the Greco-Turkish arms race, and points out several issues associated with fitting such models to arms race data. Some of the issues Brauer points out are relevant to many applications of differential equation-based models to social systems. For example, problems are often encountered with data availability, leading to complications in defining appropriate dependent variables from the data, which are required in order to validate the model. In the case of arms expenditure, for example, decisions regarding whether to take the dependent variable as the absolute expenditure on defence for each nation, or the relative amount of expenditure on defence as a proportion of that nation's GDP, can lead to varying levels of success of the fit of the model.

Parameter estimation can also be compromised as, in social systems in particular, parameter values can change very quickly. As Saperstein (2007) points out, the parameters of the original Richardson model in equation 2.3 are assumed to remain constant for timescales over which the dependent variables change. Since decisions regarding military expenditure can be made by reacting to a single event that can occur on very short timescales, there may be many scenarios in which this assumption is not valid. Saperstein (2007) goes on to define nonlinear extensions of the model in which the parameters of the system change according to the strategic aims of each nation.

Studies reporting difficulties in matching the model to empirical data sometimes overlook the principal reason for such discrepancies: the model is very simplistic. There are mechanisms not present in the model which may well play an important

role. Richardson's model is a useful descriptive tool to understand the possible states of an international system, and how the system might transition between these states. It was not intended to be used as a predictive tool to forecast defence budgets (Zinnes and Muncaster, 1984). Indeed, proponents of Richardson's model will argue that the simplicity of the model is a virtue: it can be easily analysed, understood, and be used to explain the outcomes of different scenarios, and how transitions might occur between them.

Similarly to Lanchester's model of combat, Richardson's model has been extended in a number of ways to consider the dynamics of different types of conflict. In one example, asymmetrical conflict is investigated by considering what might occur if a smaller adversary is unlikely to directly compete with a larger one, instead choosing to change its tactics by, for example, submitting to the larger nation's threats or attempting to undermine the larger nation by employing different strategies rather than directly competing by increasing the size of their own defences. In Richardson (1951) and Richardson (1960a), the model in equation 2.3 is extended to consider the possibility of submission of a nation in an arms race if the lead became too large. This model is given by:

$$\begin{aligned} \dot{p} &= -\sigma_1 p + \rho_1 q\left(1 - \upsilon_1(q-p)\right) + \epsilon_1 \\ \dot{q} &= -\sigma_2 q + \rho_2 p\left(1 - \upsilon_2(p-q)\right) + \epsilon_2, \end{aligned} \tag{2.4}$$

where $\upsilon_1, \upsilon_2 \geq 0$ are additional parameters that Richardson termed 'submissiveness', whilst all other parameters have the same interpretation as in equation 2.3. The parameters υ_1 and υ_2 determine the extent to which the reaction terms are diminished proportional to the opponent's lead in defences. Their inclusion has the effect of enabling scenarios in which, once a sufficient lead develops for one nation, their opponent will slowly begin to react less and eventually begin to reduce their defences, as they concede their position in the arms race.

Asymmetric dynamics can also occur during insurgent warfare and other types of civil violence (Ryan, 2006). In this case, whilst it is difficult to measure the dependent variable in terms of military expenditure, there may be other measures that determine the level of threat or cooperation between opponents, such as the amount of public support for either side, or the likelihood of one side initiating conflict against the other.

Karmeshu et al. (1990) consider an extension of the Richardson model that can be applied to domestic political conflict in order to investigate the interactions between a ruling and a challenger group. Similarly, models proposed by Jackson et al. (1978), Intriligator and Brito (1988) and Blank et al. (2008) are all reminiscent of Richardson's model since they incorporate dynamical processes of escalation and inhibition, as well as various extensions that might be relevant in civil violence scenarios.

The ability for models of escalation processes to be applied to a range of different types of conflict, from arms races to insurgencies, suggests that they can be interpreted as models of general conflict between two adversaries. Indeed, recently, a number of authors have taken this perspective, and proposed models of general conflict processes that build upon theories of conflict developed in psychology. The authors argue that such models can be applied to nations, groups or individuals who interact in a conflict with an opponent. No constraints are placed upon the range of situations to which the model may be applied. For example, Liebovitch et al. (2008) present the dynamical properties of the model given by:

$$\begin{aligned} \dot{p} &= -\sigma_1 p + \rho_1 \tanh q + \epsilon_1 \\ \dot{q} &= -\sigma_2 q + \rho_2 \tanh p + \epsilon_2. \end{aligned} \tag{2.5}$$

The relationship between this model and Richardson's model in equation 2.3 is clear: the interaction terms have become nonlinear functions bounded in $(-\rho_1, \rho_1)$ and $(-\rho_2, \rho_2)$, respectively. Further extensions have recently been explored in Qubbaj and Muneepeerakul (2012) and Rojas-Pacheco et al. (2013) by adding time delays to these reaction terms.

Perhaps surprisingly, given how important the consideration of space is in various conflict processes, there have been few spatial extensions of DE-based conflict models. Borrowing techniques from ecology (see, for example, Malchow et al. (2008)), some spatially-explicit models have been proposed using reaction-diffusion equations to specify how a dependent variable of interest varies in space. For example, Keane (2011a) presents a spatially extended version of the Lanchester equations and demonstrates how strategic manoeuvring of combat units can be incorporated into a spatially continuous model. Spatial Lanchester models are explored further in González and Villena (2011), in which they are derived from first principles based on assumptions

of the movement dynamics of troops. Another example is Brantingham et al. (2012) who present a spatially extended version of the Lotka-Volterra equations to model the geographic evolution of gang boundaries in Los Angeles. They observe consistencies between the model and the real world system, demonstrating that events cluster in space in a way predicted by the model. Reaction-diffusion models have also been used extensively in models of urban crime (Short et al., 2010a,b; Pitcher, 2010; Rodriguez and Bertozzi, 2010; Berestycki and Nadal, 2010). Some have argued however, that reaction-diffusion models may not be the most appropriate method of accounting for spatial dependency since such models can lack a clear theoretical argument for the continuous diffusion of the dependent variable in space (González and Villena, 2011; Ilachinski, 2004).

Another approach to modelling spatial dependencies with DEs is through the use of spatial interaction models. Spatial interaction models specify how the value of a dependent variable at one location interacts with the dependent variable at another. They can be readily employed within differential equations, which typically specify the change in that variable over time, taking into account any spatial interaction. Davies et al. (2013), for example, present a DE-based model of the London riots that employs a spatial interaction model to account for spatial dependency in contagion processes associated with rioting. The authors use their model to investigate policing strategies—in particular concerning police deployment strategies—in an effort to understand how these might affect outcomes during such extreme events.

2.5 Discussion

A range of modelling frameworks, each of which have been used for the development of spatio-temporal models of civil violence, have been introduced, and various examples considered. The amount of empirical data required to formulate the models, and the extent to which assumptions remove the model from the real world varies over the different modelling frameworks. Furthermore, this changes both the plausibility of the model, as well as the range of potential insights, as argued in Chapter 1 (see also Figure 1.1).

Exploratory approaches can be used to construct null models whose structure is directly informed by the empirical data (e.g. through the total number of events or

the number of expected events in a given spatio-temporal window). Differences between null models and empirical data can be used to infer certain characteristics of the data, and possible mechanisms for these characteristics can be considered. It has been demonstrated how exploratory approaches are particularly well-suited to analysing the spatio-temporal properties of civil violence event data. Limitations of exploratory approaches arise from their inability to explore theorised mechanisms in detail, and their reliance on accurately recorded spatio-temporal data. Reliance on past data means that exploratory approaches can not be extensively used in a predictive setting, since any predictions would rely heavily on extrapolation.

Statistical models require the specification of some hypothesised relationship between variables. Calibration of the model with empirical data, together with appropriate controls, can lead to an assessment of the extent to which variables that proxy for the proposed mechanisms covary with a dependent variable, and therefore can provide evidence that those mechanisms do indeed play a role in the data generating process. Statistical models in which structural covariates are employed as a proxy for a particular mechanism are widely used to assess the occurrence of civil violence and conflict events in space and time. Despite recent models being applied at finer spatial and temporal resolutions than have typically been used in the past, such models may still suffer from sources of error brought about by aggregation. Statistical models of individual choice may offer an alternative formulation for employing statistical models to study the spatial context of civil violence.

A significant literature in the statistical modelling of civil violence and conflict has shifted the focus from standard goodness of fit measures associated with regression models to their ability to predict the onset and occurrence of events. Even relatively parsimonious models have been shown to have some predictive value. Point processes provide a statistical modelling framework that are well-suited to predictive modelling. In particular, there are a number of point process models that have been applied to a range of problems in crime and security. Some of these have even demonstrated their ability to predict events in space and time more successfully than traditional models.

Mechanistic frameworks, such as agent-based modelling and differential equation-based modelling, enable the investigation of the logical consequences of a proposed mechanism at various levels of aggregation. If the model produces outputs in agree-

ment with empirical observation then that mechanism may play a prominent role in the real-world system. Mechanistic models can also be used to consider different scenarios on which there is little historical precedent and scarce empirical data. In this sense, mechanistic models can be extremely useful in a policy setting, as policy-makers might be interested in what might occur in the future under a range of different policy options. The appropriate level of complexity in a mechanistic model is often difficult to achieve. Simple models are often preferable due to their ability to be analytically interrogated, but can be criticised for not incorporating potentially important processes. More complex models can be also be defined, however, models that are too complex can preclude validation procedures and therefore useful insights.

The choice to construct a mechanistic model using an agent-based or equation-based framework is an important one. Although ABMs can potentially better capture the idiosyncrasies of individual behaviour, they often result in a higher level of model complexity, which is sometimes undesirable. Additionally, the wide number of analytical approaches developed to study differential equations sometimes means that DE-based models can lead to more sophisticated insights. Keane (2011b), for example, compares a spatially-explicit equation-based model of combat with an equivalent agent-based model (described in Ilachinski (2004)) and shows that many behaviours of agent-based models can be reproduced using equation-based approaches. If the results of a DE-based model can be shown to produce complex dynamics such as those in an ABM, then the analytical power given by the DE model would be preferable so that a researcher can, in theory, evaluate different regimes of behaviour; a technique which is difficult to achieve with any certainty in a simulation. Short et al. (2010b) provide an example where the analytical tractability of an equation-based model generated from an agent-based model leads to greater insights than the agent-based model alone. Some studies have combined the two approaches in an attempt to benefit from both of their advantages (Geller and Alam, 2010).

Finally, although there are some other modelling frameworks that may have been included in this thesis to investigate the spatio-temporal setting of civil violence, such as spatial game theory, bayesian networks and machine learning algorithms, the scope of the thesis has been bounded to incorporate just those approaches presented above, which were found to be the most prominent spatio-temporal approaches to modelling

civil violence in the current literature.

Chapter 3

Exploring spatio-temporal patterns of rioting with data-driven models

3.1 Introduction

The availability of extensive datasets detailing various aspects of human activity has transformed our ability to examine social systems from a quantitative perspective. Civil violence is an area of human activity to which this particularly applies. Police forces and government agencies are collecting considerable quantities of data on the locations and times at which offences associated with violence occur. The purpose of this chapter is to examine whether modelling the spatio-temporal profile of event data using an exploratory data-driven approach can lead to insights into the mechanisms by which civil violence occurs. It is then considered how these types of models might be used to aid the operational decision-making of police organisations.

Exploratory data-driven approaches typically compare carefully constructed null models to the empirical data, in order to make inferences about that data. It is common for null models to be built from initial simple—indeed, almost trivial—assumptions. Further assumptions are then subsequently incorporated that begin to increase the complexity of the model. As will be demonstrated in this chapter, the inclusion of more restrictive assumptions can lead to sophisticated insights into the range of plausible data generating processes.

To demonstrate this model framework, spatial and spatio-temporal patterns in the 2011 London riots are investigated. The aim is to construct a model for the generation of times and locations at which offences occurred during the riots, with the objective of understanding how and why the riots spread as they did. A model is first presented in which riot data is generated under the assumption of complete spatial randomness. Comparing this modelled data with the event data, it is concluded that there was significant spatial heterogeneity and autocorrelation during the London riots. The spatio-temporal profile of the rioting is then explored, first by determining whether there was significant spatio-temporal interaction between events that was above and beyond the effect of the spatial and temporal dependency of the event data and second by examining how spatio-temporal interaction influenced the local patterns generated by the times and locations at which offences occurred. The results of this study are discussed with reference to possible mechanisms for the observed patterns, and evidence for the presence of these mechanisms is evaluated. The utility of these insights is discussed both from a theoretical and a policy perspective, and the generality of the modelling

approach is considered. Finally, it is argued that the insights obtained can be used in the development of more sophisticated models.

3.2 Data aggregation

To introduce notation, which is defined without loss of generality in order to enable applicability of the methods presented across different scenarios, suppose that events occur at $(\mathbf{s}_i, t_i) \in \mathcal{D} \times \mathcal{T}$ for $i = 1, .., N$, where $\mathcal{D} \subset \mathbb{R}^2$ is a bounded spatial domain, and $\mathcal{T} \subset \mathbb{R}$ is a bounded temporal domain. Suppose also that the events $(\mathbf{s}_i, t_i)$ are ordered so that $t_i < t_{i+1}$ for $i = 1, ..., N-1$, and therefore it is often convenient to take $\mathcal{T} = [t_1, t_N]$.

Event data is often aggregated into a spatio-temporal partition of the domain $\mathcal{D} \times \mathcal{T}$. There are many reasons why event data might be aggregated. Data on civil violence is highly likely to be of a sensitive nature. At its finest level of spatial resolution, it may contain identifiers such as home addresses of suspects or other personal information. The data can also suffer from observation biases. For example, there are difficulties in obtaining accurate event times when investigating different types of crime since the occurrence of the crime is rarely directly observed (Ratcliffe, 2000). Consequently, the interval in which the crime is known to have occurred is often recorded, rather than the actual time.

To introduce notation, for subsets $\mathcal{D}_j \in \mathcal{D}$ for $j = 1, 2, ..., J$ and $\mathcal{T}_k \in \mathcal{T}$ for $k = 1, 2, ..., K$, suppose that

$$\mathcal{D} = \bigcup_{j=1}^{J} \mathcal{D}_j, \qquad \mathcal{T} = \bigcup_{k=1}^{K} \mathcal{T}_k. \tag{3.1}$$

It is further assumed that $\mathbf{s}_i \in \mathcal{D}_j$ implies $\mathbf{s}_i \notin \mathcal{D}_l$ for all $l \neq j$ and for all i. Similarly, $t_i \in \mathcal{T}_k$ implies $t_i \notin \mathcal{T}_l$ for all $l \neq k$ for all i. In other words, $\{\mathcal{D}_j\}_{j=1,...,J}$ is a non-overlapping partition of the domain $\mathcal{D}$, and, similarly, $\{\mathcal{T}_k\}_{k=1,...,K}$ is a non-overlapping partition of the domain $\mathcal{T}$.

Due to constraints in the way event data is collected and reported, the spatial partition of $\mathcal{D}$ is often defined by administrative regions that are geometrically irregular. Consequently, the subsets $\mathcal{D}_j$ can vary substantially in size for different j. In the case of the 2011 London riots, in which offence data was particularly sensitive given the political salience of the riots, the available data reported the location of offences aggregated

into census output areas within Greater London. Census output areas are a geographic partition of the UK designed for the reporting of demographic data obtained from the UK census. Each output area is designed to contain approximately 300 residents and, therefore, can vary in size according to the population density of the underlying geography.

The effects that aggregation has on analysis of spatial data has been well documented (see, for example, Weisburd et al. (2009)). One such effect is the modifiable areal unit problem which is demonstrated in detail in Openshaw (1984). It states that the choice of spatial partition of the geographic area of interest can have a large influence on the outcome of any analysis. The results obtained may be more of a consequence of the particular aggregation chosen and not a property of the underlying process. A solution is to run multiple analyses for different geographic aggregations of the data, in order to test whether results are consistent when the data is aggregated in different ways. One way of achieving this, and the method that is employed in this chapter, is to overlay a square spatial grid on the geographic area of interest. A square spatial grid easily enables the researcher to consider different aggregations of the available data by varying the spatial resolution of the grid, denoted by δs. In laying a regular spatial grid over an irregular administrative partition, care must be taken to ensure that the spatial grid is of a large enough resolution so that events occurring within a particular administrative area are mapped to the spatial grid unit in which they occurred.

The modifiable unit problem also holds for temporal aggregations, in which events are aggregated into time intervals $\mathcal{T}_k$. Similarly to the spatial case, a solution is to aggregate the data into a regular temporal partition of the time domain of interest $\mathcal{T}$ with resolution δt. Supposing that $\mathcal{T} = [t_1, t_N]$, then $\mathcal{T}_k$ is defined for $k = 1, ..., K$ so that

$$\mathcal{T} = \bigcup_{k=1}^{K} \mathcal{T}_k = \bigcup_{k=1}^{K} [t_1 + (k-1)\delta t, t_1 + k\delta t), \tag{3.2}$$

where K is chosen so that $t_N - t_1 \leq K\delta t$. The resolution δt can then be varied to test whether any conclusions are consistent across different temporal aggregations. For spatio-temporal analysis, the modifiable unit problem is addressed by performing analyses over different values of both δs and δt. In varying δs and δt, it is also possible to examine if, and how, conclusions resulting from the analysis vary over different

temporal and spatial scales.

3.3 Spatial randomness and autocorrelation

In order to motivate investigation into the spatial autocorrelation of riot events, the advances made in considering the spatial dependencies of different types of crime are first considered. Indeed, a large body of research has demonstrated that, for certain types of crime, there is significant evidence for spatial autocorrelation: the phenomenon by which the occurrence of events is more likely to be near to other events. This finding has led to subsequent studies investigating possible explanations for the presence of autocorrelation. Johnson (2008), for instance, compares two possible explanations for the presence of autocorrelation in studies of residential burglary. The first of these states that it is the occurrence of events at a particular location that increases an area's attractiveness, leading to the occurrence of further events. This is known as the boost hypothesis. The second explanation is that it is the presence of suitable time-stable environmental conditions at that particular location that make it particularly vulnerable, the so-called flag hypothesis. This particular example demonstrates the utility in using data-driven modelling approaches as a first approximation for a model of a complex process. The identification of spatial autocorrelation led to further studies that considered explanations of the phenomenon. Models based upon simple assumptions can often inform further studies by suggesting research questions. It is in this vein that this section proceeds.

In this section, a spatial analysis for the 2011 London riots is presented in order to determine whether or not it was the case that riot offences clustered in space. The aim is to determine whether further investigation into the spatial patterns of the riots might lead to more intricate insights, which might ultimately be useful from a policing perspective. A model of complete spatial randomness (henceforth abbreviated as CSR) for the event data is first considered. Rejection of CSR is often considered a "minimal prerequisite to any serious attempt to model an observed pattern" (Diggle, 2013). Indeed, if a dataset is indistinguishable from CSR then there is no spatial dependency in the data, and efforts at spatial modelling are unlikely to generate useful insights.

A series of events $(\mathbf{s}_i, t_i)$ for $i = 1, ..., N$ is *completely spatially random* when the locations of the events $\{\mathbf{s}_i\}_{i=1,...,N}$ are indistinguishable from a Poisson process.

A *Poisson process* occurs when counts of events in non-overlapping subsets $\mathcal{D}_j$ of $\mathcal{D}$ follow a Poisson distribution. Denoting the number of events that occur in the subset $\mathcal{D}_j$ by the random variable X_j and assuming that the subsets $\mathcal{D}_j$ have equal area for all j, this implies that

$$Pr(X_j = x) = \frac{\lambda^x e^{-\lambda}}{x!}, \tag{3.3}$$

for some $x \in \mathbb{Z}$ and *intensity* $\lambda \in \mathbb{R}$ for $j = 1, 2, ..., J$.

Denoting the realisation of X_j in the empirical data by x_j, then, in order to reject CSR for a given dataset, it is necessary to compare the values $\{x_j\}_{j=1,...,J}$ with realisations of X_j that would be expected under a null hypothesis of CSR. A model of CSR is therefore the first model of the empirical data proposed. This model is employed in order to detect spatial heterogeneity, which can then be explored with more complex approaches. As well as determining whether the empirical data differs from CSR, the level of autocorrelation in the data is quantified through the use of spatial statistics, which are first introduced.

3.3.1 A measure of dispersion

The comparison between the model and the empirical data is typically made through the use of a test statistic. A test statistic $\mathcal{S} \in \mathbb{R}$ is designed to be a single-valued summary of the dataset that can detect differences between different data samples (e.g. from the empirical data or the model). A test statistic that is often used when considering CSR is the index of dispersion. This is defined as

$$\mathcal{S}_d = \frac{\mathrm{Var}[X_j]}{\mathbb{E}[X_j]}, \tag{3.4}$$

where the variance and expectation of the counts are calculated over the different spatial regions $\mathcal{D}_j$, which are assumed to have equal area.

For idealised distributions, such as that of CSR, the index of dispersion can be computed analytically. For a Poisson process in which the random variable X_j has the distribution given by equation 3.3, the expected count is:

$$\mathbb{E}[X_j] = \sum_{x=1}^{\infty} x Pr(X_j = x) = \sum_{x=1}^{\infty} x \frac{1}{x!} \lambda^x e^{-\lambda} \tag{3.5}$$

from which, by removing a common factor from the sum, and using the identity $\sum_{k=1}^{\infty} y^{k-1}/(k-1)! = e^y$, it can be shown that

$$\mathbb{E}[X_j] = \lambda. \tag{3.6}$$

The variance of the same process is given by

$$\mathrm{Var}[X_j] = \mathbb{E}[X_j^2] - (\mathbb{E}[X_j])^2 = \sum_{x=1}^{\infty} x^2 \frac{1}{x!} \lambda^x e^{-\lambda} - \lambda^2, \tag{3.7}$$

from which, by removing a common factor from the sum, separating the sum into two components, one with denominator $(x-1)!$ and one with denominator $(x-2)!$, relabelling indices and using the exponential identity used in the expectation calculation, it can be shown that

$$\mathrm{Var}[X_j] = \lambda. \tag{3.8}$$

The index of dispersion for a Poisson process is therefore

$$\mathcal{S}_d = \frac{\mathrm{Var}[X_j]}{\mathbb{E}[X_j]} = 1. \tag{3.9}$$

The index of dispersion measures the extent to which event counts are distributed over different spatial units. $\mathcal{S}_d$ is equal to zero when the counts are equal over areas and are therefore completely uniformly distributed. This might occur if events form a regular point lattice. As shown in equation 3.9, $\mathcal{S}_d$ is equal to one under CSR. A value $\mathcal{S}_d \in (0, 1)$ indicates under-dispersion. In this case, the distribution of events is somewhere between complete uniformity and CSR, and events are distributed more evenly than would be expected under CSR. Values of $\mathcal{S}_d > 1$ indicate over-dispersion: there is more clustering of values than would be expected under CSR, and events are distributed unevenly across relatively few spatial units.

3.3.2 A measure of autocorrelation

Whilst the index of dispersion considers how events are distributed within areas, another test statistic is employed to consider how counts of nearby areas relate to one another. Moran's I (Moran, 1950) is an index of spatial autocorrelation that measures the extent to which areas with similar counts are proximate to each other, or, conversely, in the case of a negative value, the extent to which lower counts tend to be nearby areas with high counts. It can be used to investigate whether clustering is due to localised effects within areas—for example due to the presence of a particular target—or whether clustering is a result of more widespread regional effects that includes the surrounding spatial units. If high event counts occur near to areas with low event counts, then there is negative spatial autocorrelation. If areas with high counts are close to other areas

with high counts, and areas with low counts are near to other areas with low counts, then there is positive spatial autocorrelation. Moran's I is defined as:

$$\mathcal{S}_I = \frac{J}{\sum_{j=1}^{J}\sum_{l=1}^{J} w_{jl}} \frac{\sum_{j=1}^{J}\sum_{l=1}^{J} w_{jl}\left(X_j - \bar{X}\right)\left(X_l - \bar{X}\right)}{\sum_j \left(X_j - \bar{X}\right)^2}, \tag{3.10}$$

where J is the number of spatial units, X_j is the variable of interest, $\bar{X}$ is the mean of X_j across the different spatial units, and w_{jl} is a matrix of spatial weights that specifies the proximity of spatial units $\mathcal{D}_j$ and $\mathcal{D}_l$.

$\mathcal{S}_I$ is bounded between -1 and 1. A value equal to 1 corresponds to perfect positive autocorrelation, whilst a value equal to -1 corresponds to perfect negative autocorrelation. This statistic has been widely employed to characterise the level of spatial autocorrelation in levels of war and democracy (Gleditsch and Ward, 2000), criminal activity (Anselin et al., 2000), gang rivalry (Tita and Radil, 2011) and maritime piracy (Marchione and Johnson, 2013), amongst others.

For an idealised Poisson process, similarly to the index of dispersion, Moran's I can be calculated analytically. In particular, for spatial units of equal area, the expected value of $\mathcal{S}_I$ is $-1/(J-1)$, where J is the number of spatial units.

3.3.3 Simulating a random process

Under CSR, the test statistics $\mathcal{S}_d$ and $\mathcal{S}_I$ are both analytically tractable. In this chapter, however, more general models than CSR will be considered. For such models, the calculation of test statistics is not as simple. Realisations of more complex models can be generated through the use of simulation. These realisations can then be directly compared with empirical data. Comparison between test statistics obtained from empirical data and a simulated realisation of data generated from a null model can then either support or reject the hypothesis that the data are completely spatially random. In this section, it is shown how simulation can be used to generate an approximate realisation of a Poisson process over the same spatial partition as the available data, leading to area counts $\left\{x_j^{(1)}\right\}_{j=1,\ldots,J}$. The superscript is introduced to distinguish between realisations of the random variable X_j that are obtained from simulation and realisations that are obtained from empirical data (for which there is no superscript).

An approximate simulated Poisson process can be constructed as follows: for each of the N events, assuming that the spatial units $\mathcal{D}_j$ have equal area, one spatial unit $\mathcal{D}_j$

is chosen at random with uniform probability from the set of spatial units (i.e. with probability $1/J$) with replacement, since it is possible that more than one event can occur within a given spatial unit. Therefore, for each j, X_j is the number of times the spatial unit $\mathcal{D}_j$ was chosen in N selections. The probability that $X_j = x$ for $x = 1, 2, 3, ...$ is then given by the Binomial distribution. This is because for $X_j = x$ to hold after N selections have been made, it is necessary that j must be chosen x times whilst not chosen $(N - x)$ times, leading to:

$$Pr(X_j = x) = \frac{N!}{x!(N-x)!}\left(\frac{1}{J}\right)^x\left(1-\frac{1}{J}\right)^{N-x}. \tag{3.11}$$

It can be shown, however, that for large N, the binomial distribution approximates a Poisson process. Indeed, setting $\lambda = N/J$, leads to

$$Pr(X_j = x) = \frac{N!}{x!(N-x)!}\left(\frac{\lambda}{N}\right)^x\left(1-\frac{\lambda}{N}\right)^{N-x}. \tag{3.12}$$

Next, considering the limit as $N \to \infty$,

$$\begin{aligned}
&\lim_{N\to\infty}\frac{N!}{N^x(N-x)!}\\
&=\lim_{N\to\infty}\frac{N(N-1)(N-2)...(N-k)(N-k-1)...(2)(1)}{N^x(N-x)(N-x-1)...(2)(1)}\\
&=\lim_{N\to\infty}\frac{N}{N}\frac{(N-1)}{N}\frac{(N-2)}{N}...\frac{N-x+1}{N}\\
&=1,
\end{aligned}$$

and

$$\begin{aligned}
&\lim_{N\to\infty}\left(1-\frac{\lambda}{N}\right)^N\left(1-\frac{\lambda}{N}\right)^{-x}\\
&=\lim_{N\to\infty}\left(1+\frac{1}{-\frac{N}{\lambda}}\right)^{-\frac{N}{\lambda}(-\lambda)}1^{-x}\\
&=e^{-\lambda},
\end{aligned}$$

where the identity $\lim_{y\to\infty}\left(1+\frac{1}{y}\right)^y = e$ is used. Thus, for $N \to \infty$, equation 3.3 is obtained and it has been shown that simulating a random process in this way for a large number of events N is approximately equivalent to simulating a Poisson process. Moreover, this simulation enables the preservation of the number of events, given by N, in the simulated distribution, leading to more meaningful comparisons between the empirical data and the random process.

The next step is to compare this simulated realisation of random variables $\left\{x_j^{(1)}\right\}_{j=1,...,J}$ against the empirical counts $\{x_j\}_{j=1,...,J}$ through the use of a test statistic $\mathcal{S}$. Doing this for just one realisation of the simulated distribution is not particularly instructive: one realisation does not indicate how much the empirical distribution differs from the theoretical one. However a full permutation of all possible realisations of the dataset under a binomial distribution is computationally very intensive for large values of N and J. Therefore, a sample of G realisations from the set of all possible realisations is taken, leading to simulated realisations $\left\{x_j^{(g)}\right\}_{j=1,...,J}$ for $g = 1, 2, ..., G$, and the empirical distribution $\{x_j\}_{j=1,...,J}$ is compared against all of the distributions in this sample. If the test statistic for the empirical distribution, $\mathcal{S} \in \mathbb{R}$, sufficiently differs from the statistics generated from the simulated distributions, $\mathcal{S}^{(g)} \in \mathbb{R}$, for iterations $g = 1, 2, ..., G$, then we conclude that there is evidence to distinguish the empirical data from what would be expected under CSR.

The significance of the empirical test statistic can be calculated by considering the rank r of the empirical test statistic with respect to the simulated data, so that, for a one-tailed test,

$$r = \sum_{g=1}^{G} \mathbf{1}(\mathcal{S}^{(g)} \geq \mathcal{S}), \tag{3.13}$$

where the indicator function $\mathbf{1}(.)$ is equal to one if the condition in the bracket holds, and equal to zero otherwise. Then, following North et al. (2002), if S is a random variable defined by the test statistic, so that $\mathcal{S}^{(g)}$ are realisations of S, then the so-called p-value is defined as

$$Pr(S \geq \mathcal{S}) = \frac{r+1}{G+1}. \tag{3.14}$$

A small p-value indicates that it would have been unlikely for the data summarised by the test statistic $\mathcal{S}$ to have been observed if the data was indeed generated by a process of CSR.

3.3.4 Testing for CSR in the 2011 London riots

Data obtained from London's Metropolitan Police Service on the 2011 London riots consists of details of $3,914$ offences that occurred during the five days of unrest from the 6th-10th August. Of these, $2,868$ contained details of where the offence occurred, aggregated to the geographic level of UK census output areas. Within Greater London, within which all offences occurred, there are $24,140$ census output areas defined by the

2001 UK census. These areas have varying size, and are designed to contain approximately 300 residents. In Figure 3.1, the spatial distribution of the events is shown by plotting the centroid of the output area in which an offence occurred. The shading of each point corresponds to the number of events that occurred within that output area throughout the duration of rioting. In Figure 3.2, the cumulative frequency of the number of offences occurring within each output area is shown. There are many areas in which no offences occur, but, as Figure 3.2 demonstrates, there are a few areas in which many events occur. This would suggest that the data is likely to be clustered, however, in order to formally determine this, it is necessary to undergo the simulation procedure described below.

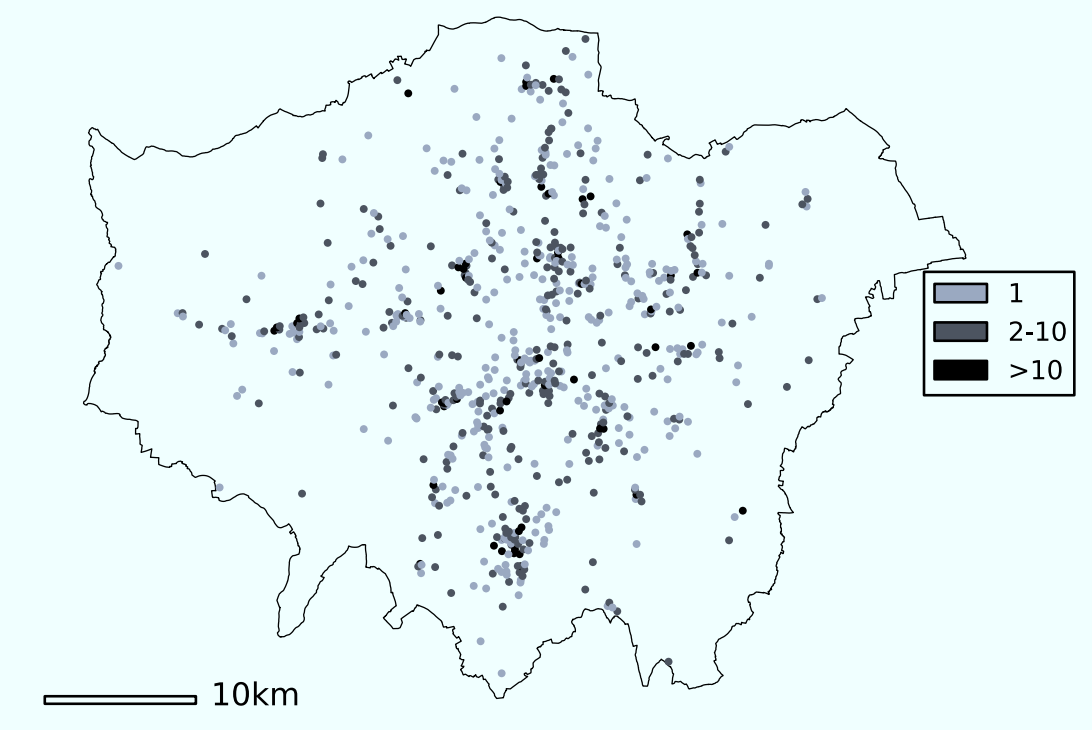

Figure 3.1: **A map of the 2011 London riots.** The centroids of the output areas in which events occurred are plotted, with the counts referring to the number of offences within each output area over the duration of the disorder.

A spatial grid with spatial resolution δs is overlaid on the geographic area of interest—the census output area geography of Greater London—the resolution of which can be varied in order to address the modifiable areal unit problem. Riot events are then mapped to the corresponding grid unit that overlays the output area in which

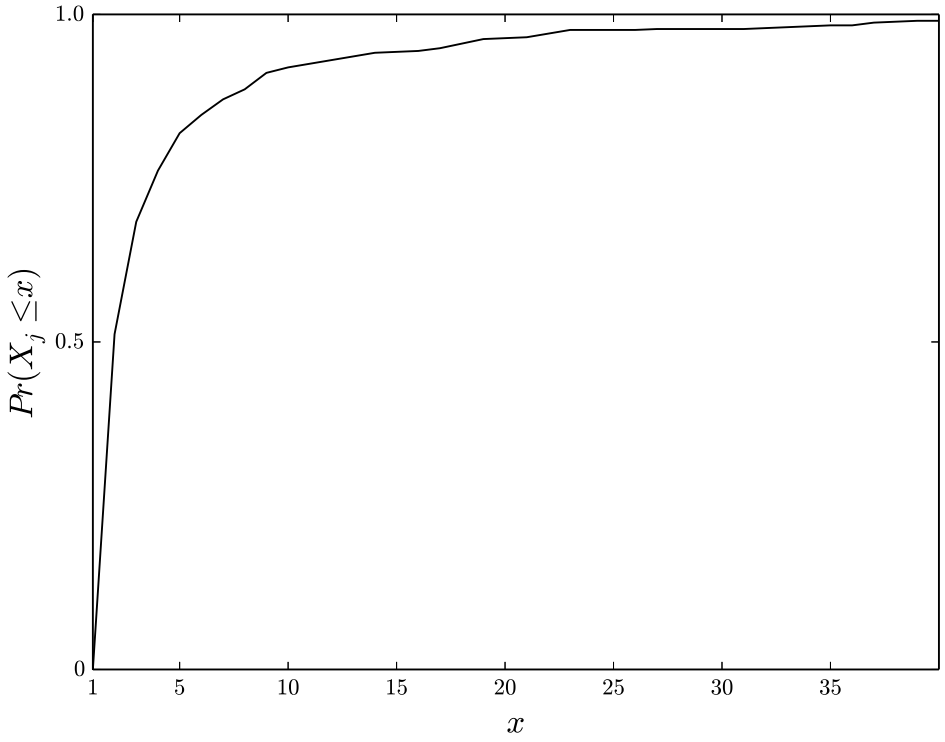

Figure 3.2: **The empirical cumulative distribution of counts of offences across output areas that contained at least one offence.** The graph shows the probability that a randomly selected output area containing at least one offence had an offence count at least as large as the value on the x-axis. The largest number of offences within a single output area is 131, however this value is omitted from the graph for clarity.

the event is recorded. In Figure 3.3, a comparison between the output area geography and a regular spatial grid of two different resolutions ($400m$ and $650m$) is shown. The mean area of an output area in which riot offences occurred is $0.15\mathrm{km}^2$. Accordingly, values of δs are chosen so as to not exceed the precision of the data. The smallest spatial resolution of the overlaid grid considered is $\delta s = 400\mathrm{m}$, so that the area of each spatial unit in the grid, $0.16\mathrm{km}^2$, exceeds the average area of the output areas within which offences occurred. On average, each event is consequently mapped to the corresponding spatial unit of the overlaid grid within which the event occurred.

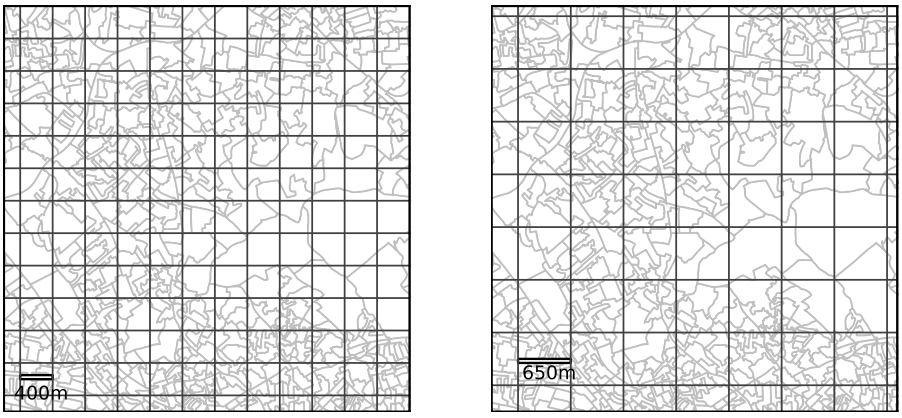

Figure 3.3: **Two regular spatial grids over the same portion of London's Output Area geography.** The resolution of the grids are $400m$ on the left and $650m$ on the right.

Following the description of testing for CSR in the previous section, $G = 499$ simulated realisations of the data under the null hypothesis of CSR are generated by randomly allocating each of the $2,868$ offences to one of the spatial grid units. Since each unit of the spatial grid has equal area, each unit is chosen with equal probability. The number 499 is chosen in accordance with previous literature employing Monte Carlo simulations. By considering equation 3.14, it can be seen that for each simulated statistic $\mathcal{S}^{(g)}$ that is greater than the empirical value of $\mathcal{S}$, the p-value increases by a value of 0.002, suggesting a potential high level of confidence in the results.

The index of dispersion and Moran's I are used as test statistics to distinguish the empirical data from the modelled data for a range of grid sizes. When calculating the Moran's I statistic, the matrix of spatial weights, with entries w_{jl}, is defined with queen

contiguity, named after the range of moves available to the queen piece in chess. That is, $w_{jl} = 1$ if spatial units j and l in the spatial grid share either an edge or a vertex, otherwise $w_{jl} = 0$. Thus, the neighbourhood of spatial unit j consists of those units that surround the focal unit j, as shown in Figure 3.4. For each spatial unit j, units outside of this neighbourhood are not considered in determining whether counts are correlated.

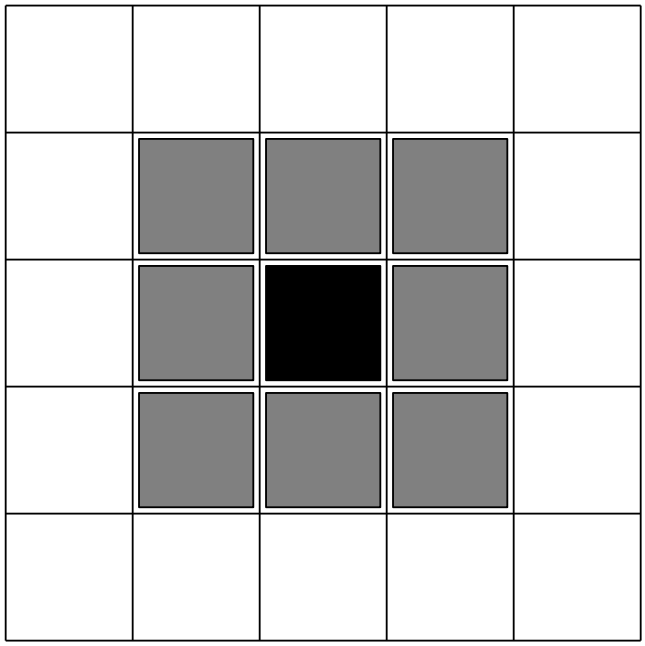

Figure 3.4: **The neighbourhood of a focal spatial unit under queen contiguity.** The grey squares are considered to be the neighbours of the black square.

Figure 3.5 shows the values of the index of dispersion, $\mathcal{S}_d$, and the value of Moran's I, $\mathcal{S}_I$, for a range of spatial grid resolutions δs. The figure also shows the values of the same statistics under the assumption of CSR. For all cases considered, the statistics of the model are less than the statistics obtained from the empirical data, leading to a p-value of 0.002 for both the index of dispersion and Moran's I. Therefore, the chance of observing the data given that the null model of CSR is true is less than 0.002, and it can be concluded that there is highly likely to be significant spatial clustering in the empirical data. This implies that the spatial distribution of the rioting warrants investigation through the use of more complex models.

The values of $\mathcal{S}_d$ are much greater than 1, indicating substantial over-dispersion. This implies that within grid units there is strong clustering of events and arises since

the majority of the events occur within a relatively small number of grid units. The values of $\mathcal{S}_I$ are also positive, indicating the presence of positive spatial autocorrelation. That is, the counts of events occurring in each unit are positively associated with the counts occurring in neighbouring units. Although being positive, the values of $\mathcal{S}_I$ are close to zero. Taking these values on their own, it might be difficult to conclude that there is positive autocorrelation since the values of $\mathcal{S}_I$ are much closer to zero than to one – the value indicating perfect spatial autocorrelation. This example demonstrates the necessity of comparing the statistic against a null hypothesis: the values of $\mathcal{S}_I$ from the empirical data are, in fact, much greater than would be expected when compared to the same number of events under CSR. Therefore, despite being a small absolute value, there is certainly evidence for positive autocorrelation, with the small absolute value of the statistic being a consequence of the sparseness of the data over the entire spatial region of interest.

3.4 Spatio-temporal interaction

When event occurrence varies in both space and time, it can be of great importance to determine whether there is also spatio-temporal dependency. Tests for spatio-temporal interaction are distinct from tests that identify the presence of purely spatial or temporal dependency (or, indeed, both): they focus on the likelihood of a further event occurring in a particular location, given the time and location at which a prior event has occurred. This information can be useful in policy-making. During outbreaks of rioting in a city, for instance, police leaders face decisions concerning the allocation of limited resources of police officers in real time. Insights into the spatio-temporal behaviour of rioting can help to answer questions such as whether police resources should remain at sites recently rioted or whether these resources would be better deployed elsewhere in the city, for example at perceived attractive targets that have not yet experienced rioting.

In this section, in order to investigate such questions, the level of spatio-temporal dependency in the 2011 London riots is determined through the use of a grid-based Knox statistic. Similarly to the test for spatial autocorrelation in Section 3.3, a model of the riots is constructed under the assumption that there is no spatio-temporal dependency. This enables the comparison between the empirical data and the data generated using a null model. Differences between the two can then be evaluated in order to de-

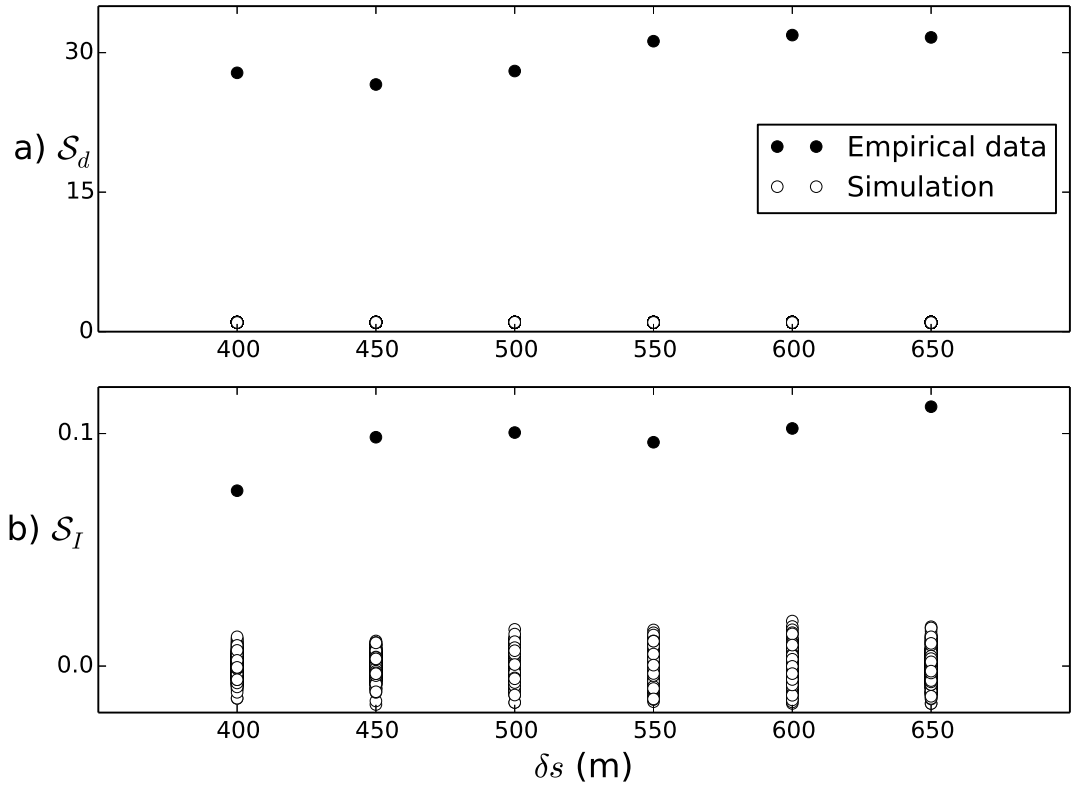

Figure 3.5: **Results of the test for CSR.** a) The values of $\mathcal{S}_d$ (in black) and $\mathcal{S}_d^{(g)}$ (in white) are shown for each iteration $g = 1, 2, ..., 499$ for different grid sizes. In this case, the points in white are so close together that the different iterations are indistinguishable. This demonstrates further how strong the spatial clustering is in the empirical data. b) The values of $\mathcal{S}_I$ (in black) and $\mathcal{S}_I^{(g)}$ (in white) are shown for each iteration $g = 1, 2, ..., 499$ for different grid sizes. In this case, the different iterations of the model are more distinguishable.

termine whether the null model provides a reasonable account of the data generating process, or whether further analyses might be required.

It was demonstrated in Section 3.3 that the distribution of the locations of offences is highly likely to be spatially clustered. As discussed at the beginning of that section, there are two prominent explanations for the spatial clustering of event data that have been investigated in the literature for different types of crime: the flag hypothesis and the boost hypothesis. These two explanations can be distinguished between by determining the level of spatio-temporal interaction between events. To explain, the flag hypothesis supposes that variations in the risk levels of different areas are due to static time-stable influences that can encourage crime. For example, in the case of residential burglary, it may be that houses with fewer visible security features are more likely to be targeted (since the burglar will perceive they are more likely to succeed) and therefore experience a higher risk of burglary. This risk will be relatively constant over time (provided that the homeowners do not improve the level of security during this time), and so, such properties will likely experience a larger number of burglaries in any given time period, when compared to another house that has many visible security features. On the other hand, the boost hypothesis supposes that properties are more at risk as a direct result of it being targeted for a relatively short period of time after an offence has occurred. If the boost hypothesis was at play, a larger number of events would be expected in the locality of a prior event, above and beyond the spatial and temporal distribution of events within the wider region of study. The boost hypothesis implies spatio-temporal interaction; whereas the flag hypothesis attributes apparent space-time clusters to a heterogeneous distribution of risk in space combined with natural variation in crime trends. Understanding the extent to which both of these mechanisms play a role can lead to policy recommendations. For instance, if the boost hypothesis is significant in influencing future levels of risk, then, after a burglary, efforts could be made to reduce the underlying risk levels, ensuring that the risk of burglary does not get too large.

In the case of rioting, the analogue of the flag hypothesis suggests that time-stable features of different areas might also influence the risk of rioting at a given location. For example, if offenders participate in rioting due to the opportunity for them to loot high-value goods, then targets containing high-value goods are likely to be more at risk of

experiencing a riot than other targets, as potential rioters perceive the greater benefit of selecting that target over others. This rational choice perspective on the part of rioters—that they select targets based on the ability for those targets to fulfil their objectives—has been explored elsewhere (e.g. Martin et al. (2009)) and there have been several efforts to understand the features of targets that make them particularly attractive to rioters (Berk and Aldrich, 1972; Rosenfeld, 1997). In Chapter 4, the environmental features of different targets, and their role in attracting rioters will be explored further. It is noted for now that environmental features of regions can certainly play a role in the spatial clustering of riots; however, if the environmental features of these regions are static and time-stable, then the times at which events occur at these locations can be taken to be independent random events with times drawn from the temporal distribution of offences over the entire geographic region of interest. The null model for tests of spatio-temporal interaction supposes that this is indeed the case and, therefore, that events occurring at a given location do not influence the likelihood of future events proximate to that location, beyond the spatial and temporal distributions of the observed data.

The riots are modelled under the null hypothesis of spatio-temporal independence by randomly permuting the event times. Considering events $(\mathbf{s}_i, t_i)$ for $i = 1, ..., N$, the set of times at which events occur, given by $\{t_1, t_2, ..., t_N\}$, is permuted as follows: choose a uniform psuedo-random integer, $k_1^{(1)}$, between 1 and N. Then swap the position of t_1 with $t_{k_1^{(1)}}$. Next, choose a uniform psuedo-random integer, $k_2^{(1)}$, between 2 and N. Then swap the position of t_2 with $t_{k_2^{(1)}}$. Continue for each $i = 3, .., N-1$ by choosing a psuedo-random integer, $k_i^{(1)}$, between i and N and then swapping the position of t_i with $t_{k_i^{(1)}}$. This results in the random permutation of event times $\left\{t_{k_1^{(1)}}, t_{k_2^{(1)}}, ..., t_{k_N^{(1)}}\right\}$. The modelled riot data under the null hypothesis of spatio-temporal independence is then given by $(\mathbf{s}_i, t_{k_i^{(1)}})$ for $i = 1, ..., N$. The modelled riot data has the same spatial distribution, given by the locations $\mathbf{s}_1, \mathbf{s}_2, ..., \mathbf{s}_N$, and the same temporal distribution, given by the times $t_1, t_2, ..., t_N$, as the original data; however, the association between them is randomised and any interdependency beyond purely spatial and temporal factors is removed.

As was the case with the CSR model in Section 3.3, comparing this single realisation of the dataset under a null hypothesis with the empirical dataset is not particularly

instructive: the significance of any differences between the two datasets is impossible to determine. However, on the other hand, taking a full permutation of the event data is computationally intensive for large values of N (there are $N!$ different possible permutations). Therefore, a sample of $G = 499$ from the possible $N!$ random permutations is taken, leading to temporal permutations $\left\{t_{k_1^{(g)}}, t_{k_2^{(g)}}, ..., t_{k_N^{(g)}}\right\}$ for $g = 1, ..., 499$, which are then compared against the empirical data.

In order to compare the empirical data with the modelled data, a test statistic is required. A common statistic for identifying spatio-temporal interaction is the Knox statistic, $\mathcal{S}_K$ (discussed from a methodological perspective in Knox (1964a) and first employed as a test of spatio-temporal interaction in Knox (1964b)). $\mathcal{S}_K$ is defined as the number of pairs of events that occur within a given space-time window of each other. If the space-time window selected for the calculation of the Knox statistic is large enough, then the Knox statistic will be given by its maximum value, $N(N-1)/2$, since all possible pairs will be included. Employing the same spatio-temporal grid as in Section 3.3, a grid-based Knox statistic is defined by taking the spatial window for significant pairs as all events occurring within first-order queen contiguity distance of the original event, as in Figure 3.4. The temporal window for significant pairs is taken to be one hour. This value is chosen so as not to exceed the resolution of the reported data, in which many of the offences are recorded as occurring to the nearest hour. Temporal resolutions of 2, 3, 4, 5 and 6 hours were also tested in order to alleviate the implications of the modifiable unit problem from a temporal perspective. These results were consistent with those for 1 hour and for reasons of clarity are not presented here.

Of the $3,914$ offences associated with the London riots that were obtained from the Metropolitan Police Service, $2,592$ contained details of both the location at which the offence took place as well as the time at which the event occurred. These were the events used in the analysis. Figure 3.6 shows the Knox statistics for the empirical data and for the simulated data for different spatial grid resolutions. The values of the Knox statistic associated with the empirical data are much larger than the values associated with the simulated data for all spatial grid sizes tested. In fact, the effect is extremely strong, with the values of the empirical Knox statistics being around four times the value when there is no spatio-temporal dependency. Since no simulated Knox statistic is larger than the empirical Knox in 499 simulations, the p-value is calculated to be

0.002, however, given the distance of the empirical result to the simulated result, it is likely that a much smaller p-value could be found through the use of further iterations.

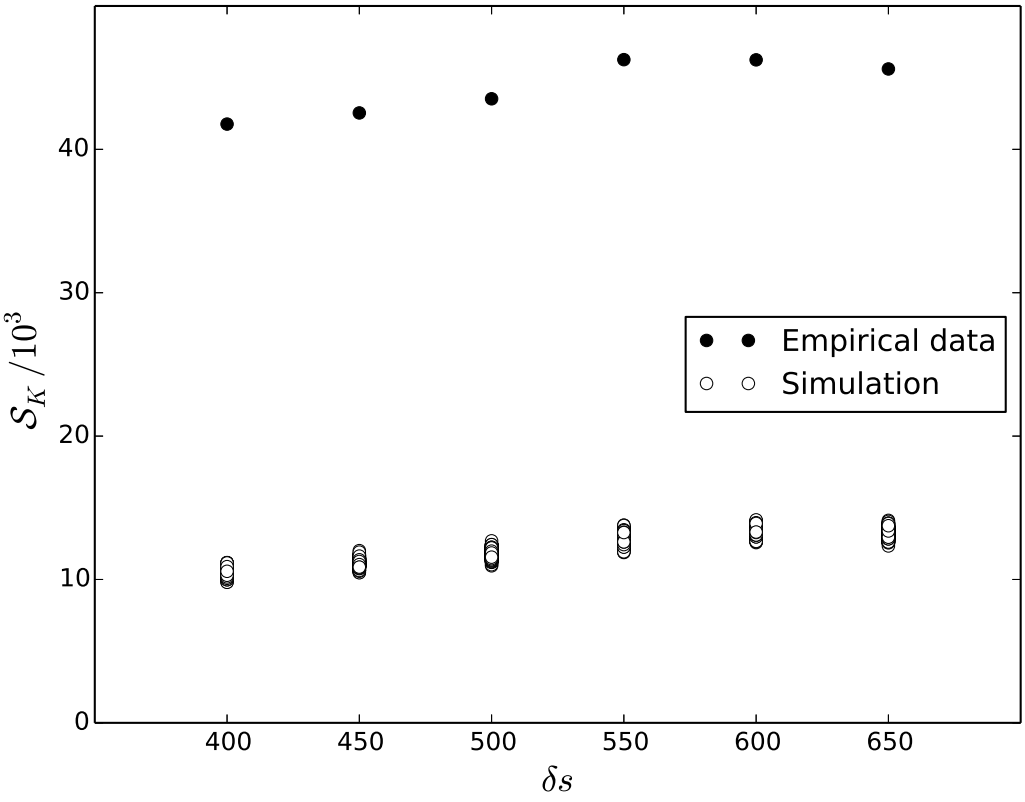

Figure 3.6: **Results of the Knox test.** The empirical Knox statistic plotted against 499 realisations of the simulated Knox statistic for a range of spatial grids.

It can be concluded that during the riots in London, there was significant spatio-temporal dependency in the event data. This finding implies that it was not just the suitability of certain locations in space, combined with the suitability of a particular time that led to riots, but that there was also strong evidence for event dependency: the occurrence of an event at a particular point in space and time increased the likelihood of observing a further event in proximity to the original event. In the remainder of this chapter, the precise nature of the interaction between proximate events is explored by considering the geographic patterns made by the riots.

3.5 Analysing local patterns of geographic diffusion

Two models have been presented so far in this chapter. The first of these assumed that riot data was generated with complete spatial randomness, and was shown to be a poor

fit to the empirical data. The second model assumed that riot offences were spatio-temporally independent, and again was rejected as a plausible model for the London riots. This is not to say, however, that proposing these models for the London riots did not produce any insights. In both of these examples, the specification of the model enabled the testing of a hypothesis regarding the nature of the spatio-temporal distribution of the riots. Moreover, it has been shown that subsequent models of rioting must account for the spatial dependency and for the spatio-temporal dependency present in the data.

In this section, more sophisticated insights into the London riots are sought by pursuing an exploratory data-driven approach. Localised patterns of offences in space and time during the riots are investigated using a novel Monte-Carlo simulation, which builds upon those presented in the previous two sections. It is argued that the investigation into the prevalence of specific patterns can aid understanding into the way in which the riots spread. The analysis presented here enables the consideration of more intricate mechanisms as explanations for the observed patterns and these are discussed.

A binary approach to the analysis of event data in a spatio-temporal grid is used. The dependent variable of interest is given by a binary tuple $(X, Y)_{(j,k)}$ for each space-time unit, indexed by the tuple (j, k). The index j denotes the spatial grid unit of interest, whilst the index k denotes the temporal window under consideration. For each (j, k), $X \in \{0, 1\}$ indicates whether at least one offence occurred in the focal space-time window of interest, and $Y \in \{0, 1\}$ indicates whether at least one offence occurred within any of the focal area's neighbouring units, which are defined with queen contiguity, as shown in Figure 3.4. Since the variables of interest are binary, they do not distinguish between the number of events occurring in each space-time window: the occurrence of a single event is recorded as being equivalent to the occurrence of many events. This restriction brings with it some limitations to the analysis, which will be discussed below; however, it also allows the primary subject of analysis to be the geographic scope of each outburst of rioting, rather than the relative intensity of each riot. The geographic scope of a riot is of significant interest to decision-makers since one objective for law enforcement officers during periods of civil disorder is to minimise the extent of the area at risk.

The same variables are used in Schutte and Weidmann (2011), who use a grid-

based analysis to model conflict events across four different civil wars, and in Rey et al. (2011), who also used a binary approach but do so over irregularly shaped spatial areas. The method proposed here advances these two studies by proposing a novel Monte Carlo simulation as a null model. The proposed model is particularly suited to scenarios involving high levels of spatio-temporal clustering, such as the present case of rioting.

The prevalence of four local patterns of riot events in space and time are investigated. These are first introduced before proposed mechanisms corresponding to each of these patterns are explored. The first type of pattern is termed *containment*. This occurs when areas already affected by disorder in one time period are also affected in the next, but when the disorder does not spread to neighbouring areas. Second, *relocation* is when the disorder moves from one locality to another, without persisting in the original location. Third, processes of *escalation* occur when rioting continues for a prolonged period in a certain area, and also spreads to contiguous areas. Finally, *flashpoints* are outbursts of co-occurring offences located in areas that are geographically distinct from areas that had recently experienced offences. In other words, they occur when areas and their neighbouring areas suddenly experience widespread disorder.

These diffusion patterns are defined by considering the change of the variable $(X, Y)_{(j,k)}$ for each space-time unit (j, k), over sequential time intervals. An instance of containment at spatial unit j and time k occurs when this variable transitions as follows:

$$(1, 0)_{(j,k)} \rightarrow (1, 0)_{(j,k+1)}. \tag{3.15}$$

Thus, containment occurs when offences take place in a focal cell repeatedly without occurring in any neighbouring cells. Similarly, an instance of relocation at (j, k) is defined as

$$(1, 0)_{(j,k)} \rightarrow (0, 1)_{(j,k+1)}, \tag{3.16}$$

so the rioting moves from one cell to at least one neighbouring cell, without persisting in the original cell. Escalation occurs when offences persist in the original cell but also spread to at least one neighbouring cells that were previously unaffected, given by

$$(1, 0)_{(j,k)} \rightarrow (1, 1)_{(j,k+1)}. \tag{3.17}$$

Flashpoints are identified if offences occur within a wider area that had not experienced

any events in the previous time step, and is therefore given by

$$(0,0)_{(j,k)} \rightarrow (1,1)_{(j,k+1)}. \tag{3.18}$$

The simplest examples of these diffusion patterns are illustrated in Figure 3.7.

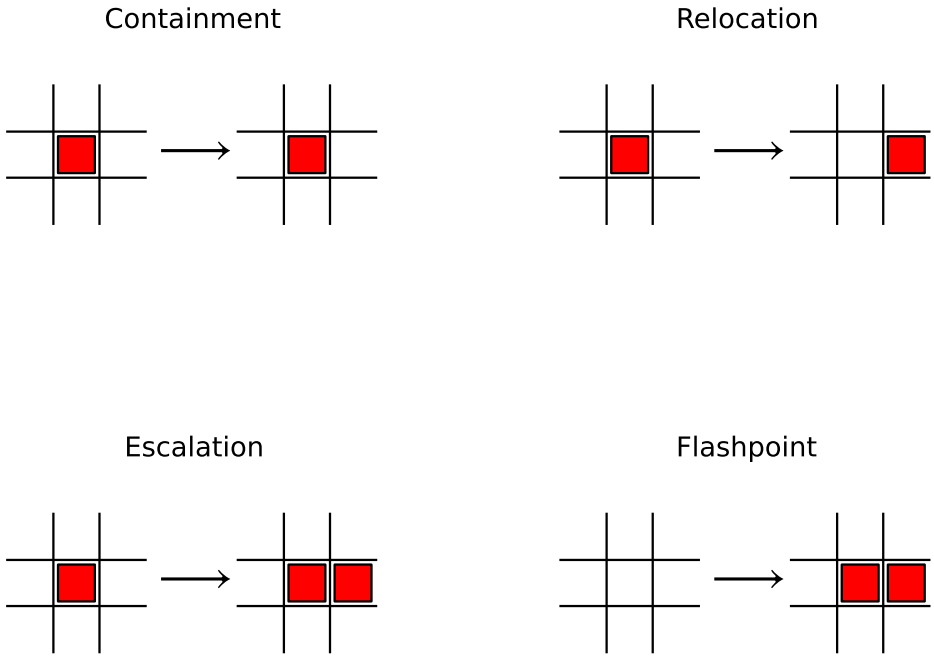

Figure 3.7: **Geographic patterns of diffusion.** An illustration of the simplest examples of each of the diffusion patterns of interest occurring in a spatio-temporal grid.

3.5.1 Proposed mechanisms for riot diffusion patterns

In order to generate more complex models of rioting and civil disorder, assumptions are required that specify how the models behave. Inspired by a data-driven approach, the models presented in this chapter are specified with relatively simple assumptions, such as spatial randomness or spatio-temporal independence. In this section, it is demonstrated how a data-driven approach can be used to suggest mechanisms for the behaviour of the system, which may then be employed to construct more intricate assumptions for future models. Mechanisms for the evolution of the 2011 London riots are discussed, before the prevalence of each of the local offence patterns in space and time are used to evaluate these mechanisms as possible causes in the observed data.

Riots involve groups of people at a given location engaging in or threatening acts of violence often for a common purpose. As was the case for the 2011 UK riots—during which, offences in London comprised just a part of the total number of offences across the UK—an outbreak of rioting may be followed by other riots, possibly in distinct geographical areas, and they can persist over a long period of time. Riots can cluster in space and time as a result of a number of processes. A key distinguishing feature of rioting from other types of urban crime is that the mutual activity of previously unacquainted offenders can potentially affect the actions of others. These influences can occur and change over very short time scales, particularly when compared to other types of urban crime, for which influences on the decision to engage in an offence might be more static and depend more on the environment in which an individual finds themselves.

Although not entirely separable, it is useful to introduce two different perspectives for considering riot processes. The first considers the interdependency between events, and supposes that the presence of rioting at a particular location directly influences the likelihood of more rioting for a certain time period afterwards. The second treats the spatio-temporal clustering of event data as a result of the confluence in space and time of conditions suitable for rioting. This distinction, although similar, is different to the distinction made between the flag and boost hypotheses discussed in Section 3.4. This is because, in this case, the environmental conditions that make an area suitable for rioting at a particular point in space can vary quite quickly in time, for example, due to the presence and actions of law enforcement officers. This is in contrast to the flag hypothesis, which relied on static environmental conditions to generate clustering of events.

In the case of the first perspective, an outbreak of rioting might be explained by a single person committing an offence, for example by committing burglary, followed by others taking the opportunity to begin looting at the same location, as they perceive the risk of being caught to be lower than it otherwise would be. Explanations using the second perspective might state that rioting was more likely at that location and at that time due to the presence of high-value goods that may have been looted, together with the lack of law enforcement officers present, and might even include factors such as the weather (in interviews conducted after the riots it was claimed that the rain helped to

put a stop to the rioting (Morrell et al., 2011)).

These two related explanations have been explored through the use of statistical models for a variety of crime and security data in Mohler (2013). In his paper, two models are compared for the clustering of event data in space and time. The first, a Hawkes process, directly models the increased likelihood of further events based on the occurrence of existing events. The second, a log Gaussian Cox process, models the clustering as a result of a random process, in which the occurrence of events do not necessarily increase the likelihood of further events.

These two perspectives are subtly different and can be difficult to distinguish between in many studies of event data (although the algorithm proposed by Mohler (2013) is a promising attempt to do so). They do, however, provide the opportunity to separate possible mechanisms that may be at play during rioting, and to consider how each perspective might be reflected in the space-time patterns introduced above. In what follows, the idea of contagion of rioting, and the argument that offences directly influence further offences is first discussed. Next, other factors that might influence the geographic diffusion of rioting, including the presence of police officers and the environment in which the riots occur are considered.

Mechanisms for Event Interdependency: Social and Geographic Contagion

Large-scale outbreaks of disorder can be consequences of underlying tensions and grievances within a widely distributed population. If news of an initial riot at a given location spreads, then others who share similar grievances, regardless of where they are, may be inspired to behave similarly in an effort to address their grievances. Considering the London riots of 2011, some have suggested that a process of contagion resulting from such grievances was at least partly responsible for the severe escalation and perseverance of observed patterns (Gross, 2011). A process of social contagion, possibly facilitated by social networks or conventional media reports, could lead to the mobilisation of more motivated offenders, and the subsequent wider engagement in disorder at particular locations and at particular times. Mobilised and motivated offenders may be attracted to particular areas, regardless of how far they would need to travel to reach them.

Social contagion refers to the mobilisation of motivated offenders, regardless of their location. Contagion may also increase the number of rioters via a more local process. Geographic contagion refers to the way an offender's decision to engage in disorder is influenced by situational precipitators, almost regardless of the decision-maker's underlying grievances. Wortley (2008) argues that situational precipitators, such as environmental cues, events or influences can prompt, pressure, permit or provoke criminal behaviour. It is possible that visible signs of rioting act as precipitators that encourage potential offenders to engage in the disorder. If those who live near to or happen to pass by ongoing riots are more likely to engage in the disorder more so than they otherwise would, then a process of geographic contagion is present. This mechanism assumes that witnessing disorder serves to prompt, pressure, permit or provoke engagement with the disorder at a particular location. Bystanders perceive that engaging in the disorder at that location is acceptable, given the circumstances. If it is perceived that the risks of apprehension are lower than they otherwise would be, bystanders may be encouraged to engage in the disorder themselves, leading to further offences nearby. The mechanism by which potential rioters are more likely to engage in rioting if offences are currently taking place in close proximity is perhaps due to the perception of safety in numbers: the perceived risk of arrest is likely to be lower in those areas where rioters substantially outnumber law enforcement agents. This mechanism has been explored in a range of other studies, two of the most widely cited of which are Epstein (2002) and Granovetter (1978).

While processes of contagion of both a geographic and non-geographic nature have been discussed in the literature, only a limited number of empirical studies have examined space-time patterns of offending during outbreaks of rioting. In a study of the US race riots in the 1960s, Spilerman (1970) tested for the presence of geographic contagion by examining the extent to which cities were more or less likely to experience riots if those nearby had recently experienced them. Finding no significant effect, he argued that widespread riots might have been stimulated by the sharing of grievances facilitated by national news coverage of injustices on television. Subsequent studies using more precise methods and data have, however, shown that collective violence may diffuse geographically at the spatial scale of cities and on the time scale of days, but have also provided evidence to suggest that contagion is more likely in cities where

news outlets such as television provide coverage of disorders occurring elsewhere (Midlarsky, 1978; Myers, 1997, 2000, 2010).

While it can be difficult to disentangle contagion effects of a geographic or non-geographic nature, it is possible to identify particular space-time patterns of events that would be anticipated if either or both mechanisms had a part to play. For example, considering patterns of riots within a city, Abudu Stark et al. (1974) provide one of the few empirical studies of the space-time dynamics of riots at a fine spatial scale, and find evidence to suggest that rioting spread both between contiguous and non-contiguous areas. The former would be expected in the case that the risk of rioting diffuses spatially, the latter where the process is not dependent upon geography. Other fine-scale empirical studies have investigated the characteristics of targets during rioting (Berk and Aldrich, 1972; Rosenfeld, 1997); however, few have directly examined localised diffusion and, consequently, the space-time dynamics of civil disorders are not currently well understood.

Considering contagion in the context of the space-time patterns introduced above and depicted in Figure 3.7, incidents of containment would be expected if the contagion effect was strongly localised. That is, if the occurrence of one offence led to the occurrence of further events at the same location. In this case, the contagion effect might be strongly influenced by local environmental factors, such as the presence of a particular retail centre that was attractive to rioters.

On the other hand, the prevalence of relocation and escalation patterns would be expected if the geographic contagion was not localised by environmental features in this way, and nearby areas offered suitable opportunities at which to offend. In these cases, rioters may be attracted to the wider area in which disorder occurs, but do not necessarily commit offences at exactly the same location, instead offending nearby: the disorder is more dynamic and moves or expands in geographic extent. Another reason for dynamic patterns could be that an initial location which experienced extensive disorder may reach some kind of capacity (for example, by running out of goods to be looted), leading to rioters that may have been attracted to that area by the ongoing rioting searching for other nearby locations in which to engage in the disorder.

Finally, the prevalence of flashpoints might indicate occurrences of social contagion in which groups of motivated individuals select areas to target by coordinating

the collective activity of at least some rioters. The organisation of sudden widespread outbreaks of disruption might be achieved through the use of social media. Blackberry Messenger—a private and instant messaging service for those with Blackberry mobile phones—was cited by the Metropolitan Police Service as one of the ways by which rioters communicated and were able to organise themselves by arranging times and locations at which to meet (Metropolitan Police Service, 2012).

Dynamic environment effects: Interaction with police

There are a variety of possible explanations for clustering in the event data. Spatial clustering may occur at a particular location because that location provides a suitable opportunity for rioters to loot high-value goods, and offences may be clustered in time due to a majority of rioters having more free time during the evening, rather than during the day.

In a similar way, there are environmental influences that may be used to explain spatio-temporal clustering of offences beyond the effects of both spatial and temporal clustering. These influences do not have to depend solely on the presence of ongoing rioting. For example, if the environmental features of places and those that surround them vary substantially in terms of their attractiveness to offenders, observed instances of containment may be highly likely, as rioting is more likely to continue at particular (attractive) locations, and not to diffuse to nearby (but dissimilar) areas. On the other hand, if rioters' spatial decision-making was less determined by such factors, instances of relocation would be more likely. These types of effects, however, are dependent on the continued occurrence of rioting and so are closely related to the effect brought about by contagion.

Perhaps the largest influence on the space-time patterns of rioting that does not explicitly depend on processes of contagion, comes from the interactions between rioters and police officers. These interactions can provide another mechanism through which disorder may spread or be suppressed. Wilkinson (2009) suggests that this is an area not sufficiently investigated in the previous literature, perhaps largely due to a lack of sufficiently detailed data on law enforcement activities. Although the study presented here suffers from a lack of data on where the police were, it is possible to comment upon the types of patterns that may be more or less prevalent based on the tactics used

by the police.

During the riots in London, the actions of the police came under great scrutiny. In particular, the public and media questioned the course of action taken by police when faced with the disorder (Riots Communities and Victims Panel, 2011). It was perceived that, in an effort to limit the spread of events, the police were standing by and containing offenders, without being drawn into the disorder to make arrests, thereby failing to protect some locations from being looted. The use of these tactics by police officers would lead to more instances of containment, as opposed to any of the other patterns described above.

The Metropolitan Police Service have stated that containment tactics were initially used to counter the riots (Metropolitan Police Service, 2012). It was claimed that this was due a combination of the severe and unprecedented scale of the riots together with a lack of resources (in terms of the number of police officers) available to react to the disorder. Specifically, they were apparently concerned that,

> "should they send officers forward into a dangerous situation to try to make an arrest, they would then no longer be able to maintain a police cordon which was critical to holding a junction or protecting a location to prevent the spread of disorder or to protect life."

Such reports suggests the presence of uncertainty with regards to the most appropriate public order tactics: should police officers attempt to contain the disorder within defined boundaries or to attempt to proactively arrest rioters. The first tactic would lead to a concentration of incidents in one area, and hence to more counts of containment patterns, whilst the second might cause the rioters, and therefore their disorder, to spread to new locations, albeit whilst some of the rioters are arrested. In the case of the latter, the number of occurrences of relocation would expected to be higher as the disorder spreads.

Since the police resource scarcity was largely viewed as being responsible for this uncertainty, extra officers were brought in from other police forces in the UK as the riots intensified (see Figure 3.8). It is widely claimed that this was the key factor in bringing an end to the prolonged period of disorder. Indeed, Her Majesty's Inspectorate of Constabulary (HMIC, 2011) stated,

> "While the immediate response to the public disorder in August was hesitant, this transformed into a decisive and effective response in which large number of assets were mobilised to regain control of the streets."

Although some have questioned whether the number of officers on the final night of the unrest was, in fact, suboptimal (Davies et al., 2013), the increase in police numbers would have enabled the police officers present during an outbreak of rioting to be more proactive in stopping on-going disorder: they may have been able to make arrests without the risk of other offenders present dispersing to nearby areas, and thereby spreading the disorder.

The relatively abrupt change in police manpower, and the subsequent arguments that this was the principal reason for the quelling of disorder, provides conditions comparable to a natural experiment, and enables the investigation into how patterns of offending changed with the police's ability to employ more effective public order tactics. As a consequence, the offence data considered in this section is split in two, to see whether this apparent change led to a change in the patterns of offences. During the first half of the riots, when police tactics were more constrained, if the on-going rioting provoked or prompted others to engage in the disorder, the unrest would be expected to spread in one of the four ways discussed above and depicted in Figure 3.7. As the range of public order tactics available to the police increased, changes in the diffusion patterns of riot events would be expected as the space-time dependency of offences would likely have been disrupted. While some places would still be expected to experience hotspots of activity, less evidence of the spreading of the disorder as time progresses is expected. Indeed, the occurrence of escalation and flashpoints would suggest that the police are not in control of the disorder as it spreads to new locations.

3.5.2 Simulating spatio-temporal independence with binary event data

The number of observed instances of containment, relocation, escalation and flashpoints are counted by considering the values of $(X, Y)_{(j,k)}$ and $(X, Y)_{(j,k+\delta t)}$ for all values of j and k. After enumerating the observed patterns of interest, it is necessary to determine the statistical significance of the counts of each pattern. Similarly to Sections 3.3 and 3.4, this is achieved by constructing a null model against which test

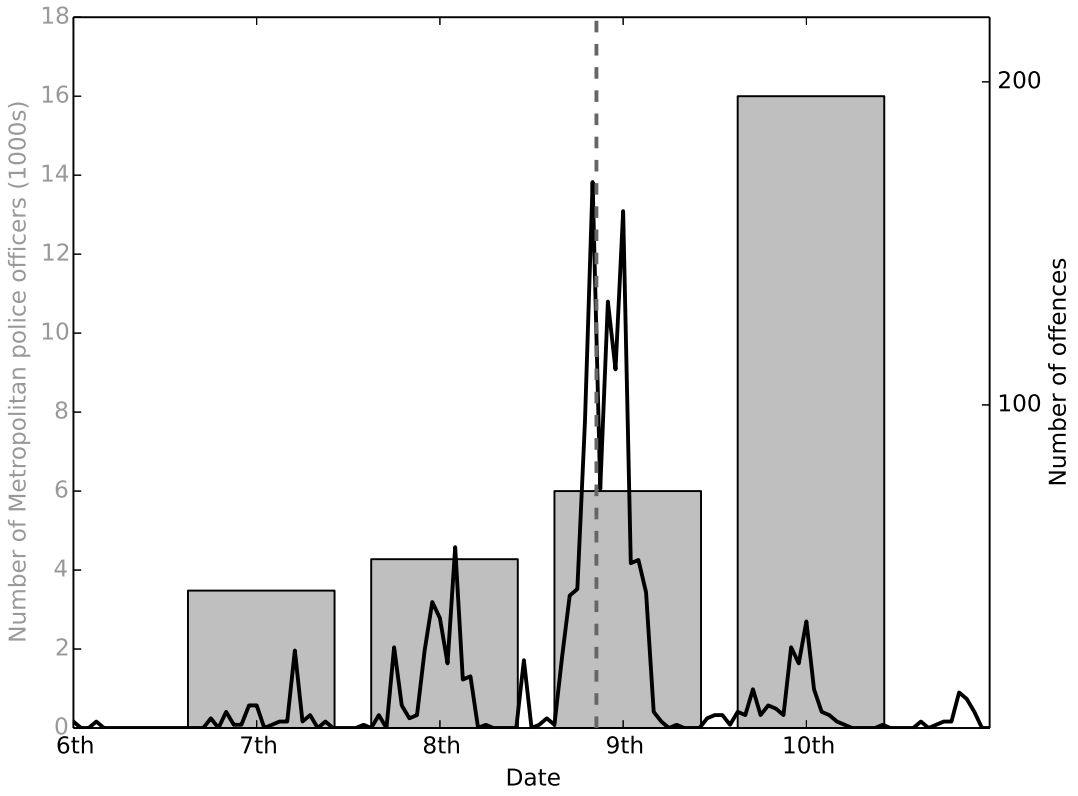

Figure 3.8: **Police officers and offences.** Bar chart of the number of police officers on the streets of London for each night throughout the duration of the disorder, and the number of recorded offences. The dashed vertical line represents the mid-point of the offence data.

statistics—in this case, the count of each type of diffusion pattern—can be compared.

A null model is sought that removes spatio-temporal dependency in the offence patterns but preserves the underlying spatial and temporal distributions of the data. Since the test statistics of this section are based upon binary interpretations of the spatio-temporal distribution of the data, the random permutation to generate the null model that was described in Section 3.4 cannot be used here. The reason for this is due to the high levels of spatio-temporal clustering in the event data. There are many space-time windows in which more than one event occurs and a few in which many events occur. Consequently, a random permutation of the times at which events occur spreads out these offences across different space-time windows that previously contained no events. Since many more space-time windows now contain events, a binary measure obtained from this permuted dataset is not comparable with a binary measure of the original dataset. In order to preserve the binary spatial distribution and the binary temporal distribution, but to randomise the spatio-temporal interaction, a different approach is required.

The simulation of the data under the null hypothesis of spatio-temporal independence requires consideration of the binary matrix B, known as the space-time contingency table. The matrix B is constructed as follows: let B be a $J \times K$ binary matrix, where J is the number of spatial units in the spatial-temporal grid and K is the number of temporal units. Define $B_{jk} = 1$ if, and only if, the number of offences in spatial unit $\mathcal{D}_j$ within temporal unit $\mathcal{T}_k$ exceeds zero. The contingency matrix B describes the distribution of events across the study region, and, for the spatio-temporal grid defined in section 3.2 with a spatial resolution $\delta s = 20$km and $\delta t = 24$ hours, is given by:

$$B = \begin{pmatrix} 1 & 0 & 0 & 1 & 1 \\ 1 & 0 & 1 & 1 & 1 \\ 0 & 0 & 0 & 0 & 0 \\ 1 & 1 & 1 & 1 & 1 \\ 1 & 1 & 1 & 1 & 1 \\ 1 & 1 & 1 & 1 & 1 \\ 0 & 0 & 1 & 1 & 1 \\ 1 & 0 & 1 & 1 & 1 \\ 0 & 0 & 0 & 0 & 0 \end{pmatrix}, \tag{3.19}$$

where the columns correspond to each temporal unit in the space-time grid (which, in this case, correspond to each of the five days of the rioting) and the rows correspond to each spatial unit.

The generation of the data under the null hypothesis involves the random sampling of binary contingency tables subject to the constraints brought about by preserving the row and column sums - the spatial and temporal distributions, respectively. To generate the expected distribution, assuming the null hypothesis of the space-time independence of events, a bipartite graph denoted by $\mathcal{G} = (V_1, V_2, E)$ is constructed, in which the sets of vertices V_1 and V_2 are partitioned so that every edge in E connects one vertex in V_1 with one vertex in V_2. Defining V_1 as the set of spatial units, indexed by j, and V_2 as the set of temporal units, indexed by k, an edge (j, k) between j and k is added if, and only if, $B_{jk} = 1$.

Figure 3.9 shows this bipartite network for $2,592$ offences associated with the 2011 London riots. These offences are the ones included in the analysis and correspond to the offences in the original dataset (for which $N = 3,914$) that contain data on the location and time at which the offence occurred.

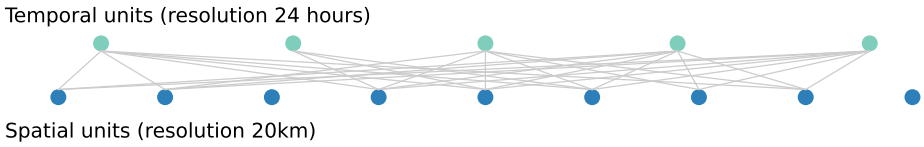

Figure 3.9: **Network visualisation of the London riot data.** The bipartite network G for the London riot data with $\delta t = 24$ hours and $\delta s = 20km$, visualising the matrix in equation 3.19.

Using a uniform pseudo-random number generator, two edges are selected. Denoting the chosen edges by (j_1, k_1) and (j_2, k_2), it is first determined whether or not the edges defined by (j_1, k_2) and (j_2, k_1) already exist. If they do not, which, for the sparse dataset associated small spatial areas during the 2011 London riots is highly likely,

then the edges (j_1, k_1) and (j_2, k_2) are removed, and the edges (j_1, k_2) and (j_2, k_1) are created.

Of course, the resulting bipartite network produced from this procedure will appear almost identical to the original network, obtained from the real data: a maximum of two edges have been removed and replaced with new edges. Thus, in order to generate a permuted dataset against which hypotheses concerning spatio-temporal dependency can be tested, the process by which two edges swap temporal nodes in the bipartite graphs is repeated many times. After sufficient number of iterations, a distinct network is constructed that becomes quite unrecognisable to the original network, although the degree of each vertex (defined as the number of edges connected to it) is equal to the degree of that same vertex in the original network. It remains to define a suitable number of iterations for this procedure that sufficiently removes the spatio-temporal dependencies from the original network.

Suppose that this process is repeated $\mathcal{M}$ times. Then $\mathcal{M}$ is the number of times that two edges are selected at random and rewired so that the edges swap end nodes, provided that the new edges created do not already exist. $\mathcal{M}$ is calculated by considering the total number of selections required to ensure that every edge is selected at least once. Since edges are selected uniformly randomly each time, and therefore some edges will almost always be selected more than once, this number will vary over different attempts at this procedure.

It is therefore supposed that this number is given by the random variable χ. $\mathcal{M}$ is chosen to be equal to the value in the distribution of χ that is greater than 95% of all the possible values that χ can take. By defining $\mathcal{M}$ in this way, it is ensured with 95% confidence that the rewiring procedure outlined above selects every edge, and, therefore, ensures that the distribution given by the null hypothesis (that there is no spatio-temporal interaction) is sufficiently random, subject to the constraints brought about by preserving the spatial and temporal distributions of offences.

The 95% confidence interval on the random variable χ is calculated by first letting χ_m be the random variable given by the number of selections required in order to select the m-th new edge, after $m - 1$ distinct edges have already been selected. Then one

realisation of χ is given by

$$\chi = \sum_{m=1}^{M} \chi_m, \tag{3.20}$$

where M is the total number of edges. The probability of selecting a new edge in the next selection after $m-1$ distinct edges have been selected is given by

$$P_m = 1 - \frac{m-1}{M}. \tag{3.21}$$

Thus, for the variable χ_m to be equal to some value, say h, there must be $h-1$ selections in which an already selected edge is chosen, followed by 1 selection in which a distinct edge is chosen. The expected value of the variable χ_m is then

$$\mathbb{E}\left[\chi_m\right] = \sum_{h=1}^{\infty} h\left(1-P_m\right)^{h-1} P_m. \tag{3.22}$$

The right hand side of equation 3.22 contains the negative of a polynomial derivative of $(1-P_m)$, and, thus

$$\mathbb{E}\left[\chi_m\right] = P_m \sum_{h=1}^{\infty} -\frac{d}{dP_m}\left(1-P_m\right)^h. \tag{3.23}$$

Swapping the derivative and summation and using the formula for the sum of a geometric series, the following is obtained:

$$\mathbb{E}\left[\chi_m\right] = -P_m \frac{d}{dP_m}\frac{1-P_m}{P_m} = \frac{1}{P_m}. \tag{3.24}$$

The variance of χ_m can be calculated similarly. The expected value of χ_m^2 is given by

$$\mathbb{E}\left[\chi_m^2\right] = \sum_{h=1}^{\infty} h^2 (1-P_m)^{h-1} P_m, \tag{3.25}$$

which, using the identity

$$\frac{d^2}{dP_m^2}(1-P_m)^{h+1} = h^2(1-P_m)^{h-1} + h(1-P_m)^{h-1}, \tag{3.26}$$

can be written as

$$\mathbb{E}\left[\chi_m^2\right] = P_m \sum_{h=1}^{\infty} \frac{d^2}{dP_m}(1-P_m)^{h+1} + P_m \sum_{h=1}^{\infty} -h(1-P_m)^{h-1}. \tag{3.27}$$

Noting that the final term in equation 3.27 contains a polynomial derivative of $(1-P_m)$, and then swapping the derivatives and summations, leads to

$$\mathbb{E}\left[\chi_m^2\right] = P_m \frac{d^2}{dP_m^2}\frac{(1-P_m)^2}{P_m} + P_m \frac{d}{dP_m}\frac{1-P_m}{P_m} = \frac{2}{P_m^2} - \frac{1}{P_m}, \tag{3.28}$$

after differentiating. Thus the variance of χ_m is then

$$\mathrm{Var}\left[\chi_m\right] = \mathbb{E}\left[\chi_m^2\right] - \left(\mathbb{E}\left[\chi_m\right]\right)^2 = \frac{1 - P_m}{P_m^2}. \tag{3.29}$$

Since the expected sum of M random variables is the sum of those expected random variables, the expected value of χ can be calculated as

$$\mathbb{E}\left[\chi\right] = \sum_{m=1}^{M} E\left[\chi_m\right] = \sum_{m=1}^{M} \frac{1}{P_m} = M \sum_{m=1}^{M} \frac{1}{M - m + 1}, \tag{3.30}$$

which can be simplified by setting $m' = M - m + 1$ and removing primes for convenience to obtain

$$\mathbb{E}\left[\chi\right] = M \sum_{m=1}^{M} \frac{1}{m}. \tag{3.31}$$

Similarly, since the random variables χ_m are independent for all values of m, the variance of χ is given by

$$\mathrm{Var}\left[\chi\right] = \sum_{m=1}^{M} \mathrm{Var}\left[\chi_m\right] = \sum_{m=1}^{M} \frac{1 - P_m}{P_m^2} = \sum_{m=1}^{M} \frac{\frac{m-1}{M}}{\left(1 - \frac{m-1}{M}\right)^2}, \tag{3.32}$$

which, by multiplying both sides of the fraction by M^3, and setting the index $m' = M - (m - 1)$ and removing primes, becomes

$$\mathrm{Var}\left[\chi\right] = M^2 \sum_{m=1}^{M} \left(\frac{1}{m^2} - \frac{1}{Mm}\right) \leq M^2 \sum_{m=1}^{K} \frac{1}{m^2} < 2M^2, \tag{3.33}$$

since $\sum_{m=1}^{\infty} 1/m^2 = \pi^2/6$.

In order to find the 95% confidence interval of χ, and therefore to find the value of $\mathcal{M}$, Chebyshev's inequality is used. Chebyshev's inequality states that for unknown distributions with known mean and known variance, the majority of values can be specified to be within a certain number of standard deviations from the mean. Formally, Chebyshev's inequality is given as

$$Pr\left(\left|\chi - \mathbb{E}\left[\chi\right]\right| \geq c\sqrt{\mathrm{Var}\left[\chi\right]}\right) \leq \frac{1}{c^2}, \tag{3.34}$$

for all positive real constants c. Thus,

$$\frac{1}{c^2} \geq Pr\left(\left|\chi - M \sum_{m=1}^{M} \frac{1}{m}\right| \geq c\sqrt{\mathrm{Var}\left[\chi\right]}\right) \tag{3.35}$$

$$\geq Pr\left(\left|\chi - M \sum_{m=1}^{M} \frac{1}{m}\right| \geq c\sqrt{2M^2}\right) \tag{3.36}$$

$$\geq Pr\left(\chi - M \sum_{m=1}^{M} \frac{1}{m} \geq c\sqrt{2M^2}\right), \tag{3.37}$$

where the first inequality arises from Chebyshev's inequality in equation 3.34, the second inequality arises from equation 3.33 and the third inequality arises since $|x| \geq x$ for all values of x. Consequently,

$$Pr\left(\chi \geq M\sum_{m=1}^{K}\left(\frac{1}{m}+\sqrt{2}cM\right)\right) \leq \frac{1}{c^2}. \tag{3.38}$$

Finally, setting $c = \sqrt{20}$ obtains

$$Pr\left(\chi \geq M\sum_{m=1}^{M}\left(\frac{1}{m}+\sqrt{40}M\right)\right) \leq 0.05, \tag{3.39}$$

and, thus for

$$\mathcal{M} \geq M\left(\sum_{m=1}^{M}(1/m+\sqrt{40}M)\right), \tag{3.40}$$

the realisation of the random variable χ is less than the value of $\mathcal{M}$ with 95% confidence. Therefore, with $\mathcal{M} = M(\sum_{m=1}^{M}(1/m+\sqrt{40}M))$, the re-wiring procedure on the bipartite network $\mathcal{G}$ selects every edge with 95% confidence.

In what follows, using this value of $\mathcal{M}$, the results of this rewiring procedure as applied to spatio-temporal grids of varying sizes and the 2011 London riot data are presented. As the results will demonstrate, this re-wiring procedure, despite not being perfectly random for some realisations of the data under the null hypothesis, is sufficiently random in order to detect differences in the prevalence of the different patterns of diffusion described above. This approach to simulation therefore usefully enables the comparison of binary test statistics against data simulated under the null hypothesis of spatio-temporal independence, but with the binary spatial and temporal distributions of the simulated data identical to the empirical data.

3.5.3 Results

In order to determine the effect of increasing police numbers, two separate analyses of the data are performed, one for each half of the data. For the first half, it is argued that the police were under resourced and unsure of the correct public order tactics to adopt. For the second half, the police numbers were much higher, and it is therefore expected that the police were able select the best approach from a wider range of public order strategies. The two time periods are split at the median time for all offences used in the analysis, to ensure that there are the same number of offences within each analysis. The median time is 20:30 on the 8th August 2011. In Figures 3.10 and 3.11, the

prevalence of each pattern of interest against 499 realisations of the data under the null hypothesis, for each spatio-temporal grid resolution, and for each half of the data, respectively, are presented. Using heat maps to represent the prevalence of each pattern, the colours in these figures show the values of the $\mathcal{Z}$-scores, calculated as the observed count of each diffusion pattern minus the mean of the counts of each diffusion pattern in the simulated data, divided by the standard deviation of the counts over the simulated distribution. Specifically, letting $\mathcal{S}$ be the count of either containment, relocation, escalation or flashpoints in the observed data, the $\mathcal{Z}$-score is defined as

$$\mathcal{Z} = \frac{\mathcal{S} - \frac{1}{G}\sum_{g=1}^{G} \mathcal{S}^{(g)}}{\sqrt{\frac{1}{G}\sum_{g=1}^{G} \left(\mathcal{S}^{(g)} - \frac{1}{G}\sum_{g=1}^{G} \mathcal{S}^{(g)}\right)^2}}, \tag{3.41}$$

where $\mathcal{S}^{(g)}$ is the value of the count of the pattern in the g-th iteration of the simulated data. The results were also tested using the empirical performance of the Monte-Carlo simulation, using the expression in equation 3.14. The distributions of the test statistics were sufficiently normal that these were results were consistent with the $\mathcal{Z}$-scores defined here. $\mathcal{Z}$-scores are used as an easily interpreted measure for the distance of a particular value from the mean. In particular, the value of the $\mathcal{Z}$-score specifies the number of standard deviations from the mean of the statistic in question. The more positive the value of each $\mathcal{Z}$-score in Figures 3.10 and 3.11, the further the distance from the statistic to the mean in the positive direction, and, therefore, the more prevalent each pattern is in the empirical data when compared to spatio-temporal independent data. On the other hand, if the $\mathcal{Z}$-score is negative, then the expected pattern is less prevalent than when compared to the spatio-temporal independent data. For the purposes of clarity, the plots in Figures 3.10 and 3.11 are conditional upon the significance of each result. This means that the cells are coloured only if the observed differences are statistically significant (based on a two-sided 95% confidence interval). If the results do not reach significance for a particular space-time window, then that window is shaded white.

According to the results shown in Figures 3.10 and 3.11, it is evident that during the first half of the riots, observed counts of escalation were much more prevalent than would be expected, assuming that the timing and location of events were independent. This finding is relatively insensitive to the space-time resolutions for the grids that were

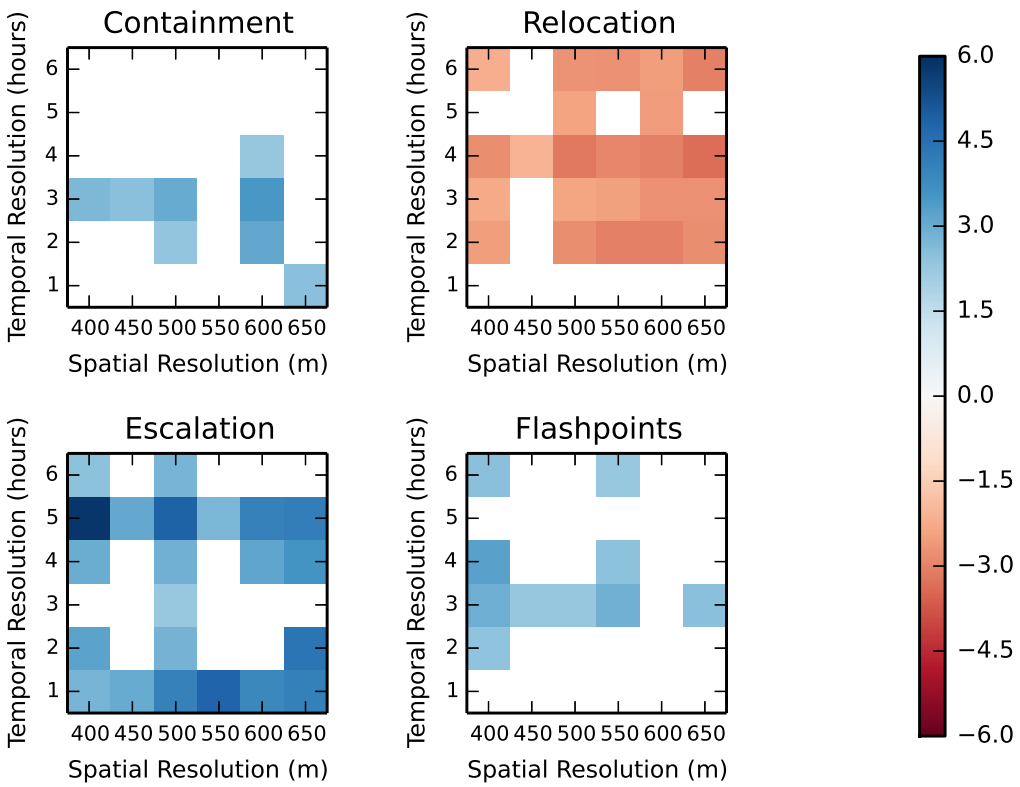

Figure 3.10: **Results for the first half of the data.** $\mathcal{Z}$-scores for each observed count outside a 95% two-sided confidence interval of the resulting distribution from the Monte Carlo simulation, for each diffusion pattern for the first half of the data. Spatial-temporal resolutions that do not reach statistical significance are shaded white.

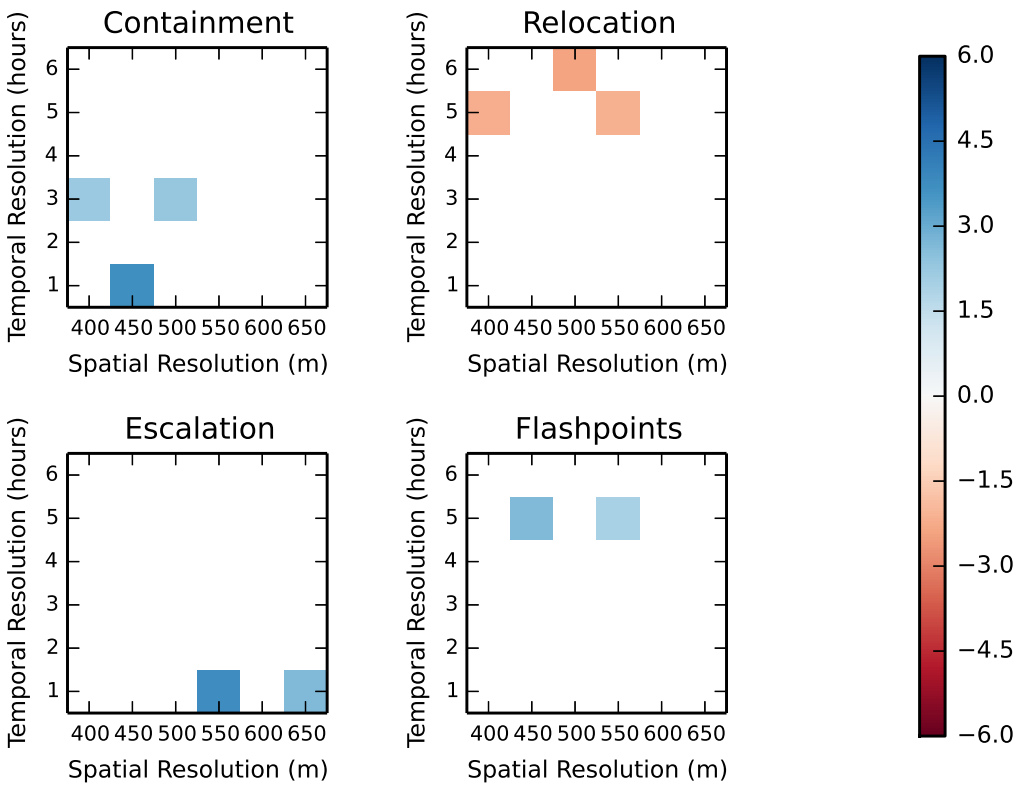

Figure 3.11: **Results for the second half of the data.** $\mathcal{Z}$-scores for each observed count outside a 95% two-sided confidence interval of the resulting distribution from the Monte Carlo simulation, for each diffusion pattern for the second half of the data. Spatial-temporal resolutions that do not reach statistical significance are shaded white.

tested. There is evidence to suggest that containment is more prevalent than would expected in the first half of the rioting, although this appears to be far more sensitive to the time window used, with the most prevalence for this type of pattern being apparent for three-hour intervals. Flashpoints were also observed significantly more than would be expected, particularly for smaller spatial units. In contrast, instances of relocation were observed significantly less frequently than would be expected across most of the grid resolutions tested.

The results for the second half of the data vary from the results for the first half quite significantly. In fact, although for the resolutions that are significant, they are significant in the same direction as in the first half of the data, there is a distinct lack of evidence that these results are consistent across different grid resolutions tested. Given that there are 36 significance tests for each pattern, corresponding to each space-time window tested, and that tests are performed at the 95% significance level, $36 \times 0.05 = 2$ false positive findings would be expected for each pattern. Thus, for the second half of the disorder, it is evident that the prevalence of the localised patterns of offences did not differ from the null hypothesis in which spatio-temporal interaction is removed.

3.5.4 Conclusions

Interpreting these results, the first conclusion that can be made is that the local patterns in space and time made by the offences in the 2011 London riots changed significantly between the first and second halves of the disorder. Moreover, it appears that spatio-temporal dependency between offences did not influence the spreading of the riots in the second half of the disorder. It was argued in Section 3.5.1, that this may be due to the increased police presence during the second half of the rioting, enabling police officers to adopt more effective public order tactics, essentially bringing a stop to the contagious nature of the riots. This suggests that the police not only supressed the overall level of the disorder, as has been argued by various reports since the riots (e.g. House of Commons (2011)), but also suppressed the role of contagion processes (e.g. escalation and flashpoints) which were a feature during the first half of the disorder.

During the first half of the riots, disorder appears to have persisted at locations already experiencing riots, sometimes without moving into the surrounding areas (containment) and sometimes spreading to those nearby (escalation). This provides support

for the idea that there were localised effects whereby rioters were attracted to sites where there was on-going disorder. The results cannot detect the effects that may be due to social contagion, in which offenders were mobilised more systematically through social media or other means, or to geographic contagion, in which those who encountered activity through their proximity to ongoing disorder were encouraged to participate; however, there is sufficient evidence that at least some form of contagion and dependency between offences took place. Distinction between these two effects is considered further in Chapter 4.

Evidence of flashpoints during the first half of rioting suggests that there were instances in which unaffected areas suddenly found themselves subject to disorder. This is consistent with the arguments put forward that groups of rioters were able to organise times and places at which to offend. The occurrence of flashpoints from a policy perspective represents an intriguing problem for the allocation of police officers. In particular, flashpoints are difficult to predict because, unlike instances of containment or escalation, which stem from locations in which rioting is ongoing, flashpoints originate in locations with no rioting nearby, which occurs many times for the sparse dataset of the London riots.

The prevalence of relocation was significantly less than expected during the first half of the disorder across a range of different grid resolutions. This is consistent with the argument that environmental features localised the contagion effect and therefore tied disorder to certain areas. The disorder was not so dynamic that it easily moved from location to location. Considering the actions of police and their influence on possible relocation, it appears that during the first half of riots they did not encourage the dispersion of rioters to other regions. Given that the occurrence of containment was significant, it appears that the policing strategy of containment was indeed effective. A common concern associated with geographically focused police activity is that it will merely displace offending to different areas (Bowers et al., 2011). Of course, different riots may have different dynamics, but in the current case, there was no evidence of this, which suggests that police action did not simply move rioting to neighbouring areas.

3.6 Discussion

Exploratory data-driven approaches, in which model assumptions are derived from empirical data, can lead to various insights. Moreover, by considering possible mechanisms for how such data may have been generated, it is possible to test hypotheses concerning these mechanisms, thereby evaluating how well these explanations are supported by the observed data. Of course, the success of a hypothesis test does not necessarily mean that the explanation proposed is the mechanism that results in the observed data, but it may help to discount certain processes. For example, when considering local patterns in space and time made by the occurrence of riot offences in this chapter, it was shown that the pattern of relocation occurred much less often than would be expected, assuming that the offences were independent. This finding rules out mechanisms for riots that result in dynamic 'hotspots' for the short timescales that were considered. Instead, as shown by the greater than expected prevalence of containment and escalation, at least for the first half of rioting, the outbursts were more static in space, perhaps as a result of the attraction of the underlying areas.

Another reason for employing data-driven approaches to modelling, particularly when first faced with an empirical dataset, is that it can often suggest assumptions that might be used to construct more descriptive or complex models. It has been argued in this chapter that important considerations when investigating riots and civil disorder are the impact of interdependency between events, the relationship between the locations of the riots and the underlying geography, and the interaction between rioters and police. In Chapter 4, two of these—interdependency between events, and the relationship with the underlying geography—will be incorporated into a behavioural model of rioter target choice. The third consideration, the interaction between rioters and police, is more difficult to incorporate due a lack of data on law enforcement activities. In Chapter 5, a case study of conflict between Naxal insurgents and police will be modelled using more descriptive models than have been presented here.

This chapter has made novel contributions to the theoretical understanding of rioting and civil disorder. In contrast to much previous research on the spatio-temporal analysis of riot patterns, the analysis presented here uses relatively fine spatial and temporal scales to examine the spatio-temporal patterns of riots. Furthermore, it has been shown that the spatio-temporal patterns of the London riots were consistent with theo-

ries of contagion, in which the occurrence of an offence at a given location increases the likelihood that another offence will occur nearby in space and time. This effect may be brought about by situational precipitators, in which the presence of rioting encourages individuals who are nearby to participate in the rioting, leading to geographic contagion. Alternatively, the contagion process could be a result of mobilising those who share similar grievances, regardless of where they are located. Social contagion can spread through a range of various media channels. These two perspectives will be considered further in Chapter 4 by investigating the distance that rioters typically travelled in order to offend. These two mechanistic explanations for the spreading of riots are consistent with the analysis presented here, suggesting both are plausible mechanisms for the spreading of rioting. They are difficult to distinguish between, and it is likely that both have a role to play.

Policy questions have also arisen through this modelling approach. The onset of rioting and civil disorder forces policy-makers to immediately decide how best to allocate scarce resources. It has been shown that the presence of more police coincided with the reduction of the local spreading of disorder in space. The prevalence of flashpoints during the first half of the riots, in which widespread disorder occurs at a given location quite spontaneously, is a phenomenon which would have been difficult to predict and it is therefore unlikely that police officers could have been present at such locations antecedently. The occurrence of flashpoints are inherently difficult to police. On the other hand, the analysis in this chapter has shown that instances of containment and escalation were more prevalent than would have been expected, assuming that the events were independent. These patterns provide more opportunity for policing. A general finding is that the rioting appeared to be fairly static as a result of the spatio-temporal interdependency, and rooted in the underlying geography for timescales over which police may be deployed. The adoption of reactive strategies by police officers, by which officers are quickly deployed to locations where rioting is ongoing, as opposed to proactive strategies, by which officers are deployed to locations which are not experiencing disorder but at which disorder may be anticipated, is perhaps a good strategy to adopt. The prevalence of flashpoints, however, suggests that police allocation should also be dynamic, and that there is a balance that needs to be struck.

In Chapter 1, it was argued that policy-makers are more trustworthy of approaches

that rely more upon the empirical data and less upon extensive assumptions that remove the model from the real world. Whilst the findings of this chapter have been shown to be robust to a variety of different grid sizes, and may be useful in informing policy-makers of the need to incorporate underlying geography into allocation problems, they are unable to offer more extensive insights into, for example, the locations which are more vulnerable than others of experiencing flashpoints. The aim of the proceeding chapters is to consider more descriptive, and, in turn, predictive models.

A number of caveats to the conclusions of this chapter are worthy of discussion. First, as is the case with any study that employs police crime data, not all incidents of disorder would have been recorded by the police, and it is unclear how much disorder went unreported. In the analysis of local patterns of diffusion, it was the geographic scope of the rioting, rather than its relative intensities in different locations that was examined. Because of this binary approach to analysis, it is hoped that the effects of underreporting have been minimised: it is reasonable to suggest that the largest source of underreporting would have occurred at the sites of the largest outbursts of disorder. Second, analyses of the kind reported here are only as good as the precision of the data available for analysis and the data utilised were not perfectly precise in terms of when and where events occurred. To mitigate this issue, a sensitivity analysis was performed by varying the spatial and temporal resolutions at which patterns were explored. Again, such issues are true of most studies of crime and disorder, but should be borne in mind.

As a tool for the analysis of event data in space and time, the methods utilised in this section can be extremely valuable to gain insights into a given dataset. These methods involve the use of Monte-Carlo simulations to compare empirical data against null models. The simulations increased in complexity - first, by assuming the number of events remains consistent with the empirical dataset, but that they occur in random locations; second, by assuming the spatial and temporal distribution of events are preserved, but spatio-temporal dependency between them removed; and third, by supposing that the binary spatial and temporal distributions are preserved by the null model. The latter of these is a novel contribution to the literature and focuses more on the geographic scope and its local diffusion patterns than on individual offences.

Chapter 4

Modelling individual target choice during rioting

4.1 Introduction

The literature on criminality and collective behaviour contains a number of theories regarding the nature by which individuals make decisions during outbreaks of civil violence such as rioting. These theories, combined with the findings of the preceding Chapter, which argued that both contagion and environmental features of targets played a significant role in the spatio-temporal distribution of rioting, are employed in this chapter to investigate the 2011 London riots from a rioter's perspective. A parametric statistical model is presented that evaluates the extent to which extant theory of offender behaviour offers explanations for the distinctive space-time patterns of the riots. The individual behaviour that is modelled is the choice of target for each offender, a key driver in the emergent spatio-temporal profile of the system.

Parametric statistical modelling requires the selection of a family of models, dependent on a vector of parameters $\boldsymbol{\beta} = (\beta_1, \beta_2, ..., \beta_n)$, from which, a particular model may be constructed by specifying a value for $\boldsymbol{\beta}$. In many cases, these values are estimated through inference procedures that incorporate the available data and find the value of $\boldsymbol{\beta}$ that provides the closest fit (in some sense) between the model and the data. A key distinction between the parametric approach to modelling in this chapter, and the nonparametric approach in Chapter 3, is that the specification of a parametric family of models requires theoretical assumptions in order to define relationships between the variables. In the nonparametric case in Chapter 3, model assumptions were either very simple (e.g. complete spatial randomness) or derived from the empirical data (e.g. by specifying the spatial and temporal distributions of the offences). The difference in this chapter is that theoretical arguments are introduced in order to construct more complex assumptions. The parameterisation of the model can then be used to test hypotheses related to these assumptions.

In what follows, a family of probabilistic models for the choices made by rioters concerning where to offend is derived. The model is a version of a random utility discrete choice model, popularised for analysing choice problems following McFadden (1974). This model distinguishes itself from traditional regression modelling since it can be derived theoretically from relatively simple assumptions concerning choice behaviour. An extension to the standard model presented in this thesis is that dynamic variables are incorporated to account for the effect of contagion influencing the target

choice of each rioter. The model is derived by considering a variety of explanations for how the characteristics of a particular area influence the likelihood that it is chosen as a location in which to riot. An inference procedure that exploits the multinomial logistic form of the model is used to estimate the parameters in the vector $\boldsymbol{\beta}$. Conclusions resulting from these estimates in the context of theories for rioter target choice are then presented.

The ability of the model to explain the spatio-temporal profile of the riots is assessed. By considering the observed riots as just one realisation of the probabilistic model, a simulation is constructed in an attempt to recreate the spatio-temporal profile of the riots. Since each rioter is modelled as an autonomous entity acting probabilistically, this simulation can be considered as a stochastic agent-based model or a microsimulation model. As discussed in Chapter 2, such models have previously been shown to be effective tools for policy development and decision-making. The simulation is therefore considered from the perspective of its possible application in the policy domain, with the findings of the model used to calculate optimal police deployment strategies for a range of riot scenarios.

4.2 A model of target choice in the 2011 London riots

The desires and objectives of individuals requires attention when developing models of social systems. In this section, a model of target choice is derived that is based on choice models more commonly found in the field of economics. The target choice of each rioter is modelled because it provides an objective measure of individual behaviour that can be related to other measures used to capture characteristics of each target and it directly impacts the spatio-temporal profile of the riots – an emergent behaviour of the system studied in Chapter 3.

Choice models suppose that a decision-maker (or an agent) is required to select one option out of a set of alternatives. In the case of rioters, each rioter must undergo a decision process that results in them first deciding to engage in the disorder, and, second, choosing the timing and location at which they engage with the disorder. Thus, at some stage during this process, they choose between a set of possible locations at which to riot. This set of locations represents the set of alternatives available to each rioter. Choice models enable us to model the possible drivers and influences behind the

choices that are made. The aim of this study is to determine the types of areas, as measured using a variety of data sources, that are particularly suitable for rioting, thereby understanding which areas might be more at risk if a similar outbreak of disorder were to occur in the future.

In order to differentiate between the different choices, it is assumed that each choice that could be made has associated to it some intrinsic value, or utility, to the decision-maker. If the decision-maker were to choose a particular option, they would then obtain that level of utility. Utility is often thought of as the difference between benefits and costs of selecting a particular option and, as well as tangible constituents, such as financial gain, can also incorporate abstract concepts, such as well-being or potential happiness of the decision-maker. As will be demonstrated in the case of rioting, utility can consist of a number of factors, including the ease of accessing a particular target, or the value of potential goods that may be looted from a target.

Modelling the choices made by decision-makers when faced with a choice set involves assigning numeric values for the utility of each choice. The utility is often modelled from the perspective of the decision-maker, and can therefore incorporate variation across decision-makers. A rule is then prescribed that determines how the decision-maker chooses a single alternative out of the choice set, based on the utility values for each possible choice. The most widely used rule for choosing amongst alternatives states that the decision-maker chooses the alternative that offers them the most utility. The model then reduces to finding the alternative that offers the highest utility from the perspective of the decision-maker. In this case, it is the relative values of the utility that determine the preferences of the decision-maker, rather than the absolute value of utility, which may not have standardised units or dimensions.

Utility maximising models have been extensively developed in the field of economics and, throughout their history, have come under criticism arguing that they are incapable of modelling the behaviour of individuals (Beinhocker, 2007). Such criticism often stems from two major arguments: first, the rule that a decision-maker always chooses the option that provides them with the most utility is flawed; and, second, that utilities are so subjective as to be meaningless: a modeller cannot understand the desires and objectives of an individual, even if that individual were acting to maximise their utility. In this chapter a model is developed with these criticisms in mind. Namely,

it is acknowledged that it is impossible to incorporate the myriad of different factors and influences that may play a role in the decision-making process. It is assumed in what follows that the decision-maker will indeed select the option that provides them with the most utility, but that it is impossible to model the utility of different options in such a way that incorporates the limitations, prejudices, and idiosyncrasies of individuals, their environment, and their understanding of the choices available, whilst also keeping track of how these perceived utilities might change over time. The idea that an individual has limited access to available information, and may be unknowingly not acting in their best interest due to this limited information, has been referred to as bounded rationality, a concept discussed in Simon (1955).

One might conclude that, since it is impossible to determine the preferences of an individual, any attempts to model choices by assigning utilities to each alternative might be in vain. In fact, many authors in a variety of different fields have shown that by modelling the choices of individuals, significant insights can often be obtained, both into the behaviour of those individuals, as well as into the characteristics of choices that make them particularly attractive to decision-makers. For example, proposing a variant of bounded rationality, which the authors term rational choice theory, Cornish and Clarke (1986) argue that the deviant behaviour of a criminal is largely driven by their desire to maximise some form of utility, subject to their understanding of the choices that are available (see also Cornish and Clarke (2008)). This perspective has been attributed to a changing focus within the field of criminology. Traditionally, the occurrence of criminality was considered a consequence of the upbringing and psychology of the offender. An individual was thought be a motivated offender as a direct result of these factors. The use of bounded rationality in models of criminality—in which the offender is merely concerned with maximising the benefits offset by the costs of taking up a particular action—has led to much modern research considering the environment and the possible circumstances that might lead to an act of crime, allowing the concept of a motivated offender to be applicable to any individual who finds themselves in a particular set of circumstances, and not just to those who exhibit a particular psychological makeup.

Supposing that the actions and choices of offenders rely upon an element of bounded rationality, models of individual decision-making have been developed that

account for at least some level of uncertainty, and which explicitly incorporate an offender's bounded access to information, as well as a researcher's inability to capture this information. In what follows, a random utility model of discrete choice is derived in which offenders are assumed to be idiosyncratic. The probabilities of an individual making a particular choice are modelled, rather than the actual choice, in order to account for unobserved variance amongst choices that may be playing a role in the utility maximising behaviour of each individual. The operationalisation of this model is considered by identifying some of the features of the choice set—the set of targets available to offenders during the London riots—that enable the estimation of the model. The estimation of the parameters in the model is outlined, before presenting the results. This section concludes by discussing the findings from the perspective of criminological and social science theories that speak to the explanation of target choice during rioting, and highlights the contributions that mathematical modelling can make to the theoretical understanding of criminality.

4.2.1 A random utility model of discrete choice

For decision-maker i, suppose that alternative j has utility $U_{ij} \in \mathbb{R}$ associated with it, for alternatives $j = 1, ..., J$, and for decision-makers $i = 1, 2, ..., N$. In other words, U_{ij} is the utility decision-maker i obtains by selecting alternative j. The set of alternatives is assumed to be mutually exclusive, exhaustive, and finite. This implies, respectively, that: choosing a particular alternative j necessarily means that choice l is not chosen for all $l \neq j$; that exactly one alternative must be chosen; and that $J < \infty$. The principal assumption is that a decision-maker will select the alternative that offers the maximum utility across all possible alternatives. That is, decision-maker i will select the alternative j with $U_{ij} > U_{il}$ for all $l \neq j$.

A random utility model estimates U_{ij} for all i and j by supposing the perception of the utility to decision-maker i is composed of two components given by

$$U_{ij} = V_{ij} + \epsilon_{ij}. \tag{4.1}$$

The first component, denoted by V_{ij}, is the observable component of the utility U_{ij}. That is, V_{ij} is the utility of alternative j according to decision maker i that is perceptible to an observer of that decision-maker. This is the portion of utility that a researcher can attempt to model. The second component, denoted by ϵ_{ij}, corresponds to the un-

observed utility. This corresponds to the desires and objectives of the decision-maker that are unknown to an observer, and can be used to incorporate idiosyncratic preferences across individual decision-makers. The unobserved component of utility cannot be accurately obtained, and thus is treated as a random error term.

The inclusion of the random error term in the utility of each alternative explicitly accounts for uncertainty in the model. Moreover, the error term is assumed to incorporate the variation in choices for each decision-maker, as well as the limitations of the model to account for such idiosyncrasies.

Assuming that the utility U_{ij} is equal to V_{ij} and therefore that the error term is equal to zero would be one way of defining the model; however, this would not account for uncertainty. Instead a random variable Z_i is introduced, defined as the choice that is made by decision-maker i. In what follows, a model is derived for the probability distribution $Pr(Z_i = j)$ for each choice $j = 1, 2, ..., J$ and for each decision-maker $i = 1, 2, ..., N$.

Assuming that each decision-maker will select the alternative that provides them with the most utility, the probability that $Z_i = j$ is equal to the probability that the utility U_{ij}, is greater than the utility of all other alternatives l for $l \neq j$. Thus,

$$Pr(Z_i = j) = Pr(U_{ij} > U_{il} \; \forall \; l \neq j). \tag{4.2}$$

Substituting equation 4.1 into equation 4.2 leads to

$$\begin{aligned} Pr(Z_i = j) &= Pr(V_{ij} + \epsilon_{ij} > V_{il} + \epsilon_{il} \; \forall \; l \neq j) \\ &= Pr(\epsilon_{il} - \epsilon_{ij} < V_{ij} - V_{il} \; \forall \; l \neq j). \end{aligned} \tag{4.3}$$

Thus, $Pr(Z_i = j)$ is equal to the value of the cumulative probability distribution of the random variable $\epsilon_{il} - \epsilon_{ij}$, which is unknown, at the value $V_{ij} - V_{il}$, which is assumed to be observable and therefore known. Defining $\boldsymbol{\epsilon}_i = (\epsilon_{i1}, \epsilon_{i2}, ..., \epsilon_{iJ})$ to be a multivariate random variable with joint probability distribution given by $f_{\boldsymbol{\epsilon}_i}(\boldsymbol{\epsilon}_i)$, then

$$\begin{aligned} Pr(Z_i = j) &= \int_{\{\boldsymbol{\epsilon}_i \in \mathbb{R}^J | (\epsilon_{il} - \epsilon_{ij} < V_{ij} - V_{il}) \; \forall \; l \neq j\}} f_{\boldsymbol{\epsilon}_i}(\boldsymbol{\epsilon}_i) d\boldsymbol{\epsilon}_i \\ &= \int_{\boldsymbol{\epsilon}_i} \mathbf{1}_i((\epsilon_{il} - \epsilon_{ij} < V_{ij} - V_{il}) \; \forall \; l \neq j) f_{\boldsymbol{\epsilon}_i}(\boldsymbol{\epsilon}_i) d\boldsymbol{\epsilon}_i, \end{aligned} \tag{4.4}$$

where $\mathbf{1}_i$ is the indicator function which is equal to 1 if the evaluated condition inside the bracket is true, and equal to 0 otherwise.

The specification of the discrete choice model is therefore reduced to specifying a functional form for the joint probability distribution $f_{\boldsymbol{\epsilon}_i}(\boldsymbol{\epsilon}_i)$, and then calculating the integral in equation 4.4. Due to the multi-dimensional nature of this integral, the vast majority of models for the distribution of $\boldsymbol{\epsilon}_i$ do not have analytical solutions, and are therefore solved numerically. For example, the multinomial probit model is constructed by assuming that $f_{\boldsymbol{\epsilon}_i}(\boldsymbol{\epsilon}_i)$ is given by the multivariate joint normal distribution with specified mean and variance. This model does not have a closed analytical form, and requires numerical calculation of the integral in equation 4.4 (although by assuming the ϵ_{ij} for $j = 1, .., J$, are independent and identically distributed, it can be reduced to a single dimensional integral).

The model that is specified here is the multinomial logit model, and is derived by assuming that the errors ϵ_{ij} for $j = 1, .., J$ are independent and identically distributed according to an extreme value type I distribution (which is also known as a Gumbel distribution). For each ϵ_{ij}, this distribution is given by

$$f_{\epsilon_{ij}}(\epsilon_{ij}) = \exp\left(-\epsilon_{ij} - e^{-\epsilon_{ij}}\right), \tag{4.5}$$

and the cumulative distribution is given by

$$F_{\epsilon_{ij}}(\epsilon_{ij}) = \exp\left(-e^{-\epsilon_{ij}}\right). \tag{4.6}$$

Following Train (2003), and assuming that, initially, ϵ_{ij} is assumed to be known but ϵ_{il} unknown, then

$$Pr(Z_i = j|\epsilon_{ij}) = Pr\left(\epsilon_{il} < V_{ij} - V_{il} + \epsilon_{ij} \; \forall \; l \neq j\right), \tag{4.7}$$

which, since ϵ_{il} are independent, is equal to the product over $l \neq j$ for all possible values of l. Thus,

$$Pr(Z_i = j|\epsilon_{ij}) = \prod_{l \neq j} Pr\left(\epsilon_{il} < V_{ij} - V_{il} + \epsilon_{ij}\right). \tag{4.8}$$

The right hand side of equation 4.8 is a product over evaluations of the cumulative distribution function $F_{\epsilon_{il}}$, so that

$$Pr(Z_i = j|\epsilon_{ij}) = \prod_{l \neq j} F_{\epsilon_{ij}}(V_{ij} - V_{il} + \epsilon_{ij}) = \prod_{l \neq j} \exp\left(e^{-(V_{ij} - V_{il} + \epsilon_{ij})}\right). \tag{4.9}$$

By applying Bayes' theorem for a conditioned probability, and evaluating the likelihood of ϵ_{ij} occurring for all possible realisations of ϵ_{ij},

$$Pr(Z_i = j) = \int_{\epsilon_{ij}} Pr(Z_i = j|\epsilon_{ij}) f_{\epsilon_{ij}}(\epsilon_{ij}) d\epsilon_{ij}, \tag{4.10}$$

which, by substituting in equations 4.9 and 4.5, becomes

$$Pr(Z_i = j) = \int_{\epsilon_{ij}} \prod_{l \neq j} \exp\left(e^{-(V_{ij} - V_{il} + \epsilon_{ij})}\right) \exp\left(-\epsilon_{ij} - e^{-\epsilon_{ij}}\right) d\epsilon_{ij}. \tag{4.11}$$

The integral in equation 4.11 can be evaluated analytically, the explicit calculation of which is shown in Train (2003, pg. 85). The solution to the integral provides the functional form of the multinomial logit model, described in closed form as

$$Pr(Z_i = j) = \frac{e^{V_{ij}}}{\sum_{l=1}^{J} e^{V_{il}}}. \tag{4.12}$$

The probability of each decision-maker i selecting alternative j is therefore given by an expression that is dependent on only the observed component of utility for each choice, and does not depend on the unknown error ϵ_{ij}. Given the observed component of utility for each alternative and for each decision-maker, this probability can be found by calculating the ratio of the exponential of the observed utility, compared against the sum of the exponentials for all alternatives. The model emphasises the comparative nature of the discrete choice model: the decision-maker is more likely to select those alternatives which offer comparatively greater observed utility. An account of the history of this model and the range of different uses is given in McFadden (2001).

There are notable consequences from the derivation of this model that are not immediately obvious. By assuming that the error terms ϵ_{ij} are independent, the resulting model leads to what is known as independence of irrelevant alternatives. That is, the ratio of choice probabilities between any two alternatives is unaffected by the presence of other alternatives, which arises due the following equation:

$$\frac{Pr(Z_i = j)}{Pr(Z_i = l)} = \frac{e^{V_{ij}}}{e^{V_{il}}}, \tag{4.13}$$

for two different alternatives j and l. Since the right hand side of equation 4.13 does not depend on any of the other alternatives, the ratio of the probability of choosing alternative j and l is constant regardless of which other options might be available. There are many thought experiments that can highlight why the inclusion of a new

option might cause the value of equation 4.13 to change. For instance, if an option j' is introduced to the alternatives, which is almost identical to option j but which is very different to option l, then it might be expected that the value in equation 4.13 would decrease: decision-makers who might have chosen option j would be more likely to switch to j' whilst decision-makers who might have chosen option l would be less likely to switch to j'.

Independence of irrelevant alternatives arises as a result of the assumption of independence over the error terms ϵ_{ij}. In many scenarios, particularly those related to spatial choice problems, this assumption is likely to be violated. In particular, it implies that a particular area is chosen as a result of just the features of that area, and not as a result of the features of areas nearby. Since it is conceivable that a rioter may offend in a particular area due to the characteristics of a neighbouring area, the errors are likely to be correlated between nearby targets. This mechanism would manifest as a spillover effect. The presence of spillover effects is consistent with the analysis of Chapter 3, which demonstrated the prominence of escalation diffusion during the riots. To account for this limitation of the model, and the fact that there may well be correlated error terms over different alternatives, there have been a number of more complex models proposed in which the integral in equation 4.4 can not be calculated analytically (Train, 2003). However, as Bernasco et al. (2013) explains, whilst such models allow for spatial dependence, they do not directly treat it as an active process, instead accounting for it indirectly as part of the error term. Accounting for spatial effects in the observed part of the model enables investigation into the spatial processes that might be at play (see also Beck et al. (2006)). This is the approach taken in this study and spillover effects are incorporated into the observed part of the model. This is discussed further in the proceeding sections.

Another consequence of the model derivation is that it can be readily extended to include time-dependent utility functions. This can enable the model to account for preferences of decision-makers or characteristics of alternatives that might change over time, resulting in a dynamic utility function. Supposing that the time period of interest can be partitioned into discrete time intervals $t_1, t_2, ..., t_K$, the utility function is given by

$$U_{ijk} = V_{ijk} + \epsilon_{ijk}, \tag{4.14}$$

where the observed utility V_{ijk} is known for each decision-maker i (for $i = 1, 2, ..., N$), for each alternative j (for $j = 1, 2, ..., J$) and for each time period k (for $k = 1, 2, ..., K$). Defining the random variable Z_{ik} to be the choice of decision-maker i at time k, an analogous derivation results in

$$Pr(Z_{ik} = j) = \frac{e^{V_{ijk}}}{\sum_{l=1}^{J} e^{V_{ilk}}}. \tag{4.15}$$

The important assumption in deriving this model is that the analogous error terms ϵ_{ijk} are not only independent and identically distributed over both i and j but also over k. That is, the error terms are required to be uncorrelated over time across decision-makers. This can be viewed as quite a restrictive assumption as the choices of decision-makers tend to be consistent over time due to time-stable preferences of individuals. In what follows, a temporally dependent model will be derived for the observed utility function V_{ij} for each rioter i and potential target j. The observed utilities V_{ij} will not be explicitly dependent on time, however, and so the limitation described here does not arise. Instead, the temporal dependence will be incorporated into the utilities' dependence on each decision-maker.

4.2.2 Modelling the observed utility for rioter target choice

In order to apply the discrete choice model in equation 4.12 to the 2011 London riots, it is first necessary to define the choice set. Since it is the target choice of each offender that is of interest, as measured by the random variable Z_i for each rioter i, the choice set is required to consist of all possible locations at which each rioter could have chosen to commit an offence. Considering all possible locations as the set of points within a particular spatial region would result in an infinite choice set, contradicting the model assumptions. Consequently, a finite partition of the geographic area within which rioter targets could have been selected is required.

Given that all offences in the dataset were observed to occur within Greater London, it is assumed that all choices that could have been made were also contained within Greater London. A partition of Greater London is therefore required which enables the characteristics of each area to be evaluated for each decision-maker, in order to construct a utility function. For reasons of data compatibility, which will become clear as the utility function is specified, this set is taken to be the set of 4,765 Lower Super Output Areas (henceforth abbreviated as LSOAs) in Greater London. LSOAs are a

geographic partition of the United Kingdom for the purposes of reporting census data. Each LSOA is designed to contain around 1,500 residents, and, consequently, the set of LSOAs vary in size according to the underlying population density.

The choice to perform the analysis at this level of aggregation was made, on the one hand, to perform a novel spatial analysis of rioting at a fine scale of resolution, but, on the other, not to make the spatial resolution so fine that problems are encountered in the inference of parameters. Indeed, the LSOA geography consists of areas that are typically smaller than the units of analysis used in previous parametric approaches to the study of rioting, which have often considered the spatial patterns of rioting at a national level (Myers, 1997, 2000, 2010; Olzak and Shanahan, 1996; Spilerman, 1970, 1971, 1976). Moreover, the level of resolution offered by the LSOA geography is also smaller than many previous applications of similar discrete choice models to other types of crime (Bernasco and Nieuwbeerta, 2005; Clare et al., 2009), although newer studies have applied the model to yet smaller geographical areas (Bernasco, 2010b; Bernasco et al., 2013). The advantage of smaller sized units of analysis in the discrete choice approach is that the explanatory variables used to construct the utility function are more representative of the population and characteristics of each area. However, potential issues with using smaller areas arise with increased difficulty in accounting for spillover effects, as well as in finding structural data at an appropriate level of resolution.

The data that will be used to calibrate the model of target choice was obtained from the Metropolitan Police Service and consists of all crimes associated with the 2011 London riots. For each offence, the data included identifiers for: the LSOA within which the offence took place; the LSOA in which the offender was recorded as living; the date and time on which the offence was estimated to have occurred; and the age of the offender; all for 2,299 offences (of the total available 3,914 records). Only these records were used in the analysis and no offender appears in the data more than once.

Table 4.1 details the types of offences committed for the 2,299 records used in the analysis. The majority of crimes were incidents of burglary or theft, which supports the common view that looting was prevalent during the riots, and therefore may have influenced the target choice of offenders. Indeed, the majority of crime types are those that would commonly be associated with rioting behaviour (cf. Abudu Stark et al. (1974)). Since the primary interest lies in identifying the factors that most consistently

influenced offender spatial decision-making during the riots, all of the data is analysed.

Offence Type	**Percentage of offences**
Burglary	59.1%
Theft	11.4%
Criminal damage	6.4%
Violence against the person	4.5%
Robbery	1.7%
Other	16.8%

Table 4.1: **The distribution of different crime types over the five days of rioting (N=2,299).**

The observed component of utility V_{ij} for offender i and target j can be modelled by considering the characteristics of the target j, its relationship to the offender i, and how this might change based on the time at which the offender chooses to engage in the disorder. It is modelled as a linear combination of n variables, denoted by $W_{1ij}, W_{2ij}, ..., W_{nij}$, so that

$$V_{ij} = \beta_1 W_{1ij} + \beta_2 W_{2ij} + ... + \beta_n W_{nij}, \tag{4.16}$$

for parameters $\beta_1, \beta_2, ..., \beta_n$.

The construction of the model requires the specification of each of these variables for all values of i and j, and, in what follows, this is described for each W_{gij}, for $g = 1, 2, ..., n$. These variables are chosen in accordance with three criminological theories that have previously been used to explain the target choice of crime and rioting. These are: the theory of crowds, crime pattern theory, and the theory of social disorganisation. These theories, each of which is discussed in more detail in what follows, describe, respectively, how: the behaviour of a crowd, and therefore the presence of rioting at a particular location, influences the likelihood of selecting that area in which to riot; how decisions made with respect to rioting are influenced by the routine activities of rioters combined with the environment and urban form of the potential locations; and how rioting is more likely to occur in areas with weak social ties.

Crowd Theory

In Chapter 3, it was argued that contagion would have played a significant role in generating the spatio-temporal patterns of the riots. In particular, evidence was found to suggest that the occurrence of offences at a particular location in space and time increased the likelihood of subsequent events occurring nearby. The effect of crowds on the dynamics of target choice is therefore the first consideration in this model.

The effect of contagion arises as a result of both planned co-offending amongst rioters, and as a precipitating influence between previously unacquainted offenders. Co-offending of burglary, in which collaborators jointly commit crimes, has been shown to typically target similar areas to those targeted by sole offenders (Bernasco, 2006). Target choice among previously unacquainted offenders, however, has rarely been considered from a modelling perspective, particularly at a relatively fine spatial scale, such as that proposed here.

In Chapter 3, two possible explanations for contagion during outbreaks of rioting were discussed. The first stated that contagion was the result of shared grievances across a widely distributed population and had little to do with the initial location of the rioter. The second argued that contagion during rioting was a result of situational precipitators, in which proximity to rioting in space and time served to prompt, permit, pressure and provoke others to partake in criminal activity (Wortley, 2008). These two perspectives imply a rational choice approach when considering the decision to engage in the disorder: potential offenders weigh up the potential benefits (e.g. the opportunity to address grievances or for criminal acquisition) against the potential costs (cost of arrest or political prosecution). Perhaps surprisingly, much early research into rioting did not take a similar view. In fact, early theories concerning the behaviour of crowds during rioting, such as those posited by Le Bon (1896; 1960) and Freud (1921), suggested that crowds were irrational, 'animal-like', and that the behaviour of the crowd could only be considered from the perspective of an irrational collective mind, with targets more or less selected at random. Within such crowds, individuals were supposed to be unable to control their own behaviours, were 'swept up', and adopted the incentives of this collective mind. From the perspective of complex systems, this interpretation of the aggregation of behaviour implies that it is the interactions between individuals that is most prominent in determining the macro-level outcomes, rather than the internal

incentives and choices of the individuals.

Since this early work, however, researchers have argued that the process of rioting is, in fact, driven by a more rational process (Berk and Aldrich, 1972; Berk, 1974; Mason, 1984; McPhail, 1991). According to such accounts, individuals decide whether to engage in the rioting based on the available information and some internal cost-benefit calculation. Even after individuals have decided to engage, they have more control over their actions than is suggested by early accounts of collective violence. For instance, there is evidence that targets can be chosen selectively by rioters (Auyero and Moran, 2007; Berk and Aldrich, 1972; Rosenfeld, 1997), and, indeed, that, by considering those targets, more can be learnt about the mechanisms at play during riots (Martin et al., 2009). In this interpretation of crowds, in contrast to earlier theories, the incentives and choices of the individual play a more prominent role in the aggregation of crowd behaviour. Moreover, this viewpoint supports the approach taken in this section, suggesting that, consistent with rational choice theory, an element of rationality is present in the decision-making of individuals.

Recent treatments of crowds have often incorporated individual incentives with some degree of rationality, but also allow individuals to be influenced by the actions of those around them. For example, Gordon et al. (2009) extend a traditional economic model that estimates an individual's 'willingness to pay' for a certain good, in order to incorporate the impact of interaction between individuals. This perspective of crowd behaviour, in which individuals, or agents, influence the behaviour of others, each of whom has their own set of behaviours, attributes, or objectives, and which might vary widely over the population, has also previously been considered in models of rioting and civil disorder (Granovetter, 1978; Midlarsky, 1978; Myers, 2000; Epstein, 2002).

As emphasised in Myers (2000), care must be taken in interpreting the influence of crowds, in order to avoid confusion between irrational actors having no choice in getting swept up in rioting—as would be the case in contagion of a disease, and traditional theories of crowd behaviour—and actors that are perhaps more willing to engage in disorder due to the precipitating influence of crowd behaviour after weighing up the costs and benefits of doing so. Using the perspective of bounded rationality, the latter view is the one that is taken here. It is important to be clear that such an argument does not assume that offenders cease to act like rational agents, but that the decision to

engage in a criminal event can be rather dynamic and may be influenced by more than an individuals internal desires or motivations.

In order to incorporate riot precipitators into the model of target choice, it is assumed that the utility of each target depends on the number of riot-related offences that have recently occurred at that target. It is hypothesised that, all other things being equal, areas in which riots have recently occurred will be more likely to be selected by rioters in which to offend.

To measure the effect that prior offences at a location have on the spatial decision-making of a new potential rioter, for each rioter decision, the number of detected offences that occurred for a certain time period before the decision is made to offend are counted. The sum of this calculation is denoted by $W_{1ij}^{\delta t}$, where the subscript j corresponds to the target area, the subscript i refers to the decision-maker, which implicitly determines the time at which the decision to offend is made, and the superscript δt denotes the time period before the decision is made over which offences contribute to the count. For example, for $\delta t = 12$, the sum of prior offences in a given area is taken to be the number of offences that occurred in the previous 12 hours from the time at which the decision to offend is made.

The variable $W_{1ij}^{\delta t}$ is taken to depend on the time at which offender i commits their offence. Although implicitly dependent on time, the model is not the same as the temporal version of the discrete choice model in equation 4.15, as decision-makers do not make a decision at every discrete time interval. Instead, only one decision for each offender is made. It is assumed that the time at which each offence occurs is given, and that an offender becomes motivated to commit their offence at this particular time due to processes that are not under direct consideration here. For this reason, the variable is indexed by the decision-maker i, which is assumed to incorporate information on when the decision is made, rather than any explicit temporal dependency as in equation 4.15.

A question that was not addressed in Chapter 3 was the length of time that any increased level of attractiveness due to ongoing rioting lasts at a particular area. That is, for how long does the precipitating influence of prior events at a given location last? Turning again to the literature on criminology, this influence has been widely studied in the case of the increased attractiveness of targets of residential burglary (Bowers and Johnson, 2005; Johnson and Bowers, 2004), in which the effect of increased risk due to

a recent burglary has been observed to last for up to two months. Given the highly dynamic nature of the riots, its short time-scale, and the fact that each offender is included in the dataset only once (which is in contrast to the literature on burglary in which at least part of the increased attractiveness at a particular site is often attributed to offenders returning to where they have successfully burgled previously), it is anticipated that the time scales over which increased risk may be observed are much shorter. To test this, models are run with $\delta t = 6$, 12, and 24 hours, and the relative success of each of these models is evaluated.

In selecting these variables, models were also run with $\delta t < 6$; however, singularities were encountered in the calibration procedure due to there being insufficient variance in the variable $W_{1ij}^{\delta t}$. $\delta t = 6$ was the minimum value for which the model was successfully calibrated and is therefore used as the minimum value in this study.

Crime Pattern Theory

There have been many attempts at explanations of the spatial and temporal clustering of crime. Environmental criminology is specifically concerned with explaining how environmental effects—which can incorporate a range of spatial and temporal processes—influence the prevalence of different types of crime (Brantingham and Brantingham, 1981). Much of this theory builds upon the routine activity approach, which asserts that the necessary conditions for crime to occur are the convergence in space and time of: a motivated offender; a suitable target; and the absence of a capable guardian (Cohen and Felson, 1979). According to this approach, routine activity patterns—defined as the locations and times at which individuals are more likely to be found as a direct result of their everyday behaviour, for example on the route to work before the start of the working day or at recreational areas in the evening—shape the opportunities for this convergence. From this perspective, crime is seen as opportunistic: offenders are largely believed to come across opportunities to commit crimes as a result of their everyday routines, rather than purposefully going out of their way to commit a particular offence. The routine activity approach stimulated great interest in understanding crime as a (bounded) rational process that focused on the environmental circumstances in which crime occurs, rather than the underlying psychological makeup of offenders.

Resulting from this interest, crime pattern theory argues that the patterns brought

about by the occurrence of crime in space and time are a direct result of those areas being more likely to coincide with the routine activity patterns of potential offenders (Brantingham and Brantingham, 1993). Moreover, crime pattern theory considers how routine activity patterns shape awareness of criminal opportunities, and how this may lead to the emergence of spatial concentrations of crime. According to crime pattern theory, people create mental maps of their routine activity patterns, which typically consist of routine activity nodes (locations at which individuals frequently visit, or at which they spend much of their time), and the routes that the individual takes to travel between these nodes. It is asserted that it is at these locations that crimes are more likely to be committed by an individual.

Prominent features of the urban environment are expected to lie within the awareness spaces of a range of different people, including many potential offenders. In particular, much of the population of London and other urban areas around the world, are highly likely to retain local landmarks—including retail centres, transport hubs such as train stations and schools—within their awareness spaces as routine activity nodes, which makes these areas more likely to experience crime. Bernasco and Block (2009) provide evidence that this is indeed the case with these examples in a study of robbery in Chicago.

Consequently, on the basis of crime pattern theory, it is hypothesised that during rioting, with all other things being equal, offenders will be more likely to choose locations to offend that are nearby schools, public transport hubs, retail centres and locations that are proximate to the city centre, as these represent locations which are likely to be prominent within the mental maps of a wide range of rioters.

In order to incorporate these effects into the model of V_{ij}, W_{2j} is taken to be the number of key stage 4 schools (roughly equivalent to secondary schools for those aged 11-16) in each LSOA and is counted using data from the UK Department of Education.

W_{3j} is taken to be a binary indicator of whether or not an underground station is located within the LSOA j. The locations of underground stations are obtained from Open Street Map (www.openstreetmap.org). Crime pattern theory does not only assume that transport hubs are areas that much of the population would be familiar with, and therefore more likely to be located in the mental maps of offenders, but also that transport hubs are likely to be areas travelled through as potential rioters move

between prominent locations in their awareness spaces.

W_{4j} is taken to be a measure of retail floorspace within each target area j, obtained from the Valuation Office Agency floorspace data for the year 2004 (see www.planningstatistics.org.uk). Specifically, it is taken to be the number of $250m^2$ portions of retail floor space within each area j, where the units are chosen to aid interpretation of the resulting parameter estimates. In the case of rioting, retail centres in particular may be targeted simply because they contain opportunities for looting, rather than as a direct result of that location being present in the routine activity nodes of offenders. Nevertheless, it is expected that retail centres will act as crime attractors, and that, where they are targeted, the retail centres chosen will be those that are likely to be within an offender's awareness space.

Finally, W_{5j} is taken to be the distance between the centroid of the target LSOA j and the centre of London (measured as a point just south of Trafalgar Square: longitude -0.1277, latitude 51.5073) in kilometres.

In the framework of the discrete choice model outlined in Section 4.2.1, it is possible to incorporate variables into the observed utility V_{ij} that not only depend on the target location j but which also depend on the offender i who is making the choice of where to offend. This enables further variables inspired by crime pattern theory to be incorporated. In particular, although overlapping mental maps provide the opportunity to capture routine activity nodes for a wide range of the population, the best indicators for routine activity nodes are likely to more specific to each individual.

For the 2011 London riots, given that the offender data details not only where the crime occurred but also where the offender resided, it is possible to incorporate into V_{ij}, for each offender i, the distance between the area in which the offender resided and the area j in which that offender could have chosen to engage in the disorder. This contributes to the utility of each area a measure of how far the target is from where the rioter is most likely to have been based and the locations with which the rioter is likely to be most familiar. Supposing that the awareness space of an offender is more likely to contain areas near to where that offender resides, it would be expected that targets closer to the residential area of each rioter are more likely to experience rioting.

In fact, there has been much prior research into the so-called journey to crime: the distance between an offenders residential location and the location at which they

commit their crime. Supporting the principle proposed by Zipf (1949), that individuals are most likely to take up the option that provides the most reward for the least effort, studies of the journey to crime indicate that, despite the many and varied opportunities available to them, most offenders commit crime close to their home location (for a recent review of this literature, see Townsley and Sidebottom (2010)).

To operationalise a measure of journey to crime, the Euclidean distance between the LSOA centroid within which each offender was recorded as living, and the LSOA centroid of each target area was calculated, and incorporated as one of the variables in the model for the observed utility, denoted by W_{6ij}.

In the case that an offender committed an offense within the LSOA within which they reside, the distance between the more precise locations at which they were recorded as living and at which they committed their offence was computed. These more precise locations are given by the centroids of the census output area, the finest level of aggregation at which the data are available.

Figure 4.1 shows the distribution of these journey to crime distances. Consistent with previous studies, and in line with the expectations of crime pattern theory, a clear pattern of distance decay can be observed. Moreover, the scale and central tendency of the distribution of distances travelled is very similar to that for other types of crime (Rossmo, 2000).

Offender awareness of a location is expected to be inversely related to the distance between that location and their routine activity nodes. For studies into the journey to crime, distance is considered to be a measure of impedance that affects the likelihood of an individual becoming familiar with a particular area. However, factors other than distance can influence awareness in this way. For example, features of the urban environment, such as natural barriers (e.g. rivers) or transport links (e.g. train stations), may impede or facilitate the ease with which people can travel to, and hence become familiar with, a particular location. In their study, Clare et al. (2009) examined the extent to which features of the physical environment, such as major highways and rivers, act as barriers to an offender's choice of burglary location. They found that the presence of either feature between an offender's home location and a potential target area decreases the likelihood that the latter will be selected. Furthermore, studies of gang activity in Los Angeles have found that such environmental boundaries appear to sig-

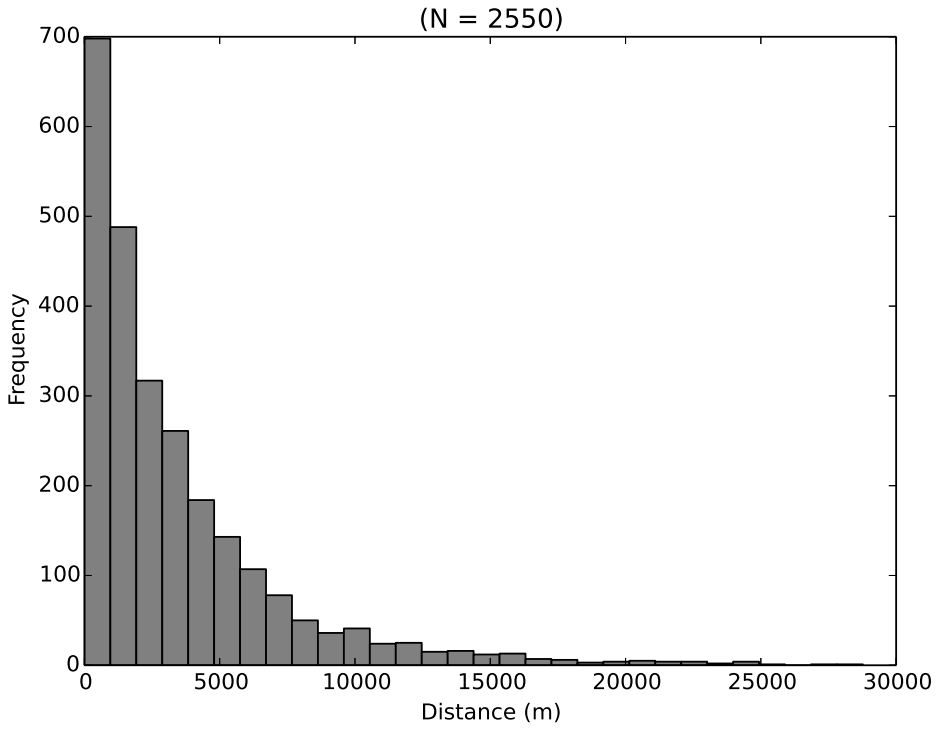

Figure 4.1: **Histogram of the distance between residential location and offence location.** The distances are calculated as the Euclidean distance between the centroids of the LSOAs recorded as the residential area and the crime area of each offender.

nificantly influence the spatial patterns of gang rivalries (Tita et al., 2003; Radil et al., 2010).

In the case of London, it is likely that the greatest such barrier and, thus, influence of this kind on the spatial decision-making of offenders, is the River Thames. The Thames divides London into distinct northern and southern areas, and, while there are bridges that connect North and South London, the presence of the Thames can substantially impede movement between the two. Given the size of the river and the scope for natural barriers to shape offender awareness spaces, it is expected that offenders will be less likely to cross the river in order to offend. In order to incorporate this effect into the model, each LSOA is coded as being located either north or south of the Thames so that, for any LSOA pair, it is possible to indicate whether the two areas are located on the same side of the river. The variable W_{7ij} is then defined to be an indicator variable that determines whether or not the residential area of offender i and the target area j are located on the same side of the River Thames.

Finally, since the model for V_{ij} is a linear combination of the variables W_{gij}, for $g = 1, 2, ..., n$, it is possible to disaggregate them by considering different types of offender. To explain why this might be desirable, it is first considered how the awareness spaces of individuals might vary over different offenders. Previous research has suggested that the awareness space of offenders is unlikely to remain static throughout an individual's lifetime (Bernasco, 2010a). As people move houses, jobs, and take up new activities, they are likely to encounter areas they have not encountered before. These experiences will all contribute in some way to the mental map of an individual. Moreover, it is hypothesised that the mental map of minors—those under the age of 18—will have a more restricted mental map, than compared to both their own mental map when they are older, but also to the mental maps of older individuals. Because of this, it might be the case that older offenders have a wider range of locations in which they can choose to offend. They might also have more means to travel there, as older offenders can be expected to have more disposable income to travel via public or private transport. It is therefore hypothesised that adult offenders are more likely to travel further than their younger counterparts (such findings have been reported for other types of crime in Snook et al. (2005); Townsley and Sidebottom (2010)).

Figure 4.2 shows the age distribution of offenders. A large proportion of the of-

fenders were under the age of twenty, however, offenders across the age spectrum are represented, creating the skewed distribution observed; a distribution that is very similar to the typical age-crime curve (Stolzenberg and D'Alessio, 2008). In particular, this figure demonstrates that there were a significant number of offenders under the age of 18, and so, the journey to crime variable W_{6ij} is separated by an indicator function into:

$$\beta_6 W_{6ij} + \beta_6^a I_a(i) W_{6ij}, \tag{4.17}$$

where $I_a(i)$ is equal to one if offender i is over the age of 18, and equal to zero otherwise. β_6 therefore measures the effect that distance has on the utility of each area to juveniles, whilst $\beta_6 + \beta_6^a$ measures the same effect but for adults.

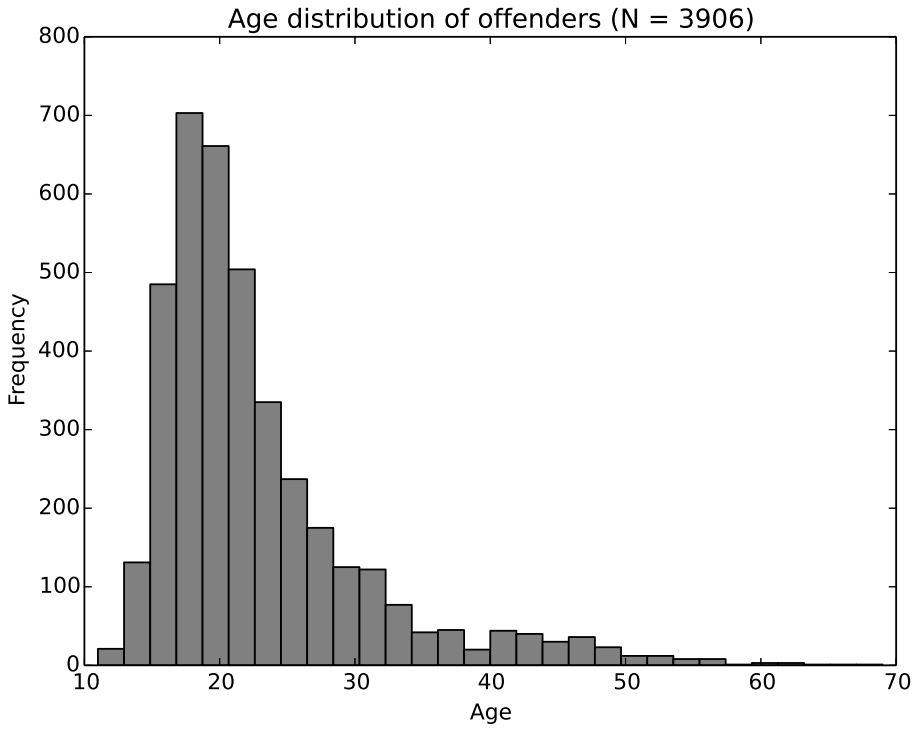

Figure 4.2: **Age distribution of offenders.** Of the total available 3,914 offences contained in the data, 3,906 contained the age of the offender.

To further distinguish between the offending behaviour of minors and adults, it is noted that some nodes of activity, such as schools, work locations and retail centres, might feature more prominently in the awareness spaces of particular age groups. Young offenders might be more likely to target areas that contain routine activity nodes

that are particularly relevant to them, such as schools. Therefore, in a similar way to the journey to crime variable, the variable used to denote the count of schools in each area is also disaggregated as follows:

$$\beta_2 W_{2j} + \beta_2^a I_a(i) W_{2j}, \tag{4.18}$$

with analogous interpretations for β_2 and β_2^a.

Social Disorganisation

The theory of social disorganisation largely stems from the influential work of Shaw and McKay (1969), who investigated the relationship between neighbourhood characteristics and the spatial distribution of crime and delinquency in the US city of Chicago. They concluded, amongst other things, that the areas within Chicago containing residents who were economically disadvantaged, ethnically diverse and who were residentially mobile, were more likely to have higher rates of crime and delinquency.

Social disorganisation theory was used as an explanation of this effect, and asserts that the inability of a community to jointly identify common social values, and to subsequently exert effective informal social controls, substantially increases the crime and delinquency within an area. That is, for neighbourhoods in which there is a strong sense of community and mutual cooperation, residents are more likely to intervene to prevent crime. Reviews of the development of social disorganisation theory can be found in Bursik (1988) and Kubrin and Weitzer (2003).

Tests for social disorganisation theory typically identify conditions that might lead to a lack of social cohesion, which can be affected by a number of different neighbourhood characteristics. For neighbourhoods with a transient population, for example, brought about by a large flux of inward and outward migration, it is asserted that there will be relatively fewer opportunities for the formation of stable social ties, leading to the lack of social cohesion which fosters inability to jointly act to prevent and mitigate crime. Other conditions identified as having an impact on the resulting crime and delinquency rates include ethnic heterogeneity (it is argued that diversity amongst individuals can act as a barrier to social cohesion as different communities can fail to share consensus), family disruption (close family is often viewed as a first opportunity to exert such informal social control), and deprivation (rather than having a direct result on levels of crime, it is argued that within disadvantaged neighbourhoods, communities

may lack the resources and organisational base of their more affluent counterparts, and so are less likely to exert formal control) (Sampson and Groves, 1989; Sampson et al., 1997; Bernasco, 2006).

In the case of rioting, in accordance with previous studies, the level of social disorganisation of an area can influence the likelihood of disorder occurring there in slightly different ways. First, cohesive neighbourhoods may exert control over their own residents to reduce the likelihood that they will engage in disorder or form a rioting crowd. Since most of the rioting occurred nearby the residential areas of the rioters (see Figure 4.1), it is likely that if this explanation has a role to play, there would be a reduced risk of rioting in areas with greater social cohesion. Second, signs of cohesion within a neighbourhood might affect whether offenders, regardless of where they live, choose to engage in disorder within that neighbourhood. In this case, social cohesion might be seen as acting as a social barrier to deter rioters from targeting or coalescing in a given neighbourhood (Bernasco (2006) argues this from the perspective of target choice for residential burglary).

It is therefore reasonable to hypothesise that there is an increased likelihood of areas being selected as targets for rioting if those areas have greater levels of social disorganisation. In order to incorporate the impact of social disorganisation into the measure of observed utility for each rioter, three measures of each target area are calculated. It should be noted that in this study the levels of social disorganisation are measured indirectly (as in Shaw and McKay (1969)), rather than through the use of survey samples that attempt to more directly measure local social processes (Sampson and Groves, 1989; Sampson et al., 1997).

The first variable estimates the extent to which the population in a given area j is transient by considering the inward and outward migration within each area. This is done using a measure of population churn, as outlined in Dennett and Stillwell (2008), which quantifies the residential migration of individuals. Specifically, this measure is given by

$$W_{8j} = \left(\frac{D_j + O_j + M_j}{P_j} \right) \times 10, \tag{4.19}$$

where D_j is the in-migration to area j over a particular period of time, O_j is the out-migration from the area and M_j is the total migrants that relocate from one residence to another whilst remaining within the same area j over that time period. P_j is the popu-

lation of area j. Using the best data available for this purpose, the values of D_j, O_j and M_j were obtained for each LSOA in Greater London from the 2001 UK Census. This data was obtained by asking census participants for their usual address one year earlier. The multiplicative factor of 10 was chosen as a scaling factor to aid interpretation of the resulting estimates, which otherwise has no bearing on the results.

The second variable to incorporate into the estimate of observed utility for each target measures the ethnic heterogeneity of each target area. The index of qualitative variation (Agresti and Agresti, 1978; Wilcox, 1973) is used, and defined as

$$W_{9j} = \left(1 - \sum_{k=1}^{E} e_{kj}^2\right) \times 10, \tag{4.20}$$

where E is the total number of distinct ethnic groups and e_{kj} is the proportion of individuals belonging to ethnic group k, that reside in area j. W_{9j} is interpreted to be a measure of the probability that two individuals selected at random from the population of zone j will be of different ethnicity. The data is again obtained from the 2001 UK Census, which specifies the number of residents of different ethnicities in each LSOA in Greater London. The different ethnic groups specified and included in the model are: White British, White Irish, Other White, White and Black Caribbean, White and Black African, Other Mixed, Indian, Pakistani, Bangladeshi, Other Asian, Caribbean, African, Other Black, Chinese, Other Ethnic Group. Again, the scaling factor of 10 was chosen to aid parameter interpretation.

A potential source of error with the findings associated with these variables is that the data used to estimate neighbourhood levels of ethnic diversity and population churn are based on data from the 2001 UK census. These data were used as they are the most recent that are available, and, in using them, it is assumed that the demographics (and changes in them) of an area are relatively stable on the time-scale of a decade.

Finally, a measure of deprivation is incorporated into the observed utility of each target choice. Denoted by W_{10j}, this is given by the Index of Multiple Deprivation, a measure used extensively in the UK to determine disadvantaged areas (McLennan et al., 2011). The estimates from 2010 are used as they are the most recent available, and just one year away from the time at which the riots occurred.

Spillover effects and controls

Several variables have been defined and have been argued to help capture the observed component of utility of each target area for each offender and, in the case of contagion, over different periods of time. In addition to the variables discussed above, a measure of population density of each target area is also included in the model, denoted by W_{11j}. This is included to control for its potential effects and is obtained using the Mid-2010 Population Estimates for LSOAs by the UK Office for National Statistics.

It was discussed in Section 4.2.1 that the inclusion of spatially lagged variables in the specification of the observed utility can mitigate some of the unintended effects that arise due to independence of irrelevant alternatives. Spatial spillover occurs when a rioter is attracted to a particular area not due to the attributes of that area, but to the attributes of a neighbouring area. If this were to occur, then the errors in the utility of each target area would no longer be independent, violating the assumptions of the model. In the case of the London riots, for example, it may be that an offender chose to go to an area that contained an underground station. They then might have walked from the underground station to a neighbouring area and found a suitable opportunity to offend in that neighbouring area. In this situation, the effect of having an underground station in a neighbouring area influences the attractiveness of the area that the rioter chose, and so the unobserved portion of utility over these choices is no longer independent, as assumed by the model. To account for this, the attributes of neighbouring areas can be incorporated into the utility of each area, in an attempt to capture the correlation across the unobserved utility within the observed utility, thereby ensuring that the errors remain independent and the model assumptions are not violated. To do this, a similar approach to Bernasco et al. (2013) is used. In what follows, the spillover effects accounted for in the model are described.

In Chapter 3, it was shown how the occurrence of offences in a particular location can increase the likelihood of offences occurring in neighbouring locations. Since the number of prior offences is incorporated within the model in the variable $W_{1ij}^{\delta t}$, it is natural to also include a spatially lagged version of this variable. It is therefore hypothesised that areas will be more likely to be selected by rioters if neighbouring areas have recently experienced rioting. The number of offences that occur in neighbouring areas to the target area j within δt hours preceding the time at which rioter i decides to

engage in the disorder is denoted by $W^{\delta t}_{12ij}$.

In order to test for further spatial spillover effects, three neighbourhood variables are also incorporated into the model of observed utility. These are: the average number of schools in neighbouring areas, denoted by W_{13j}; an indicator variable to determine whether the neighbouring area contained an underground station, denoted by W_{14j}; and the average retail floor space in neighbouring areas, denoted by W_{15j}. All neighbouring areas are defined with queen contiguity: areas need to just share a single point of a boundary in order to be classed as neighbours.

Extending equation 4.16 to incorporate the variables discussed, leads to the final model for the observed utility of each target area j, for each offender i:

$$\begin{aligned} V^{\delta t}_{ij} =& \beta^{\delta t}_1 W^{\delta t}_{1ij} + \beta_2 W_{2j} + \beta^a_2 I_a(i) W_{2j} + \beta_3 W_{3j} + \beta_4 W_{4j} + \beta_5 W_{5j} \\ &+ \beta_6 W_{6ij} + \beta^a_6 I_a(i) W_{6ij} + \beta_7 W_{7ij} + \beta_8 W_{8j} + \beta_9 W_{9j} + \beta_{10} W_{10j} \\ &+ \beta_{11} W_{11j} + \beta^{\delta t}_{12} W^{\delta t}_{12ij} + \beta_{13} W_{13j} + \beta_{14} W_{14j} + \beta_{15} W_{15j}, \end{aligned} \tag{4.21}$$

where the vector of parameters $\boldsymbol{\beta} = (\beta_1, \beta_2, ...\beta_{15})$ is to be estimated from the data. For ease of notation in what follows, equation 4.21 is written in vector notation as

$$V^{\delta t}_{ij} = \boldsymbol{\beta}.\mathbf{W}^{\delta t}_{ij}, \tag{4.22}$$

where $\mathbf{W}^{\delta t}_{ij}$ is the vector of variables associated with offender i and target j and includes the indicator function $I_a(i)$. Each of the distinct variables included in this model is outlined in Table 4.2, together with the theoretical perspective from which the argument for including each variable stems.

4.2.3 Parameter estimation

Without specifying a particular value for the vector of parameters $\boldsymbol{\beta}$, the discrete choice model determines a family of models. Equation 4.12 specifies the form by which the observed components of utility influence the probability that a given alternative is selected, whilst equation 4.21 determines the way in which observed utilities are derived from data associated with each alternative. Moreover, the role of equation 4.21 is to proxy the effect of the theoretical perspectives discussed in Section 4.2.2 into the utility of each target. In this section, the vector of parameters $\boldsymbol{\beta}$ is estimated using the offence data from the 2011 London riots. In doing so, the model becomes fully specified, enabling the estimation of the probability that rioter i would have selected target j, for

Variable	Parameter	Description	Expected effect of higher values on attractiveness	Theoretical perspective
$W_{1ij}^{\delta t}$	$\beta_1^{\delta t}$	Previous offence count	Increase	CT
W_{2j}	β_2, β_2^a	Number of schools	Increase, particularly to juveniles	CPT
W_{3j}	β_3	Underground station indicator	Increase	CPT
W_{4j}	β_4	Retail floorspace	Increase	CPT
W_{5j}	β_5	Distance to city centre	Decrease	CPT
W_{6ij}	β_6, β_6^a	Distance between residence and target	Decrease, particularly to juveniles	CPT
W_{7ij}	β_7	Thames between residence and target	Decrease	CPT
W_{8j}	β_8	Churn rate	Increase	SDT
W_{9j}	β_9	Ethnic diversity	Increase	SDT
W_{10j}	β_{10}	Deprivation	Increase	SDT
W_{11j}	β_{11}	Population density	None	Control
$W_{12ij}^{\delta t}$	β_{12}	Previous offence count in neighbouring areas	Increase	Spillover
W_{13j}	β_{13}	Number of schools in neighbouring areas	Increase	Spillover
W_{14j}	β_{14}	Number of underground stations in neighbouring areas	Increase	Spillover
W_{15j}	β_{15}	Average retail floorspace in neighbouring areas	Increase	Spillover

Table 4.2: **The variables used to estimate the observed utility of each target.** The theoretical perspective from which each variable stems is also shown and the following abbreviations are used: Crowd theory = CT; Crime pattern theory = CPT; Social disorganisation theory = SDT.

every i and j, given the offences that have occurred up until the point in time at which rioter i engages with the disorder.

Furthermore, by selecting the value of $\boldsymbol{\beta}$ that results in the best fit between the model and the offence data, it is possible to observe the influence of each of the variables in equation 4.21 on the observed utility, and the resulting probability distribution. If, for some g, β_g is estimated to be equal to zero, then that variable is asserted to play little role in the attractiveness of targets to rioters, according to the data used in the calibration procedure. Alternatively, if β_g is estimated to be positive with a high level of confidence, then the associated variable is positively associated with the attractiveness of each target: higher values of that particular variable at a target are thought to increase its attractiveness. Conversely, if β_g is estimated to be negative with a high level of confidence, then higher values of the associated variable are thought to decrease attractiveness.

The log-likelihood function

The form of the discrete choice model is particularly suitable for maximum-likelihood estimation, in which the parameter vector is selected that maximises the likelihood of observing the data over all possible values of $\boldsymbol{\beta}$. Specifically, the likelihood function is defined as

$$\begin{aligned}&\mathcal{L}(\boldsymbol{\beta}|Z_N = z_N, Z_{N-1} = z_{N-1}, ..., Z_1 = z_1)\\&\quad = Pr(Z_N = z_N, Z_{N-1} = z_{N-1}, ..., Z_1 = z_1|\boldsymbol{\beta}),\end{aligned} \tag{4.23}$$

where a lower case variable z_i denotes the realisation of the random variable Z_i. Equation 4.23 states that the value of the likelihood function is the probability of observing the empirical data, given the modelled joint probability distribution together with a particular value for $\boldsymbol{\beta}$. Applying Bayes rule to the joint distribution, and conditioning so that conditional dependencies are applied to the events in chronological order, it can be shown that

$$\begin{aligned}&\mathcal{L}(\boldsymbol{\beta}|Z_N = z_N, Z_{N-1} = z_{N-1}, ..., Z_1 = z_1) =\\&\quad Pr(Z_N = z_N|Z_{N-1} = z_{N-1}, Z_{N-2} = z_{N-2}, ..., Z_1 = z_1)\\&\quad \times Pr(Z_{N-1} = z_{N-1}|Z_{N-2} = z_{N-2}, Z_{N-3} = z_{N-3}, ..., Z_1 = z_1)\\&\quad \times ... \times Pr(Z_1 = z_1).\end{aligned} \tag{4.24}$$

Using the model for the probability distribution in equation 4.12, the conditional probability for a random variable Z_i is assumed to be given by

$$Pr(Z_i = z_i | Z_{i-1} = z_{i-1}, Z_{i-2} = z_{i-2}, ..., Z_1 = z_1) = \frac{e^{V_{ij}^{\delta t}}}{\sum_{l=1}^{J} e^{V_{il}^{\delta t}}}, \tag{4.25}$$

where $V_{ij}^{\delta t}$ is given as in equation 4.21. The probabilities can be taken to be equivalent to conditional probabilities because the model for the probability distribution depends on the history of the system, and specifically on the realisations of random variables $Z_{i'}$ for $i' < i$. In other words, each decision-maker selects the alternative that offers them the most utility using the information on where rioters have previously offended. Consequently, the likelihood function is given by

$$\mathcal{L}\left(\boldsymbol{\beta} | z_N, z_{N-1}, ..., z_1\right) = \prod_{i=1}^{N} \prod_{j=1}^{J} \left(\frac{e^{V_{ij}^{\delta t}}}{\sum_{l=1}^{J} e^{V_{il}^{\delta t}}} \right)^{\mathbf{1}(z_i = j)}, \tag{4.26}$$

where $\mathbf{1}(z_i = j)$ is an indicator function, equal to one if $z_i = j$, and equal to zero otherwise.

In order to maximise the likelihood function, it is often computationally more efficient to maximise the logarithm of the likelihood function, and this case is no exception. This is possible since the logarithm is a monotonically increasing function, and thus the maximum of the logarithm of a function occurs at the same location as the maximum of the function. Taking the natural logarithm, and substituting in equation 4.22, equation 4.26 becomes

$$\ln \mathcal{L}\left(\boldsymbol{\beta} | z_N, z_{N-1}, ..., z_1\right) = \\ \sum_{i=1}^{N} \sum_{j=1}^{J} \mathbf{1}(z_i = j) \boldsymbol{\beta}.\mathbf{W}_{ij}^{\delta t} - \sum_{i=1}^{N} \sum_{j=1}^{J} \mathbf{1}(z_i = j) \ln \left(\sum_{l=1}^{J} \exp(\boldsymbol{\beta}.\mathbf{W}_{il}^{\delta t}) \right). \tag{4.27}$$

The maximum likelihood estimator for $\boldsymbol{\beta}$ occurs when

$$\left(\frac{\partial \ln \mathcal{L}}{\partial \beta_1}, \frac{\partial \ln \mathcal{L}}{\partial \beta_2}, ..., \frac{\partial \ln \mathcal{L}}{\partial \beta_n} \right) = (0, 0, ..., 0). \tag{4.28}$$

Differentiating the terms in equation 4.27, it can be shown that, for $g = 1, 2, ..., n$,

$$\frac{\partial}{\partial \beta_g} \sum_{i=1}^{N} \sum_{j=1}^{J} \mathbf{1}(z_i = j) \boldsymbol{\beta}.\mathbf{W}_{ij}^{\delta t} = \sum_{i=1}^{N} \sum_{j=1}^{J} \mathbf{1}(z_i = j) \mathbf{W}_{gij}^{\delta t}, \tag{4.29}$$

and that

$$\begin{aligned}
&\frac{\partial}{\partial \beta_g} \sum_{i=1}^{N} \sum_{j=1}^{J} \mathbf{1}(z_i = j) \ln \left(\sum_{l=1}^{J} \exp(\boldsymbol{\beta}.\mathbf{W}_{il}^{\delta t}) \right) \\
&\qquad = \sum_{i=1}^{N} \sum_{j=1}^{J} \mathbf{1}(z_i = j) \frac{\sum_{l'=1}^{J} W_{gil'}^{\delta t} \exp(\boldsymbol{\beta}.\mathbf{W}_{il'}^{\delta t})}{\sum_{l=1}^{J} \exp(\boldsymbol{\beta}.\mathbf{W}_{il}^{\delta t})} \\
&\qquad = \sum_{i=1}^{N} \sum_{j=1}^{J} \mathbf{1}(z_i = j) \sum_{l'=1}^{J} W_{gil'}^{\delta t} Pr(Z_i = l') \\
&\qquad = \sum_{i=1}^{N} \sum_{l'=1}^{J} W_{gil'}^{\delta t} Pr(Z_i = j'), \qquad (4.30)
\end{aligned}$$

where the final equality arises due to the fact that $\sum_{j=1}^{J} \mathbf{1}(z_i = j) = 1$ (i.e. that each rioter makes exactly one choice). Consequently, the derivative of the log-likelihood in equation 4.27 is:

$$\begin{aligned}
&\frac{\partial}{\partial \boldsymbol{\beta}} \ln \mathcal{L}\left(\boldsymbol{\beta} | z_N, z_{N-1}, ..., z_1\right) = \\
&\qquad = \sum_{i=1}^{N} \sum_{j=1}^{J} \mathbf{1}(z_i = j) \mathbf{W}_{ij}^{\delta t} - \sum_{i=1}^{N} \sum_{j=1}^{J} \mathbf{W}_{ij}^{\delta t} Pr(Z_i = j) \qquad (4.31) \\
&\qquad = \sum_{i=1}^{N} \sum_{j=1}^{J} \left(\mathbf{1}(z_i = j) - Pr(Z_i = j)\right) \mathbf{W}_{ij}^{\delta t}. \qquad (4.32)
\end{aligned}$$

Thus, the value of $\boldsymbol{\beta}$ that maximises the log-likelihood satisfies

$$\sum_{i=1}^{N} \sum_{j=1}^{J} \left(\mathbf{1}(z_i = j) - Pr(Z_i = j)\right) \mathbf{W}_{ij}^{\delta t} = 0. \qquad (4.33)$$

In McFadden (1974), it is shown that the function $\ln \mathcal{L}(\boldsymbol{\beta})$ is strictly concave, and, therefore, that if a value $\boldsymbol{\beta}$ satisfies equation 4.33, and is a local maximum, then it is also the global maximum. This result, together with the existence criteria detailed in McFadden (1974), ensures that robust and efficient estimation procedures are available to calibrate the model. Moreover, these properties have led to the model in equation 4.12, with linear-in-parameter observed utility functions V_{ij} being used widely for the analysis of choice problems.

Optimisation

Using the offence data from the 2011 London riots, 2,299 choice events are used to calculate the likelihood function, together with the data detailing attributes of each alternative, as described in section 4.2.2. The value of $\boldsymbol{\beta}$ that maximises the log-likelihood

is found using the Survival package in the statistical software R (Therneau, 2014). This particular package has been widely used in the estimation of multinomial logistic regression models and is employed here due to its convergence speed with a large number of observations in the calculation of the likelihood function. The optimisation procedure that this software performs is based upon the algorithm presented in Gail et al. (1981).

Since the calculation of the maximum likelihood estimator requires the comparison of each of the 2,299 offenders with each of the 4,765 choices available to that offender (corresponding to the LSOA geography in Greater London), the amount of computation required is very large, and, in this case, the computational power available to run the optimisation (64-bit version of R running on 3.2 GHz Intel Core i3 with 4GB RAM) is quickly exceeded.

One way of circumnavigating the need to include all of the required data, and to consequently reduce the computational requirements, is to use sampling methods. These approaches estimate the likelihood function by, for each offender, selecting a random sample of alternatives that were not chosen, in order to compare against the location that was chosen. Such approaches have been shown to produce consistent estimates for the parameter values (Bernasco et al., 2013).

For this study, however, sampling methods are not used and instead the entire dataset is incorporated by splitting up the analysis and running separate optimisation procedures for each day of rioting. Running a separate optimisation for each day is possible using the available computational power, and, furthermore, enables the examination of if and how the parameter estimates varied on each day of rioting. If the parameter estimates are consistent over the different days tested, it would provide evidence that the conclusions that may be drawn from them are robust under the data for the different days (which involves different offenders since each offender appears in the dataset only once).

The number of offences that occur for each day of rioting, and therefore the number of offences included in each optimisation procedure, together with the number of LSOAs which contain offences during each day, is shown in Table 4.3.

For purposes of clarity, and to avoid making conclusions from an insufficient amount of data, the results for the first and last day of rioting—the 6th and 10th

Dates	Number of Arrest Records	Number of LSOAs Affected
6th August 2011	54	20
7th August 2011	232	42
8th August 2011	1,477	247
9th August 2011	446	162
10th August 2011	90	55
Total	2,299	436

Table 4.3: **The number of offences and the number of LSOAs affected by day of rioting.** The total number number of LSOAs affected is the total number of LSOAs that experienced rioting over the 5 days.

August—are excluded from the presentation in what follows. Therefore, only results for the 7th, 8th and 9th of August are reported, which included 93.7% (2,155) of available records.

Overall model fit and selection of δt

The first task is to determine the most appropriate value of δt. The value of δt corresponds to the time interval prior to each offence over which the count of previous offences at each area, and within each neighbouring area, is calculated. Maximum likelihood estimators are found for each day of unrest for $\delta t = 6$, $\delta t = 12$ and $\delta t = 24$. The overall fit of each model is assessed, and described below, and the most appropriate value for δt is used in the presentation of results that follows.

As well as different optimisation procedures employed for different values of δt, two different optimisation procedures are run in order to examine the spillover effects. The first model assumes that $\beta_{12}^{\delta t} = \beta_{13} = \beta_{14} = \beta_{15} = 0$, so that the effects of neighbouring areas do not influence the probability that a target is selected. The second model assumes that these same parameters are not fixed and are calibrated in the same way as the others.

The models with and without the spillover effects are separated due to the anticipated high levels of collinearity between the spatially lagged variables and the variables associated with each target area, which can lead to problems in the interpretation of parameter estimates. A model without neighbourhood effects would be preferred from

the perspective of minimising collinearity in the explanatory variables, but a model with these effects would be preferred from the perspective of mitigating the impact from independence of irrelevant alternatives. If the inclusion of spatial spillover effects has little effect on the estimation of the other parameters, then there will be more confidence in the robustness of the parameter estimates.

In order to consider the effectiveness of the model as a whole, and to measure the extent to which it is able to reproduce the observed data, a pseudo r-squared statistic is calculated for each model run. Denoting the maximum likelihood estimator by $\bar{\boldsymbol{\beta}}$, this statistic compares the value of the log-likelihood function $\ln \mathcal{L}(\boldsymbol{\beta})$ with $\boldsymbol{\beta} = \bar{\boldsymbol{\beta}}$ and the value of the same function with $\boldsymbol{\beta} = \mathbf{0}$. Specifically, R^2 is defined as

$$R^2 = 1 - \frac{\ln \mathcal{L}(\bar{\boldsymbol{\beta}})}{\ln \mathcal{L}(\mathbf{0})}. \tag{4.34}$$

When $\boldsymbol{\beta} = \mathbf{0}$, the observed component of the utility of each choice is equal to 0, and there is an equal probability that each site is chosen. In this case, there are no distinguishable features accounted for across the possible choices. Given that the log-likelihood $\ln \mathcal{L}(\boldsymbol{\beta})$ is a measure of the probability that the model with parameter $\boldsymbol{\beta}$ will result in the observed data, the value of R^2 indicates the extent to which the model estimated with the parameter $\bar{\boldsymbol{\beta}}$ increases this probability against a null model in which targets are selected uniformly randomly. It can be interpreted as the extent to which the model with the parameter $\bar{\boldsymbol{\beta}}$ explains the variance observed in the model.

The values of R^2 for each of the models calibrated—for each day under consideration, for each value of δt, and for both inclusion and exclusion of spillover effects—are shown in Figure 4.3. Considering first the variation with different values of δt, it is not immediately clear which value provides the best model. For instance, the model with $\delta t = 12$ appears to have a higher R^2 value on the 7th August but the model with $\delta t = 24$ has a slightly higher value on both the 8th August and the 9th August. This is consistent across models both with spillover effects and without. In order to determine the value of δt that provides the best fit to the data, a weighted average R^2 is calculated given by the weighted mean R^2 over each day, weighted according to the number of offences occurring on each day, given in Table 4.3. These averaged R^2 values are shown in Table 4.4. This table shows that the value of δt resulting in the model with the overall best fit is $\delta t = 24$. In what follows, this is the value of δt that is employed.

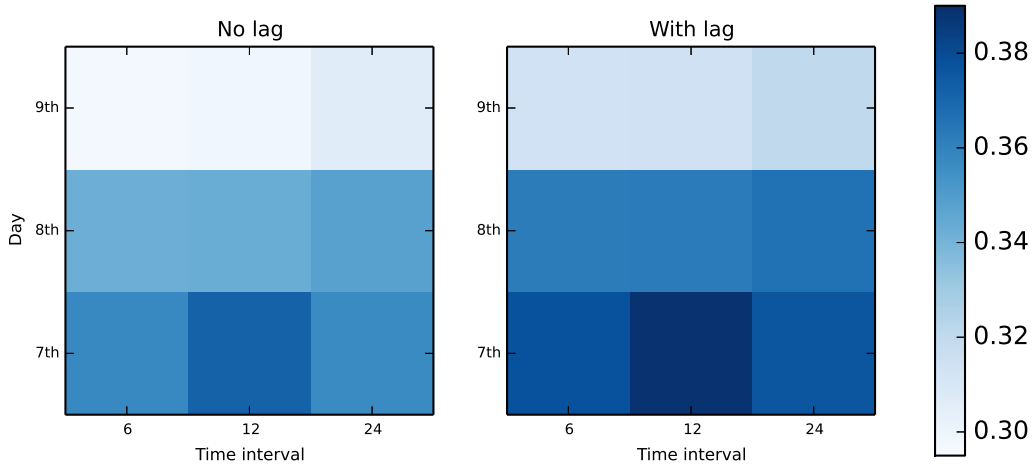

Figure 4.3: **$\mathbf{R^2}$ values for each of the different models tested.** The darker the shading, the higher the value of R^2, and the better the fit to the data. The model without spillover effects is shown on the left, and the model with spillover effects is shown on the right. The time interval used corresponds to the value of δt.

Model	**Weighted R-squared**
6hr without spillover	0.3352
12hr without spillover	0.3374
24hr without spillover	0.3405
6hr with spillover	0.3544
12hr with spillover	0.3561
24hr with spillover	0.3581

Table 4.4: **Weighted $\mathbf{R^2}$ values.** These are calculated by taking the average of each R-squared value over each day of rioting, weighted linearly according to how many offences occur on each day of unrest.

Considering overall model fit, the average R^2 across all days of rioting for the case with $\delta t = 24$ is 0.3405 without spillover effects and 0.3581 with spillover effects. The first observation that can be made is that the model performs well in explaining the variation of target choice in the data: the likelihood function increases by around 35% when explanatory variables are included. In particular, McFadden (1979) states that values between 0.2 and 0.4 represent an excellent fit to the data. It should be noted that the R^2 values are typically much lower for maximum likelihood estimation than R-squared values that can be calculated in ordinary least-squares regression. This is because the model uses probabilities to estimate a binary choice (whether each area is chosen). Consequently, the R^2 can only be equal to one if the choices that are made are estimated with probability equal to one, and the choices that are not made are estimated with probability zero. Uncertainty in the model necessarily decreases the value of the R^2 in a way that does not occur with ordinary least squares regression, and thus the values are typically lower.

Testing for unobserved heterogeneity in the dynamic variable

Before the results are presented for the parameter estimates, a final complication brought about by the inclusion of dynamic variables in the attributes of each area is addressed. The variable used to estimate the role of recent offences on rioter target choice, denoted by $W_{1ij}^{\delta t}$, may in fact not be capturing the desired effect: that the increased likelihood of area j being selected is a direct consequence of previous offences in that area. This is because it may instead be capturing unobserved heterogeneity that is not otherwise incorporated in the model.

Unobserved heterogeneity arises when factors that are largely responsible for influencing the choices of individuals are not included in the model. Whilst it is hoped that, in the derivation of the model, the large majority of such factors have been incorporated in some way, it may be that some have been missed due either to a lack of theoretical understanding of target choice during rioting or due to the lack of available data.

Similarly to the variables already present in the observed utility function, unobserved heterogeneity can be either time stable or dynamic. An example of dynamic unobserved heterogeneity may arise from the behaviour of police, which is likely to

influence the choice of target, but which has not been included in the model due to a lack of data on law enforcement activities. Static unobserved heterogeneity may arise due to the presence of particular retail stores at certain locations or the locations of police stations, the inclusion of which in the model may have unnecessarily increased its complexity.

Since the variable $W_{1ij}^{\delta t}$ counts the number of rioters who choose area j in the δt hours prior to each offence, it may be that it is actually capturing either dynamic or static unobserved heterogeneity: areas with high values of $W_{1ij}^{\delta t}$ may have high values because those areas attracted more rioters due to its characteristics that are not captured by the model.

The extent to which this variable measures static unobserved heterogeneity can be directly tested. To do this, the model is calibrated using the same optimisation procedure for each of the three days under consideration with just three variables: the distance between the residential area of each rioter and their potential target, denoted by W_{6ij}; the number of rioters who had engaged in the disorder at each potential target in the previous 24 hours; and the number of rioters who had engaged in the disorder at each potential target throughout the remainder of the duration of the disorder (that is, the total number of rioters at each location, minus the number who had offended within the previous 24 hours), denoted by $W_{16ij}^{\delta t}$. The distance between a residential area and target area is included in this version of the model as it was considered to be the variable that accounts for most of the variation in the target choice of rioters.

The parameter estimates and their 95% confidence interval are shown in Table 4.5. The parameters associated with counts of an area, both for the previous 24 hours, as well as for all other times, are significant, and greater than one, indicating that the presence of offences in a particular area does indeed increase the likelihood that it is selected for rioting. Since both estimates are significant, it can be concluded that offences in the previous 24 hours, as measured by the variable $W_{1ij}^{\delta t}$, includes effects above and beyond what would be anticipated from static unobserved heterogeneity, since otherwise the static unobserved heterogeneity would be captured by the variable $W_{16ij}^{\delta t}$. Results are next presented that include the variable $W_{1ij}^{\delta t}$ under the assumption that it is indeed capturing some form of contagion process. However, it should be borne in mind that there is some level of unobserved heterogeneity not accounted for in the

Date	**Parameter**	**Exponentiated parameter estimate**	**95% confidence interval of estimate**
7th Aug	$\beta_1^{\delta t}$	1.173	[1.156,1.191]
7th Aug	β_6	0.628	[0.598,0.659]
7th Aug	$\beta_{16}^{\delta t}$	1.060	[1.055,1.065]
8th Aug	$\beta_1^{\delta t}$	1.049	[1.046,1.053]
8th Aug	β_6	0.588	[0.576,0.601]
8th Aug	$\beta_{16}^{\delta t}$	1.079	[1.076,1.081]
9th Aug	$\beta_1^{\delta t}$	1.040	[1.030,1.042]
9th Aug	$\beta_6^{\delta t}$	0.560	[0.537, 0.584]
9th Aug	$\beta_{16}^{\delta t}$	1.120	[1.106, 1.126]

Table 4.5: **Parameter estimates and their associated confidence intervals for the test of unobserved heterogeneity.**

model, which may well arise from processes such as police action on which there is no available data.

Results

In Figure 4.4, the results of the optimisation procedure are presented for $\delta t = 24$ without spillover effects. In Figure 4.5, spillover effects are included. For each component of the parameter vector $\boldsymbol{\beta}$, exponentiated point estimates are shown that maximise the log-likelihood function, subject to the conditions in equation 4.33. A 95% normal confidence interval is also shown for each parameter. The exponentiated value of the parameter β_g is the multiplicative effect of a one-unit increase in attribute W_{gij} on the odds that decision-maker i selects target j. The odds are defined as the probability that i selects j, divided by the probability that i does not select j. If $e^{\beta_g} = 1$ then there is no association between that variable and offender spatial decision-making during the London riots. Values above one suggest that the likelihood of an area being chosen is positively associated with the variable considered, and values below one suggest a negative association. The value of each exponentiated parameter in Figures 4.4 and 4.5 can therefore enable the interpretation of each attribute in the model.

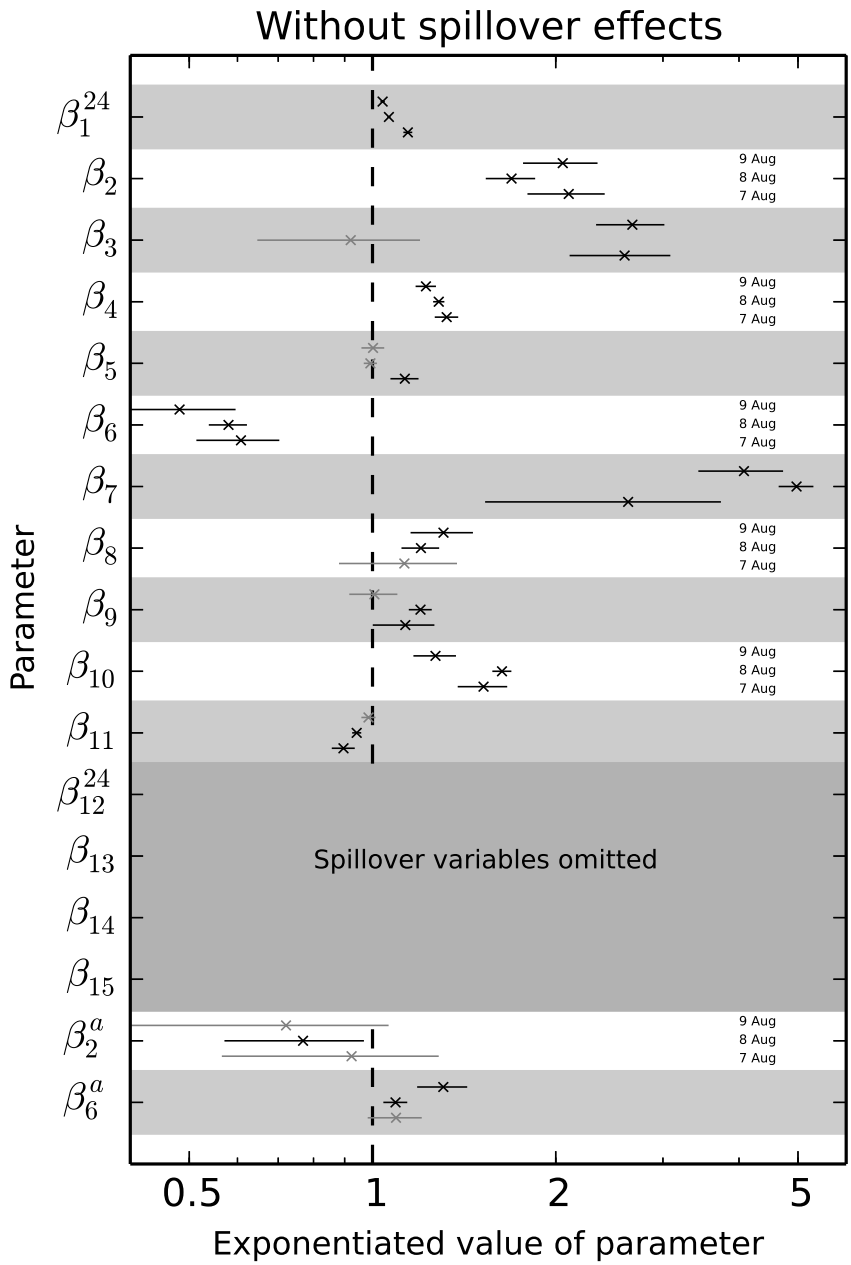

Figure 4.4: **Exponentiated parameter estimates of the discrete choice model for $\delta\mathbf{t} = \mathbf{24}$.** This model excludes spillover effects. For each parameter, three point estimates are shown as crosses, one for each day under consideration. Each estimate also has a corresponding 95% confidence interval, shown as an error bar. The error bar is shaded grey if it crosses zero, otherwise it is shaded black. If it is shaded black, it implies that the associated parameter is significant at the 0.05 level. The description of each parameter is given in the supporting text.

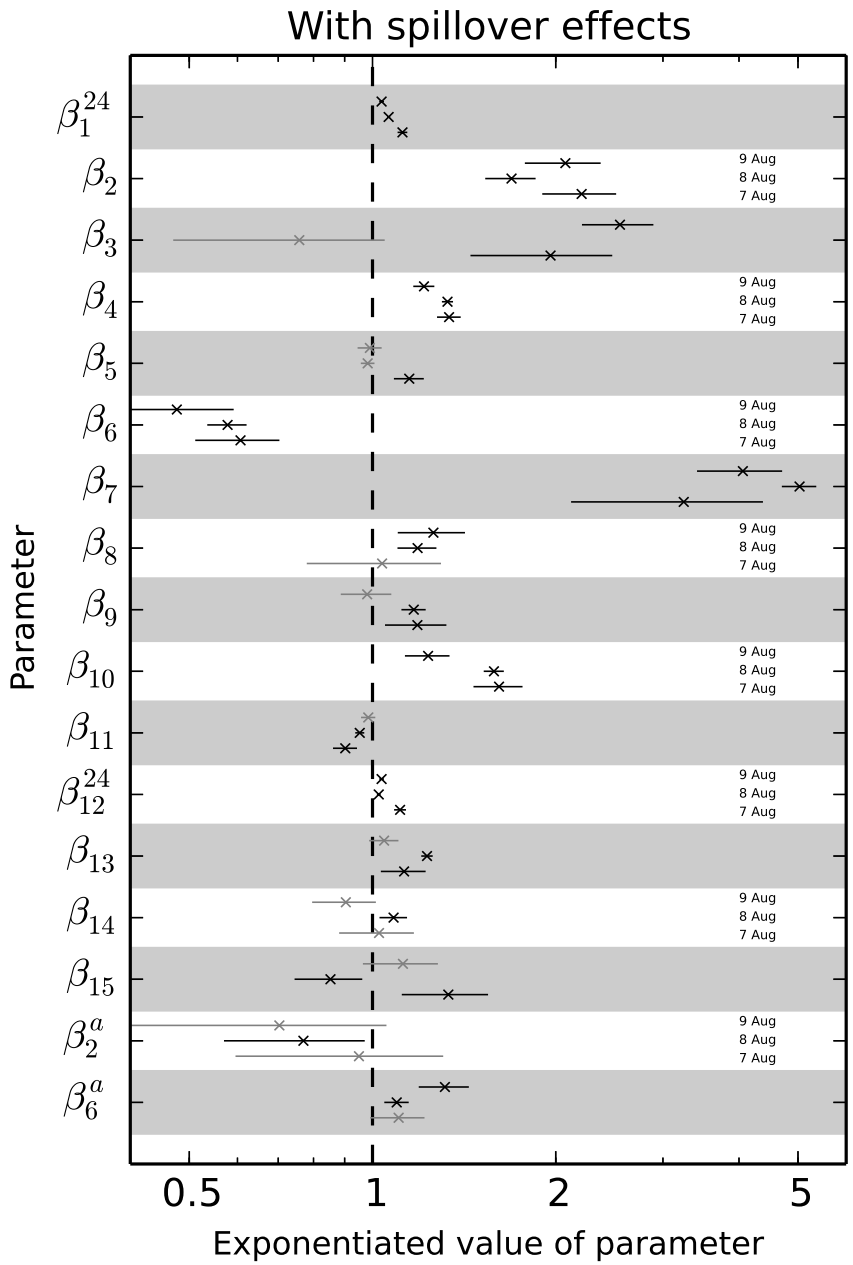

Figure 4.5: **Exponentiated parameter estimates of the discrete choice model for $\boldsymbol{\delta t = 24}$.** This model includes spillover effects. For each parameter and model run, three point estimates are shown as crosses, one for each day under consideration. Each estimate also has a corresponding 95% confidence interval, shown as an error bar. The error bar is shaded grey if it crosses zero, otherwise it is shaded black. If it is shaded black, it implies that the associated parameter is significant at the 0.05 level. The description of each parameter is given in the supporting text.

Interpretation of estimates

In this section, each parameter estimate from the results presented in Figures 4.4 and 4.5 is considered in turn, and each associated hypothesis related to the theoretical perspectives introduced in section 4.2.2 is discussed in the context of these findings. The results with the spillover variables omitted are first investigated, corresponding to Figure 4.4.

Taking the first parameter, β_1^{24}, which measures the effect that offences occurring in the previous 24 hours at each location has on the attractiveness of that target, the estimates are consistently positive and significant. Although the magnitude of the exponentiated variable is only slightly greater than one, the relatively small confidence intervals for the parameter estimate suggest that this is a highly significant finding. This finding supports the analysis of Chapter 3: ongoing rioting can act as a situational precipitator, in which rioters are encouraged to engage in the disorder more so than they otherwise would. To illustrate, on the 7th September, the odds of an area being targeted by an offender increased by a factor of 1.143 for every additional (detected) offence that occurred in that area in the previous 24 hours.

Similar statements can be made for each day of unrest; however, when considering how this variable changes over the three days of rioting—from 1.143 on the 7th, to 1.064 on the 8th, to 1.039 on the 9th—the temporal distribution of offences throughout the duration of rioting requires consideration. This is because the number of offences that occur within any 24 hour period prior to an offence changes significantly over time, and such a change may well affect the parameter estimates. Indeed, since the parameter estimates measure the increased attractiveness of each area due to a single extra offence with all other things equal, one might expect to experience diminishing returns on the extent to which attractiveness can increase as the number of rioters increases. That is, the increased attractiveness per rioter is likely to decrease with more rioters: it has been hypothesised elsewhere that the first rioter can be the most important in influencing the chance of a full scale outburst (Granovetter, 1978). Since the parameter estimates considered here decrease with each passing day, and since the number of rioters increased from the 6th August to the 8th August (see Table 4.3), the period of time prior to events on the 9th August would, in all likelihood, include the greatest number of rioters. Thus, if there was a diminishing effect on the increased attractiveness as the number of rioters

at each site increases, then the estimates of the parameters for this variable would be expected to decrease over time, which is indeed what is observed.

The parameter estimates for β_2, corresponding to the presence of schools in the target area, are all positively associated and significant at the 0.05 level with the choices made. Thus, rioters were more likely to offend in areas containing schools. It was argued in Section 4.2.2 that this is likely to occur due to the role of schools in the collective routine activity nodes of offenders. Considering all offenders, the odds of a rioter selecting an area for each additional school contained within that area increases by a factor of between 1.692 and 2.101 for each of the days under consideration.

In order to further test the hypothesis that the role of schools in the target choice of offenders was a result of those schools being prominent in the routine activity nodes of offenders, an interaction parameter was also estimated to determine the extra effect brought about by the offender being over the age of 18. Although only significant at the 0.05 level for the 8th August, there is some indication that the effect of schools on the decision making of adults is less prominent than it is for juvenile offenders. For instance, on the 8th August, the point estimate of $e^{\beta_2^a}$ is 0.769, meaning that the total impact of schools will be around 23% less for adult offenders. This provides some support for the theory that routine activity nodes are likely to change and diminish for individuals as they get older.

The effect from the connectivity of an area, proxied by an indicator of the presence of an underground train station given by β_3, was, for the 7th and 9th August, positively associated with the chance that the area was selected. In fact, on those days, the odds of an area being targeted by an offender more than doubled if it contained a station. This provides further support that those areas in the routine activity nodes of offenders were more likely to be targeted. On the 8th August, the estimate was not significant, and, curiously, was in the opposite direction to the other two days. This might be explained by the fact that, on the 8th August, the rioting was much more widespread than on the other days and so the ease of accessibility might have been less of a concern for rioters on this particular day.

The effect of retail centres, as measured by β_4, was positively associated and significant with the likelihood of an area being selected for all days considered. For every additional $250m^2$ of retail floorspace in an area, the odds that it was selected as a lo-

cation in which to riot increased by a value of between 1.22 and 1.32, all other things being equal. Whilst this finding might be interpreted as evidence for the targeting of routine activity nodes, which may include retail centres, it may also be a result of many of the offences during the riots being associated with looting of high-value goods.

The effect on target attractiveness from its distance to the city centre, as measured by β_5, did not appear to play a consistent role, as the estimate was only significant for one of the days tested. On the 7th August, the exponentiated coefficient was statistically significant and positively associated with the choice of target, suggesting that rioters were more likely to offend further away from the city centre. However, on the 8th August and 9th August, the effect was indistinguishable. One reason for the apparent absence of the influence of this variable may be that, for a city like London, the city centre may be too crude to represent a routine activity node for all offenders.

The point estimates for β_6 are significantly negatively associated with the choices made by rioters for each day of unrest. Since β_6 measures the effect of Euclidean distance between the offender's residence and their riot location, this suggests that areas further away from a rioter's residence were less likely to be selected, which is entirely consistent both with the theory of crime patterns and studies investigating the journey to crime. Indeed, given the distance decay shown in Figure 4.1, this finding is to be expected. For interpretation, the odds of an offender selecting an area reduces by a factor of between 0.482 and 0.608 for each additional kilometre of distance between their residence and that target area, all other things being equal.

Two of the three estimates of β_6^a are statistically significant at the 0.05 level, suggesting that the magnitude of the exponentiated parameter estimate for the journey to crime variable is closer to one for adults than it is for juveniles. This indicates that, as hypothesised in Section 4.2.2, the effect of distance on the target choice of rioters is more pronounced for juvenile offenders, and adult offenders did indeed appear to travel further to commit their crimes. This could be a result of the extended awareness spaces of adults perhaps combined with their increased means to travel farther.

The influence of the River Thames, as measured by β_7, was significantly positively associated with rioter target choice, and consistent across all days. The odds of an offender selecting an area were up to five times higher if that area was on the same side of the river as the area in which they lived, all other things being equal. This supports

the hypothesis derived from crime pattern theory, which states that the river acts as a natural barrier to the awareness spaces of offenders.

With respect to social disorganisation, as measured by population churn, ethnic diversity and deprivation, whose effect is measured by β_8, β_9 and β_{10} respectively, the parameter estimates were, in general, positively associated with target choice, although some results were not statistically significant at the 0.05 level. In particular, areas with a higher level of deprivation were more likely to be selected on each day of the riots. The odds of an area selected increased by a factor between 1.269 and 1.632 for each unit increase in the measure of deprivation. The likelihood of an area being selected increased by a factor of between 1.2 and 1.3 for each unit increase in the measure of churn of that area, although the effect was not statistically significant on the 7th August. The effect of attractiveness on target choice increased by a similar amount for ethnic diversity on the 7th and 8th August but was not significant on the 9th. Thus, areas with higher levels of churn, ethnic diversity and deprivation were more likely to be targeted, thereby supporting theories of social disorganisation, which state that in areas with higher values of such variables, the residents are less likely to have the ability to collectively prevent such crimes from occurring.

As discussed in Section 4.2.2, there are two mechanisms by which this effect is likely to come about. Cohesive neighbourhoods might exert control over their residents to reduce the likelihood that they would engage in the disorder. Alternatively, signs of social cohesion, or collective action, might act as a barrier to deter rioters from targeting a neighbourhood. Such action was reported as helping to stop some of the rioting that took place in the United States during the summer of 1967 (Corman, 1967), and, while not systematic, anecdotal evidence from media coverage of the London 2011 riots suggested that in some areas residents acted collectively to prevent rioters from targeting their neighbourhoods.

With respect to population density, and the parameter estimate for β_{11}, it would appear that, while the strength of the effect decayed over the course of the three days, with it being statistically insignificant at the 0.05 level on the final day, offenders tended to select areas with lower population density. In this model, population density is included as a control and is not discussed with respect to a particular hypothesis. This finding does, however, demonstrate the value of including this variable in the model

specification.

In Figure 4.5, in which estimates of the exponentiated coefficients for the spillover variables are also presented, it can be seen that the results are consistent with those discussed so far, both with respect to the direction in which the effect acts, as well as to the significance of each variable. Thus, it can be concluded that the inclusion of spillover effects does not drastically alter the parameter estimates of the other variables. This demonstrates that the findings are robust, and implies that the substitution patterns captured by the spillover variables do not unduly impact the other estimates.

The spillover effect from prior offences, as measured by β_{12}^{24}, is significant and positive for all days under consideration. The occurrence of offences in neighbouring areas therefore appears to increase the attractiveness of areas to rioters. These results are consistent with the findings of Chapter 3 in which evidence for the spreading of offences in space and time was demonstrated. Considering the spillover effects for the presence of schools, underground train stations and retail areas, as measured by β_{13}, β_{14} and β_{15}, respectively, the results are more mixed, with significant effects at the 0.05 level detected for schools on the 7th and 8th August, for underground stations on the 8th August and for retail areas on the 7th and 8th August.

The interpretation of the individual spillover parameters is complicated due to high levels of collinearity with non-spillover variables that arise due to spatial autocorrelation of those variables. The importance of including the spillover effects is largely to determine whether the non-spillover parameters are consistent when the spillover effects are included. Since this appears to be the case, this provides evidence for the robustness of the parameter estimates and the model itself. In particular, variables associated with crowd theory, crime pattern theory and social disorganisation theory have been shown to provide robust estimates for influences on rioter target choice. Consistency of many of these estimates over the different days tested implies consistency in the decision-making of rioters, providing some evidence for the presence of (bounded) rationality in rioter target choice.

4.3 Simulating the 2011 London riots: Towards a policy tool

Mechanistic models of rioting, in which model assumptions specify how system entities behave, can be used to generate different scenarios whereby hypothetical outbreaks of rioting are simulated. These hypothetical scenarios can be compared against empirical observation and the mechanisms that are used to construct the model can be evaluated. In this section, a novel microsimulation model of rioter target choice is proposed, based upon the statistical model of target choice presented in Section 4.2. First, the model is described and evaluated as a mechanistic model for rioter target choice. The model is novel due to the way it incorporates theoretical perspectives via the target choice model described in Section 4.2. The extent to which it improves upon prior models of rioter behaviour is discussed. Second, the potential for the model to be used in a policy-making context is explored by using it to propose solutions for police resource allocation during rioting.

4.3.1 Microsimulation of target choice

Microsimulations and agent-based models are, in many cases, indistinguishable. They both model the behaviour of individuals and are concerned with how local behaviour aggregates to global outcomes (both techniques are introduced in more detail in Chapter 2). Efforts at separating the two approaches typically consider the extent to which empirical data forms model assumptions; or whether the objective for constructing the model is for the quantitative prediction of a real-world phenomenon, as is the case for microsimulation models, rather than for the explanation of how that phenomenon emerges through the behaviour of system entities, which is often the case for agent-based models (Birkin and Wu, 2012). The model presented here uses the model from Section 4.2, which is based on empirical data, to form its assumptions. Furthermore, its potential as a component model for the quantitative prediction of riot locations is considered. For these reasons, the term ‘microsimulation’ is preferred.

The objective of a microsimulation model is to generate realisations of individuals, based on aggregated empirical data, which might have applicability within a policy setting (Ballas et al., 2005). Microsimulation models typically consist of an empirical dataset of a particular population, which is used to specify the initial conditions, to-

gether with a series of probability distributions that may be conditional upon a range of factors. Pseudo-random number generators combined with these probability distributions are then used simulate certain characteristics associated with each individual in the population, such as the decisions that they make over a period of time.

The successful estimation of parameters in the statistical model of discrete choice in Section 4.2 suggests that an appropriate decision to be simulated is the target choice of rioters during the 2011 London riots. The probability distribution defined by the model in Section 4.2 is conditional upon the initial location of each rioter, the age of the rioter, the time at which the rioter decides to engage with the disorder, and the characteristics of the riot scenario up until that time. Thus, this model is well suited to being applied within a microsimulation framework.

The model is described as follows: suppose that each offender, indexed by i for $i = 1, 2, ..., N$, resides within an LSOA in Greater London, denoted by $s_i^{(o)}$, and is deemed to commit their offence at time t_i, corresponding to the hourly interval within which the offence occurred. Let $I_a(i)$ indicate whether offender i is an adult or under the age of 18, and let $s_i^{(d)}$ denote the LSOA that was chosen according to the empirical data. Suppose also that the offences are ordered so that $t_i < t_{i+1}$ for $i = 1, 2, ..., N-1$. Since the discrete choice model presented in Section 4.2 depends on the riot scenario up until each rioter makes their decision as to where to engage with the disorder, the history of the system at time t, denoted by $\mathcal{H}(t)$, is defined by the set

$$\mathcal{H}(t) = \left\{ (t_i, s_i^{(d)}) | t_i < t \right\}. \tag{4.35}$$

The variable to be simulated is the target choice of each offender. Since there is uncertainty surrounding the choice that each offender makes, a random variable Z_i is modelled. Realisations of Z_i are required to correspond to the LSOA which offender i selects as a target within the simulation; thus, the set of possible values for Z_i is given by the set $\mathcal{D} = \{1, 2, 3, ..., 4765\}$, where each member of $\mathcal{D}$ corresponds to an LSOA.

The probability mass function of Z_i prescribes the probability with which each member of the set $\mathcal{D}$ becomes a realisation of Z_i, and therefore determines the probability with which each LSOA is chosen by offender i in the model. In Section 4.2, the model estimated was for the probability mass function of Z_i, conditional upon the origin of the offender, their age, the time at which the offence occurred, and the history

of the system at that time. Denoting this function by f_{Z_i}, then

$$f_{Z_i}(j|s_i^{(o)}, I_a(i), \mathcal{H}(t_i)) = Pr(Z_i = j|s_i^{(o)}, I_a(i), \mathcal{H}(t_i)) = \frac{e^{V_i^{\delta t}(j)}}{\sum_{l=1}^{J} e^{V_i^{\delta t}(l)}}, \tag{4.36}$$

where $V_i^{\delta t}(j)$ is the observed component of utility gained by offender i if they were to select option $j \in \mathcal{D}$.

A candidate for the function $V_i^{\delta t}(j|s_i^{(o)}, I_a(i), \mathcal{H}(t_i))$ was constructed in Section 4.2 where it was written $V_{ij}^{\delta t}$; however, not all of the components of the model were deemed to be significant predictors for the behaviour of rioters. As a consequence, the model taken in this section is chosen to only include the variables which provided the most predictive power, assessed by the corresponding confidence interval associated with each variable. Thus, the following function is defined:

$$\begin{aligned} V_i^{\delta t}(j) =& \beta_1^{\delta t} W_{1ij}^{\delta t} + \beta_2 W_{2j} + \beta_2^a I_a(i) W_{2j} + \beta_3 W_{3j} \\ &+ \beta_4 W_{4j} + \beta_6 W_{6ij} + \beta_6^a I_a(i) W_{6j} + \beta_7 W_{7ij} + \beta_{10} W_{10j}, \end{aligned} \tag{4.37}$$

where the terms are denoted as in Section 4.2 and measure, respectively, the effect from: offences occurring in target area j during the previous δt hours to t_i; schools in target area j; underground train stations in target area j; retail floorspace in target area j; the distance between the offender's residence and target area j; whether or not target area j is on the same side of the river Thames as the offender's residence; and deprivation in target area j. As well as explaining a large amount of the variance in the data, these variables also capture the three theoretical perspectives—crowd theory, crime pattern theory, and social disorganisation theory—discussed in the derivation of the model. The measure for the number of rioters in the previous δt hours, $W_{1ij}^{\delta t}$, is taken with $\delta t = 24$, in accordance with Section 4.2.

The values of the vector $\boldsymbol{\beta} = (\beta_1^{\delta t}, \beta_2, \beta_2^a, \beta_3, \beta_4, \beta_6, \beta_7, \beta_7^a, \beta_{10})$ are selected in accordance with the estimation of these parameters in Section 4.2. For offender i, the corresponding parameter $\boldsymbol{\beta}$ is found by sampling independently from the joint normal distribution with mean given by the point estimates of $\boldsymbol{\beta}$ from Section 4.2 and standard deviation given by the corresponding standard errors. Recall that three sets of parameters were estimated: one for each day of rioting under consideration. The choice of distribution for each parameter therefore also depends upon the day on which the offence occurred.

Random sampling of the parameter values is employed to better reflect the uncertainty associated with each parameter over the different decision-makers. The resulting model is related to a mixed logit specification, in which the parameters themselves are random variables described by a corresponding distribution function (see, for example Train (2003)). The simulation itself might be thought of as a mixed logit model with independent normally distributed parameters, with means and variances given by the conditional logistic regression estimated in the previous section. Although the parameters might, in reality, be likely to covary with decision-makers, the assumption of independence is used as an approximation, and merely as a means of incorporating variation across decision-makers.

The simulation proceeds as follows:

1. Set $i = 1$.

2. At time t_i, offender i commits their offence at some location. Calculate the value of $f_{Z_i}(j|s_i^{(o)}, I_a(i), \mathcal{H}(t_i))$ for each $j \in \mathcal{D}$.

3. For each j, find the value of the function

$$F_{Z_i}(j|s_i^{(o)}, I_a(i), \mathcal{H}(t_i)) = Pr(Z_i \leq j|s_i^{(o)}, I_a(i), \mathcal{H}(t_i)) = \sum_{l=1}^{j} f_{Z_i}(l|s_i^{(o)}, I_a(i), \mathcal{H}(t_i)), \tag{4.38}$$

   which forms an increasing function on the set $\mathcal{D}$, taking values in the interval $[0, 1]$.

4. Generate a pseudo-random number between 0 and 1, denoted by $\mathcal{R}$.

5. Find a realisation of Z_i, given by $z_i = F_{Z_i}^{-1}(\mathcal{R})$.

6. If $i < N$, set $i \to i + 1$ and return to step 2, otherwise stop.

This simulation produces a set of chosen target areas, $z_1, z_2, ..., z_N$, where the lower case notation is used to correspond to the realisation of the random variable Z_i for $i = 1, 2, ..., N$. The outputs of this simulation represent a riot scenario in which the rioters behave according to the discrete choice model derived in Section 4.2. If the model is able to recreate the observed riot data, then it provides evidence to suggest that

the theoretical perspectives discussed in Section 4.2 are both necessary and sufficient to explain rioter target choice. Furthermore, if the model can provide accurate realisations of riots, then it may be possible for the model to be employed as a predictive tool. In what follows, a comparison between the model outputs and the empirical data is first made, before considering a potential policy application.

4.3.2 Comparison of the model with empirical data

A full out of sample validation of the model is not possible since it has been estimated using all of the available empirical data for each day. This was done in order to gain the best possible understanding into the range of mechanisms that might underlie rioter target choice. Nevertheless, an assessment of the model can be made by determining the extent to which the incorporated mechanisms are able to both quantitatively and qualitatively predict the distribution of rioting in the sample data.

In order to assess the model, it is noted that each realisation is the result of a number of stochastic elements, and, thus, to get a more complete understanding of the model outputs, a sample of 100 realisations is made, resulting in chosen target areas $z_1^{(g)}, z_2^{(g)}, ..., z_N^{(g)}$ for $g = 1, 2, ..., 100$. To determine whether the model is capable of producing similar output to the observed phenomenon, the average number of rioters that targeted LSOA j over the 100 simulations of the model, given by

$$\bar{C}_j = \frac{1}{100} \sum_{g=1}^{100} \sum_{i=1}^{N} \mathbf{1}(z_i^{(g)} = j), \tag{4.39}$$

where $\mathbf{1}(.)$ is an indicator function equal to one if the condition inside the bracket is satisfied, and equal to zero otherwise, is compared against the actual counts of events that occurred in LSOA j for $j = 1, 2, ..., J$.

Figure 4.6 is a bar chart in which the x-axis represents the 30 LSOAs that were most targeted by the rioters according to the empirical data. The bars in the positive direction correspond to the empirical count of offences in each LSOA and the bars in the negative direction correspond to the values of $\bar{C}_j$ that are obtained from the 100 iterations of the simulation for the corresponding LSOAs j. Although a significant discrepancy between the model and the data is observed, there is some indication that the most targeted LSOAs were also those that were most targeted according to the simulation. This implies that the model might indeed be able to contribute to the prediction of

riot locations; however, it doesn't necessarily capture all of the underlying behaviour of the rioters. In particular, the values of the counts in the empirical data are much larger than the counts resulting from the simulation, suggesting that there was greater clustering in some areas observed than is accounted for in the model.

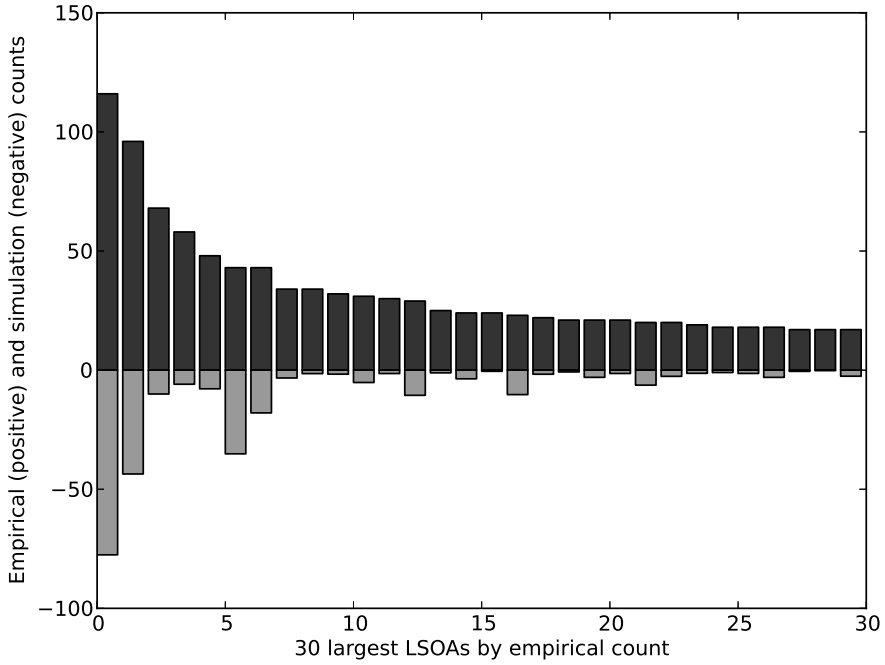

Figure 4.6: **Rioter counts for the 30 most targeted LSOAs according to the empirical data.** The positive bar chart shows the empirical counts, and the negative bar chart shows the averaged simulated counts.

If the model is to be used as a forecasting tool in a policy setting, one must also be wary of the false positive rate of the simulation, which might occur when the model erroneously predicts that an particular location will be targeted. Figure 4.7 shows a bar chart in which the x-axis represents the 30 LSOAs that were most targeted according to the averaged simulation counts, given by $\bar{C}_j$ for $j = 1, 2, ..., J$. The majority of locations most selected by rioters in the simulation were also those areas selected according to the empirical data. There are, however, two notable outliers that deserve attention.

The largest outlier, the second most selected as a target according to the simulation, experienced no offences according to the empirical data. This particular LSOA represents a region in North London containing five schools. Since the count of schools

was used as an attractiveness factor in the model of target choice, which, for this LSOA would have been five times as strong, many simulated rioters selected it as a suitable location at which to commit their offence. Possible explanations for why this area was not selected by rioters according to the empirical data may be that the effect from schools is not additive, and that a school indicator function, taking values 0 or 1, would have been a more appropriate measure of the effect from schools, rather than the count. Another explanation may be that the effect from the presence of schools in each LSOA is, in reality, dependent upon a range of other area-level attributes such as retail floorspace. Nonlinear utility functions can be used to model such dependencies.

Another outlier, representing the fifth most selected LSOA according to the simulation, contains part of London's largest retail centre in the area around Oxford Street. According to the empirical data, this LSOA experienced no riot offences. Since retail floorspace is an attractiveness factor within the simulation, the large retail floorspace of this particular LSOA in comparison to all other areas is likely to have attracted a greater proportion of rioters. Possible explanations for why rioters perceived the very centre of London's retail district as a poor target according to the empirical data may be the perception that, within the centre of London, there may be more law enforcement officers available to counter any riots, which may increase the chances that each rioter will be arrested. Furthermore, larger retail centres may also have higher levels of security, meaning that looting and other riot related offences are difficult to commit.

Although each simulation of the riots has the same number of offences as in the empirical data by construction, the average of the variance of counts across each simulation is 3.29, compared to 11.90 for the empirical data. The offences are therefore more spread out over the LSOAs in the simulation of the riots than is actually observed. This suggests that, although the model goes someway to explaining the target choice of rioters, it does not incorporate all possible explanations as to why rioters selected certain locations over others. Nevertheless, although there are discrepancies between the model and the empirical data with respect to the counts of offences that occurred within each LSOA, the present model may still be of use in a policy setting if it is able to broadly reproduce the spatial patterning of the riots. To determine this, it is next considered whether, with as few outliers as possible, the simulation broadly consistently highlights those areas that were most vulnerable to experiencing riots. For this purpose,

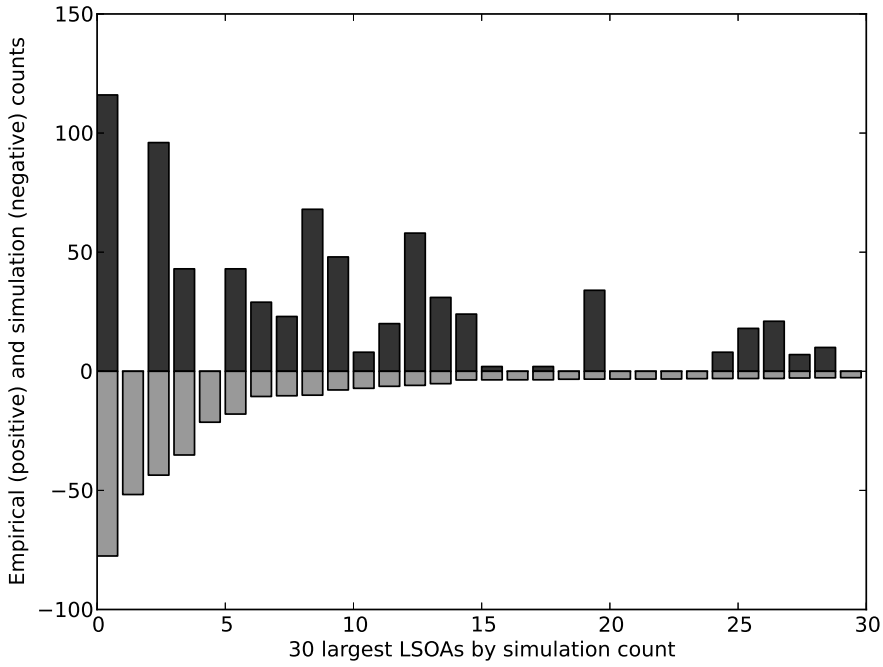

Figure 4.7: **Rioter counts for the 30 most targeted LSOAs according to the average of the simulations.** The positive bar chart shows the empirical counts, and the negative bar chart shows the averaged simulated counts.

another metric is employed: the ratio of the count of the LSOA to its rank, where the LSOAs are ranked according to the number of offences that occur within it. The inclusion of the rank of each LSOA is to reduce the dependency of the following tests on just the counts of offences, which have been shown to include notable discrepancies. If the model is able to broadly highlight the areas most at risk, then it may be of use for the prediction of the location of riots.

Figure 4.8 plots the ratio of the count of offences to its rank for each LSOA, comparing the empirical data to the averaged simulated data. If the model is a good fit to the data, a positive correlation would be expected. Although there is a significant amount of variation between the model and the simulated data, a positive correlation is also observed. The Pearson's product moment correlation coefficient is 0.906, confirming a strong positive correlation and suggesting that the simulation is indeed capable of reproducing some of the more general patterns observed in the empirical data.

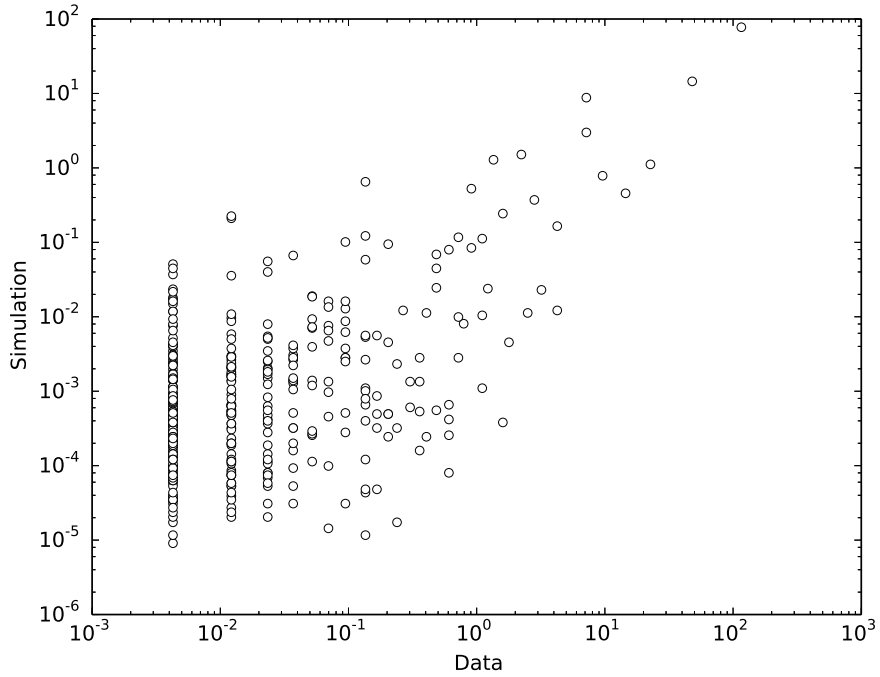

Figure 4.8: **Ratio of count to rank for each LSOA for both the empirical data and the simulation.** The ranks are obtained by sorting the LSOAs according to their count. The plot is shown on a log-scale for clarity.

4.3.3 The model as a component in a policy tool

In this section, it is demonstrated how the microsimulation model presented in section 4.3.1 might be used within a policy context. The strategic deployment of police during a city-wide outbreak of rioting, as observed in London, is an important policy issue. Police allocations can be made in anticipation of rioting, and are dynamic, meaning that law enforcement officers can move towards nearby sites at which rioting occurs. The objective for police commanders, therefore, is to optimally allocate law enforcement officers over different areas in the city so that the maximum number of police officers are within a short travel distance of anticipated riot locations, enabling police to arrive quickly once rioting occurs.

In order to understand which locations might be best for deployment, the microsimulation model described in Section 4.3.1 is used to generate realisations of riot scenarios. In what follows, a dynamic allocation algorithm is proposed that uses the outputs of such realisations to produce potential deployment distributions in London.

Suppose that G riot realisations are given by $z_1^{(g)}, z_2^{(g)}, ..., z_N^{(g)}$ for $g = 1, 2, ..., G$, as in Section 4.3.1. Let the count of offences that occur in LSOA j (for $j = 1, 2, ..., J$) in the g-th realisation be denoted by $C_j^{(g)}$ and suppose that the number of police officers available to be deployed prior to a potential riot outbreak is given by L. For scenarios in which the police are unable to be present over the entire region in which riots are anticipated, as was the case during the riots in London, it can be expected that $L \ll J$.

When considering potential deployments, the police will consider the number of police officers that may be required for any given number of rioters at each location. In this section, the number of police officers required to alleviate the threats posed by one rioter (in terms of the damage they may incur on property and danger to civilians) is assumed to be given by the parameter ν. To explain, a riot of 50 rioters would require a deployment of 50ν police officers to be quelled.

The anticipated riot intensity at LSOA j is defined to be

$$\ln\left(\frac{1 + C_j^{(g)}}{1 + \nu L_j^{(g)}}\right), \tag{4.40}$$

where $L_j^{(g)}$ is the number of police officers deployed to area j in iteration g. This particular form is chosen partly because it increases logarithmically with increasing rioter count, meaning that whilst the intensity will be significantly increased when a single

rioter decides to engage with a small disorder—indicating that the disorder is showing significant signs of growth—a rioter joining an already large disorder will increase the intensity by a smaller amount since it is of relatively less importance in comparison to the already large disorder. In addition, the measure deceases logarithmically with increasing $\nu L_j^{(g)}$, suggesting that a small number of police can drastically reduce the threats posed by a small disorder but that the allocation of additional police to larger disorders, at which there is already a significant police presence, does not have a similar reduction. The addition of 1 to both the numerator and denominator avoids the measure being undefined for all non-negative values of $C_j^{(g)}$ and $L_j^{(g)}$.

The allocation of police should also incorporate the time it takes for police to travel between expected rioter sites, since once rioting emerges in certain locations, police officers may wish to arrive quickly to alleviate its impact and to prevent the riot from growing. The proximity between two LSOAs l and j is defined to be

$$\exp(-\upsilon d_{lj}), \tag{4.41}$$

where d_{lj} is taken here to be the Euclidean distance between the centroids of LSOA j and LSOA l in kilometres and υ is a positive parameter. Other implementations might consider alternative distance metrics, such as road travel time between two LSOAs. The form of this function is useful since it obtains a maximum value of 1 only for the LSOA in which police are already located, and decreases quickly for nearby LSOAs. Therefore, greater emphasis is placed on police being more inclined to remain where they are, rather than travelling too far, and, arriving at a location at which the presence of police is no longer required. The parameter υ controls the extent to which emphasis is placed upon nearby locations, rather than locations farther away.

Using the two components of riot intensity and proximity, a measure of deployment utility is next defined. The idea behind this measure is to determine the benefit of allocating a single police officer to a particular LSOA, whilst accounting for their ability to travel to nearby potential riot sites and, simultaneously, accounting for the police that might already be located nearby. Denoting deployment utility for LSOA l and iteration g by $\mathcal{Y}_l^{(g)}$, the measure is defined as

$$\mathcal{Y}_l^{(g)} = \sum_{j=1}^{J} \ln\left(\frac{1+C_j^{(g)}}{1+\nu L_j^{(g)}}\right) e^{-\upsilon d_{jl}}. \tag{4.42}$$

In order to produce a full allocation of the L available police, a dynamic allocation is required. To explain, after each police officer has been allocated to the LSOA with the maximum value of $\mathcal{Y}_l^{(g)}$, the value of $\mathcal{Y}_l^{(g)}$ requires recalculation, taking into account the effect of the previous deployment. Thus, a suitable algorithm for the allocation of police according to the microsimulation model is given by the following procedure:

1. Set $L_l^{(g)} = 0$ for $l = 1, 2, ..., 4765$.
2. Calculate $\mathcal{Y}_l^{(g)}$ as in equation 4.42 for each LSOA l.
3. Find the maximum value of $\mathcal{Y}_l^{(g)}$ over all LSOAs and allocate one police unit to that location. Update the values of $L_l^{(g)}$ to reflect this deployment.
4. If there are still more police to allocate, return to step 2, otherwise stop.

The average value of the deployment utility over $G = 100$ iterations with $L_j^{(g)} = 0$ for each LSOA j and iteration g and with $\nu = \upsilon = 1$, is shown in Figure 4.9 as a heat map. LSOAs that are shaded darker have a higher initial deployment utility associated with them, and are therefore areas where rioting is predicted to occur. According to the simulation, there are two prominent areas that have the highest level of deployment utility: one above the river Thames and one below the river Thames (the river is indicated by the white line through the centre of Greater London). The value of the deployment utility of an LSOA j, in comparison to the other LSOAs, can be thought of as the relative importance of allocating police officers to that particular area and this figure shows the spatial distribution of this measure.

As a final comparison between the microsimulation model described in Section 4.3.1, the equivalent value of the deployment utility calculated with the empirical counts of offences, rather than the simulated counts $C_j^{(g)}$, is shown in Figure 4.10. Again, the darker the shading of the LSOA, the higher the deployment utility and more value is assigned to that particular area. In this case, the darker areas of the map are more localised, with three or four prominent areas at which the deployment utility is highest.

Although there is some discrepancy between the model outputs and the empirical data, there is agreement in terms of the broad pattern. In particular, the model appears

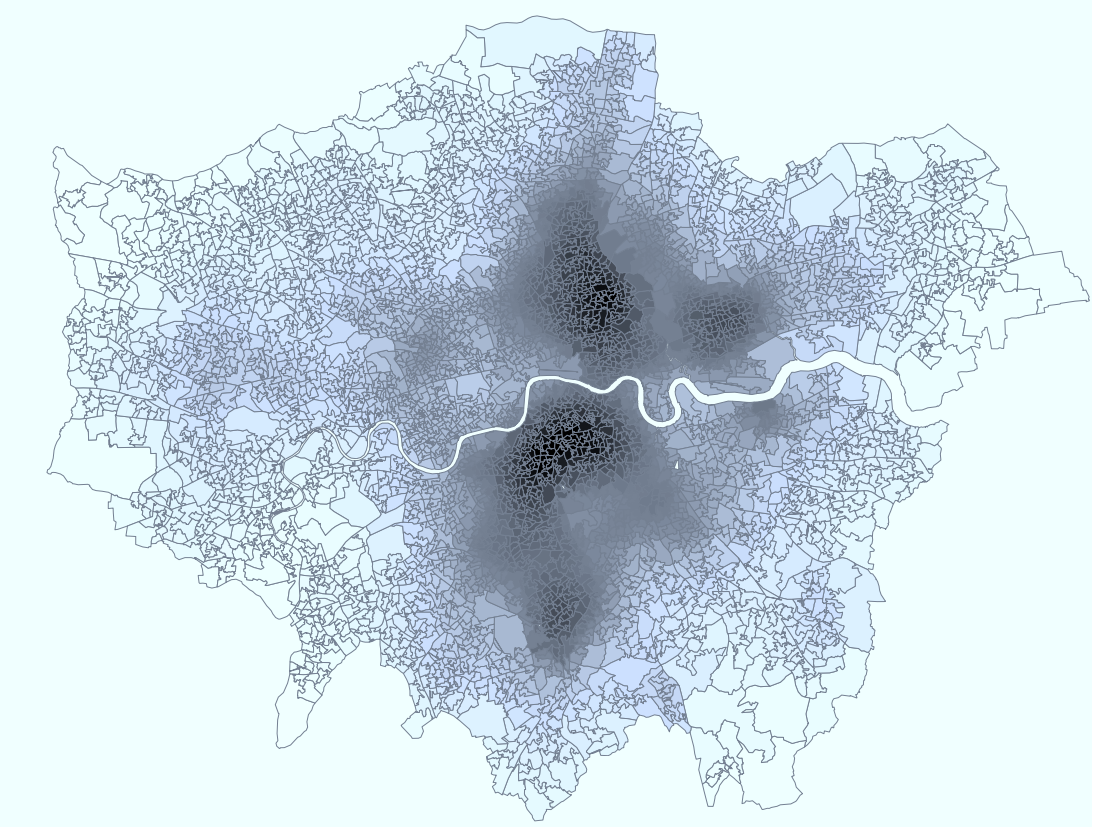

Figure 4.9: **The simulated deployment utility for each LSOA in Greater London.** The average value of $\mathcal{Y}_j^{(g)}$ over $g = 1, 2, ..., 100$ iterations is calculated assuming that no police officers have been deployed. This value corresponds to the shading of each LSOA j. Darker shades indicate higher levels of deployment utility. The rioter counts for each LSOA are those estimated from the microsimulation model in Section 4.3.1. The river Thames is indicated by the white line through the centre of London.

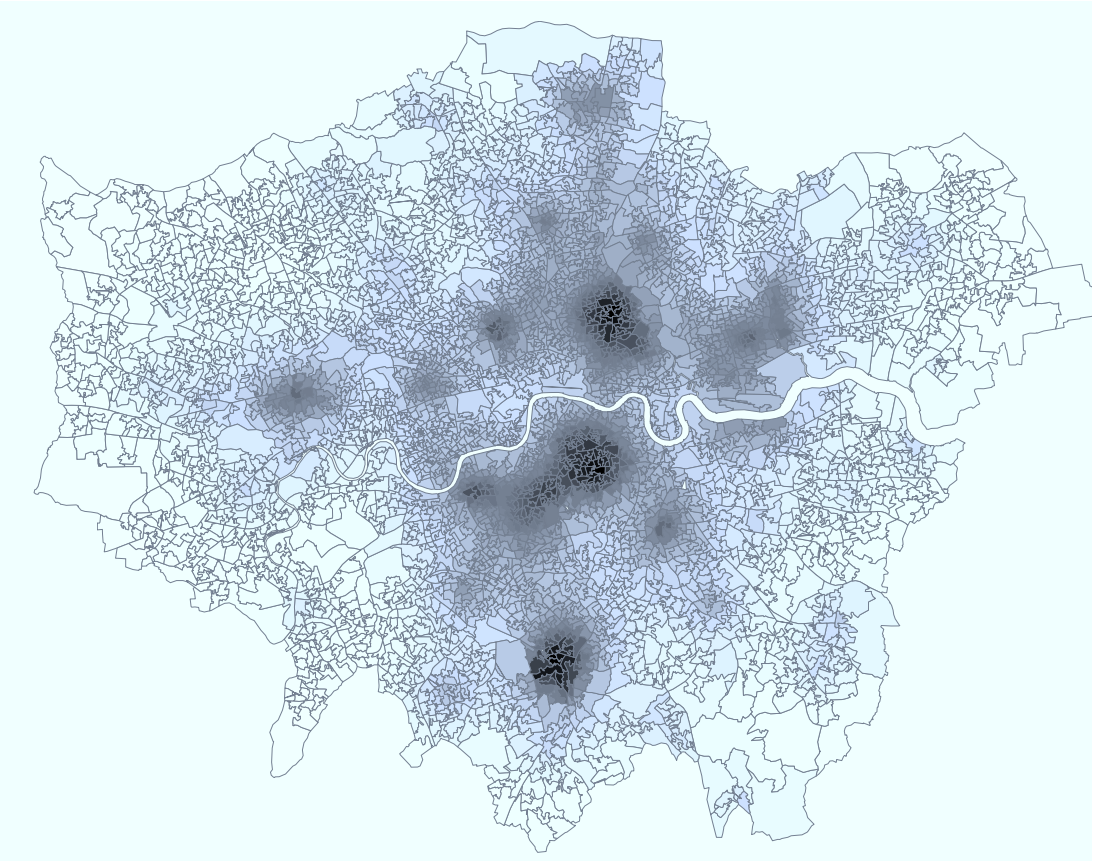

Figure 4.10: **The empirical deployment utility for each LSOA in Greater London.** The value of $\mathcal{Y}_j$ is calculated assuming that no police officers have been deployed. This value corresponds to the shading of each LSOA j. Darker shades indicate higher levels of deployment utility. The rioter counts for each LSOA are obtained from the data. The river Thames is indicated by the white line through the centre of London.

to generate a number of peaks of deployment utility in broadly similar areas to the deployment utility calculated with the empirical data. The distribution of the deployment utility with the actual data appears to be strongly clustered in certain locations in comparison to the model, where the clusters are much larger. Potential explanations for this effect include the fact that the deployment utility for the model is calculated using the average of a number of simulations, and thus may become more smooth. Another explanation may be due to the fact that the variance of the counts of offences is much greater for the empirical data than was observed in the simulation. The simulation led to the occurrence of offences that were more spread out in space, and the results presented here reflect this.

As a policy tool, the model presented here is, as yet, incomplete. It cannot be used on its own to predict the locations of future riots due to its conditional dependence upon certain features of the empirical data. Each of the factors upon which the model is conditional requires the development and implementation of separate sub-models. The model is conditional on the age and residential locations of each offender, the time at which each offender chooses to commit their offence, and the history of the riot up until one hour prior to the point at which the model is used. Models for rioter age and residential location might be developed by exploring further the characteristics of the rioters who have previously engaged in rioting combined with demographic statistics from London. Models for the timing of rioter offences might be used to explore further mechanisms of contagion. In particular, such models will be required to specify precisely how a rioter chooses to engage in the disorder, and not just where they choose to do so. The history of the system can be provided by real-time police recording during a riot. Such models are not explored further in this thesis so as to not detract from its principle objective: understanding how different models might be used to gain insight into the spatio-temporal characteristics of civil violence. Instead, the presentation of a policy model of target choice in this section has provided a proof of concept that statistical models of this type might be usefully incorporated into predictive policy models.

Another limitation of this model is that it does not account for the effect that the deployment of police officers may have on the target choice of rioters. Further development of the model might incorporate such effects although this was not possible in the present study due to a lack of available data on law enforcement activity. Game

theory might usefully contribute to the models developed here since both rioters and police might aim to strategically position themselves in an attempt to maximise their utility (see, for example, Oléron Evans and Bishop (2013)).

Finally, rioting is a dynamic phenomenon that occurs over relatively short time periods (the London riots occurred over five days in total). The optimal allocation of policing is therefore likely to vary on shorter timescales than is accounted for here, and further work might account for this.

4.4 Discussion

Difficulties in the mathematical modelling of social systems arise because the behaviours of individuals and their interactions with others are complicated and uncertain. Individuals can behave with inconsistency under seemingly similar situations. Policy-makers, however, can benefit greatly from the generation of modelled scenarios. Such scenarios can, for instance, enable training of decision-makers, or can enable the testing of crowd control measures, which are almost impossible to test during outbreaks of rioting due to the challenge of making key decisions in real-time.

Previous models of rioting have typically taken the perspective that simplicity is a virtue. In this section, almost as an alternative to this perspective, insights have been obtained from theories in the social sciences, which have been built up over many decades of qualitative and quantitative studies into the behaviour of both individuals and crowds. By incorporating well-developed theories into a model of rioter target choice, and having calibrated this model against the London riot data to estimate the parameters and assess the goodness of fit of the model, a simulation has been proposed that produces realisations of riot scenarios. It has been demonstrated how this model might be used in a policy-making context, through the optimisation of the allocation of police officers based on model outputs.

There are many new contributions presented in this chapter. The novel application of a discrete spatial choice model to rioter target choice has provided further evidence that, across the three days of rioting considered, there is evidence to suggest that offenders selectively chose targets. This supports previous research on target selection of rioting. Furthermore, the estimation of model parameters suggest that it is largely the factors that have been used to influence offender spatial decision-making for a range of

different crime types that can be used to explain target selection in rioting. Considering the different theories examined, factors associated with crime pattern theory—namely, the distance an offender travels between their residence and their offending location, whether or not the Thames is to be crossed, and the presence of schools, retail centres and transport hubs—all appear to contribute to the spatial decision-making of rioters. The consistency of the findings, both in terms of their alignment with the hypotheses articulated in Section 4.2.2, and the patterns observed across the days for which results were presented, provide further support for crime pattern theory as a model of offender spatial decision-making. These findings emphasise the value of crime pattern theory as a means of explaining offender target selection in extreme circumstances such as those associated with riots, for which some scholars have previously argued that rational decision-making is abandoned.

The findings provide further support that the riots were highly contagious, as the occurrence of ongoing rioting at a particular location significantly increased the likelihood that that area was to be selected. There was also support for the idea that social disorganisation theory had a part to play, and areas which had fewer means of exerting social control of a particular area were more likely to have experienced riots. The extent to which the model explains the variance in the empirical data is fairly high, improving upon a model based on uniform random choice of target areas by rioters by around 35%.

A simulation model that is based on this discrete choice model has also been outlined, in order to consider how such statistical modelling might be employed within a policy setting. Models of rioting can have a direct and immediate impact on policy decision-making, as the presence of crowds and riots often requires decisions to be made with regards to how they are managed in real-time. The use of models to generate crowd and rioting scenarios can be used to understand what a good set of strategies or actions might be in order to increase safety or alleviate the negative effects of rioting, such as looting or property damage. Models of crowds have previously been used when designing the fastest evacuation routes from buildings (Zarboutis and Marmaras, 2004), to decide on optimal street layouts (Batty et al., 2003), and to design crowd control strategies at mass gatherings (Helbing et al., 2007).

Some have argued that many of these agent-based models do not sufficiently cap-

ture the range of realistic behaviours that might be expected of individuals in such scenarios (Aguirre et al., 2011; Drury and Stott, 2011). In particular, there is concern that recent simulation and agent-based models of rioting are too simplistic, and that they are based more upon early theories of 'panic' and irrationality, such as those articulated by Le Bon (1896; 1960) and Freud (1921), rather than based on the more recent theoretical research which argues that individuals in fact tend to exhibit more rationality in their behaviour. Models that incorporate the behaviours of agents according to these more recent theoretical developments are beginning to demonstrate greater utility by generating more realistic scenarios (a recent example is the agent-based model of Torrens and McDaniel (2013) who incorporate the interaction behaviour between rioters and the more immediate urban environment in which the riot takes place). The simulation model presented in this chapter directly incorporates a complex decision-making process on the part of each rioter, based on theories that attempt to explain offender behaviour. In this sense, the model represents a significant contribution to modelling of riots.

There are limitations to the model presented in this chapter that require discussion. The applicability of statistical models in the policy domain has been previously questioned (Ward et al., 2010) since statistical models that have been thought to explain empirical data rather well have been shown to be largely inappropriate when testing predictions or forecasts. This is largely due to the problems associated with overfitting the model on the available data. In this chapter, the model is calibrated with data from the 2011 London riots, which is just one example of a riot process. It has been shown that the model explains variance in the empirical data rather well; however, it may be that it will not be of any use in predicting new or out of sample riot scenarios, such as those occurring at different times, and those occurring at different locations. This effect is hoped to have been mitigated by basing the model assumptions on existing criminological theory. Another question that might be considered is whether the model can be applied to scenarios outside of London. Cultural, social and geographic effects may well play a role in determining the attractiveness levels associated with the variables tested elsewhere. Indeed it may be that a different city with a different transport network, and with different convergence of routine activity spaces, leads to different parameter estimates and different conclusions as to the important factors of

rioter target choice.

There are a variety of choice models that could have been chosen to model the decision-making of rioters. The conditional logit discrete choice model was chosen due to its attractive properties: the likelihood function is globally concave with linear utility functions, ensuring a maximum likelihood estimator is unique, and thus the model is very computationally efficient. In addition, the model can readily incorporate spatial spillover effects, mitigating the impact from independence of irrelevant alternatives and correlated error terms. The choice of model can be justified by considering its potential use in the policy domain. In particular, if the model were to be employed in real-time, updating parameters based on where and when offences are occurring, then such computational efficiency would be highly desirable.

If the simulation described in Section 4.3.1 is to be ultimately useful from a policy perspective, then it cannot rely upon the data used in the simulation to determine the locations of where rioters originate, and the time at which they choose to offend. A method for identifying the likely locations of rioter's origins and the times at which they decide to engage in the disorder is therefore required.

It has been shown that the likely origin of a rioter is a significant predictor for the target of each offender. An advantage of the modelling procedure presented in this chapter is that it is able to distinguish between the attractiveness of two otherwise identical areas based purely on their relationship to the locations at which rioters may be located, and the time at which the offence occurs. Models that do not account for where rioters come from, and which merely examine the association between where offences occur and the characteristics of those areas, may be more prone to highlighting apparently vulnerable areas that are not at risk since they are somewhat isolated from the rioter population. Similarly, areas that would otherwise not be particularly vulnerable may be so if there is a high density of potential offenders living near to them. Thus, it is important to explicitly consider the initial distribution of rioters when the vulnerability of targets depend on characteristics such as distance from the rioting population. Some models for the initial distribution of rioters and their decision to become motivated to engage in the disorder have been considered elsewhere in the literature (Davies et al., 2013; Torrens and McDaniel, 2013), and an extension to the work presented in this chapter would be to integrate these models within a policy framework, in which

parameters might be updated in real-time.

One important process that has been missing from this chapter, and which, for the riots in London in particular, would have played a significant role, is the behaviour of the police, and the reaction of rioters to that behaviour. This is largely due to a lack of data on where the police were at different periods of time, and the range of tactics that were employed to counter the riots. In the following chapters, competition between different actors during civil violence in space and time is considered in more detail, first by employing spatio-temporal point processes, and then by employing a deterministic differential equation based model.

Chapter 5

Point process modelling of two adversaries in space and time

5.1 Introduction

Acts of hostility between two adversaries are often the manifestation of ongoing and intractable violence. In many cases, our understanding of a particular outbreak of civil violence can be improved by analysing these events. Mapping the locations and frequencies of hostile events can be useful from a policy-making perspective to indicate the intensity and geographic extent of the violence, as well as its evolution over time (O'Loughlin et al., 2010a). However, as has been shown elsewhere in this thesis, the development of more sophisticated models that incorporate data, combined with some assumptions as to how the conflict might be evolving, can be used to better understand the underlying mechanisms, and can sometimes be used to forecast how civil violence might evolve in the future.

In this chapter, the spatio-temporal dependency of hostile events between two adversaries is modelled with a stochastic model. Direct interaction between adversaries is a mechanism that has not yet been explicitly modelled in this thesis, but it has formed the basis of many previous models of conflict (for example, competition type mechanisms are used as the basis for the differential equation models of both Lanchester (1916) and Richardson (1960a)). Many models that consider interactions between adversaries, particularly those at fine spatio-temporal scales, are abstract models used to articulate hypothesised interactions. This is in contrast to what follows, in which, a novel dataset is employed to parameterise a model of insurgent and counterinsurgent activity. Datasets containing detailed information on the actions of different adversaries at a local level are only more recently becoming widespread in the study of civil violence (for examples, see Braithwaite and Johnson (2012); Kocher et al. (2011); O'Loughlin et al. (2010a); Lyall (2009), amongst others).

A stochastic model is employed in order to account for natural variation from the proposed mechanisms in the empirical data. This approach also enables access to a range of tools developed to perform hypothesis testing of model assumptions. Specific hypotheses concerning how the occurrence of events depends on the history of the conflict will be articulated and tested. Empirical data is incorporated in the modelling process to test specific assumptions, as well as to ascertain overall model fit.

In what follows, a range of stochastic multivariate, and in some cases nonlinear, point process models are constructed. This type of model is chosen for two principal

reasons: first, it is flexible enough to enable the examination of a series of hypotheses concerning causal mechanisms as to how civil violence might evolve, and, second, similar models have been applied to crime and security events elsewhere and have been shown to successfully forecast the timing and location of future conflict events (see, for example, Zammit-Mangion et al. (2012)). Moreover, similar models can also provide insights regarding resource allocation for law enforcement agencies, and can be applied in a policy setting to reduce levels of crime and violence (Mohler, 2014). This particular modelling approach is chosen over others in order to contribute to this burgeoning research area by building a novel spatio-temporal model that is capable of incorporating competition type dynamics prevalent in a range of different conflict models.

This chapter fits into the thesis by exploring a well-studied mechanism incorporated into previous conflict models within a novel spatio-temporal point process framework. Furthermore, it progresses the thesis further along the spectrum of models introduced and discussed in Chapter 1. Models such as those proposed in this chapter can provide insight through the better understanding of proposed mechanisms, and, if a model is successful, through forecasting the evolution of civil violence. The models presented in this chapter also incorporate empirical data and uncertainty, enabling better forecasts than might be obtained from deterministic approaches. The broader question that this chapter sets out to address is whether such modelling approaches that combine causal mechanisms with empirical data can be more usefully employed in policy-making than other modelling frameworks.

In what follows, the case study used in this chapter is first described then proposed mechanisms for the conflict are discussed in the form of a series of hypotheses. A series of multivariate stochastic point process models are derived that incorporate these mechanisms. Parameters are estimated using a maximum likelihood approach, and their confidence obtained using parametric bootstrap methods. The models are then evaluated first with respect to the articulated hypotheses, and then by considering the extent to which the model explains variation in the empirical data. The extent to which the models can usefully inform policy-making concerning the case studied is considered with an out-of-sample test, and the comparative advantages of this modelling approach over others is discussed.

5.2 The Naxal insurgency and police response in Andhra Pradesh

For a number of decades, the Naxal movement (introduced in section 1.4.2) engaged in attacks against both civilians and the state. This hostility was the result of a long-standing commitment by the Naxals to armed struggle against the state in order to address wide-ranging grievances. Andhra Pradesh was one of the most affected Indian states during this time, and its government came under criticism for their apparent ambivalence towards the violence, failing to devise a long-term strategy that improved the security situation (Basu, 2011). At the height of hostilities in 2006, the Indian Prime Minister Manmohan Singh stated that the Naxals represented the "single largest internal security threat to India" (Basu, 2011). In recent years, the level of violence has substantially reduced; however, for much of the previous decade, violence and hostility increased periodically, often to unprecedented levels.

Data was obtained from police forces in India that detailed hostile events associated with the Naxal insurgency for ten years between 2000 and 2010 in the state of Andhra Pradesh. The data consisted of official police records of Naxal-related violence or threat recorded in the 1,642 police stations within the state.

Over the course of the duration of this dataset, there is evidence to suggest that the police adopted various counterinsurgency strategies. For instance, during a period in 2004, in which various splinter groups of the Naxal movement combined to form a unified and potentially diplomatic group, counterinsurgency actions were ceased completely in the hope that a diplomatic solution to the conflict could be found. During other periods, the police took up strict counterinsurgency action. Activities resulting from such police action were not detailed in the data; however, aggressive counterinsurgency activity, which involved the killing of Naxals during shootouts, were known to have been adopted as a result of fieldwork described in Belur (2010). As a result, it is assumed that events described in the dataset as an "exchange of fire" between Naxal and police, and which resulted in at least one Naxal fatality, were largely caused by strategic counterinsurgency activities. It has been claimed that using this description for Naxal fatalities is a way of legally justifying extrajudicial killings (Belur, 2010).

Using the assumption that incidents describing an "exchange of fire" and during

which at least one Naxal was killed corresponds to a counterinsurgency event undertaken by the police, it is possible to partition the dataset into events initiated by Naxals and counterinsurgency events initiated by the police. As a consequence, the dataset employed in this chapter is distinct from the data on the London riots investigated in previous chapters. During the London riots, the behaviour of the police was unknown and could not be empirically tested within the models presented. In this case, data on the activities of both adversaries in the conflict can be used to explicitly consider the effect of actions of one side on the actions of the other. Moreover, the scarce availability of such datasets elsewhere implies that the model presented in this chapter provides a significant contribution to existing literature concerning the spatio-temporal modelling of sub-national conflict between two adversaries.

In total, there are 4,820 incidents in the dataset, which covers the entire state of Andhra Pradesh. For each event i, a three-dimensional tuple is constructed, given by $(t_i, \mathbf{s}_i, m_i)$, where $t_i \in \mathcal{T}$ denotes when event i took place, $\mathbf{s}_i \in \mathcal{D}$ denotes where the event took place, and $m_i \in \{0, 1\}$ is a mark that indicates whether incident i was initiated by Naxals ($m_i = 1$) or was initiated by police as part of their counterinsurgency campaign ($m_i = 2$). The sets $\mathcal{D}$ and $\mathcal{T}$ represent the spatial and temporal domains of the model, which are next described.

The models developed in this chapter will be continuous in time; however, the data on the Naxal conflict is discrete in time, with a daily temporal resolution. The first day included in the dataset is the 1st January 2000 and the final day is 7th August 2010 (3,872 days in total). Taking $\mathcal{T} = [0, 3872]$, the date of each event is translated into continuous time by initially setting t_i to be equal to midnight on the day on which the event occurred. In section 5.5, concurrent events are distinguished by a randomisation procedure, which is explained in the relevant part of the text.

The domain $\mathcal{D}$ represents the geographic area of interest and, due to the resolution at which the data is available, is taken to be composed of the union of non-overlapping districts, as

$$\mathcal{D} = \bigcup_{j=1}^{J} \mathcal{D}_j, \tag{5.1}$$

where each $\mathcal{D}_j$ corresponds to a district in Andhra Pradesh. According to the 2011 Indian census, there are 23 districts in the state of Andhra Pradesh. In one of these

districts, Hyderabad, just two events were recorded. Since this district comprises of the city of Hyderabad, and therefore is small in its geographic extent, and does not experience a large amount of violence, this district and the two events that occur within it are omitted from the analysis.

In 2014, the state of Andhra Pradesh was bifurcated, and the state of Telangana was formed consisting of nine districts that were previously part of Andhra Pradesh. Andhra Pradesh itself remained but now consisted of just 13 districts. The state bifurcated to more closely align language, ethnicity and old political ties. 3,387 of the 4,820 incidents in the dataset (70%) occurred within the districts that formed the new state Telangana. For reasons of computational tractability, the domain $\mathcal{D}$ is initially chosen to consist of the 9 districts in Telangana, and the analysis is restricted to just these events. In particular, the models outlined below are calibrated using incidents that occur within these 9 districts. This restriction ensures that the models proposed can be calibrated over reasonable time frames. Furthermore, this restriction enables the remaining data to be used for out-of-sample model testing, in order to determine whether the model of insurgency in the Telangana state also applies in the state of Andhra Pradesh (specifically, only four districts are used in the out of sample data – those four districts that contained at least 100 events over the period of study). Therefore, initially, $J = 9$ and, for each event i, it is sufficient to take $\mathbf{s}_i = s_i \in \{1, 2, ..., 9\}$, denoting the district within which the event took place.

The spatial distribution of both police and Naxal initiated events in Telangana and Andhra Pradesh across the entire time period of interest is shown as a thematic map in Figure 5.1. The temporal distribution of incidents occurring on each day within each district is shown in Figure 5.2. This figure also distinguishes between Naxal and police intiated events, and includes total counts of each type of event that occurred in each district. In total, there are 586 police events and 4,234 Naxal events, of which, 424 police events and 2,963 Naxal events are contained within the nine districts that make up Telangana. Examining these figures, it can be observed that the vast majority of events occur within a relatively small number of regions, with the highest number of events occurring in the Warangal district. Furthermore, the intensity of police attacks follows closely the intensity of Naxal attacks in space, suggesting that the two types of events may well be dependent upon one another (although, one should be cautious

not to confuse correlation with causation). In what follows, stochastic point process models of these events are derived by considering a variety of mechanisms that may have influenced their occurrence.

5.3 Hypotheses for a model of the Naxal conflict

In this section, a series of hypotheses related to the Naxal insurgency are stated and discussed. These hypotheses serve to articulate the underlying assumptions of the models derived in this chapter and are intended to build upon prior work investigating the spatial and temporal properties of civil violence. Moreover, the hypotheses presented are described in general terms, so that they can be considered in the context of other examples of civil violence. The hypotheses will be evaluated using the case study of the Naxal insurgency after the models have been derived and their parameters estimated.

First, the timings of events are considered. Many studies have investigated the timing of events associated with human behaviour and have shown that homogeneous Poisson process models of event occurrence, in which events are equally likely to occur in any given point in time, are often inappropriate (Barabási, 2005). Events tend to cluster in time and there can be long periods in which no events occur. Recently, many scholars have considered the timings of events associated with human conflict, terrorism, and insurgencies, and have shown similar effects. Moreover, together with the distribution for the frequency of the severity of each event, the inter-event time distribution has been shown to exhibit heavy-tails, and to be remarkably robust, implying extensive temporal clustering (Bohorquez et al., 2009; Johnson et al., 2011; Clauset and Gleditsch, 2012; Johnson et al., 2013; Picoli et al., 2014).

Elsewhere, inhomogeneous and history-dependent temporal point process models have been shown to improve upon simple Poisson process models for terrorist and insurgent event occurrence in Iraq (Lewis et al., 2011), Israel and Northern Ireland (Mohler, 2013), Afghanistan (Zammit-Mangion et al., 2012), Indonesia (Porter and White, 2012), and the Philippines and Thailand (White et al., 2013). In these examples, enabling events to cluster in time more so than would be expected under a Poisson process leads to improved model fit.

Attempts to explain the temporal clustering of insurgent and terrorist attacks typically consider the decision-making and operations of the terrorist organisation commit-

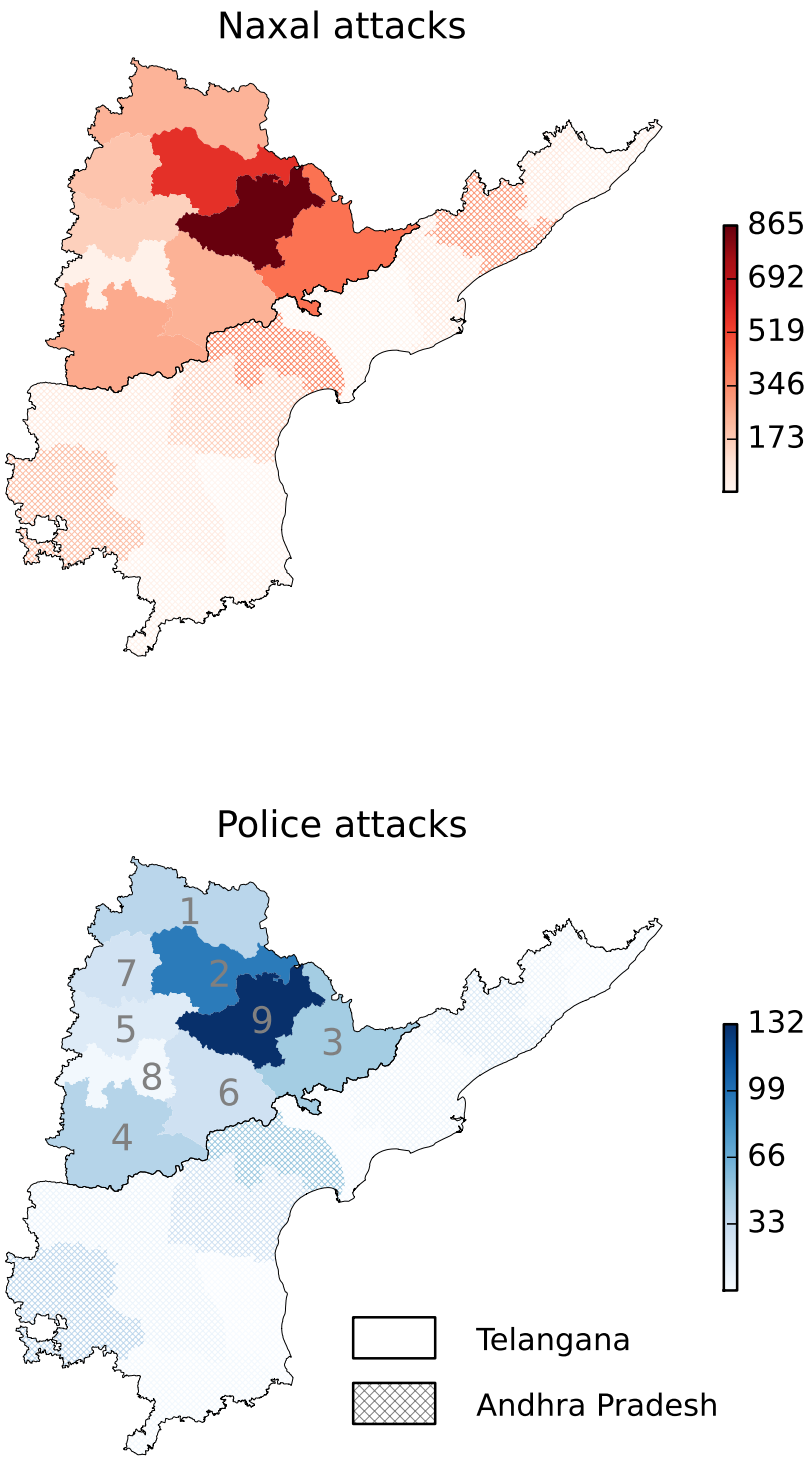

Figure 5.1: **A choropleth map of Andhra Pradesh and Telangana showing the spatial distribution of event data.** The top map shows the count of Naxal initiated events that occur within each district over the entire time domain of interest, and the bottom map shows the count of police initiated events that occur within each district. The districts not in Telangana are hatched. The numbers in the districts of Telangana in the lower map correspond to the numbered districts in Figure 5.2.

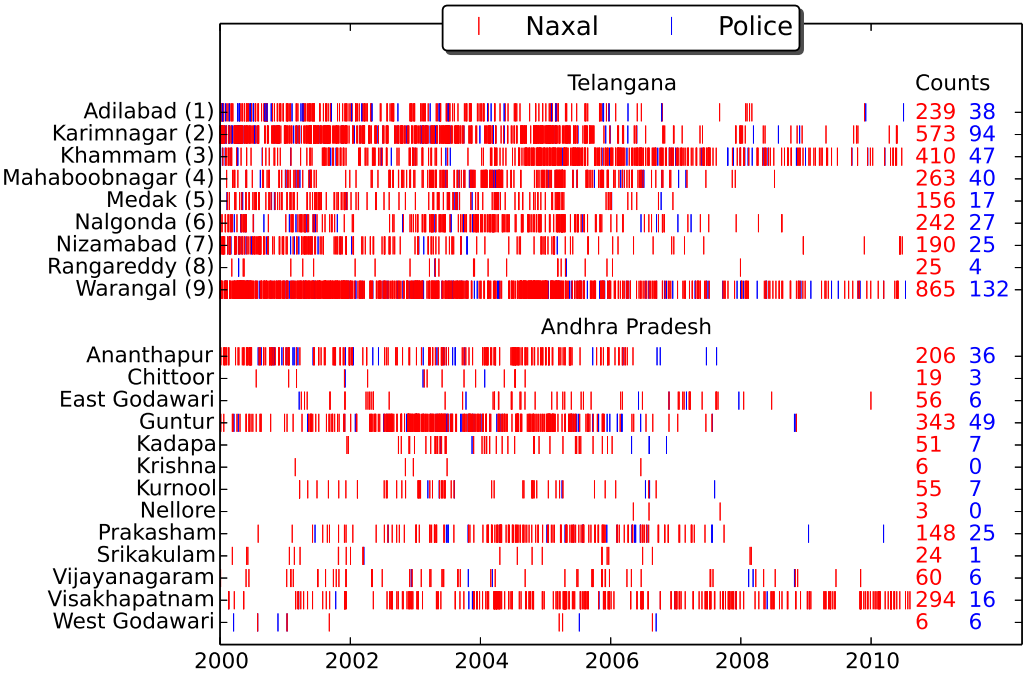

Figure 5.2: **The time series of the event data for each district in Telangana and Andhra Pradesh.** The events are colour coded, with points in blue denoting police initiated events and points in red denoting Naxal initiated events. The numbers beside the names of the districts in Telangana correspond to the numbers in the lower map in Figure 5.1.

ting them. Employing a rational choice perspective, Townsley et al. (2008) argue that insurgents are more likely to commit further attacks after a prior successful attack as an efficient method of operating, and in order to minimise the effort expended in planning new attacks. Insurgents may also be more likely to commit further attacks shortly after a prior attack, as they will be more likely to have access to the weapons, organisational structure, and other capabilities necessary to carry it out.

Bohorquez et al. (2009) attribute the patterns in the timing and severity of attacks to the inevitable coalescence and fragmentation amongst different insurgent groups, combined with a decision-making mechanism by which each terrorist group attempts to choose the best time to attack in order to maximise media coverage of that attack. In contrast, Clauset and Gleditsch (2012) distinguish between the frequency at which insurgent groups commit attacks, and the severity of those attacks, and construct a model based on organisational growth and recruitment. They conclude that terrorist groups increase the rate at which attacks are committed as they become larger and more experienced, contributing to the temporal clustering. The severity of attacks is shown to be independent of both the size and experience of terrorist groups, but larger terrorist groups tend to have higher attack fatality rates as a result of committing attacks more regularly.

The first hypothesis states that insurgent events cluster in time, and, in particular, that they can exhibit escalation, whereby the occurrence of one event increases the likelihood of observing another event for a certain period of time. This increased risk is expected to diminish if no further events occur (in accordance with previous studies such as LaFree et al. (2012) and Braithwaite and Johnson (2012)). This leads to:

Hypothesis 1: The likelihood of insurgent violence is increased for a period of time after insurgent violence.

Counterinsurgent activity may also be temporally clustered, as it responds to variation in political strategies aimed at diminishing the threat from insurgents; to the actions of insurgents; and to other intelligence obtained. In some cases, the counterinsurgent activities have been shown to be even more time-autocorrelated than the insurgent events themselves (O'Loughlin and Witmer, 2012; Braithwaite and Johnson,

2012).

For Andhra Pradesh in particular, the government were reported to periodically adopt both less strict and more severe counterinsurgency strategies, which correspond with the activities recorded in the data. It has been reported, for instance, that during the period before elections in Andhra Pradesh, the police were more lenient towards the insurgents in an attempt to increase government support amongst civilians with insurgent sympathies (Basu, 2011). Conversely, there were periods during which prolonged counterinsurgency strategies were adopted, leading to the Naxals being consistently targeted over a period of time. This leads to the second hypothesis:

Hypothesis 2: The likelihood of counterinsurgent activity is increased for a period of time after counterinsurgent activity.

As well as the temporal clustering of insurgent and terrorist attacks, many studies have demonstrated the presence of spatial and spatio-temporal clustering by considering the locations of events. For instance, inspired by evidence of spatio-temporal clustering in a range of different crime types, Townsley et al. (2008) and Johnson and Braithwaite (2009) investigate different types of terrorist activity in Iraq and show that pairs of events are much more likely to be located near to each other in both space and time when compared to a null hypothesis of event independence. The same observation was found in Chapter 3 when investigating the spatio-temporal patterns of the 2011 London riots.

Spatio-temporal clustering of events leads to hotspots of insurgent activity in which a higher than expected number of events occur. These hotspots may grow, diffuse, or decline over time. Such hotspots of insurgent activity have been identified using a variety of analytic techniques designed to investigate spatio-temporal dependency in Afghanistan and Pakistan (O'Loughlin et al., 2010a; Zammit-Mangion et al., 2012), Spain and El Salvador (Behlendorf et al., 2012), and the Northern Caucasus of Russia (O'Loughlin et al., 2011; O'Loughlin and Witmer, 2012). In all of these cases, strong, localised patterns of conflict were demonstrated, which can, in some cases, it is argued, be used as the basis for the prediction of future events.

The actions of counterinsurgents have also been shown to be spatio-temporally

clustered, perhaps as a result of their response to the actions of insurgents (Braithwaite and Johnson, 2012) (which will be discussed further in what follows), or through the organisation of policing activities at local police force level. Strong localisation of event patterns in space leads to the following hypothesis:

Hypothesis 3: The influence of prior events is strongest at nearby locations.

Counterinsurgency is likely to play a role in the timing and location of Naxal attacks; however, it is not clear what effect it may have. On the one hand, counterinsurgency may have the desired effect of weakening insurgent capacity so that they are unable to commit future attacks; however, on the other, counterinsurgency may serve to fuel hostility by worsening the grievances of the insurgents; increase civilian support for the insurgency; and make them more willing to engage in retaliation. Indeed, tit-for-tat behaviour, in which insurgents and counterinsurgents repeatedly engage in retaliation has been demonstrated in the Iraq insurgency (Linke et al., 2012); the North Caucasus (O'Loughlin and Witmer, 2012); and the Israeli-Palestinian conflict (Haushofer et al., 2010).

The impact of any counterinsurgency action is likely to depend significantly on the types of counterinsurgent strategies adopted. However, evidence has shown that even highly indiscriminate counterinsurgent operations can serve to benefit both the counterinsurgents by reducing the number of subsequent attacks (Lyall, 2009) and the insurgents, by shifting local support and control in favour of the insurgency (Kocher et al., 2011).

In a few cases, studies have distinguished between the different types of counterinsurgent action employed, and have shown that, for example, more discriminatory counterinsurgent activity is more likely to reduce the likelihood of future insurgent attacks in Iraq (Braithwaite and Johnson, 2012); that different strategies and military interventions in the Northern Ireland conflict had different effects on the likelihood of future insurgent attacks (LaFree et al., 2009); and that isolating the insurgency is more effective than direct combat in Russia's North Caucasus (Toft and Zhukov, 2012).

The specific counterinsurgency strategies adopted by the police in the Naxal conflict are not detailed in the data, although are known to result in Naxal loss of life. The

following two hypotheses are included to determine the change in likelihood of future insurgent activity given the occurrence of counterinsurgent events:

Hypothesis 4: The likelihood of insurgent violence is increased for a period of time after counterinsurgent activity.

Hypothesis 5: The likelihood of insurgent violence is decreased for a period of time after counterinsurgent insurgent activity.

A hypothesis is also included to determine whether or not counterinsurgent activities are more likely to occur following insurgent activities, as shown in the identification of tit-for-tat behaviour in previous conflicts.

Hypothesis 6: The likelihood of counterinsurgent activity is increased for a period of time after insurgent violence.

The final hypothesis is concerned with how insurgent conflict diffuses in space and time. There is a large literature on the factors that facilitate international conflict contagion (see, for example, Salehyan and Gleditsch (2006), Buhaug and Gleditsch (2008) and Braithwaite (2010)); however, the literature on the equivalent factors for the spreading of sub-national insurgent activity and other types of civil violence at a local level is comparatively small. Some authors have sought to determine the characteristics of areas that make them well-suited to the expansion of insurgent activity by considering, for example, the distance of the area from the established authority (Raleigh and Hegre, 2009; Buhuag et al., 2009); the terrain of an area (Do and Iyer, 2010); accessibility by road (Zhukov, 2012); and communication links between areas (Myers, 2000). The relative capability of the insurgents has been shown to significantly influence the role that some of these factors play (Holtermann, 2015).

In many cases, however, the geographic proximity of susceptible areas to areas with ongoing violence can serve as a good indication of the risk of violence spreading. Theoretically, insurgents typically look to secure territorial bases before working to expand their controlled areas through the support and recruitment of civilians (McColl,

1969). Although the relative success of these strategies are likely to have an influence on the locations of violence, Schutte and Weidmann (2011) argue that such insurgent conflicts exhibit escalation diffusion, by which areas neighbouring those with ongoing conflict events are likely to experience events themselves in the future. Additionally, O'Loughlin and Witmer (2012) show that retaliation between insurgents and counter-insurgents decays spatially by considering geographic neighbouring areas; Weidmann and Ward (2010) show the benefits of including spatial lags within a predictive model of conflict; and Weidmann and Zürcher (2013) provide evidence that the impact of conflict events decays exponentially in both space and time. Consequently, the final hypothesis is:

Hypothesis 7: The effect of prior events will be stronger on neighbouring districts than on non-neighbouring districts.

In what follows, the hypotheses articulated here are used to construct a series of multivariate point process models for the occurrence of Naxal and police initiated events. These models are then calibrated against the available data and the hypotheses evaluated.

5.4 Point process models of the Naxal conflict

In this section, Hawkes processes are introduced, and a series of models derived with increasing complexity. Hawkes processes are a type of point process, and provide a versatile modelling framework capable of incorporating each of the hypotheses described in Section 5.3. The notation in the definitions that follow is in accordance with the data associated with the Naxal insurgency outlined in Section 5.2.

A point process is a collection of random events $\{(t_i, s_i, m_i)\}_{i=1,2,3,\ldots,N}$ ordered so that $t_i \leq t_{i+1}$, where t_i denotes the time at which event i occurred, s_i denotes the spatial region within which the event took place, and m_i is a mark to denote the type of event that occurred. The point process is simple if this inequality is strict for all values of i. If the collection of each type of event for each spatial region is considered as a separate process, as will be the case in the models that follow, then the point process is multivariate.

More formally, a multivariate point process is defined as a series of counts

$$Z_j^{(l)} : \mathcal{T} \to \{z \in \mathbb{Z} | z \geq 0\}, \tag{5.2}$$

on some temporal domain $\mathcal{T} = [0, \bar{t})$ for some maximum time $\bar{t} \in \mathbb{R}$, defined by

$$Z_j^{(l)}(t) = \sum_{\substack{t_i < t \\ s_i = j \\ m_i = l}} \mathbf{1}_{t_i}([0, t)), \tag{5.3}$$

where $\mathbf{1}_{t_i}([0, t))$ is an indicator function, which is equal to one if $t_i \in [0, t)$ and equal to zero otherwise. The subscript j is used to refer to the spatial region within which events contribute to the count $Z_j^{(l)}$, and the superscript l is used to denote the type of event, which, in what follows, will either be an event initiated by Naxals ($l = 1$) or an event initiated by police ($l = 2$). The summation in equation 5.3 applies to events (t_i, s_i, m_i) with $s_i = j$ and $m_i = l$. That is, each type of event in each region is counted separately. For example, the count $Z_3^{(1)}$ counts Naxal events that occur within the 3rd spatial region under consideration. Models will be specified for $Z_j^{(l)}$ for $l = 1, 2$ and for $j = 1, 2, ..., 9$, corresponding to the 9 spatial regions within the state of Telangana (see Section 5.2 and, in particular, Figures 5.1 and 5.2).

The history of the system until some time t, $\mathcal{H}(t)$, is defined to be the set of events that have occurred before time t, so that

$$\mathcal{H}(t) = \{(t_i, s_i, m_i) | t_i < t\}. \tag{5.4}$$

The conditional intensity function, $\lambda_j^{(l)} : \mathcal{T} \to \mathbb{R}$, associated with the count $Z_j^{(l)}$, describes the expected number of events that occur at each point in time. The function is constructed by considering the expected number of events that occur in time intervals of length δt per unit time, and then considering the limit of this number as $\delta t \to 0$. Formally, given the history of the system $\mathcal{H}(t)$, the conditional intensity function associated with the count $Z_j^{(l)}$ is defined as

$$\lambda_j^{(l)}(t|\mathcal{H}(t)) = \lim_{\delta t \to 0} \frac{\mathbb{E}\left(Z(t + \delta t) - Z(t) | \mathcal{H}(t)\right)}{\delta t}. \tag{5.5}$$

For a given j and l, if $Z_j^{(l)}(t)$ is simple and finite for all $t \in \mathcal{T}$, then the associated conditional intensity function $\lambda_j^{(l)}(t|\mathcal{H}(t))$ is unique (Daley and Vere-Jones, 2003). It follows that in order to define a particular simple and finite point process given by

$Z_j^{(l)}$, it is sufficient to specify the function $\lambda_j^{(l)}(t|\mathcal{H}(t))$. Many models of point processes specify a functional form for the conditional intensity function, rather than for the count, and this is also the approach that is taken here.

In the sections that follow, six models are proposed which will be used evaluate the hypotheses in Section 5.3. The models are constructed with increasing complexity, with each subsequent model designed at capturing a further mechanism that may be at play during the Naxal conflict.

5.4.1 Model 1: The Poisson process

Model 1 is a Poisson process, which is defined by setting the conditional intensity function $\lambda_j^{(l)}$ to be equal to a positive constant. The model will initially be taken to consist of just two distinct parameters for all l and j: one for the rate at which insurgent initiated events occur, and one for the rate at which police initiated events occur. Thus, model 1 can be written as:

$$\lambda_j^{(1)}(t) = \mu_1, \qquad \lambda_j^{(2)}(t) = \mu_2. \tag{5.6}$$

for positive constants μ_1 and μ_2 and for $j = 1, 2, ..., 9$. This model assumes that the probability of an event occurring in time intervals of the same length is constant over the entire duration of the period of interest. There is no dependence of $\lambda_j^{(l)}$ on $\mathcal{H}$ and so the model has no memory.

Just two distinct parameters are required in equation 5.6, and are used to distinguish between the type of event that occurs. This implies that the rate at which events occur is assumed to be constant across the different spatial regions under consideration. However, Figures 5.1 and 5.2 demonstrate how the number of events varies substantially in space. A spatially disaggregated model, in which different Poisson rates are estimated for each district, can also be specified as

$$\lambda_j^{(1)}(t) = \mu_{1j}, \qquad \lambda_j^{(2)}(t) = \mu_{2j}, \tag{5.7}$$

for $j = 1, 2, ..., 9$, denoting the spatial region of each intensity function. Equation 5.7 will be referred to as Model 1a in what follows, and requires 18 parameters to fully specify it.

5.4.2 Models 2 and 3: Self-exciting Hawkes processes

The Poisson process is often used as a baseline model against which more complex models can be evaluated. Indeed, for many processes observed in the real-world, particularly those involving human decision-making, a Poisson process is not appropriate (Barabási, 2005). This is because the models in equations 5.6 and 5.7 are unable to account for scenarios in which the rate at which events occur varies in time. This can occur, for example, when events are highly temporally clustered. As a consequence, a wide range of temporally dependent conditional intensity functions have been proposed. One example is the inhomogeneous Poisson process, which occurs when the conditional intensity function $\lambda_j^{(l)}(t)$ takes the form of an explicit function in t.

A more complex model of point processes can be obtained by allowing $\lambda_j^{(l)}$ to depend on a random variable, giving rise to what are known as doubly stochastic processes. One of the most well-known is the Cox process (Cox, 1955). As demonstrated in equation 5.5, however, $\lambda_j^{(l)}(t)$ can also be dependent upon $\mathcal{H}(t)$, allowing models to retain information of the events that have occurred up until time t and to vary accordingly.

One such model is the Hawkes process, named after Alan Hawkes who introduced and first analysed the model in Hawkes (1971). The motivation for this model was to account for point processes in which the occurrence of events increases the probability of further events occurring in the near future. In order to introduce the model, a simplified scenario is considered, in which, a one-dimensional point process is modelled using the conditional intensity function λ. Sub- and super-scripts are removed from the notation for clarity.

For a conditional intensity function λ, corresponding to a single-dimensional counting process Z, with history $\mathcal{H}(t)$, a Hawkes process is defined by setting

$$\lambda(t|\mathcal{H}(t)) = \mu + \sum_{t_i<t} \kappa(t - t_i), \tag{5.8}$$

for some $\mu > 0$, known as the background rate, and for some function $\kappa(t)$. The background rate μ may be either a constant or a time-dependent function, meaning that the first term in equation 5.8 corresponds to, respectively, a homogeneous or inhomogeneous Poisson process. The function $\kappa(t)$ is called the triggering kernel, and determines the increase in intensity that is due to the occurrence of events, or triggers.

Typically, $\kappa(t)$ will be positive, meaning that the occurrence of an event increases the probability of observing further events, and decreasing in t, meaning that the increased intensity due to the occurrence of each event decays over time (although negative and increasing triggering functions will also be used later in this chapter).

It is shown in Hawkes and Oakes (1974) that if $\mu > 0$ and

$$0 < \int_0^\infty \kappa(t)dt < 1, \tag{5.9}$$

then a unique Hawkes process exists on the real line. Furthermore, in this same article, by defining the Hawkes process as a branching process, it is shown that, under the same conditions, the process is stationary: given a sufficiently long history of the process, it is invariant in time. In this case, the expected long-term intensity of the process is given by

$$\mathbb{E}(\lambda) = \frac{\mu}{1 - \int_0^\infty \kappa(t)dt}. \tag{5.10}$$

The formulation of the model as a branching process is useful intuitively. A Hawkes process arises when mother events, occurring with probability μ, can, with a certain probability defined by the triggering kernel, "give birth" to daughter events, which, in turn, can generate further daughter events. Provided that the triggering kernel satisfies the condition in equation 5.9, then the process is stable and does not blow up in finite time.

These existence, uniqueness and stability characteristics, combined with the model's capability for representing clustering of events in time, have led to it being applied to a wide range of different scenarios including earthquake frequency (Ogata, 1988), neuron spike trains (Johnson, 1996), email correspondence (Blundell et al., 2012) and financial trades (Bowsher, 2007; Embrechts et al., 2011). In particular, there have been many applications of Hawkes processes to the timing of events related to problems in crime and security (Egesdal et al., 2010; Lewis et al., 2011; Porter and White, 2012; White et al., 2013; Mohler, 2013).

A common choice of the function $\kappa(t)$, and the one that is proposed in Hawkes (1971), is an exponential decay function. Following the normalising convention of the decay function in Liniger (2009), this is defined as

$$\kappa(t) = \alpha\omega e^{-\omega t}, \tag{5.11}$$

for constants $\alpha > 0$ and $\omega > 0$. The inclusion of ω in both the exponential and as a product with the exponential leads to

$$\int_0^\infty \omega e^{-\omega t} dt = 1, \tag{5.12}$$

and so the process is well-defined and stationary according to the results outlined in Hawkes and Oakes (1974) if, and only if, $0 < \alpha < 1$.

The value of $\alpha\omega$ is the amount that is added to the conditional intensity at the moment event i at $t = t_i$ occurs. This extra intensity then decays as $t - t_i$ increases. Therefore, $\alpha\omega$ is equal to the expected number of additional events per unit time that are a direct result of the occurrence of each event.

The parameter ω defines the rate of decay, and determines the timescale over which a significant level of increased intensity is added to the overall intensity function after each event. Small values of ω imply $\kappa(t)$ decays slowly, and, therefore, the additional intensity that is due to each event remains significant for a long time. Conversely, large values of ω imply a faster decay, and additional intensity due to each event is only significant for a shorter amount of time.

The reciprocal of ω can be interpreted as a characteristic time-window over which the majority of the increased risk due to a triggering event dissipates, and, therefore, is the time over which additional events can occur that are directly due to the triggering event. If the events are taken to be Naxal associated events, then ω^{-1} can be thought of as the time over which a further event is planned and executed that is considered a direct result of each triggering event. This same interpretation is used in Lewis et al. (2011) to determine the time taken to plan and execute insurgent attacks in Iraq.

The effect of additional intensity due to triggering events also depends on α, which dictates the magnitude of the added intensity that is due to each event. Moreover, since the expected additional number of attacks per unit time that are due to each triggering event is given by $\alpha\omega$, and since the parameter ω^{-1} is a characteristic time window over which these additional events typically occur, the expected number of new events that are directly due to each triggering event is given by $\alpha\omega\omega^{-1} = \alpha$, and thus α can be thought of as the mean number of additional events that are directly due to each triggering event.

The total mean number of descendent events that are due to each triggering event

forms a geometric series, as this number includes not just the events that are directly due to a triggering event, but also those events that are directly due to those triggered events with the same probability. Thus the total mean number of descendent events per event is:

$$\sum_{i=1}^{\infty} \alpha^i = \frac{\alpha}{1-\alpha} \tag{5.13}$$

where i denotes the generation of each event (i.e. the n-th generation has on average α^n direct descendents).

Using equation 5.13, the stationary conditional intensity in equation 5.10 can be derived by noting that, for an exponentially decaying triggering kernel, as in equation 5.11,

$$\int_0^{\infty} \kappa(t)dt = \alpha. \tag{5.14}$$

Next, if background events are occurring at rate μ and for each background event there are on average $\alpha/(1-\alpha)+1$ events (where the addition of one is to count the event arising from the background rate itself), then, assuming stationarity (and that the process has an infinite history), the average rate is given by the product of these two values. That is, by the rate at which background events occur multiplied by the average number of subsequent events each background event stimulates, given by

$$\mu\left(\frac{\alpha}{1-\alpha}+1\right) = \frac{\mu}{1-\alpha}. \tag{5.15}$$

Figure 5.3 plots the conditional intensity function of a Hawkes process described by equation 5.8 with an exponentially decaying triggering kernel given in equation 5.11, in which events occur at times t_1, t_2 and t_3. It demonstrates how the occurrence of events significantly increases the short-term probability of future events occurring. By varying the parameters α, the magnitude of the excitation can be adjusted, whilst the parameter ω varies the duration of the decay.

To model events associated with the Naxal insurgency, two multivariate self-exciting Hawkes process models are proposed. These two models each contain six parameters to be estimated. The first model neglects spatial effects, and assumes that, regardless of where events occur, they contribute to the excitation of the model equally in all spatial regions. The second model estimates the conditional intensity function differently for each spatial region, by assuming that excitation is only brought about by

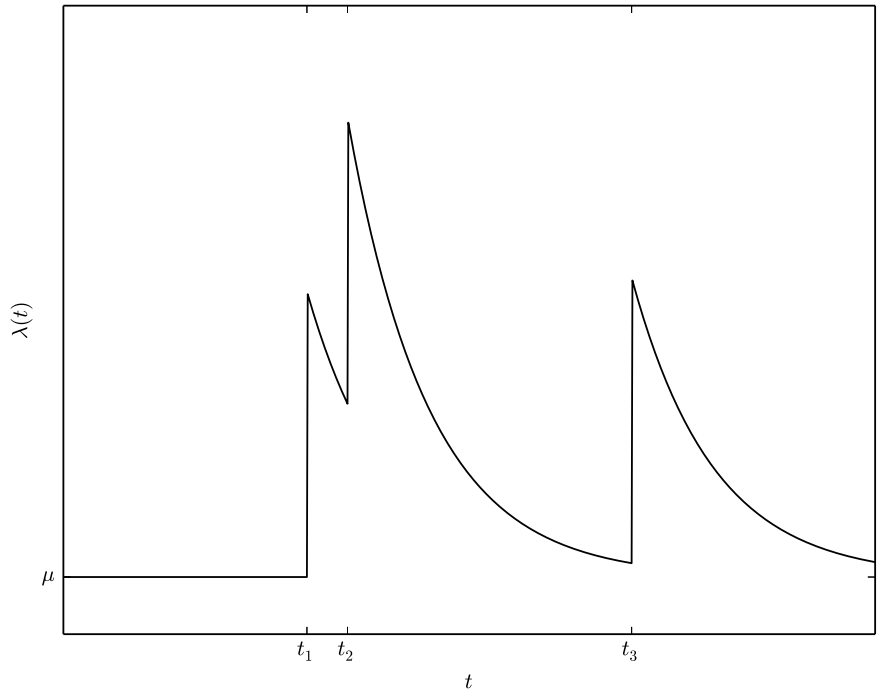

Figure 5.3: **An example of a Hawkes process with events occurring at $\mathbf{t_1}$, $\mathbf{t_2}$ and $\mathbf{t_3}$.**

events occurring within the same spatial region. The first model is given by

$$\lambda_j^{(l)}(t|\mathcal{H}(t)) = \mu_l + \sum_{\substack{t_i<t \\ m_i=l}} \alpha_{ll}\omega_l e^{-\omega_l(t-t_i)}, \tag{5.16}$$

whilst the second model can be written as

$$\lambda_j^{(l)}(t|\mathcal{H}(t)) = \mu_l + \sum_{\substack{t_i<t \\ m_i=l \\ s_i=j}} \alpha_{ll}\omega_l e^{-\omega_l(t-t_i)}, \tag{5.17}$$

where an additional condition on the sum has been added to distinguish equation 5.17 from equation 5.16. If the model in equation 5.17 leads to a substantial improvement over the model in equation 5.16 with regards to explaining the variance in the data, then it can be concluded that local excitation provides a better mechanism for modelling the conflict than global excitations.

Note that the background rates in equations 5.16 and 5.17, μ_l, depend on the type of event, given by l, but not on the spatial region, given by j. Analogously to the model in equation 5.7, models can also be constructed with spatially varying background rates,

resulting in multilevel models. However, models with background rates that are constant in space will initially be favoured, since the estimation of multilevel background rates precludes out-of-sample model testing. Spatial variation will be incorporated into the model via the triggering kernel, and not the background rates. This decision is justified in Section 5.5.3.

5.4.3 Model 4: Mutually-exciting Hawkes processes

In his original paper, in order to account for scenarios in which the occurrence of a certain type of event influences the probability of observing a different type of event, Hawkes (1971) also introduced mutually-exciting processes. These are able to account for interactions across event types, and, as a consequence, are particularly suited to the case study of the Naxal insurgency. Model 4 is given by

$$\lambda_j^{(l)}(t|\mathcal{H}(t)) = \mu_l + \sum_{\substack{t_i<t \\ m_i=1 \\ s_i=j}} \alpha_{l1}\omega_l e^{-\omega_l(t-t_i)} + \sum_{\substack{t_i<t \\ m_i=2 \\ s_i=j}} \alpha_{l2}\omega_l e^{-\omega_l(t-t_i)}, \tag{5.18}$$

for parameters $\alpha_{l1} > 0$, $\alpha_{l2} > 0$, and $\omega_l > 0$ for $l = 1, 2$. The parameters α_{12} and α_{21} determine the strength of the mutual excitation, and have a similar interpretation to the one-dimensional case. That is, the parameter α_{12} measures the expected number of additional events of type 1 (Naxal events) that are brought about as a result of excitation from events of type 2 (police events), and vice-versa for α_{21}. The interpretation of these parameters can be considered in terms of retaliation between Naxal and police. As in the previous model, the parameter ω_l determines the rate of decay of increased risk for events of type l and the background rate μ_l determines the rate at which events that are not descendants of triggering events occur. The decay parameters ω_l do not depend on the type of triggering event that occurs for reasons of analytical tractability as fast estimation algorithms rely on decay rates being constant over event types. Instead, all variation from different triggering events is captured in the corresponding excitation parameters.

General properties of multivariate mutually-exciting Hawkes processes, including existence and uniqueness criteria, are detailed in Liniger (2009) (see also Embrechts et al. (2011)). In particular, if the parameters ω_1 and ω_2 are strictly positive, and all other parameters are non-negative, then analogous results to the one dimensional Hawkes process can be established. That is, if the spectral radius of the matrix formed by the

parameters $A = (\alpha_{ll'})_{l,l'=1,2}$ is less than one, then the process exists and is unique on the real line (Embrechts et al., 2011). Moreover, within each spatial region j, the expected value of the intensity function associated with each type of event is given by the vector:

$$\begin{pmatrix} \mathbb{E}\left(\lambda_j^{(1)}\right) \\ \mathbb{E}\left(\lambda_j^{(2)}\right) \end{pmatrix} = (I_2 - A)^{-1}\boldsymbol{\mu}, \tag{5.19}$$

where I_2 is the 2-dimensional identity matrix and $\boldsymbol{\mu} = (\mu^{(1)}, \mu^{(2)})^T$ (Liniger, 2009).

5.4.4 Model 5: Spatial Hawkes processes

A model is required that incorporates and distinguishes between effects from neighbouring regions, and effects from non-neighbouring regions. For each spatial region j, denote by $\mathcal{N}(j)$ the set of indices corresponding to spatial regions that share a border with j, and denote by $(j \cup \mathcal{N}(j))^c$, the remaining set of non-neighbouring districts. For each district j, the effect from triggering events occurring in each of these sets of districts is modelled by an exponentially decaying triggering kernel with parameters that vary over each of the sets, but which are not dependent on j. Thus, the conditional intensity function for district j is given as

$$\begin{aligned} \lambda_j^{(l)}(t|\mathcal{H}(t)) =& \mu_l + \sum_{l'=1}^{2} \sum_{\substack{t_i<t \\ m_i=l' \\ s_i=j}} \alpha_{ll'1}\omega_l e^{-\omega_l(t-t_i)} \\ &+ \sum_{l'=1}^{2} \sum_{\substack{t_i<t \\ m_i=l' \\ s_i\in\mathcal{N}(j)}} \alpha_{ll'2}\omega_l e^{-\omega_l(t-t_i)} \\ &+ \sum_{l'=1}^{2} \sum_{\substack{t_i<t \\ m_i=l' \\ s_i\in(j\cup\mathcal{N}(j))^c}} \alpha_{ll'3}\omega_l e^{-\omega_l(t-t_i)}. \end{aligned} \tag{5.20}$$

The subscript 1, 2 or 3 is added to each of the excitation parameters to denote, respectively, excitation associated with events occurring within the same district, excitation associated with events occurring in neighbouring districts, and excitation associated with events occurring in non-neighbouring districts.

This results in 12 excitation terms to be estimated, together with 2 decay parameters and 2 background rate parameters. The parameters in the triggering kernels do not depend on the district j and so, whilst still incorporating the spatial structure of the case

study, are used to detect more general structural dynamics associated with the spreading of Naxal insurgency across the entire state, rather than the detection of specific hot spots of activity.

5.4.5 Model 6: Nonlinear spatial Hawkes processes

In the models considered so far, the excitation parameters are constrained to be non-negative, leading to an excitation effect: as events occur, the intensity function increases, rather than decreases. In order to consider inhibition effects, as specified by hypothesis 5 in Section 5.3, it should be possible for the intensity function to decrease as events occur, suggesting that the excitation parameters might be negative and be associated with an inhibition process. Relaxing the constraint that the excitation terms must remain positive brings about complications that result in a nonlinear intensity function. Specifically, the intensity function becomes

$$\begin{aligned}\lambda_j^{(l)}(t|\mathcal{H}(t)) = \Bigg(& \mu_l + \sum_{l'=1}^{2} \sum_{\substack{t_i<t \\ m_i=l' \\ s_i=j}} \alpha_{ll'1}\omega_l e^{-\omega_l(t-t_i)} \\ & + \sum_{l'=1}^{2} \sum_{\substack{t_i<t \\ m_i=l' \\ s_i\in\mathcal{N}(j)}} \alpha_{ll'2}\omega_l e^{-\omega_l(t-t_i)} \\ & + \sum_{l'=1}^{2} \sum_{\substack{t_i<t \\ m_i=l' \\ s_i\in(j\cup\mathcal{N}(j))^c}} \alpha_{ll'3}\omega_l e^{-\omega_l(t-t_i)} \Bigg)_+ ,\end{aligned} \tag{5.21}$$

where $(.)_+$ denotes the positive part of the function, such that

$$(x)_+ = \begin{cases} x & x \geq 0 \\ 0 & x < 0. \end{cases} \tag{5.22}$$

The positive part of the function is taken to ensure that the intensity function cannot become negative, which would be inconsistent with its definition as a limit of a non-negative counting process. The parameters $\alpha_{ll'1}$, $\alpha_{ll'2}$ and $\alpha_{ll'3}$ for $l, l' = 1, 2$ can now be negative, and thus the model can exhibit inhibition, as well as excitation.

Theorem 7 of Brémaud and Massoulie (1996) implies that there exists a unique stationary process with intensity function given by equation 5.21 if the matrix formed of the absolute values of the excitation parameters has spectral radius strictly less than one.

Since spatial interaction arises in this model, this matrix is constructed by including one row for each intensity function, with entries given by the excitation parameter associated with events that occur in each of the different regions considered. With 9 districts of Telangana, each with potentially 2 types of event occurring, this matrix has dimension equal to 18.

Introducing nonlinearity brings about complications in the estimation of the parameters, which are detailed in Section 5.5. To the knowledge of the author, such nonlinear models of Hawkes processes have not been applied to the spatio-temporal properties of problems in crime and security and thus the exploration of this model makes a significant contribution to the literature.

5.5 Parameter estimation

In this section, the parameters of the models described in Section 5.4 that provide the best fit to the empirical data are obtained. Maximum likelihood estimation is employed to find the most likely set of parameters, given the observations in the calibration data. As described in Section 5.2, the models are calibrated using events in the dataset that occurred within the nine districts that form the state of Telangana. The maximum likelihood procedure is first described, together with an efficient algorithm for calculating the likelihood function in the case of negative excitation parameters, addressing the difficulty associated with nonlinear models. Next, another algorithm is outlined, which enables the calculation of confidence intervals associated with estimated parameters by employing bootstrap techniques. The resulting parameter estimates for each model, and corresponding confidence intervals are then presented and conclusions are discussed.

5.5.1 Likelihood for nonlinear multivariate Hawkes processes

In line with many previous studies of parametric point process modelling, the unknown parameters are estimated using the method of maximum likelihood. The specification of a linear Hawkes process model via its conditional intensity function leads to an analytical expression for the log-likelihood function. For a single-dimensional linear Hawkes process with conditional intensity function given by

$$\lambda(t|\mathcal{H}(t)) = \mu + \sum_{t_i<t} \alpha\omega e^{-\omega(t-t_i)}, \tag{5.23}$$

for some history $\mathcal{H}$, with a vector of parameters $\boldsymbol{\theta} = (\mu, \alpha, \omega)$ such that $\mu, \alpha, \omega > 0$, and sample data with events occurring at times $\{t_i\}_{i\in\{1,2,3,\ldots,N\}}$, the log-likelihood function is given by

$$\log \mathcal{L}(\boldsymbol{\theta}|\mathcal{H}(t)) = \sum_{t_i<T} \log \lambda(t_i|\mathcal{H}(t);\boldsymbol{\theta}) - \int_0^T \lambda(s|\mathcal{H}(s);\boldsymbol{\theta})ds, \tag{5.24}$$

where $T \in \mathbb{R}$ is a point in time defining the end of the period of study, so that $T \geq t_N$. The values of $\boldsymbol{\theta}$ that maximise the log-likelihood have been shown to consistently approximate the true values of the process (Ozaki, 1979; Ogata, 1981). The log-likelihood in equation 5.24 can be thought of as a comparison between the value of the conditional intensity function at the times at which events occur, against the values of the function at all other times, as given by the integral of the intensity function over the duration of the sample data. Larger values of the log-likelihood therefore correspond to a series of events that are well predicted by the conditional intensity function, and the parameters $\boldsymbol{\theta}$ that maximise the value of the log-likelihood are those that most closely match the model to the empirical data.

The log-likelihood of a linear multivariate Hawkes process is described in Embrechts et al. (2011) and, using the notation of this chapter, is given by

$$\begin{aligned}\log \mathcal{L}(\boldsymbol{\theta}|\mathcal{H}(t)) = &\sum_{j=1}^{9}\sum_{l=1}^{2}\sum_{\substack{t_i<t\\ m_i=l\\ s_i=j}} \log\left(\lambda_j^{(l)}(t_i|\mathcal{H}(t);\boldsymbol{\theta})\right)\\ &- \sum_{j=1}^{9}\sum_{l=1}^{2}\int_0^T \lambda_j^{(l)}(s|\mathcal{H}(s);\boldsymbol{\theta})ds.\end{aligned} \tag{5.25}$$

Maximising the function in equation 5.25 leads to the parameter values that maximise the intensity function $\lambda_j^{(l)}$ at the point at which each event $(t_i, s_i = j, m_i = l)$ occurs, whilst minimising the sum of all intensity functions at all other times, and therefore leads to the parameter values that most closely match the model with the empirical data.

Liniger (2009) outlines how the first term on the left hand side of equation 5.25, the sum of the logarithms of each intensity function for the particular type of event at the time at which that event occurs, can be approximated using a recursive formula. In what follows, the calculation of the likelihood is described using Model 5. Equivalent expressions for Models 1 to 4 can be obtained by setting the relevant excitation parameter(s) to zero. Supposing that the first event occurs at time t_1, the algorithm proceeds

by setting

$$\lambda_j^{(l)}(t_1) = \mu_l, \tag{5.26}$$

for $j = 1, 2, ..., 9$ and $l = 1, 2$. Thus, the initial intensity for each type of event is assumed to be equal to its background rate. Then, the intensity functions at all other event times t_i for $i = 2, 3, ..., N$ can be calculated exactly as

$$\lambda_j^{(l)}(t_i) = \mu_l + e^{-\omega_l(t_i - t_{i-1})}\left(\lambda_j^{(l)}(t_{i-1}) - \mu_l\right) + \alpha_{lm_{i-1}\tilde{s}_{i-1}}\omega_l e^{-\omega_l(t_i - t_{i-1})}, \tag{5.27}$$

where $\tilde{s}_{i-1} \in \{1, 2, 3\}$ is used to denote the spatial domain within which the event at time t_{i-1} occurred relative to the spatial region j (i.e. to determine whether the event at time t_{i-1} occurred within district j, within $\mathcal{N}(j)$ or within $(j \cup \mathcal{N}(j))^c$, respectively). The use of the recursive scheme in equations 5.26 and 5.27 greatly increases the speed with which equation 5.25 can be numerically computed.

The integrals in the second term of the right hand side of equation 5.25 can be computed analytically for linear intensity functions by observing that

$$\int_0^T \alpha_{ll'n}\omega_l e^{-\omega_l(s-t_i)}ds = \left[-\alpha_{ll'n}e^{-\omega_l(s-t_i)}\right]_0^T = \alpha_{ll'n}\left(1 - e^{-\omega_l(T-t_i)}\right), \tag{5.28}$$

for $n = 1, 2, 3$. Therefore,

$$\begin{aligned}\int_0^T \lambda_j^{(l)}(s|\mathcal{H}(s);\boldsymbol{\theta})ds =& \mu_l T + \sum_{l'=1}^{2}\sum_{\substack{t_i<t\\ m_i=l'\\ s_i=j}} \alpha_{ll'1}\left(1 - e^{-\omega_l(T-t_i)}\right) \\ &+ \sum_{l'=1}^{2}\sum_{\substack{t_i<t\\ m_i=l'\\ s_i\in\mathcal{N}(j)}} \alpha_{ll'2}\left(1 - e^{-\omega_l(T-t_i)}\right) \\ &+ \sum_{l'=1}^{2}\sum_{\substack{t_i<t\\ m_i=l'\\ s_i\in(j\cup\mathcal{N}(j))^c}} \alpha_{ll'3}\left(1 - e^{-\omega_l(T-t_i)}\right),\end{aligned} \tag{5.29}$$

which can be easily computed for any given history $\mathcal{H}(T)$.

In the case of nonlinear multivariate Hawkes processes, such as the one defined by the intensity function in equation 5.21, an analytical expression of the integrals in the log-likelihood is not tractable, and, therefore, the expression described in equation 5.29 cannot be used for fast computation.

Instead, the integrals in equation 5.25 are solved numerically. A numerical scheme that discretised the entire temporal region of interest, however, would be very computationally expensive. In particular, to calculate the function in equation 5.25 in the

linear case, when there is no inhibition, the value of the intensity function only requires evaluation at the time points when events occur. A numerical discretisation of the integral typically requires the evaluation of the function at a much higher resolution and therefore adds significantly to the computational cost.

In an attempt to alleviate the reliance on computational power in the calculation of the likelihood function in equation 5.25, an algorithm is proposed that utilises the analytical solution to the integral when there is no inhibition, as given in equation 5.29. To explain, an efficient way of approximating the integral

$$\int_0^T \lambda_j^{(l)}(s|\mathcal{H}(s))ds \tag{5.30}$$

is sought when

$$\lambda_j^{(l)} = \left(\hat{\lambda}_j^{(l)}\right)_+, \tag{5.31}$$

for some function $\hat{\lambda}_j^{(l)}(t)$, which, for some values of t, is negative. The integral given by

$$\int_0^T \hat{\lambda}_j^{(l)}(s|\mathcal{H}(s))ds, \tag{5.32}$$

is calculated using the analytic expression in equation 5.29. Then, using the trapezoidal rule for numerical integration, and supposing that the temporal domain $[0, T]$ is discretised by a uniform partition $0 = t'_0 < t'_1 < ... < t'_n = T$ for some integer n such that $t_i = t'_r$ for some r for every event i, then

$$\begin{aligned}\int_0^T \lambda_j^{(l)}(s|\mathcal{H}(s))ds = \int_0^T \hat{\lambda}_j^{(l)}(s|\mathcal{H}(s))ds \\ - \frac{1}{2}\sum_{r=1}^{n} H(-\lambda_j^{(l)}(t'_{r-1}))\left(t'_r - t'_{r-1}\right)\left(\lambda_j^{(l)}(t'_{r-1}) + \lambda_j^{(l)}(t'_r)\right) + \epsilon_n,\end{aligned} \tag{5.33}$$

where $H(x)$ is the Heaviside step function, given by

$$H(x) = \begin{cases} 0 & x \leq 0 \\ 1 & x > 0, \end{cases} \tag{5.34}$$

and ϵ_n is an error term satisfying

$$|\epsilon_n| \leq \frac{T^3 \max_{t \notin \{t'_0, t'_1, ..., t'_n\}} |\lambda_j^{(l)\prime\prime}(t)|}{12n^2}, \tag{5.35}$$

a well-known property of the trapezoidal rule. Note that since the event times are contained within the set $\{t'_0, t'_1, ..., t'_n\}$, and since the function $\lambda_j^{(l)}(t)$ is smooth for all

values of t at which events do not occur, $\max_{t \notin \{t'_0, t'_1, \ldots, t'_n\}} |\lambda_j^{(l)\prime\prime}(t)|$ is finite and the error term tends to zero as n increases.

For a suitable partition on the interval $[0, T]$, the integral in equation 5.30 can be well approximated using the expression in equation 5.33. Specifically, the integral is approximated by the analytical computation of equation 5.32, from which the negative parts are subtracted, which are approximated using the trapezoidal rule, where event times are contained in the set of interval boundaries for the partition of the temporal discretisation. In many practical scenarios, particularly when the magnitude of excitation is greater than the magnitude of inhibition, there are relatively few time periods for which the function $\hat{\lambda}_j^{(l)}$ is negative. As a consequence, the computation in equation 5.33 greatly improves the speed by which the integrals in equation 5.25 can be computed when compared to a full discretisation over the entire temporal region. The values of the parameters $\boldsymbol{\theta}$ that maximise the log-likelihood in equation 5.25, which are obtained by calculating the value of equations 5.26, 5.27 and 5.29, and using equation 5.33 if the function $\lambda_j^{(l)}$ is nonlinear, with the empirical event history $\mathcal{H}(T)$, are therefore the values that lead to the closest fit between the empirical data and the model.

In the dataset on the Naxal conflict, there were a small number of days on which a large number of events of the same event type occurred within the same spatial region. In the analysis that follows, some of the events occurring on these days were removed from the dataset in order to prevent the model calibration attributing too much influence to these days, which are likely to have occurred as a result of an exogenous process, rather than the more natural dynamics of the violence that the model aims to capture. Specifically, to do this, the daily count of events of each event type and within each spatial region is obtained and the cumulative distribution of these counts is calculated. On days whose counts exceed the 99-th percentile of the cumulative distribution of the non-zero counts, a number of events are removed from the dataset so that the count on each of these days is equal to the count at the 99-th percentile. After this process, the maximum number of events of each type within each spatial reigon occurring on each day is three. Events that take the count beyond three are thus removed from the analysis and treated as outliers.

Finally, in order to ensure that the parameter values calculated for the conditional intensity function correspond to a unique point process, the process is required to be

simple, meaning that no two events can occur simultaneously. For the dataset on the Naxal conflict, there are 1,480 events which occur on the same day as at least one other event. For these events, a uniform random number between 0 and 1 is generated and added to the event time, leading to an empirical dataset that can be considered a simple point process. The potential consequences of this step were tested in what follows by repeating the parameter estimation with different realisations of the empirical history. Although minor changes were detected, there were no significant deviations from the estimates that follow as a result of this process. This is explained further in what follows.

The Nelder-Mead algorithm (Nelder and Mead, 1965) within the SciPy package of the Python programming language is used to maximise the log-likelihood function. Constraints are employed to ensure the decay parameters ω_l and the background rate parameters μ_l are positive by adding a penalty to the objective function when any of these parameters become negative. Furthermore, the decay parameters ω_l are also constrained to be less than one, so that the characteristic time window over which triggered events are supposed to occur cannot be less than one day, corresponding to the temporal resolution of the data. The Nelder-Mead algorithm is used since it uses only function evaluations of the objective function it maximises, rather than also values of gradients and higher derivatives. In this case, this is desirable since the log-likelihood function in equation 5.25 is discontinuous in the parameter $\boldsymbol{\theta}$ due to jumps that occur in the intensity function as a result of these constraints.

5.5.2 Parametric bootstrapping of confidence intervals

As well as obtaining the parameter estimates that lead to the best fit between the model and the data, maximum likelihood approaches can also often be used to obtain standard errors of those parameter estimates (as was the case in Chapter 4, with the conditional logistic regression). In such cases, the standard errors are calculated from the Hessian of the log-likelihood. In this chapter, however, some of the models tested are nonlinear, and the accuracy of standard errors obtained from the Hessian of the log-likelihood has not been well-established beyond a few individual case studies (Bowsher, 2007).

In order to construct a confidence interval of each parameter estimate, a numerical technique is employed called parametric bootstrapping. This numerical procedure

consists of two stages. First, a simulated history of the time period of interest is constructed, in which events are supposed to occur at the rate given by the conditional intensity function with parameters given by those obtained from the maximisation of the log-likelihood function. Second, the Nelder-Mead algorithm is employed to maximise the log-likelihood function in equation 5.25 based on this simulated history of the system. It is important to emphasise that the maximisation of equation 5.25 based on this simulated data does not use the empirical data, instead using the simulation version of the system that is based on the model with parameters that are calculated from data.

These two stages result in parameter estimates associated with simulated histories of the system defined by the model with the maximum likelihood estimators as parameters. If the model were able to perfectly recreate the empirical data, then the bootstrap procedure would be expected to produce the same parameter estimates as those found by the maximum likelihood optimisation procedure with the empirical data. On the other hand, if the model produces events with a very different space-time profile to the empirical data, then it is likely that the resulting parameter estimates will be very different to those found by the maximum likelihood procedure with the empirical data. Thus, this procedure produces an assessment of the extent to which the model is able to reproduce the empirical data at the parameter level. The resulting difference between the parameters calculated from the empirical model and the parameters calculated from the simulated model can be used to assess the extent to which the value of each parameter is likely to lead to similar spatial-temporal distributions of events as the empirical data. This deviation can therefore be used to assess the confidence associated with the estimate for each parameter.

Following this two stage procedure—the simulation of events using the model calibrated with the empirical data, followed by the subsequent parameter estimation based on that history—just once is not particularly instructive since the generation of each scenario is a random process, and the minimisation procedure may find different solutions. However, repeating this process a number of times can lead to a distribution of estimated parameters based on a series of simulated versions of the data that were generated from the same model. Consequently, this procedure is repeated 250 times and a 95% normal confidence interval for each parameter estimate is obtained by calculating the empirical standard error of the resulting distribution of simulated parameters.

It remains to explain how the times, locations, and types of events are obtained when generating simulated histories of the system. The simulation of point processes over a given period of time is typically performed using so-called thinning algorithms. Thinning algorithms have been developed in order to simulate the event times of point processes for any given conditional intensity function using uniform pseudo random number generators. The procedure described below is based on the methods first introduced in Lewis and Shedler (1979) and then modified in Ogata (1981) (see also Daley and Vere-Jones (2003)). It has been adapted here to coincide with the notation and multivariate nature of the point process described by the conditional intensity function in equation 5.21, the model from which all others can be derived by placing constraints on the parameters. The thinning procedure generates a series of random numbers at a rate given by an upper bound on the conditional intensity function, denoted by λ^* say. This generates more than the number of events required, and so a random thinning procedure is used to delete some of these events, and, in doing so, constructs a process that corresponds to the conditional intensity function $\lambda_j^{(l)}$ for $j = 1, 2, ..., 9$ and $l = 1, 2$. The algorithm proceeds as follows:

1. Set $t = 0$.

2. Calculate an upper bound on the intensity function at this time and denote this by λ^*.

3. Generate a exponentially distributed random variable $\mathcal{R}_{\exp}$ with rate λ^*, by transforming a uniform random variable $\mathcal{R}' \in [0, 1]$ according to

$$\mathcal{R}_{\exp} = -\frac{\ln(\mathcal{R}')}{\lambda^*}. \tag{5.36}$$

   The next event in a Poisson process with intensity λ^* is therefore supposed to occur at time $t + \mathcal{R}_{\exp}$.

4. Generate a second uniform random variable $\mathcal{R} \in [0, 1]$.

5. Set $j = 0$ and $l = 1$.

6. For district j and event type l, calculate the conditional intensity function $\lambda_j^{(l)}(t+$

$\mathcal{R}_{\text{exp}}$) and the cumulative sum

$$F_j^{(l)}(t) = \frac{1}{\lambda^*} \sum_{\substack{j' \leq j \\ l' \leq l}} \lambda_{j'}^{(l')}(t + \mathcal{R}_{\text{exp}}). \tag{5.37}$$

7. If $\mathcal{R} < F_j^{(l)}(t + \mathcal{R}_{\text{exp}})$ then assume that the Poisson event at time $t + \mathcal{R}_{\text{exp}}$ is an event of type l and occurs within district j. Add this event to the simulated history $\mathcal{H}(t + \mathcal{R}_{\text{exp}})$, set $t \to t + \mathcal{R}_{\text{exp}}$ and return to step 2.

8. Otherwise, consider the next district and/or event type by updating the indices j and/or l and return to step 6. If the districts and event types have been exhausted then the Poisson event occurring at time $t + \mathcal{R}_{\text{exp}}$ is deemed not to have occurred according to the conditional intensity functions given by $\lambda_j^{(l)}$ and is ignored. In this case, set $t \to t + \mathcal{R}_{\text{exp}}$.

9. In order to match the simulation as close to the empirical data as possible, the number of events that occur in the simulation is required to be equal to the number of empirical events in the dataset, given by N. Thus, if the number of events that have not been removed in steps 2-8 exceeds N, then go to step 9. Otherwise, return to step 2.

10. Since the absolute times at which events are deemed to occur is dependent on the upper bound that is chosen (but the relative rate at which events occur have been thinned according to the model), the events are rescaled so that the N events occur over the same time-scale as the original data set.

The upper bound λ^* at each potential event time $t + \mathcal{R}_{\text{exp}}$ is defined to be the sum of the conditional intensity functions $\lambda_j^{(l)}$ over $j = 1, 2, ..., 9$ and $l = 1, 2$, where each function is calculated assuming that the event at time $t + \mathcal{R}_{\text{exp}}$ is of type l and occurs within j. This can be written as:

$$\lambda^*(t + \mathcal{R}_{\text{exp}}) = \sum_{l=1}^{2} \sum_{j=1}^{9} \lambda_j^{(l)} \left(t + \mathcal{R}_{\text{exp}} | \mathcal{H}(t) + \{(t + \mathcal{R}_{\text{exp}}, j, l)\}\right). \tag{5.38}$$

As well as being used in the parametric bootstrap procedure to generate simulated histories of the system according to the model, this thinning procedure can also be employed to simulate predictions as to how the system might evolve, assuming model correctness.

5.5.3 Results

In this section, the results of the maximum likelihood optimisation for each of the models specified in Section 5.4 are presented, together with estimated standard errors obtained from the parametric bootstrap procedure for the final model. The implications of these results for the hypotheses in Section 5.3 are discussed.

Table 5.1 presents the maximum likelihood parameter estimates for Models 1-6 in Section 5.4 together with the value of the log-likelihood function at the parameter estimate, and the value of Akaike's Information Criterion in order to compare the relative success of each of the models proposed. Each realisation of the empirical history relies on a random process in order to remove concurrent events, and so the log-likelihood function was maximised 100 times based on different realisations of the empirical history that arises as a result of this random procedure. The results presented are the mean values obtained from this process. The standard deviations of the estimates are not reported as the estimated results are consistent across model types for each realisation of the empirical history and were small in comparison to the estimates. Akaike's Information Criterion (henceforth abbreviated as AIC) provides a measure with which to compare models, and to determine whether a model that incorporates a particular process or mechanism is an improvement on simpler models. The AIC is given by

$$AIC = -2 \ln \mathcal{L} + 2P, \tag{5.39}$$

where P is the number of parameters in the model. The value of the AIC is a trade-off between the value of the log-likelihood, for which larger values correspond to a better model fit, and the number of parameters included in that model to obtain that fit. Models with a lower AIC are preferred, highlighting the preference for simpler models with fewer parameters if the addition of extra parameters does not sufficiently improve the model fit.

Table 5.2 presents the bootstrapped 95% confidence intervals of the estimates for Model 6, which led to the lowest AIC value, and can therefore be considered as the best fit to the data. The procedure for generating these intervals was described in Section 5.5.2. The implications of these results are next discussed.

Model 1 assumes that Naxal events in each spatial region occur with a rate given by the constant μ_1 and that police events in each spatial region occur with a rate given

Table 5.1: **Parameter estimates for each of the six models described in Section 5.4**. Parameters proceeded by the same dagger symbol in Model 2 are constrained to be equal in order to model the effect from events occurring over the entire district. For the excitation terms, the first subscript refers to the type of event affected, the second subscript refers to the influencing event, and the third subscript refers to the relevant relative spatial region within which the influencing event occurred. For example, α_{122} is the additional number of Naxal attacks (type $l = 1$) that occur due to police events (type $l = 2$) within neighbouring districts (relative spatial region 2.)

	Model 1	Model 2	Model 3	Model 4	Model 5	Model 6
μ_1	.0838	.0047	.0066	.0064	.0023	.0023
μ_2	.0122	.0025	.0023	.0005	.0003	.0003
α_{111}		.1049†	.9226	.8704	.7801	.7780
α_{112}		.1049†			.0346	.0389
α_{113}		.1049†			.0020	.0017
α_{121}				.3766	.3942	.4075
α_{122}					.0000	-.0307
α_{123}					.0109	.0137
α_{221}		.0881‡	.8156	.3808	.3512	.3725
α_{222}		.0881‡			.0189	.0429
α_{223}		.0881‡			.0031	.0856
α_{211}				.0842	.0788	.1365
α_{212}					.0000	.0005
α_{213}					.0000	-.0313
ω_1		.0655	.0298	.0331	.0427	.0423
ω_2		.0404	.0102	.0197	.0221	.0115
$\ln \mathcal{L}(\boldsymbol{\theta})$	-12456	-11585	-10572	-10518	-10488	-10446
AIC	24916	23182	21157	21048	20989	20903

Table 5.2: **Bootstrapped 95% confidence intervals of each parameter obtained with Model 6.** Each of the entries is rounded to four decimal places.

	Estimate	Lower	Upper
μ_1	.0023	.0000	.0050
μ_2	.0003	.0000	.0026
α_{111}	.7780	.7233	.8327
α_{112}	.0389	.0210	.0568
α_{113}	.0017	-.0076	.0110
α_{121}	.4075	.2456	.5694
α_{122}	-.0307	-.0955	.0341
α_{123}	.0137	-.0292	.0566
α_{221}	.3725	.0418	.7032
α_{222}	.0429	-.0459	.1317
α_{223}	.0856	.0245	.1467
α_{211}	.1365	-.0076	.2806
α_{212}	.0005	-.0257	.0267
α_{213}	-.0313	-.0984	.0358
ω_1	.0423	.0148	.0698
ω_2	.0115	.0005	.0184

by μ_2. This model resulted in the worst fit to the data out of all of the models tested. A spatially disaggregated Poisson process model was also tested, consisting of 18 parameters, corresponding to the rates at which each type of event occurs in each of the 9 spatial regions under consideration. This was done to determine the improved performance of the model when spatial heterogeneity is considered. This model (Model 1a) is not reported in Table 5.1 but led to an AIC value of $23,244$.

Model 2, corresponding to a self-exciting Hawkes process in which excitation of the intensity function occurs when an event of the same type happens anywhere in any of the districts considered, shows a significant improvement on both the non-spatial Poisson process in Model 1, and the spatially disaggregated version of the Poisson process that was also tested in Model 1a, as can be seen by the lower AIC. Therefore, a self-exciting Hawkes process is a better model for explaining the variance in the data than both Model 1 and its spatially explicit alternative. This suggests that the dominant mechanism is not the spatial heterogeneity but the temporal clustering of the event data.

According to the parameters estimated for Model 2, for each Naxal event that occurs, the model predicts a further 0.1049 Naxal events will occur, and that, for each police event that occurs, a further 0.0881 police events will occur, as indicated by the excitation parameters α_{111}, α_{112}, and α_{113}, determining Naxal self-excitation, and the parameters α_{221}, α_{222}, and α_{223}, determining police self-excitation. Three parameters for each excitation are reported in Table 5.1, to highlight the fact that the excitation occurs over the entire spatial region of interest, whether the event occurs in the same district, a neighbouring district, or a non-neighbouring district. Although three parameters are reported for each excitation, only one parameter is adjusted as the model is calibrated, and thus the parameters for the different types of excitation are constrained to be equal to one another. The decay parameters, 0.0655 for Naxal events, and 0.0404 for police events, suggest that the excitation for Naxal events decays slightly more quickly back to baseline levels than for police events. Indeed, the characteristic time window over which the Naxals plan and carry out further attacks as a result of an attack, is 15 days, whilst police attacks due to excitation are likely to occur up to 24 days from a triggering event.

Model 2 lends support for hypotheses 1 and 2 articulated in Section 5.3. In particular, the improved model fit when a mechanism is incorporated to increase the intensity

for future events of the same type, suggests that the likelihood of a Naxal event occurring is increased for a period of time after a Naxal event and that the likelihood of a police event occurring in also increased in the aftermath of a police event.

Model 3 contains the same number of calibrated parameters as Model 2; however, the triggering kernel in Model 3 for each event type only incorporates events that occur within the same district. This model is spatially-explicit since the conditional intensity functions within each spatial region now vary from each other, depending on the number of events that occur in each district. A large improvement in the model fit is observed, with the AIC reducing by nearly 10%. Furthermore, the excitation parameters estimated—0.9226 for the Naxal events and 0.8156 for the police events—are much larger than the excitation parameters in Model 2. The model predicts that, for each event that occurs, nearly one further event of the same type will occur in the same spatial region. The decay parameters suggest that, for Naxal events, this extra event will occur up to a month after the triggering event, whilst for police events, this extra event will occur up to three months after the triggering event. These findings lend support for hypothesis 3 in Section 5.3: the influence from previous events is much stronger on districts in which those previous events occur.

A multi-level version of Model 3 was also estimated but is not reported here. This was done in order to test whether the inclusion of spatially varying background rate parameters significantly altered the results. If the resulting parameter estimates were significantly different from those reported in Table 5.1, then it may be that, rather than capturing the excitation effects due to the occurrence of events, the model is capturing the spatial heterogeneity. The parameter estimates for the triggering kernel in the multilevel model—which were not made spatially explicit—were consistent with those reported in Table 5.1. The AIC value for the multi-level model was $21,126$ and, thus, the decrease in the AIC value from Model 3 was the smallest reduction of all the models tested. As a consequence, and in order to perform out-of-sample testing of the model in what follows, models with constant background rates over the spatial region of interest were preferred.

Model 4 incorporates interacting excitation effects between different event types within the same spatial region. The excitation parameters are constrained to be positive in order to detect whether any retaliatory effects are present in the dataset. The param-

eters α_{121} and α_{211}—representing the excitation of the Naxal intensity function due to the occurrence of local police events, and the excitation of the police intensity function due to the occurrence of local Naxal events, respectively—that result in the closest fit between the model and the data are both greater than zero, indicative of an interaction effect. For each police initiated event that occurs, this model predicts an average of 0.3766 further Naxal attacks and, for each Naxal event, an average of 0.0842 police events are predicted. In comparison to Model 3, the self-excitation rates are reduced to 0.8704 and 0.3808 for Naxal events and police events respectively, suggesting that some of the excitation found in Model 3 can be better explained by interaction effects. Indeed, the AIC for Model 4 is lower than that found for Model 3, suggesting an improved model. Moreover, the results lend support for hypothesis 4 and hypothesis 6: 'tit-for-tat' retaliatory behaviour is observed between the Naxals and police.

Model 5, which introduces excitation effects from events occurring in neighbouring and non-neighbouring districts, further improves model fit, as indicated by the lower AIC value. In addition, the estimated parameter values provide some support for hypothesis 7: self-excitation rates appear to decay as events occur further from the region of interest. That is, for events of both types, self-excitation is strongest in the district within which the events take place, weakens by an order of magnitude for events that occur in neighbouring districts, and weakens by a further order of magnitude for events that occur elsewhere in Telangana.

Two of the mutual-excitation parameters become negative when inhibition effects are incorporated in Model 6: the impact of police events in neighbouring districts on the rate of Naxal events, and the impact of Naxal events in non-neighbouring districts on police events. However, neither of these effects are significant at the 95% level, according to the bootstrap estimates in Table 5.2.

The confidence intervals for parameters measuring excitation effects on police intensity from Naxal events contain the value zero and thus there is insufficient evidence to conclude that police were retaliating to Naxals according to this model. This puts into doubt the conclusion of hypothesis 6 stated above: although the point estimates for retaliation are positive, there is sufficient uncertainty with this estimate to question any positive finding. The confidence interval obtained for α_{221}, capturing the local self-excitation of police events, is also relatively large. The uncertainty associated with

the parameters for police events might be explained by the relatively small number of police events that occur in comparison to Naxal events.

The remaining confidence intervals, as detailed in Table 5.2, are relatively consistent with the parameter estimates of Model 6. Table 5.2 provides a parameter level assessment of the accuracy of the model specification. Furthermore, evidence has been presented that either supports or refutes each of the hypotheses presented in Section 5.3.

5.6 Model evaluation

In this section, a global assessment of the model is made, first by considering the extent to which the model explains the occurrence of events, and, second, to determine how successful the model is able to predict events that are not used in the model calibration. The tests that follow are important steps that must be taken before any such model can be considered for use in a policy setting, and are particularly important if the model is to be used for forecasting and predicting the evolution of conflict based on its history.

A residual analysis is performed to ensure that the variation of the values of the modelled intensity functions at the event times is consistent with the actual event times, and that no significant mechanisms for the generation of those events have been omitted, given the event data. Next, by performing a receiver operating characteristic analysis and by constructing the precision-recall curve using out-of-sample data, it is determined whether the model is capturing a general process for the production of events by insurgents and counter-insurgents during the Naxal conflict, or whether the model has been over-fitted to the calibration data.

5.6.1 Residual analysis

The goodness of fit of the overall model to the empirical data can be assessed by a residual analysis. The procedure in this section corresponds closely to the procedure outlined in Peng (2003) for single-dimensional point processes and in Schoenberg (2003) and Peng et al. (2005) for multi-dimensional point processes.

A residual process of length N_s is the result of a random selection of N_s events from the full event space, chosen as examples of events which are poorly predicted by the model. Events are considered to be poorly predicted if the value of the correspond-

ing intensity function is small prior to their occurrence. A residual process of length N_s of a point process of length N given by (t_i, s_i, m_i) for $i = 1, 2, ..., N$ is constructed by randomly sampling without replacement N_s events from the list of N events, where each event i is selected with some probability P_i.

Defining P_i by

$$P_i = \frac{\left(\lambda_{s_i}^{(m_i)}(t_i^-)\right)^{-1}}{\sum_{i'=1}^{N} \lambda_{s_{i'}}^{(m_{i'})}(t_{i'}^-)^{-1}}, \tag{5.40}$$

where t_i^- is used to denote the time just before event i occurs, leads to a residual process that selects events that occurred when, on average, the intensity function is at its smallest.

If the model explains all the variance in the data, then events that occur when the intensity functions are at their smallest will appear to have no temporal dependency. If there was extensive temporal clustering within the residual process, then the model is likely to be underestimating the excitation as a result of those events during the periods of clustering. Conversely, if there a large periods of time during which no events occur in the residual process, the intensity function is likely to be overestimating the likelihood of event occurrence during that time.

If the residual process is approximately a Poisson process with constant intensity throughout the duration of the conflict, then the model can be considered to reliably calculate the likelihood with which events are anticipated to occur throughout the duration of the period of study. In particular, if the residual process resembles a Poisson process for the duration of the study period then the model is appropriate for the entirety of this duration. This is particularly important for the case of the Naxal conflict considered in this chapter, since the period of study is over 10 years. Potential sources of error may arise if the process dramatically changed its underlying dynamics during this time.

Residual processes of the Naxal conflict using Model 6 are constructed with chosen length 91. This length was chosen since it is the number of background events expected to have occurred over all districts and events types according to the calibrated background rate of Model 6. 1000 residual processes are generated and compared with 1000 Poisson processes of rate $91/3872 = 0.024$, calculated since 91 events are required to occur over a duration of 3872 days with constant rate. The Poisson processes are constructed by simulating successive event times, utilising the result that inter-event

times between two successive events in a Poisson process are exponentially distributed with mean given by the reciprocal of the Poisson intensity.

The residual processes are compared with the Poisson processes using a quantile-quantile (Q-Q) plot. A Q-Q plot compares the rate at which events occur in two separate processes by plotting the number of quantiles of events that have passed in each process for different points in time. Beginning with $t = 0$, the Q-Q plot is constructed by adding δt to t for some $\delta t << 1$, and then calculating the proportion of events in each process that have occurred up until time t. This generates a line in Q-Q space (the region $[0, 1] \times [0, 1] \in \mathbb{R}^2$). Since the two distributions for comparison here each have 1000 realisations, such a line cannot be drawn and, instead, the 95% confidence intervals in Q-Q space are plotted. The two solid lines in Figure 5.4 correspond to the 95% confidence interval of the Q-Q plot distribution for a residual process compared against a Poisson process, and the grey shaded region represents the 95% confidence interval of the Q-Q plot distribution for the simulated Poisson processes compared against a Poisson process. For clarity, the aggregate results for both Naxal initiated events and police initiated events are explored, rather than retaining the individual counts for each district.

For the residual process to be an approximate Poisson process, and therefore for the model to be a good fit to the data, the solid lines are required to coincide with the grey shaded region in the plots in Figure 5.4. For Naxal events, shown on the left hand side of Figure 5.4, the solid lines correspond relatively closely with the grey shaded region, suggesting that the model provides a reasonable fit to the data. For police events, the fit is less good, suggesting that the dynamics associated with the production of police events is not well described by the models proposed here. Perhaps this is to be expected: police are likely to operate under more constraints than their Naxal counterparts, and may be unlikely to react as quickly as the identified retaliation and excitation processes found as part of the Naxal attacks. The different strategies adopted by the police in various attempts to quell the insurgency may have also meant that a Hawkes process with constant background and excitation rates over the duration of the study period is not a good description of event occurrence. Models that change over time to reflect different counterinsurgent strategies may improve the ability to explain counterinsurgent events.

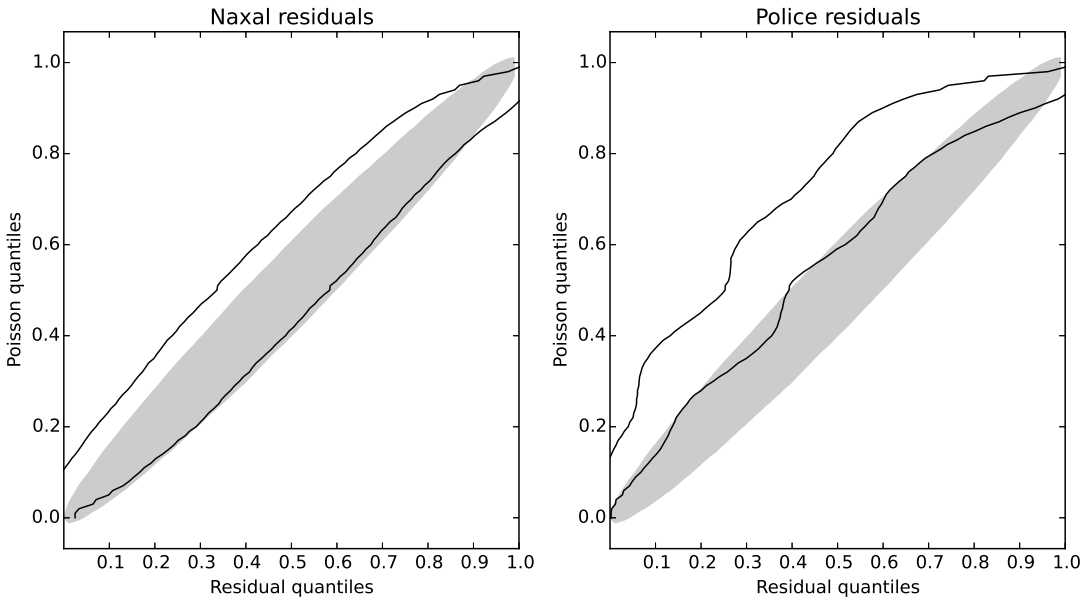

Figure 5.4: **A Q-Q plot to compare the Poisson process with the process obtained from the residual analysis in section 5.6.1 with Model 6 for Naxal events (left-hand side) and police events (right-hand side).** The shaded region shows the 95% confidence interval Q-Q plot of two Poisson processes, whilst the solid lines show the 95% confidence interval of the residual process against a Poisson process. The confidence interval of the residual process is obtained by repeating the sampling procedure described in Section 5.6.1 1000 times.

5.6.2 Out of sample predictive performance

The performance of a model can be assessed by its ability to predict events that were not used in the calibration procedure. This is particularly important if the model is to be used in a policy setting to assess the likelihood of events occurring. In what follows, two tests of predictive performance are employed: a receiver operating characteristic analysis and a precision-recall analysis.

Receiver operating characteristic (ROC) analysis is a visual approach to determine how well a model is able to classify a set of new observations into one of two classes: positive and negative. Originally developed in the study of signal detection, ROC analysis has subsequently been considered in a range of fields for assessing the goodness of fit of classifier models (Fawcett, 2006; Ward et al., 2010). ROC analysis is performed by plotting a ROC curve, which compares the rate at which the model is able to successfully identify positive observations, the true positive rate, against the rate at which the model mistakenly assigns an observation to be positive when in fact it is negative, the false positive rate.

In order to perform a ROC analysis, the model of Naxal violence must first be transformed into a classifier model. Although point process models such as the ones developed in this chapter are naturally continuous in time, a temporal discretisation of the model is applied in order to define the units of observation that require classification. This is done by taking each day within each spatial unit and of each type of event as a separate observation. Denoting the time unit of the k-th day under consideration by $\mathcal{T}_k = [t^{(k)}, t^{(k+1)}]$, the classifier model is required to determine whether or not at least one incident of type l occurred in spatial region j on day $\mathcal{T}_k$.

To specify the classifier model, a threshold approach is employed. For a given threshold $\tau > 0$,

$$\lambda_j^{(l)}(t^{(k)-}) \geq \tau, \tag{5.41}$$

implies that the model predicts at least one event to occur on day k, in spatial region j of event type l, and

$$\lambda_j^{(l)}(t^{(k)-}) < \tau, \tag{5.42}$$

implies that no event is predicted to occur. Note that the value of the intensity function is calculated at the beginning of each observation day and does not include any of the

events that occurred on that day.

To plot the ROC curve, the true positive rate and the false positive rate for a given threshold τ is required. The true positive rate is given by the total number of events that were successfully predicted by the model divided by the total number of positive events in the dataset (given by the number of days on which events occur within each spatial region of each event type), and the false positive rate is given by the total number of events mistakenly predicted by the model (i.e. those that did not occur in the dataset but were predicted to occur by the model), divided by the total number of observations that contained no events.

For each value of τ, the above calculation provides one point in ROC space. In order to plot the ROC curves, different values of τ are considered and the same calculation of the true positive rate and the false positive rate is made. The choice of τ is made so that the resulting curve is convex, as detailed in Davis and Goadrich (2006). The curves resulting from a ROC analysis omit a useful statistic for comparing models, given by the area under the curve (AUC). The AUC is equal to the probability that a new positive event will rank higher than a new observation with no event, and therefore provides a measure of reliability of the model for a given sample.

In Figure 5.5, three ROC curves are plotted. The solid curve is calculated using out of sample data. That is, the true positive rate and false positive rate are calculated for observations that were not used in the calibration of the model. The out of sample data consists of the Naxal events that occurred within the 4 districts of Andhra Pradesh, which contained at least 100 events, and which did not form part of the new state of Telangana and therefore were not used in the parameter estimation procedure. When calculating the model, excitations from other districts (i.e. neighbouring and non-neighbouring districts) were incorporated but only the out of sample events specified were predicted. The second curve is calculated using the in-sample data, containing events that occurred within the districts forming Telangana, and which were used to calibrate the parameters. Finally, a third ROC curve is plotted using an indiscriminate model, which randomly assigns positive events for each observation with probability τ.

The ROC curves for Model 6 are those that are plotted in Figure 5.5 since this was the model that provided the lowest AIC statistic. Typically, AUC values of above 0.8 are considered to correspond to a good model and therefore a relatively high level

of discrimination between positive events and negative events is observed for both in-sample and out-of-sample tests. Additionally, the AUC value for the out-of-sample data is very close to the AUC value for the in-sample data, suggesting that the model has not been overfitted to the calibration data, and that it is in fact capturing some of the general mechanisms underlying the production of conflict events.

There are problems associated with the ROC-curve when the associated data is highly skewed. The ROC-curve shows the proportion of events successfully predicted against the proportion of non-events successfully predicted. Since these are proportions, they do not depend on the actual number of events that occurred. The denominator of the false positive rate is the number of observations that were successfully predicted by the model to contain no events. If the number of observations with no events is much greater than the number of observations with an event (as is the case with the data used in this study), then the classifier successfully predicts nothing to happen for a large proportion of observations, and the false positive rate becomes very close to one very quickly, giving the impression that there is a large level of discrimination between positive events and non-positive events. For analysis of events that are relatively rare, the ROC curve tends to provide a large AUC, regardless of the actual success of the model.

To alleviate these limitations associated with the ROC curve, another approach to analysing classifier models is often presented, known as the precision-recall (PR) curve. Supposing that the classifier model has positively classified an observation, and thus the model predicts at least one event of a particular type to occur in a given spatial region on a given day, then *precision* is defined as the probability that this event will actually occur. Supposing that at least one event of a particular type occurs in a particular spatial region on a given day, then *recall* is defined as the probability that the model would have positively classified this observation, and therefore predicted the event to occur. The PR curve therefore shows the trade off between enabling the model to predict the actual events, whilst making sure that it does not predict too many events that do not happen.

The advantage of the PR curve is that it does not depend on the number of observations which were successfully predicted to have not occurred by the model, and therefore the biases that feature in the ROC curve do not occur here. The disadvantage

of the PR curve is that it is highly dependent on the number of events that occur in the dataset. Whereas the ROC curve can be used for different sample sizes, the PR curve must be applied on the same sample. For this reason, only the out of sample PR curve is plotted.

Figure 5.6 shows the PR curve for the out of sample classifier for model 6 and compares the model against an indiscriminate model on the same sample. The curve is constructed using the algorithm described in Davis and Goadrich (2006). It demonstrates how, for some threshold values of τ, if the model predicts an event to occur then there will be up to around a 20% chance that the event will actually occur. At the same time, if an event occurs, the model will have up to around a 20% chance of correctly predicting that event.

The ROC analysis and the PR analysis subtly demonstrate different aspects of the performance of the model. The closeness between the ROC curve for the out of sample data and the ROC curve for the in-sample data suggest that the model has not been overfitted to the available data. The PR curve demonstrates the models predictive performance when applied to out-of-sample data. The PR curve is unbiased with respect to the successful prediction of no events occurring but cannot be used to compare over different datasets. Although there is significant room for improvement, the values reported are much greater than is possible from using an indiscriminate model. In addition, it is worth emphasising that the models proposed are relatively parsimonious and only employ the history of the system as predictive variables. Incorporating a range of structural variable may further improve its performance (Zammit-Mangion et al., 2012).

5.7 Discussion

This chapter has proposed novel multivariate and nonlinear Hawkes process models for the modelling of insurgent violence, together with a range of tools for their calibration and evaluation. Point process models are a versatile modelling framework well-suited to the study of civil violence, but are only beginning to be employed in this domain. The work presented here is intended to contribute to this emerging study area.

The models presented in this chapter have led to theoretical advances in the understanding of insurgent violence. It has been shown, for instance, that considering

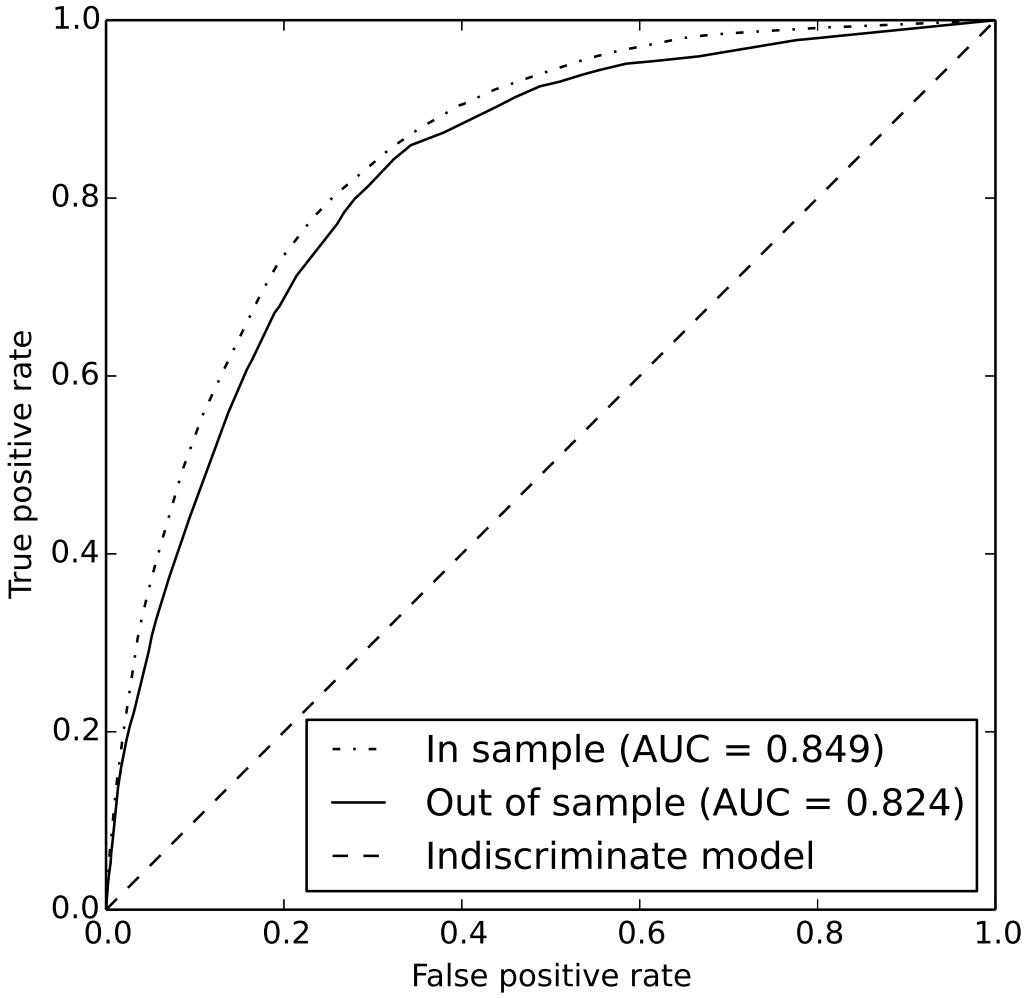

Figure 5.5: **Receiver operating characteristic (ROC) curves for: i) out of sample prediction of Naxal and police events using Model 6; ii) in-sample prediction of Naxal and police events using Model 6; and iii) an indiscriminate model that randomly assigns events to each day with a certain probability.** The out of sample analysis is performed on four districts in Andhra Pradesh that contained at least 100 events that were not used in the calibration of model parameters. The in-sample analysis is performed on all events used in the model calibration.

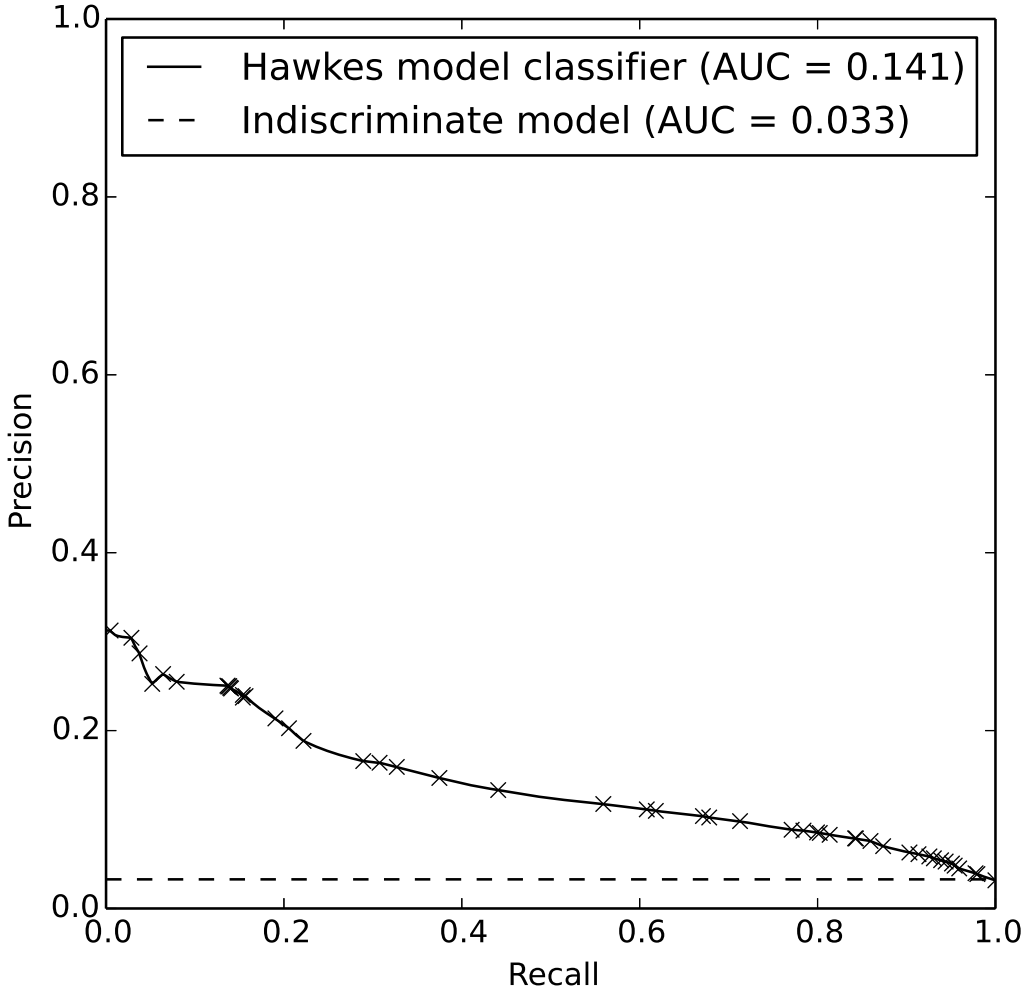

Figure 5.6: **Precision recall curves for the out of sample classifier of Model 6 (solid line) and an indiscriminate model that assigns new observations to be positive with probability τ (dashed line).**

the escalation of both insurgent and counterinsurgent actions leads to a significant improvement in the fit associated with point process models of civil violence. Incorporating the spatial dependency of the violence has also been shown to improve modelling performance, as evidenced by the improvement of the model when self-excitation acts locally, and when spatial interaction effects are incorporated through neighbouring district and non-neighbouring district excitation (although the effects from neighbouring and non-neighbouring districts were less strong).

There was evidence to suggest that insurgents retaliated to police events: the occurrence of a police event was found to increase the likelihood of Naxal events. This suggests that the counterinsurgent actions of the police that resulted in the death of at least one Naxal did, on average, little to improve the security situation in the short term.

The timings of police events were less well predicted by the model. Although positive parameters were found for the excitation of police intensity as a result of Naxal events, these estimates were not significant at the 95% level, according to the parametric bootstrapping procedure. The lack of model fit for police events suggests that another model may be more appropriate, such as one that varied in time according to the different counter-insurgent strategies adopted.

For Naxal events, the close fit between the residual process and a Poisson process for Naxal events suggests that the dynamics underlying the production of insurgent events appears relatively consistent over the ten years of the study period. Of course, the data used does not capture the whole picture, as it relies on police actions resulting in Naxal loss of life and does not account for their other activities. Others might also point to the fact that insurgent activity reduces significantly in the latter stages of the period of study. Nevertheless, this reduction in violence was not inconsistent with the Hawkes model, and thus this demonstrates that the model can be a powerful tool in the prediction of event occurrence.

There have been a number of modelling contributions made in this chapter. A series of point process models were constructed with increasing complexity to test a number of hypotheses inspired by current literature on civil violence, conflict and insurgencies. The models themselves are novel in that they incorporate the multivariate nature of the data, spatial interaction effects and nonlinearities brought about by inhibition. The calibration procedure for maximum likelihood estimation when the con-

ditional intensity function consists of the positive part of a possibly negative function is a new contribution to the literature. In addition, the consolidated presentation of bootstrap estimations of parameter-level confidence intervals, residual analysis for determining goodness of fit, and techniques for assessing the out of sample predictive performance of a classifier model derived from the point processes serves to demonstrate the potential applicability of the model.

There are numerous aspects of the conflict that this study has not taken into account. The close correspondence between the in-sample and out of sample ROC curves in Figure 5.5 suggest that the model has not been overfitted to the calibration data, and therefore that other mechanisms may well improve the model fit, beyond that which is demonstrated in the residual analysis in Section 5.6.1. Two examples of influences that might be incorporated into future models include the role of civilians in the conflict, and particular features of each of the spatial regions that might make them either more or less likely to experience conflict events, two factors that have been extensively studied previously in the context of civil violence. Limitations also arise due to the model's inability to account for coordinated attacks that occur simultaneously. The models relied on the assumption of a simple point process, which enabled unique conditional intensity functions to be proposed. The models are also subject to potential sources of error due to the choice of spatial units employed. In this case, the choice of spatial units was made in accordance with the available data since fine scale location data was not available.

This chapter progresses further along the modelling spectrum introduced in Chapter 1. General mechanisms have been incorporated into a model of civil violence, namely, the self- and mutual-excitation of events, and the spatial dependency of those excitations, combined with empirical data on the history of the conflict. Compared to the model of rioter target choice in Chapter 4, less empirical data has been employed, and the mechanisms proposed are more general. In Chapter 6, a further step along this spectrum will be made, in which a deterministic model is proposed based on the mutual interaction of adversaries.

Chapter 6

Spatial deterministic modelling of conflict between two adversaries

6.1 Introduction

Deterministic models reproduce exactly the same behaviour for two identical starting positions or initial system states. There is no randomness in the behaviour of system entities, and the system will behave precisely as specified by the model for each initial state. If the apparent random nature of much empirical data can be interpreted as fluctuations from a more deterministic process, then deterministic models can be used to model complex systems by specifying the behaviour of individual system entities and their interactions for a range of possible scenarios.

One of the reasons for employing such approaches is that deterministic models are amenable to a range of powerful mathematical techniques capable of exploring and providing insights into the logical consequences that follow from the model specification. Consequently, inappropriate implications that result from the proposed mechanisms are highlighted, and these mechanisms can be assessed with regards to their suitability for describing the system. In this sense, deterministic models are useful for evaluating the extent to which our understanding of how a system works provides a plausible account of the observed phenomenon. Furthermore, if a mechanism is considered to be appropriate, analytical tractability can provide intricate insights into the system it models.

The formulation of differential equations is one way of constructing deterministic models of complex systems. Differential equations model the rate of change of a dependent variable with respect to an independent variable, and can be naturally formulated for a wide range of systems. Additionally, since differential equations have been analysed largely in the context of physical systems for hundreds of years, a large range of tools and analytical concepts exist to interrogate such models. These tools are largely concerned with the evolution and behaviour of the modelled system state in phase space–the space defined as the union of all possible system states—and the consideration of how this might change through either the variation of parameters associated with the model, or through perturbations of the model itself. Two properties of a deterministic model that might be of interest include the stability of system states and the robustness of that stability to possible changes.

Differential equations are well-equipped to model a range of both temporal and spatio-temporal processes and, in Chapter 2, many examples are given related to the study of conflict and civil violence. One of these, the Richardson arms race model, is

considered in this chapter in more detail. This example is used to demonstrate techniques to analyse differential equations, and to consider how such techniques might provide insights into an observed phenomenon. The relative simplicity of this model ensures wide applicability to a range of conflict scenarios, and not just to the military aims of competing nations, a fact that has been exploited in other studies.

Inspired by the findings earlier in this thesis and elsewhere that highlight the need for incorporating spatial dependency in models of human conflict, a novel spatial extension to the Richardson model is presented, which enables the direct consideration of space on the interactions of competitive adversaries. This spatially explicit model is distinct from existing spatial models of conflict, which typically rely on partial differential equations or agent-based simulations to model spatial dependencies. It is argued why this approach to spatial disaggregation, which is based on entropy-maximising spatial interaction models, is well-suited to modelling spatial dependency in civil violence. Advantages arise due to the model's ability to incorporate non-smooth spatial domains and more general metric spaces. Moreover, it is argued that, in contrast to other types of spatial models, this model is more in line with Richardson's original incentives for developing his model: that simple, heuristic results can lead to powerful insights, as well as a framework for investigating conflict processes.

After deriving this spatial model, which to the knowledge of the author has not been proposed elsewhere previously, a range of analytical techniques are applied in order to gain insights into its properties. Starting with highly simplified scenarios, for which the behaviour of the model can be wholly determined, its complexity is slowly increased by considering higher-dimensional phase spaces and corresponding parameter spaces, leading to an understanding of the model's dynamics in more general scenarios.

A supercritical pitchfork bifurcation in the solution path of the model is identified within a region of the phase space in which real-world systems are likely to be located. This bifurcation is shown to be persistent under a wide range of parameter choices, and its consequences are discussed. In particular, it is shown how this bifurcation comes about as a result of the spatial disaggregation of the model, and emphasises the importance of considering spatial dependency in such models.

This chapter fits into this thesis by considering a modelling approach that has been widely employed to model social systems, and, in doing so, introduces and analyses a

new model capable of capturing spatial dependencies in civil violence and other types of conflict. Although stochastic models might be better at capturing the apparent randomness with which social systems appear to exhibit, and therefore might be more adept at prediction and the estimation of model uncertainty, deterministic models can still be used to provide insights into our understanding of social processes. Furthermore, deterministic models can often be specified at a more abstract level than many statistical models, and, as such, their findings can be translated across a range of examples. This chapter progresses further along the spectrum of model types introduced in Chapter 1, and enables the comparison between the insights obtained by this model, and insights obtained by the types of models considered elsewhere in this thesis. This perspective will be summarised in Chapter 7.

6.2 The Richardson model

As described in Chapter 2, the Richardson model was initially conceived as a model of arms expenditure between two nations in the lead up to war. As a consequence, the dependent variables, given here by p and q, were taken to be the level of military expenditure of two nations. The model is given by the following two-dimensional linear system of ordinary differential equations:

$$\begin{aligned} \frac{dp}{dt} &= \dot{p} = -\sigma_1 p + \rho_1 q + \epsilon_1 \\ \frac{dq}{dt} &= \dot{q} = \ \rho_2 p - \sigma_2 q + \epsilon_2, \end{aligned} \tag{6.1}$$

where parameters σ_1 and σ_2 determine the influence on the change in defence expenditure proportional to existing expenditure, and ρ_1 and ρ_2 determine the rate of the action-reaction relationship between the two adversaries. The terms ϵ_1 and ϵ_2 are those associated with the external grievances. Typically, ρ_1 and ρ_2 will be positive, as military defences of one side will cause increasing defences of the other. σ_1 and σ_2 are also typically positive: Richardson hypothesised that there will be some inhibition associated with an increasing military arsenal, perhaps through pressures placed upon the government of each nation by their electorate.

In order to analyse the system in equation 6.1, it is first written in vector form as

$$\begin{pmatrix} \dot{p} \\ \dot{q} \end{pmatrix} = \begin{pmatrix} -\sigma_1 & \rho_1 \\ \rho_2 & -\sigma_2 \end{pmatrix} \begin{pmatrix} p \\ q \end{pmatrix} + \begin{pmatrix} \epsilon_1 \\ \epsilon_2 \end{pmatrix},$$

or, equivalently,

$$\dot{\mathbf{p}} = P\mathbf{p} + \boldsymbol{\epsilon}, \tag{6.2}$$

where the vectors $\mathbf{p} = (p, q)$ and $\boldsymbol{\epsilon} = (\epsilon_1, \epsilon_2)$ and the matrix

$$P = \begin{pmatrix} -\sigma_1 & \rho_1 \\ \rho_2 & -\sigma_2 \end{pmatrix},$$

have been defined.

Given an initial condition, $\mathbf{p}_0 = (p_0, q_0)$, a solution of equation 6.2 defines the resulting trajectory, or solution curve, $\mathbf{p}(\mathbf{p}_0, t)$, with $\mathbf{p}(\mathbf{p_0}, 0) = \mathbf{p_0}$. In general, it can be shown that, for suitable systems (i.e. those whose derivatives are defined locally by continuously differentiable functions, f), solution curves to the differential equation $\dot{\mathbf{p}} = f(\mathbf{p})$ exist locally to $\mathbf{p}_0$ and are unique (Guckenheimer and Holmes, 1983, pg. 3).

Of particular interest when faced with an ordinary differential equation is not just on the identification of particular solution curves, but consideration of a family of solution curves. There may, for instance, be different solution curves which eventually result in exactly the same long-term behaviour. When this is the case, it is instructive to identify the set of all initial conditions that result in the same long-term behaviour. This set of initial conditions is commonly known as the basin of attraction of that particular long-term system state.

For general systems of differential equations, there are a range of different types of long-term behaviours, however just two are considered initially: divergence to infinity, and convergence to a single equilibrium point. Both of these behaviours will be shown to be present in the Richardson system, meaning that, according to the model, defence levels of both nations will either tend to a constant, or continue escalating (or de-escalating, depending on the sign of infinity). It is first shown analytically how these behaviours can occur, before discussing the real-world implications for the different types of behaviour. Although the analysis initially presented is straightforward, it is nevertheless instructive to understand the possible behaviours of the system, and to understand how insights might be obtained from deterministic models more generally.

Equilibrium points occur when solution curves in the p-q plane stop changing, so

that $\dot{\mathbf{p}} = 0$. For the system in equation 6.2, this occurs at the points (p_e, q_e) for which

$$-\sigma_1 p_e + \rho_1 q_e + \epsilon_1 = 0 \tag{6.3}$$

$$-\sigma_2 q_e + \rho_1 p_e + \epsilon_2 = 0. \tag{6.4}$$

If $\sigma_1\sigma_2 \neq \rho_1\rho_2$, then, by adding ρ_2 multiplied by equation 6.3 to σ_1 multiplied by equation 6.4, and by adding σ_2 multiplied by equation 6.3 to ρ_1 multiplied by equation 6.4, it can be shown that there is a unique solution given by

$$(p_e, q_e) = \left(\frac{\sigma_2\epsilon_1 + \rho_1\epsilon_2}{\sigma_1\sigma_2 - \rho_1\rho_2}, \frac{\sigma_1\epsilon_2 + \rho_2\epsilon_1}{\sigma_1\sigma_2 - \rho_1\rho_2} \right). \tag{6.5}$$

Alternatively, if $\sigma_1\sigma_2 = \rho_1\rho_2$, then if

$$\sigma_2\epsilon_1 + \rho_1\epsilon_2 = 0, \qquad \sigma_1\epsilon_2 + \rho_2\epsilon_1 = 0,$$

there are infinitely many equilibrium values in the p-q plane, otherwise there are none.

Looking first at the case in which $\sigma_1\sigma_2 \neq \rho_1\rho_2$, the equilibrium point in equation 6.5 is the only point in the p-q plane at which the system is stationary: at this point, both $\dot{p}$ and $\dot{q}$ are equal to zero. The constant term $\boldsymbol{\epsilon}$ can be eliminated from equation 6.2 by changing variables using the mapping $\mathbf{p}' = \mathbf{p} - P^{-1}\boldsymbol{\epsilon}$ (the determinant of P is $\sigma_1\sigma_2 - \rho_1\rho_2$, which is set as nonzero, which ensures the inverse to P exists). Removing primes for convenience, the system becomes

$$\dot{\mathbf{p}} = P\mathbf{p}, \tag{6.6}$$

and the change of variables has the effect of moving the equilibrium point to the origin.

Since the system is linear in the dependent variables, any two linearly independent solutions $\mathbf{p}_1(t)$ and $\mathbf{p}_2(t)$ can be combined to form a general solution

$$\mathbf{p}(t) = c_1\mathbf{p}_1(t) + c_2\mathbf{p}_2(t)$$

which spans the p-q plane, where, for each initial condition $\mathbf{p}_0$, the unknown constants c_1 and c_2 are chosen so that $\mathbf{p}(0) = \mathbf{p}_0$.

Since the analogous one-dimensional differential equation $\dot{y} = ay$ has solutions of the form $y(t) = ke^{at}$, solutions of the system in equation 6.6 are sought in the form $\mathbf{p}(t) = \mathbf{v}e^{\lambda t}$ for some $\lambda \in \mathbb{R}$ and $\mathbf{v} \in \mathbb{R}^2$. This yields

$$\lambda\mathbf{v}e^{\lambda t} = P\mathbf{v}e^{\lambda t},$$

and, therefore, λ and $\mathbf{v}$ are, respectively, an eigenvalue and eigenvector of P.

If $\mathbf{v}_1$ and $\mathbf{v}_2$ are two linearly independent eigenvectors of P, with corresponding eigenvalues λ_1 and λ_2 (which may be complex), then the two solutions are linearly independent and the general solution is given by their linear combination, so that

$$\mathbf{p}(t) = c_1\mathbf{v}_1 e^{\lambda_1 t} + c_2\mathbf{v}_2 e^{\lambda_2 t} \tag{6.7}$$

for constants c_1 and c_2 which are specified by the initial conditions. Furthermore, it can also be shown that, for a given initial condition $\mathbf{p}_0$, the general solution in equation 6.7 is unique (Hirsch et al., 2004).

If $\mathbf{v}_1$ and $\mathbf{v}_2$ are linearly dependent, then another, linearly independent solution is required in order to construct the general solution in the plane. This linearly independent solution can be derived from the generalised eigenvector $\mathbf{v}_3$, defined as $(P - \lambda I_2)\mathbf{v}_3 = \mathbf{v}_2$, where I_2 is the two-dimensional identity matrix, and the corresponding solution is given by $\mathbf{p}_3(t) = t\mathbf{v}_1 e^{\lambda t} + \mathbf{v}_3 e^{\lambda t}$ (see, for example, Britton et al. (1963, pg. 996)).

The analytic form of the general solution enables us to see how the qualitative dynamics depend crucially on the eigenvalues. In fact, it is possible to categorise the different types of qualitative behaviour that might arise by considering the range of possible eigenvalues for a given matrix P. Previous authors (e.g. Hirsch et al. (2004, pg. 63), Strogatz (1994, pg. 137)) have sought to demonstrate the range of behaviour for linear systems of the form in equation 6.6 by presenting the trace-determinant diagram in Figure 6.1. This arises because the eigenvalues λ_i for $i = 1, 2$ of the two-dimensional matrix P are defined by its trace, $\mathrm{Tr}(P)$, and determinant, $\mathrm{Det}(P)$, according to

$$\lambda_i^2 - \mathrm{Tr}(P)\lambda_i + \mathrm{Det}(P) = 0.$$

In particular, the relationship between the trace and determinant determine the type of equilibrium. For the Richardson system in equation 6.6, the trace, $\mathrm{Tr}(P) = -(\sigma_1 + \sigma_2)$, is the negative of the sum of the inhibition parameters, while the determinant, $\mathrm{Det}(P) = \sigma_1\sigma_2 - \rho_1\rho_2$, is a measure of the size of inhibition parameters in comparison to the action-reaction parameters.

In Figure 6.2, the dynamics locally to the equilibrium of the system in equation 6.6 are shown. The parameters used for each of these cases are chosen to correspond

with the points in Figure 6.1. Note that cases brought about by equalities (i.e. those lying on the lines in Figure 6.1) are not shown as these are special cases to separate the more common dynamics shown in real systems that do not require equality.

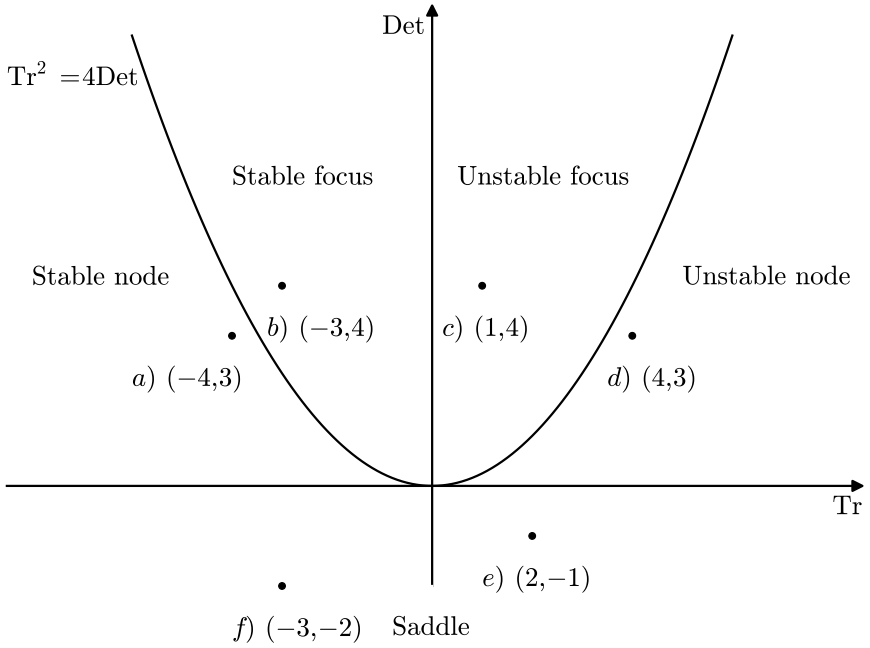

Figure 6.1: **The trace-determinant diagram for linear planar systems.** For a given two-dimensional system, $\dot{\mathbf{p}} = P\mathbf{p}$, the location of the matrix P on this diagram determines the type of the equilibrium at the origin. The points a)-f) correspond to the subfigures in Figure 6.2, which show the qualitative dynamics for each case.

6.2.1 Nodes

For $\mathrm{Det}(P) > 0$, if $\mathrm{Tr}(P)^2 > 4\mathrm{Det}(P)$, the equilibrium is known as a node. Solution curves near to a node equilibrium are determined by the relative strength of the eigenvalues and the directions of each associated eigenvector (see Figures 6.2(a) and (d) for an attractive and a repelling equilibrium, respectively). If $\mathrm{Tr}(P)^2 = 4\mathrm{Det}(P)$, then the eigenvalues are repeated, and solution curves move in only one direction either towards or away from the equilibrium value. If $\mathrm{Det}(P) = 0$ and $\mathrm{Tr}(P) \neq 0$, then one of the eigenvalues is equal to zero and there are infinitely many fixed points on a line that solution curves either move towards or away from in a perpendicular direction.

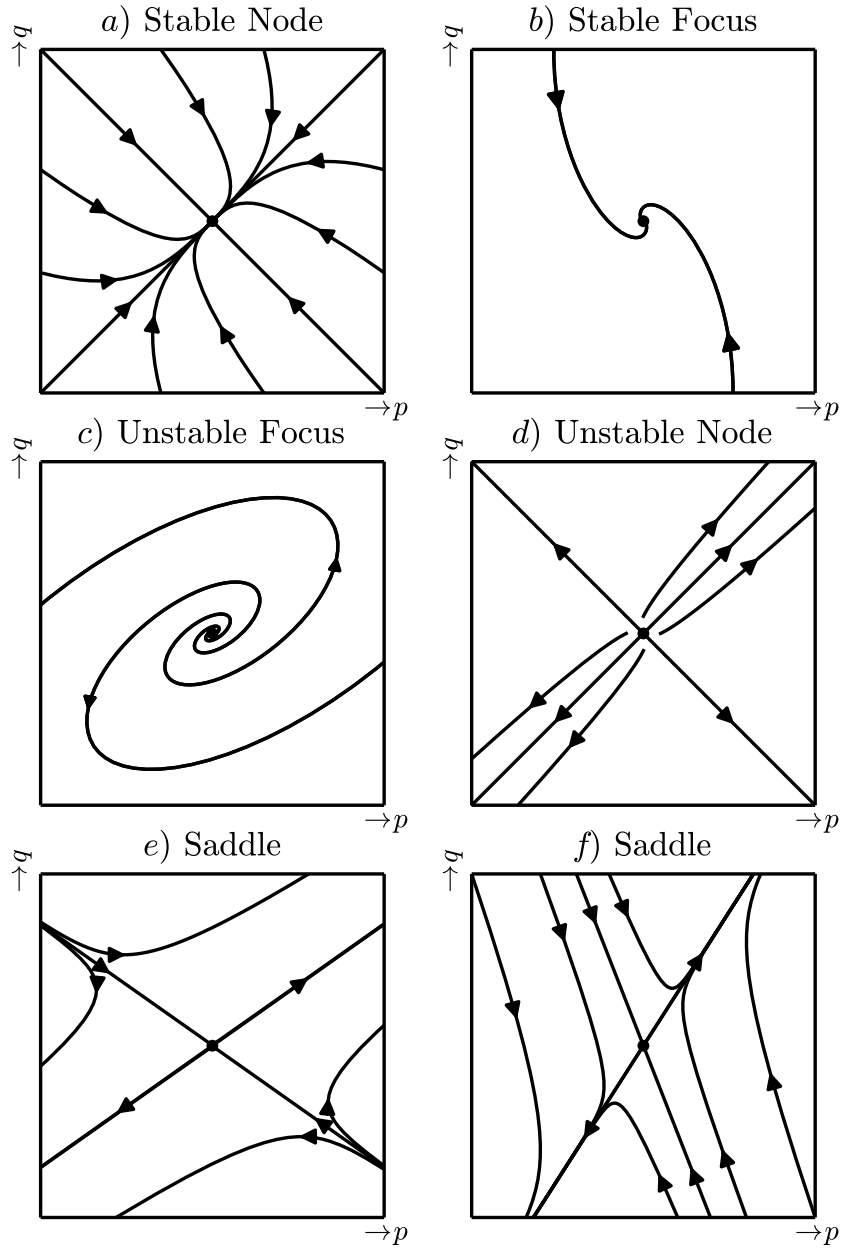

Figure 6.2: **The dynamics around the equilibrium value of the Richardson model in equation 6.6 for different parameter values**. The parameters are chosen to coincide with each point in Figure 6.1.

For $\mathrm{Det}(P) > 0$ and $\mathrm{Tr}(P)^2 > 4\mathrm{Det}(P)$, if $\mathrm{Tr}(P) > 0$ then both eigenvalues are real and positive and almost all trajectories diverge to infinity. In this case, nations are reacting to their own defence levels, as well as the levels of their adversary, without any inhibition. There is no damping in the system and it is consequently very unstable, with interactions compounding the escalation effect. Richardson argued that σ_1 and σ_2 are typically positive (which is to say there is some inherent damping behaviour), and it will therefore be assumed that $\mathrm{Tr}(P) < 0$.

For $\mathrm{Det}(P) > 0$, $\mathrm{Tr}(P) < 0$ and $\mathrm{Tr}(P)^2 > 4\mathrm{Det}(P)$, both eigenvalues are real and negative and trajectories converge to the equilibrium value. In fact, given the assumption that $\mathrm{Tr}(P) < 0$, the condition that $\mathrm{Det}(P) > 0$ is necessary and sufficient to result in a stable equilibrium. Thus, two nations will typically only cease changing their defence levels if the sum of the inhibition parameters is positive, so that there is some damping in the system, and if those inhibition terms outweigh the escalation parameters. In this case, nations are being restrained by their internal dynamics—perhaps through pressures placed upon them by the electorate—rather than reacting to the threatening actions of their adversary. This heuristic result agrees with common sense, and begins to hint at how Richardson's model might be applied to real-world scenarios.

6.2.2 Foci

Another type of stable equilibrium can occur when $\mathrm{Det}(P) > 0$ and $\mathrm{Tr}(P) < 0$. If $\mathrm{Tr}(P)^2 < 4\mathrm{Det}(P)$ then the eigenvalues are complex conjugates and, since $e^{i\theta} = \cos\theta + i\sin\theta$, there is rotation of solutions curves and they spiral towards (see Figure 6.2 (b)) or away from (see Figure 6.2 (c)) the equilibrium. This is known as a focus.

If $\mathrm{Tr}(P) = 0$ with $\mathrm{Det}(P) > 0$, then the real part of the complex eigenvalues is equal to zero and solution curves are periodic circular trajectories centred on the equilibrium. By comparing (b) and (c) in Figure 6.2, it can be seen that the closer to the determinant axis in Figure 6.1 the system is, the more rotation there is in the solution curves. For instance, in Figure 6.2(b), the equilibrium is a focus which is far from the determinant axis, and thus has very quick convergence to the equilibrium value. The system is highly dissipative, and in many practical situations it can be difficult to detect the difference between a node and a focus. In Figure 6.2(c), the equilibrium is a focus

which is close to the determinant axis and therefore has solution curves that are much slower, and the system is more conservative. In this case, however, the equilibrium is also unstable and so solution curves are diverging away from the equilibrium. In many practical situations, due to the noisiness of available datasets, it is possible that such instability, which is very close to conservative periodic orbits, can be mistaken for either conservative behaviour, or even a stable equilibrium.

6.2.3 Saddles

If $\mathrm{Det}(P) < 0$, then one eigenvalue has negative real part, and the other has positive real part, and the equilibrium is a saddle. Saddles have the characteristic that there is one direction in which solutions converge to the equilibrium and another direction in which solutions diverge to infinity. All other solutions are a linear combination of the behaviour in these two directions, which are defined by the eigenvectors associated with the negative and positive eigenvalues respectively, and therefore typically eventually diverge to infinity. Two saddles are shown in Figures 6.2 (e) and (f).

Saddles provide further insights of real-world escalation processes: they occur when $\mathrm{Det}(P) = \sigma_1\sigma_2 - \rho_1\rho_2 < 0$, which implies that the action-reaction parameters outweigh the inhibition parameters. In this scenario, the system can be susceptible to arms races. More insight into this scenario can be obtained by considering the eigenvectors of the matrix P. Assuming, without loss of generality, that $\rho_1 \neq 0$ holds in all cases of interest (since if both $\rho_1 = \rho_2 = 0$ then there are no action-reaction dynamics, and if $\rho_1 = 0$ but $\rho_2 \neq 0$, then the equations are relabelled), the eigenvectors are given by

$$\mathbf{v}_1 = \begin{pmatrix} \sigma_1 + \lambda_1 \\ \rho_1 \end{pmatrix}, \qquad \mathbf{v}_2 = \begin{pmatrix} \sigma_1 + \lambda_2 \\ \rho_1 \end{pmatrix}.$$

Saddles occur when both eigenvalues are real, with one being positive and one being negative. Denoting the positive eigenvalue by λ_1, then, if $\sigma_1 > 0$ and $\rho_1 > 0$, which Richardson argued occurs in most cases of interest, the eigenvector associated with the positive eigenvalue points in the direction of the positive quadrant in the plane. Almost all solution curves then either diverge to (∞, ∞) or $(-\infty, -\infty)$. As Richardson stated, there is either a 'drift toward war' or a 'drift toward closer cooperation' (Richardson, 1960a). For a given parameter set, the condition on which of these occur depends on the initial conditions. If the initial condition lies above the line defined by the eigenvector

associated with the negative eigenvalue then solutions diverge to positive infinity, whilst if the initial conditions lie below this line, then solutions diverge to negative infinity. In either case, the system is unstable, and the state of each individual nation is largely determined more by international dynamics than by internal processes.

6.2.4 Richardson policy options

According to Richardson's model, a nation hoping to avoid an escalating arms race with an adversary has several ways in which they can increase the stability of the system. The impacts of these strategies on the system parameters are summarised in Figure 6.3. They can, for instance, attempt to enforce a stable equilibrium by increasing the value of $\mathrm{Det}(P) = \sigma_1\sigma_2 - \rho_1\rho_2$. They can do this either by decreasing their escalation parameter, as shown in Figure 6.3(a) or by increasing their inhibition parameter, as shown in Figure 6.3(b).

As another strategy, if they perceive the system to be unstable, and in the form of a saddle, they can attempt to change the location of the system on the p-q plane so that any initial conditions will lie below the eigenvector associated with the negative eigenvalue. This could be done by decreasing the level of defences, or increasing the level of cooperation with their adversary.

Alternatively, they could attempt to alter the direction of the eigenvector associated with the negative eigenvalue so that the current state of the system falls below this line, and the system will result in an escalating process of cooperation. This could be done by altering the parameters in the system in order to minimise the difference between $\mathbf{v}_1$ and $\mathbf{v}_2$ by ensuring that λ_1 and λ_2 are as close as possible. Given that the eigenvalues are equal when $\mathrm{Tr}(P)^2 = 4\mathrm{Det}(P)$, this again involves increasing the value of the determinant.

Finally, the position of the equilibrium can be changed by varying the level of grievances determined by $\boldsymbol{\epsilon}$ as shown in Figure 6.3(c). If $\mathrm{Det}(P) < 0$, an objective might be to minimise grievances so that the equilibrium point is as close to the origin as possible, thereby increasing the possibility that the state of the system will lie in the half of the plane which results in an escalation of cooperation.

Of course, even if a nation were to make these changes, there is no guarantee that their adversary will not change their dynamics in order to put the system back on

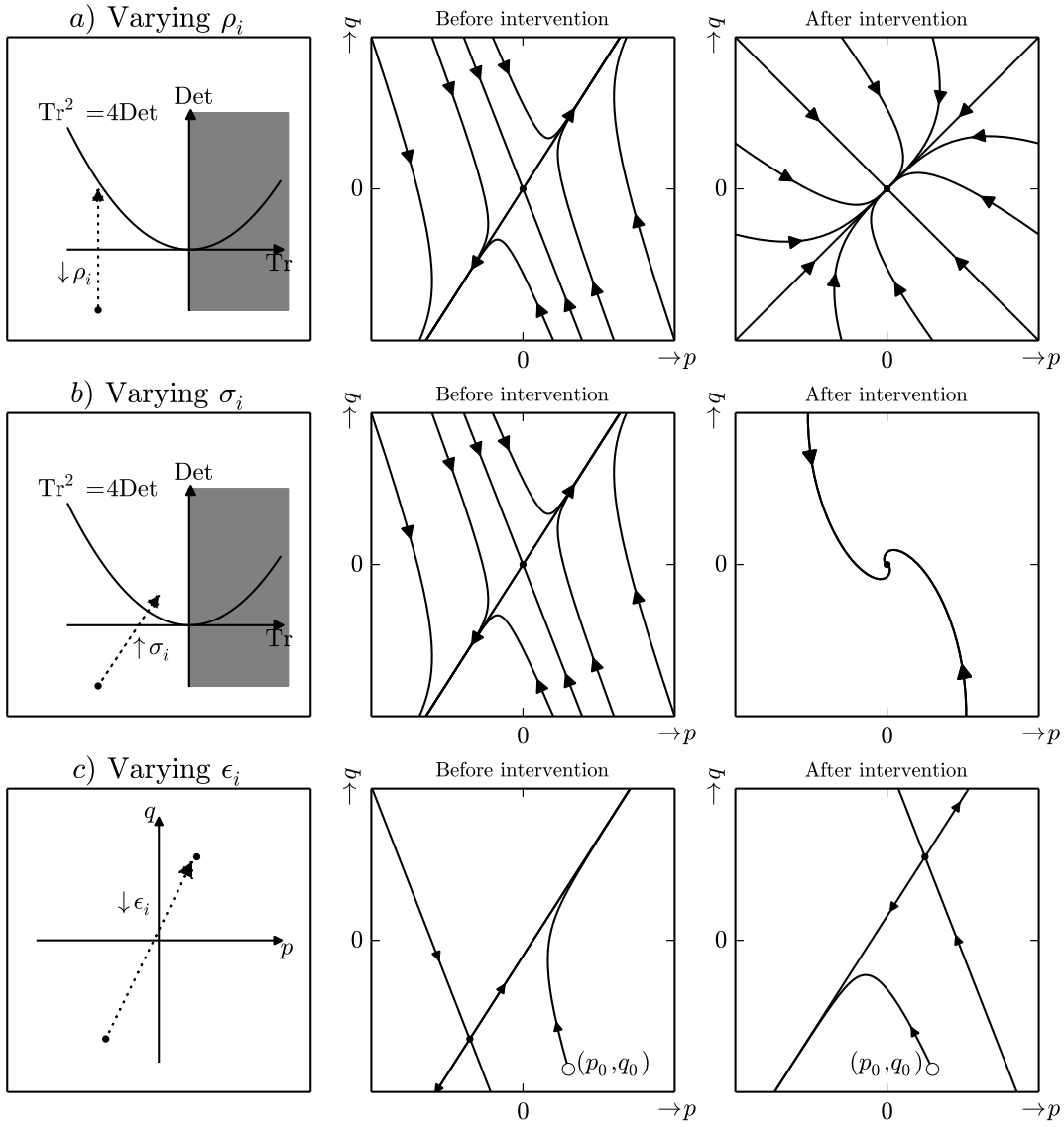

Figure 6.3: **Unilateral policy options available to nation i**. a) shows the change in the system according the trace-determinant diagram from Figure 6.1 when ρ_i is decreased and b) shows the change when σ_i is increased. Note that the half plane with $\mathrm{Tr}(P) > 0$ is shaded since if $\sigma_1, \sigma_2 > 0$, as Richardson hypothesised, the system will not lie in this portion of the plane. c) shows the impact of nation i reducing external grievances when the system is a saddle. The equilibrium point will move towards the positive quadrant, meaning that for initial conditions given by (p_0, q_0), the system will tend towards greater cooperation, rather than greater hostility.

a course to an escalating arms race. The Richardson model is useful in highlighting the possible consequences of a 'mechanical' arms race. As Richardson described, the model is "merely a description of what people would do if they did not stop to think" (Richardson, 1960a, pg. 12). This implies a view of international conflict whose consequences, once set in motion, cannot be escaped. Subsequently, authors have considered various ways of extending the Richardson model in order to incorporate some notion of decision-making on the part of the adversaries. Some, for example, have considered the Richardson model from the perspective of control theory and game theory, in which nations act according to a set of predefined objectives (Intriligator and Brito, 1976; Gillespie et al., 1977; Bennett, 1987). Although more closely considering the decision-making of individuals that lead to the system outcomes, such approaches can lose some of the generality that a more descriptive model can sometimes afford.

The analysis of the Richardson model has been presented using the language of military arms races, in which two nations retaliate by increasing their level of military expenditure. As explained in Chapter 2, the dependent variables might also represent more abstract measures of conflict, or through measures that can be interpreted through means other than expenditure. Indeed, it has been argued elsewhere that the model represents a very general conflict escalation process and, as such, can be considered to model a wide range of potential systems in which two adversaries are subject to retaliation. The ability for the model to consider such processes during conflicts such as insurgency and other types of civil violence is the reason it has been presented in this chapter. For the remainder of this chapter, the dependent variables p and q are taken to be a more general and abstract measure of hostility between two adversaries.

6.3 Spatial disaggregation of the Richardson model

It has been demonstrated in this thesis and elsewhere that spatial dependency in models of civil violence captures important processes. Consequently, deterministic models that do not explicitly model these spatial dependencies have more restrictive assumptions than those that do. It is advantageous, therefore, to consider how to incorporate space in such models, so that a modeller may assess whether or not the inclusion of space is required in any given scenario.

In this section, the Richardson model of conflict escalation is spatially disaggre-

gated in two different ways. First, a partial differential equation (henceforth abbreviated as PDE) is derived, which is inspired by a spatial disaggregation of the competitive Lotka-Volterra model used to model gang rivalries in Brantingham et al. (2012). This approach to incorporate spatial dependency is widely used in ecological models (Malchow et al., 2008), and has also been used in a range of differential equation-based models of human conflict. Some limitations of this approach are discussed, and, as a result, it is concluded that a different approach might also be utilised. Consequently, a second method for the spatial disaggregation of conflict models is presented that uses an entropy maximising spatial interaction model to account for interdependencies between spatial regions. It is argued that this spatial disaggregation addresses some of the limitations encountered with the PDE approach since it can be applied to more general metric spaces. Additionally, it is argued that this model holds an advantage over simulation approaches, such as agent-based simulation, due to its suitability for interrogation using non-linear dynamical systems analysis. The discussion in what follows is related closely to previous studies investigating the role of spatial disaggregation in deterministic models, such as Durrett and Levin (1994).

6.3.1 A PDE disaggregation of the competitive Lotka-Volterra system

The non-spatial competitive Lotka-Volterra model is first presented, in order to motivate the spatial disaggregation of deterministic ordinary differential equations. This model describes competition between two species, and has been well-studied, usually in an ecological context. Given the populations of two species, p and q, the equations that govern their evolution are

$$\begin{aligned} \dot{p} &= r_1 p \left(1 - \frac{p + \zeta_{12} q}{K_1}\right) \\ \dot{q} &= r_2 q \left(1 - \frac{q + \zeta_{21} p}{K_2}\right), \end{aligned} \tag{6.8}$$

for parameters r_1, r_2, ζ_{12}, ζ_{21}, K_1 and K_2. The interpretation of the model is as follows: r_1 and r_2 represent growth rates—that is, birth rates minus natural death rates—of the two populations p and q, respectively. K_1 and K_2 are the carrying capacities of the environment for the populations p and q, respectively. These are the maximum possible values for each of the populations that the environment is able to support and sustain.

The parameters ζ_{12} and ζ_{21} are competition terms and determine the rate at which the population of p is decreased by the presence of the population q and the rate at which the population of q is decreased by the presence of population q, respectively.

Using a similar analysis to the Richardson model that was presented in Section 6.2, it can be shown that certain parameter values and initial conditions lead to either the peaceful coexistence of the two species, or the extinction of one species due to the presence of the other. This analysis is well presented in Strogatz (1994, pg. 155) for parameter values $r_1 = K_1 = 3$, $r_2 = K_2 = 2$, $\zeta_{12} = 2$ and $\zeta_{21} = 1$, in which the dependent variables are taken to be populations of rabbits and sheep competing over the same patch of grass.

By re-labelling the parameters of the model in equation 6.8, the model can be related to the Richardson model, as highlighted in Epstein (1997). In particular, by setting

$$\epsilon_1 = r_1 \qquad \sigma_1 = \frac{r_1}{K_1} \qquad \rho_1 = -\frac{r_1\zeta_{12}}{K_1},$$

and similarly for ϵ_2, σ_2 and ρ_2, the system in equation 6.8 can be written as

$$\begin{aligned} \dot{p} &= p(-\sigma_1 p + \rho_1 q + \epsilon_1) \\ \dot{q} &= q(\ \rho_2 p - \sigma_2 q + \epsilon_2), \end{aligned} \tag{6.9}$$

which is reminiscent of the functional form of the Richardson model in equation 6.1, but with a multiplicative dependent variable term in each equation. If the initial conditions of this system are in the positive quadrant, the multiplicative term ensures that either component of the dependent variable cannot become negative. It is also interesting to note that this system has the same equilibrium value as the Richardson system, together with three other equilibria brought about by the non-linearity. The Richardson equilibrium corresponds to the peaceful coexistence of the two species.

In Brantingham et al. (2012), a spatially explicit version of the competitive Lotka-Volterra model is used to model two gangs that compete over territorial boundaries in a city, in which the dependent variables of the system vary in space as well as time. Rather than considering the population of two types of gangs, as is often the case with the competitive Lotka-Volterra system, the dependent variables, $p(\mathbf{x}, t)$ and $q(\mathbf{x}, t)$, are taken to be the density of gang-related activities attributed to gang 1 and gang 2, respectively. Thus, the locations and timings of gang-related activities are modelled

using spatially continuous functions p and q, and their values at $(\mathbf{x}, t)$ correspond to the risk of observing a gang-related activity at $(\mathbf{x}, t)$.

The spatially-explicit competitive Lotka-Volterra model that Brantingham et al. (2012) propose is given by

$$\begin{aligned} \frac{\partial p}{\partial t} &= D_1 \bigtriangledown^2 p + p(-\sigma_1 p + \rho_1 q + \epsilon_1) - \delta_1 p \\ \frac{\partial q}{\partial t} &= D_2 \bigtriangledown^2 q + q(\ \rho_2 p - \sigma_2 q + \epsilon_2) - \delta_2 q, \end{aligned} \tag{6.10}$$

where diffusion coefficients D_1 and D_2 are introduced, together with extra inhibition parameters δ_1 and δ_2. The inhibition terms $\delta_1 p$ and $\delta_2 q$ serve to incorporate intrinsic linear growth or decay of gang-related activities. The operator $\bigtriangledown^2$ is known as the Laplacian and can be written as

$$\bigtriangledown^2 = \frac{\partial^2}{\partial x^2} + \frac{\partial^2}{\partial y^2}, \tag{6.11}$$

providing the model's diffusive dynamics in accordance with Fick's laws of diffusion (De La Barrera, 2005). In particular, this model supposes that gang-related activities will spread from areas in which high levels of gang-related activities occur to areas in which low levels of gang-related activities occur. The authors argue that such dynamics are justified due to the tendency for gangs to seek new territory that has not experienced previous gang-related activities. Such expansion is halted by barriers in the urban environment, and the behaviours and spatial extent of the opposing gang, according to the other terms in the equation.

Given evidence for expansion, the diffusive assumption is often suitable; however, in considering more general scenarios, this assumption may not always be appropriate. In what follows, a PDE version of the Richardson model is presented, which is disaggregated in the same way as the Lotka-Volterra system in equation 6.10. The applicability of the model to more general spaces is considered, and the assumptions used in deriving this model are critiqued.

6.3.2 A PDE disaggregation of the Richardson model

It is possible to spatially disaggregate the Richardson model in equation 6.1 using an analogous diffusive approach to Brantingham et al. (2012). Given spatially continuous dependent variables $p(\mathbf{x}, t)$ and $q(\mathbf{x}, t)$, which now correspond to the more general

concept of conflict or contempt between two adversaries, a spatially disaggregated PDE Richardson model is given by

$$\begin{aligned} \frac{\partial p}{\partial t} &= D_1 \bigtriangledown^2 p - \sigma_1 p + \rho_1 q + \epsilon_1 \\ \frac{\partial q}{\partial t} &= D_2 \bigtriangledown^2 q + \rho_2 p - \sigma_2 q + \epsilon_2, \end{aligned} \tag{6.12}$$

where D_1 and D_2 are diffusion coefficients, $\bigtriangledown^2$ is the operator defined in equation 6.11, and the remaining parameters are interpreted according to the original Richardson model.

A number of assumptions implicit in this model may be undesirable when the model is applied to particular conflicts, such as insurgencies or other types of civil violence. First, as with the model by Brantingham et al. (2012) in equation 6.10, the diffusive dynamics imply that dependent variables will naturally spread from areas with high concentration to areas of low concentration. This implies that, according to this model, the intensity of the conflict will tend to spread out over a geographic area over time.

As has been shown in this thesis and elsewhere; however, the occurrence of civil violence can be very highly clustered in space, with a large majority of events occurring over a long time scale within a few small areas. It was shown in Chapter 3, for instance, that relocation of offences during the 2011 London riots, perhaps the most analogous with the types of diffusive dynamics discussed here, occurred much less often than would be anticipated had the events been modelled independently. At the same time, occurrences of containment, corresponding to conflicts that remain stationary and do not spread, occurred at a higher rate than could have been anticipated if the events were independent. Of course, it is possible for conflicts to spread spatially, but forcing models to observe this dynamical behaviour is potentially restrictive. Such models sometimes unnecessarily use physical analogies from the study of fluid dynamics that may not always be appropriate (Durrett and Levin, 1994; González and Villena, 2011).

Second, the model requires the dependent variables $p(\mathbf{x}, t)$ and $q(\mathbf{x}, t)$ to be smooth functions, in order to ensure that their second partial derivatives exist. Since data is often aggregated into discrete geographic areas, this implies that such models often require the construction of kernel density estimators, particularly if they are to be applied to real-world data. This requires further modelling assumptions to be

made regarding the choice of estimator and the value of any parameters required by that estimator. Furthermore, discontinuities may be required within the model due to geographical features over which the conflict may be more unlikely to spread, such as rivers, roads, or geopolitical boundaries. There are some techniques, however, that exist to incorporate such effects (see, for example, Smith et al. (2010)).

Finally, solutions to partial differential equations require the specification of spatial boundary conditions, which, in many cases may be difficult to define if the spatial area of interest has no natural boundary that contains the dynamics.

All of these factors suggest that a number of additional, and, in some cases, restrictive assumptions are required for the model to be made spatially explicit through the use of PDEs. In what follows, a different approach for the spatial disaggregation of the model is employed in an effort to preserve more of the generality associated with the original Richardson model than is afforded by PDE approaches.

6.3.3 An entropy-maximising spatial interaction disaggregation

In this section, the Richardson model in equation 6.1 is spatially disaggregated using an entropy maximising spatial interaction model that has been developed to address social systems with spatial dependency. Spatial interaction models have been employed previously within both static and dynamic spatial models to consider retail systems (Harris and Wilson, 1978; Wilson, 2008); international migration (Dennett and Wilson, 2013); rioting (Davies et al., 2013); international trade (Fry and Wilson, 2012) and ecological dynamics (Wilson, 2006).

To begin, consider a two-dimensional manifold $\mathcal{M}$, on which conflict between two adversaries takes place. Suppose that one adversary is located at the points $\mathbf{x}_1, \mathbf{x}_2, ..., \mathbf{x}_N \in \mathcal{M}$. In other words, the adversary is disparately distributed over $\mathcal{M}$, perhaps due to the positions of military bases, allied settlements, or gang safe houses, depending on the application of the model. Similarly, suppose that their adversary is located at the points $\mathbf{y}_1, \mathbf{y}_2, ..., \mathbf{y}_M \in \mathcal{M}$.

In order to maintain generality, the dependent variables for the system are taken to be general measures of conflict, hostility or contempt towards each adversary. In the disaggregated system, however, a measure of conflict at each location is tracked. In other words, the variables to be considered are $p_1, p_2, ..., p_N$, which correspond to lev-

els of hostility associated with locations $\mathbf{x}_1, \mathbf{x}_2, ..., \mathbf{x}_N$, respectively, and $q_1, q_2, ..., q_N$, which correspond to levels of hostility associated with locations $\mathbf{y}_1, \mathbf{y}_2, ..., \mathbf{y}_M$, respectively.

It is assumed similar mechanisms to the original Richardson model influence the variable p_j, for each index j. That is, $\dot{p}_j$ depends on three terms: the action-reaction term that itself depends on the adversary who is distributed over the manifold, representing the retaliatory dynamics driving the system; a measure of inhibition, representing each adversary's natural inclination to avoid conflict; and external grievances that may be present at $\mathbf{x}_j$.

The action-reaction term within the equation for $\dot{p}_j$ is assumed to depend on the variables $q_1, q_2, ..., q_M$, representing the level of hostility of their adversary. In particular, it is proposed that this term is given by a weighted sum of these terms, with corresponding *weighting factors* $w_{lj} \in [0, 1]$, which serve to specify the proportion of q_l that contributes to the action-reaction dynamics of p_j for every l and j. These weighting factors will be modelled explicitly in what follows. Following Richardson, the second term, representing inhibition mechanisms, is taken to be proportional to the hostility of p_j and the third term, representing external grievances associated with the hostility p_j, is taken to be a constant.

With an analogous equation for q_l, for some index l, but with corresponding action-reaction weighting factors denoted by v_{jl}, the disaggregated Richardson model is

$$\begin{aligned} \dot{p}_j &= -\sigma_1 p_j + \rho_1 \sum_{l=1}^{M} q_l w_{lj} + \epsilon_1 \iota_j, \qquad j = 1, ..., N, \\ \dot{q}_l &= \rho_2 \sum_{j=1}^{N} p_j v_{jl} - \sigma_2 q_l + \epsilon_2 \kappa_l, \qquad l = 1, ..., M, \end{aligned} \tag{6.13}$$

where, as before, ρ_1 and ρ_2 specify the intensity of the action-reaction dynamics, σ_1 and σ_2 specify the extent to which there is inhibition to growth in hostility, and $\epsilon_1 \iota_j$ and $\epsilon_2 \kappa_l$ are the levels of external grievance associated with p_j and q_l, respectively.

Since the model is a disaggregation of the full Richardson model, it is assumed that the dynamics of the aggregated system—that is, the system defined by the hostility of each adversary as a whole—follows the original Richardson dynamics. Thus, it is

assumed that

$$\sum_{j=1}^{N} w_{lj} = 1, \qquad l = 1, ..., M \tag{6.14}$$
$$\sum_{l=1}^{M} v_{jl} = 1, \qquad j = 1, ..., N$$

and that

$$\sum_{j=1}^{N} \iota_j = 1, \tag{6.15}$$
$$\sum_{l=1}^{M} \kappa_l = 1,$$

so that

$$\sum_{j=1}^{N} \dot{p}_j = \rho_1 \sum_{l=1}^{M} q_l - \sigma_1 \sum_{j=1}^{N} p_j + \epsilon_1, \tag{6.16}$$
$$\sum_{l=1}^{M} \dot{q}_l = \rho_2 \sum_{j=1}^{N} p_j - \sigma_1 \sum_{l=1}^{M} q_l + \epsilon_2.$$

Setting $p = \sum_{j=1}^{N} p_j$ and $q = \sum_{l=1}^{M} q_l$, it can be seen that the system in equation 6.16 is equivalent to the system in equation 6.1. Therefore, the dynamics for the aggregated system can be inferred from the analysis in section 6.2. This is an important feature of the model and is utilised in the analysis sections of this chapter in what follows.

In order to derive an explicit form for the model in equation 6.13, further assumptions are required. It is assumed that $\iota_j = 1/N$ and $\kappa_l = 1/M$, so that external grievances impact p_j and q_l similarly over different values of j and l. This assumption can be generalised, although such generalisations are not considered in this thesis.

In order to find an explicit analytical expression for w_{lj} and v_{jl}, constraints are imposed that describe how these weightings depend on the spatial distribution of the locations of each adversary and the measures of hostility. These constraints are analogous to the derivation of the entropy maximising spatial interaction model described in Wilson (2008).

In order to define the constraints, a metric $d : \mathcal{M} \times \mathcal{M} \to \mathbb{R}$ is introduced. Taking two locations, $\mathbf{x}_j, \mathbf{y}_l \in \mathcal{M}$, $d(\mathbf{x}_j, \mathbf{y}_l)$ is a measure of impedance, distance, or cost between $\mathbf{x}_j$ and $\mathbf{y}_l$. Metrics are symmetric and thus $d(\mathbf{x}_j, \mathbf{y}_l) = d(\mathbf{y}_l, \mathbf{x}_j)$.

Considering first the weightings w_{lj}, it is assumed that the weighted mean distance over all possible locations is constant so that

$$\sum_{l=1}^{M}\sum_{j=1}^{N} w_{lj} d(\mathbf{x}_j, \mathbf{y}_l) = c_1, \tag{6.17}$$

for some positive constant c_1. Since $w_{lj} \geq 0$ by construction and since $d(\mathbf{x}_j, \mathbf{y}_l) \geq 0$ for all i and j (which is another property of a metric), then when $d(\mathbf{x}_j, \mathbf{y}_l)$ is large, w_{lj} will be small, meaning that two adversaries located a long way away from each other will have a small effect on each other; whereas, when $d(\mathbf{x}_j, \mathbf{y}_l)$ is small, w_{lj} is large, and two nearby adversaries will be influenced by each other. Impedance, therefore, has a diminishing effect on the magnitude of the resulting weighting, and formulates Tobler's first law of geography within the model, forcing nearer things to be more related than farther things (Tobler, 1970).

Whilst the constraint in equation 6.17 specifies the relationship between the distance metric and the weightings w_{lj} in what will be the final model, a second constraint specifies the relationship between the weights and the hostility measures $p_1, p_2, ..., p_j$ as

$$\sum_{l=1}^{M}\sum_{j=1}^{N} w_{lj} \ln p_j = \ln\left(\prod_{l=1}^{N} \bar{p}_{w_{l\cdot}}\right) = c_2 \tag{6.18}$$

for some constant c_2. $\bar{p}_{w_{l\cdot}}$ in equation 6.18 is the weighted geometric mean, weighted according to w_{lj} for $j = 1, 2, ..., N$, for each adversary l. This is a measure of central tendency associated with the hostility measures $p_1, p_2, ..., p_N$. The product of these measures of central tendency are constrained to be constant for all possible weightings w_{lj}. The geometric mean is used instead of the arithmetic mean for mathematical simplicity in what follows. For an adversary at $\mathbf{y}_l$, this constraint forces the weighting w_{lj} to be proportional to a power of p_j, as will be shown in what follows.

Following Wilson (1970), it is assumed that the weightings w_{lj} for $l = 1, ..., M$ and $j = 1, ..., N$ can be considered to arise from a thermodynamic system comprising of a large number of very small distinct units that are able to flow from locations $\mathbf{y}_l$ to $\mathbf{x}_j$. The weighting w_{lj} represents the proportion of these small units at l that flow to j when the thermodynamic system is in equilibrium. In previous applications of the model, the individual units that flow have included money and people; however, for the present purposes, in which a general model of conflict is sought, the quantity

flowing from i to j is assumed to be a conceptual measure of threat. This is a novel interpretation of the following well-known derivation of the model, and, as will be demonstrated, enables a link between this modelling framework and a range of conflict models, such as the general Richardson model that is derived here.

For $l = 1, ..., M$ and $j = 1, ..., N$, the set of flows given by $\{w_{lj}\}$—where the bracket notation corresponds to the set of all flows w_{lj} for $l = 1, 2, ..., M$ and $j = 1, 2, ..., N$—can be realised by a number of different so-called micro-states, in which w_{lj} is the proportion of all units flowing from $\mathbf{y}_l$ to $\mathbf{x}_j$.

To illustrate this further, consider the scenario in which there are just four distinct units of threat (as opposed to a large number of units in the full derivation). Suppose also that these four units can flow from either $\mathbf{y}_1$ or $\mathbf{y}_2$—the locations of one adversary—and can flow to either $\mathbf{x}_1$ or $\mathbf{x}_2$—the locations of another adversary. Denote the number of units that flow from l to j by $\tilde{w}_{lj}$, where the tilde notation is used to distinguish the counts of these units in contrast to the proportion. Then, given no constraints on the types of flows that are possible, the most likely distribution of the flow of threat is the realisation in which a single unit of threat flows from from $\mathbf{y}_1$ to both $\mathbf{x}_1$ and $\mathbf{x}_2$ and a single unit flows from $\mathbf{y}_2$ to both $\mathbf{x}_1$ and $\mathbf{x}_2$ so that $\tilde{w}_{lj} = 1$ for all l and j. With four units, there are exactly

$$W\left(\{\tilde{w}_{lj}\}\right) = \frac{4!}{1!1!1!1!} = 24 \tag{6.19}$$

possible scenarios, or 'micro-states', which result in this same distribution of flows. In contrast, the scenario in which $\tilde{w}_{11} = 4$ whilst $\tilde{w}_{lj} = 0$ for $(l, j) \neq (1, 1)$ has exactly one corresponding micro-state in which all units of threat flow from $\mathbf{y}_1$ to $\mathbf{x}_1$. Thus, the first scenario is considered to be more likely to occur, and is used as the distribution of the flows within the model.

For a large number of threat units given by T, the number of possible micro-states that give rise to a specific set of flows $\{\tilde{w}_{lj}\}$ can be calculated as

$$W\left(\{\tilde{w}_{lj}\}\right) = \frac{T!}{\prod_{lj} \tilde{w}_{lj}!}.$$

$W\left(\{\tilde{w}_{lj}\}\right)$ is the number of ways in which a particular realisation of the distribution given by $\{\tilde{w}_{lj}\}$ can arise, and is therefore a measure of the likelihood of observing the

set of values $\{\tilde{w}_{lj}\}$. This measure can be simplified by taking the logarithm to obtain:

$$\ln\left(W\left(\{\tilde{w}_{lj}\}\right)\right) = \ln(T!) - \sum_{lj} \ln(\tilde{w}_{lj}!),$$

and, by substituting Stirling's approximation, which states that, for large n,

$$\log(n!) \approx n \ln n - n,$$

the following is obtained:

$$\ln\left(W\left(\{\tilde{w}_{lj}\}\right)\right) = \ln(T!) - \sum_{lj} \left(\tilde{w}_{lj} \ln(\tilde{w}_{lj}) - \tilde{w}_{lj}\right). \tag{6.20}$$

The final term in equation 6.20 is

$$\sum_{lj} \tilde{w}_{lj} = T \tag{6.21}$$

and is therefore equal to a constant. $T!$ is also constant, thus, in order select the distribution $\{\tilde{w}_{lj}\}$ with the highest likelihood of being observed (provided all micro-states are equally possible), it is sufficient to take the distribution $\{\tilde{w}_{lj}\}$ that maximises the entropy of the system, defined as

$$S\left(\{\tilde{w}_{lj}\}\right) = -\sum_{l=1}^{M}\sum_{j=1}^{N} \tilde{w}_{lj} \ln \tilde{w}_{lj}. \tag{6.22}$$

Maximising the value of S in equation 6.22, whilst satisfying the constraints in equations 6.14, 6.17 and 6.18 (which also hold for $\{\tilde{w}_{lj}\}$ since $Tw_{lj} = \tilde{w}_{lj}$) produces an unbiased maximum likelihood estimate of the flows subject to exactly these constraints and no other assumptions. In what follows, proportions $\{w_{lj}\}$ are used rather than actual counts of the units of threat, since the function in equation 6.22 can be maximised without loss of generality by maximising the function

$$S\left(\{w_{lj}\}\right) = -\sum_{l=1}^{M}\sum_{j=1}^{N} w_{lj} \ln w_{lj}. \tag{6.23}$$

This result provides the model of the weightings required, and is obtained using the method of Lagrangian multipliers. Following this method, the points at which

$$\nabla\Lambda = 0, \tag{6.24}$$

where Λ is defined as

$$\Lambda(\{w_{lj}\}, \alpha, \beta, \{\gamma_l\}) = -\sum_{l=1}^{M}\sum_{j=1}^{N} w_{lj} \ln w_{lj} + \alpha \left(\sum_{l=1}^{M}\sum_{j=1}^{N} w_{lj} \ln p_j - c_2 \right) \quad (6.25)$$
$$- \beta \left(\sum_{l=1}^{M}\sum_{j=1}^{N} w_{lj} d(\mathbf{x}_j, \mathbf{y}_l) - c_1 \right)$$
$$- \sum_{l=1}^{M} \gamma_l \left(\sum_{j=1}^{N} w_{lj} - 1 \right),$$

for so-called Lagrangian multipliers α, β and γ_l for $l = 1, ..., M$, are the points at which the value of S in equation 6.22 is maximised subject to the constraints in equation 6.14, 6.17 and 6.18. Differentiating with respect to each w_{lj}, and with respect to each of the Lagrangian multipliers gives

$$\frac{\partial \Lambda}{\partial w_{lj}} = -\ln(w_{lj}) - 1 + \alpha \ln(p_j) - \beta d(\mathbf{x}_j, \mathbf{y}_l) - \gamma_l,$$

for $l = 1, ..., M$ and $j = 1, ..., N$, and

$$\frac{\partial \Lambda}{\partial \alpha} = \sum_{l=1}^{M}\sum_{j=1}^{N} w_{lj} \ln p_j - c_2$$
$$\frac{\partial \Lambda}{\partial \beta} = \sum_{l=1}^{M}\sum_{j=1}^{N} w_{lj} d(\mathbf{x}_j, \mathbf{y}_l) - c_1$$
$$\frac{\partial \Lambda}{\partial \gamma_l} = \sum_{j=1}^{N} w_{lj} - 1,$$

for $l = 1, ..., M$. If the constraints are satisfied, then equation 6.24 is satisfied when

$$w_{lj} = \frac{p_j^{\alpha} \exp(-\beta d(\mathbf{x}_j, \mathbf{y}_l))}{\exp(1 + \gamma_l)}.$$

for $l = 1, ..., M$ and $j = 1, ..., N$. The constraint in equation 6.14 can be used to eliminate γ_l, since

$$\sum_{j=1}^{N} \frac{p_j^{\alpha} \exp(-\beta d(\mathbf{x}_j, \mathbf{y}_l))}{\exp(1 + \gamma_l)} = 1,$$

and so

$$\exp(1 + \gamma_l) = \sum_{j=1}^{N} p_j^{\alpha} \exp(-\beta d(\mathbf{x}_j, \mathbf{y}_l)).$$

Thus, the weighting factors w_{lj}, being the values that maximise the entropy in equation 6.22, subject to the constraints in equations 6.14, 6.17 and 6.18, can be written as

$$w_{lj} = \frac{p_j^{\alpha} e^{-\beta d(\mathbf{x}_j, \mathbf{y}_l)}}{\sum_{j'=1}^{N} p_{j'}^{\alpha} e^{-\beta d(\mathbf{x}_{j'}, \mathbf{y}_l)}},$$

for parameters α and β, and where the subscript j' has been introduced to distinguish it from j. The weighting w_{lj} determines the extent to which q_l influences the reactive retaliatory behaviour of p_j. It can be interpreted as a weighted comparison of p_j against $p_{j'}$ for $j' = 1, 2, ...N$, weighted according to the distances between $\mathbf{y}_l$ and $\mathbf{x}_{j'}$, and $\mathbf{y}_l$ and $\mathbf{x}_j$.

By writing

$$p_{j'}^{\alpha} = \exp\left(\alpha \ln p_{j'}\right), \tag{6.26}$$

for $j' = 1, 2, ..., N$, it can be seen that the model has a similar functional form to the discrete choice model used to model rioter target choice in Chapter 4. Indeed, the two models are known to be equivalent (Fotheringham and O'Kelly, 1989). One might therefore interpret the weightings w_{lj} as the attractiveness perceived by the adversary at $\mathbf{y}_l$, of each target at $\mathbf{x}_j$ for $j = 1, 2, ..., N$. In this case, 'attractiveness' is a function of hostility levels p_j and distance $d(\mathbf{x}_j, \mathbf{y}_l)$. The use of the term 'attractiveness', however, should be used with caution, as this implies that an adversary is attracted to target adversaries with high hostility, which may not be reflective of the purposeful choices of each adversary, but rather a necessary precaution. It is for this reason that the entropy-maximisation derivation proposed here is used, as opposed to the formal discrete choice framework outlined in Chapter 4.

By an analogous derivation, a similar expression may be derived for the retaliatory effect on q_l from p_j, with corresponding weightings v_{jl}, given by

$$v_{jl} = \frac{q_l^{\gamma} e^{-\delta d(\mathbf{y}_l, \mathbf{x}_j)}}{\sum_{l'=1}^{M} q_{l'}^{\gamma} e^{-\delta d(\mathbf{y}_{l'}, \mathbf{x}_j)}}, \tag{6.27}$$

for further new parameters γ and δ, and subscript l'.

Returning to equation 6.13, and substituting in the expressions for w_{lj} and v_{jl}, the spatially-explicit Richardson model for two adversaries disparately distributed over a manifold $\mathcal{M}$ with associated distance metric $d : \mathcal{M} \times \mathcal{M} \to \mathbb{R}$, is given by

$$\begin{aligned} \dot{p}_j &= -\sigma_1 p_j + \rho_1 \sum_{l=1}^{M} q_l \frac{p_j^{\alpha} e^{-\beta d(\mathbf{x}_j, \mathbf{y}_l)}}{\sum_{j'}^{N} p_{j'}^{\alpha} e^{-\beta d(\mathbf{x}_{j'}, \mathbf{y}_l)}} + \frac{\epsilon_1}{N} \\ \dot{q}_l &= -\sigma_2 q_l + \rho_2 \sum_{j=1}^{N} p_j \frac{q_l^{\gamma} e^{-\delta d(\mathbf{y}_l, \mathbf{x}_j)}}{\sum_{l'}^{M} q_{l'}^{\gamma} e^{-\delta d(\mathbf{y}_{l'}, \mathbf{x}_j)}} + \frac{\epsilon_2}{M}, \end{aligned} \tag{6.28}$$

for $j = 1, 2, ..., N$ and $l = 1, 2, ..., M$.

The model in equation 6.28 extends Richardson's model by explicitly incorporating the impact of space via the metric d. Advantages over other methods of modelling spatial conflict processes (such as partial differential equations or multi-agent simulations) include the explicit and relatively general assumptions required to derive the model, together with its concise analytical form, enabling the model to be interrogated analytically to obtain insights. Since few restrictions have been placed upon the distance metric, the model can be applied to a range of conflict processes. For example, it might be applied to international arms races, in which spatial effects between nations plays a role in their armament decision-making processes (see, for example, Goldsmith (2007) who demonstrates such spatial dependency in military arms expenditure). The metric may also be constructed to incorporate non-spatial measures such as historic ties between nations as a means of reducing the effect of the corresponding threat weighting.

Moreover, the model is general enough to be applied to any conflict process involving retaliatory dynamics and spatial dependency. It was discussed in Chapter 2 how similar models—some with explicit spatial dependency, and some without—have been considered in the context of gang rivalries, psychological conflict, and civil and insurgent conflicts, amongst others. To the knowledge of the author, the model in equation 6.28 is novel and has not been investigated elsewhere previously. For this reason, the generality of the model is preserved and, for the time being, specific applications are not considered. Thus, in what follows, this model is explored using techniques from non-linear dynamical systems analysis to obtain general insights into its properties and to demonstrate some of its logical implications.

6.4 Nonlinear dynamical systems analysis

In this section, a range of tools that have been developed to analyse nonlinear dynamical systems are employed to obtain insights into the model in equation 6.28. The types of insights sought include the understanding of the range of possible long-term behaviours of the system, and an appreciation of how varying the model's parameters changes this behaviour. As in section 6.2, in which the linear Richardson model was considered from a dynamical systems perspective, it is not just individual solution curves for a specific initial condition, denoted here by $(\mathbf{p}(t_0), \mathbf{q}(t_0)) =$

$(p_1(t_0), ..., p_N(t_0), q_1(t_0), ..., q_M(t_0))$, that are of interest, but also families of solution curves, which can be used to determine the range of possible behaviours that might arise for any initial condition within a given subset of the phase space.

To begin, some simplifying assumptions are made. In what follows, a reduced parameter space is considered in which $\alpha = \gamma = 1$, $\delta = \beta$, and $\sigma_1 = \sigma_2 = \sigma$. Respectively, these imply: that $\dot{\mathbf{p}}$ depends linearly on $\mathbf{p}$ in both the numerator and denominator of the action-reaction term (which combine to form a nonlinear function); that both adversaries react to impedance on $\mathcal{M}$ at the same rate; and that both adversaries react to internal constraints at the same rate. In accordance with Richardson's original model, the parameters ρ_1, ρ_2, σ_1, σ_2, ϵ_1 and ϵ_2 are set to be nonnegative. The parameter β is also taken to be nonnegative, to ensure that distance plays a diminishing role in the weighting factors w_{lj} and v_{jl}.

It is possible to simplify the model further, this time at no cost to the generalisability of the model, by rescaling the system. Indeed, substituting

$$t = \frac{1}{\sigma}\hat{t}, \qquad \rho_i = \sigma\hat{\rho}_i, \qquad \epsilon_i = \sigma\hat{\epsilon}_i, \tag{6.29}$$

into the model eliminates the parameter σ. Relabelling the parameters by removing hats, and taking into account the other simplifying assumptions, the model in equation 6.28 becomes

$$\begin{aligned} \dot{p}_j &= -p_j + \rho_1 \sum_{l=1}^{M} q_l \frac{p_j e^{-\beta d(\mathbf{x}_j, \mathbf{y}_l)}}{\sum_{j'}^{N} p_{j'} e^{-\beta d(\mathbf{x}_{j'}, \mathbf{y}_l)}} + \frac{\epsilon_1}{N} \\ \dot{q}_l &= -q_l + \rho_2 \sum_{j=1}^{N} p_j \frac{q_l e^{-\beta d(\mathbf{y}_l, \mathbf{x}_j)}}{\sum_{l'}^{M} q_{l'} e^{-\beta d(\mathbf{y}_{l'}, \mathbf{x}_j)}} + \frac{\epsilon_2}{M}. \end{aligned} \tag{6.30}$$

There are five parameters in equation 6.30 whose effect on the system dynamics requires exploration. ρ_1 and ρ_2 are analogous to the action-reaction terms for each adversary in the original Richardson model and are anticipated to play a similar role. That is, as they increase, the system is expected to become more unstable. A similar comparison can be made for ϵ_1 and ϵ_2, which are external grievance terms, and are anticipated to play a role in the magnitude of resulting solution curves. The parameter β, however, has no analogy within the original Richardson model. Its inclusion in equation 6.30 is as a direct result of the spatial disaggregation.

In the sections that follow, the model in equation 6.30 is considered in a series of idealised scenarios. From these scenarios, modest insights into the model can be

obtained. It will be demonstrated how some of these insights are consistent with the behaviour of the model in more complicated scenarios, leading to more useful insights that might be employed within case studies. Initially, the dimension of the dependent variable, given by $N + M$, is minimised, since low-dimensional non-linear systems are often the easiest to analyse. To this end, the model is first considered with $N + M = 3$, which is the lowest dimension of the dependent variable for which the model admits non-trivial spatial disaggregation of conflict dynamics ($N = M = 1$ leads to Richardson's original system). Next, a scenario is considered with $N + M = 4$, and then $N + M = 8$. Finally, the model is investigated in a general number of dimensions, using the findings of the more simple scenarios to instruct the analysis.

6.4.1 A three-dimensional scenario

The first scenario to be considered is the simplest with non-trivial spatial disaggregation. Without loss of generality, this is given by the case when $N = 2$ and $M = 1$, so that one adversary is distributed over two locations—at positions $\mathbf{x}_1, \mathbf{x}_2 \in \mathcal{M}$—and the other adversary remains at just one location, given by $\mathbf{y} \in \mathcal{M}$. This scenario can be thought of as one step below a macro-level model in which the spatial dependency is completely aggregated (and therefore given by the original Richardson model).

In order to fully specify the model, the metric d is defined. A metric is required that distinguishes between the locations $\mathbf{x}_1$ and $\mathbf{x}_2$, and, for analytic simplicity, is set here so that

$$d(\mathbf{x}_1, \mathbf{y}) = 0, \qquad d(\mathbf{x}_2, \mathbf{y}) = 1,$$

so that the distance between $\mathbf{x}_1$ and $\mathbf{y}$ is negligible, whilst $\mathbf{y}$ and $\mathbf{x}_2$ are different locations on $\mathcal{M}$. The resulting three-dimensional system can be written as

$$\begin{aligned} \dot{p_1} &= -p_1 + \rho_1 \frac{q p_1}{p_1 + p_2 e^{-\beta}} + \frac{\epsilon_1}{2} \\ \dot{p_2} &= -p_2 + \rho_1 \frac{q p_2 e^{-\beta}}{p_1 + p_2 e^{-\beta}} + \frac{\epsilon_1}{2} \\ \dot{q} &= -q + \rho_2 (p_1 + p_2) + \epsilon_2. \end{aligned} \tag{6.31}$$

The first constraint specified in the spatial disaggregation of the model in equation 6.14 ensures that the aggregated system, taken to be the sum of the hostility levels over the different locations of each adversary, is equivalent to the system as described by the

original linear Richardson model. The dynamics of the variables $p = p_1 + p_2$ and q are therefore given by equation 6.1. Consequently, the linear stability analysis presented in Section 6.2 can also be utilised here. During this analysis, it was determined that the Richardson model has a unique equilibrium which is stable if, and only if, $\sigma_1\sigma_2 - \rho_1\rho_2 > 0$ and $\sigma_1 + \sigma_2 > 0$. Translating these criteria using the same rescaling as in 6.29, and taking into account the constraints placed upon parameters, the aggregated system converges to a stable equilibrium if, and only if,

$$\rho_1\rho_2 < 1,$$

and this equilibrium is given by

$$p = p_1 + p_2 = \frac{\epsilon_1 + \rho_1\epsilon_2}{1 - \rho_1\rho_2}, \qquad q = \frac{\epsilon_2 + \rho_2\epsilon_1}{1 - \rho_1\rho_2}. \tag{6.32}$$

Equation 6.32 defines a line in three-dimensional (p_1, p_2, q)-space as the intersection of two planes. If the stability criteria are satisfied then the system converges to this line. If $\rho_1\rho_2 > 1$, then the aggregated system is unstable and almost all solution curves diverge to infinity.

For the remainder of this section, it is assumed that $\rho_1\rho_2 < 1$, so that all solution curves in the aggregated system converge to a stable equilibrium, and all solution curves in the three-dimensional system in equation 6.31 converge to the line defined by equation 6.32. It remains to find the dynamics of the system on this line, representing the behaviour of the system that is due to spatial disaggregation.

The dynamics on the line of equation 6.32 can be found through a change of variables to separate the model into two components: the original linear Richardson system, which is well-understood, and the unknown dynamics brought about by spatial disaggregation. To this end, the variables

$$p = p_1 + p_2, \qquad r = p_1 - p_2,$$

are introduced.

Re-writing the system in equation 6.31 in terms of the variables p, q and r, leads

to

$$\dot{p} = -p + \rho_1 q + \epsilon_1 \tag{6.33}$$

$$\dot{q} = -q + \rho_2 p + \epsilon_2 \tag{6.34}$$

$$\dot{r} = -r + \rho_1 q \frac{p(1 - e^{-\beta}) + r(1 + e^{-\beta})}{p(1 + e^{-\beta}) + r(1 - e^{-\beta})}, \tag{6.35}$$

which isolates the dynamics of the aggregated system with the unexplored dynamics on the line defined by 6.32. Equations 6.33 and 6.34 correspond to the Richardson model in equation 6.1 with $\sigma_1 = \sigma_2 = 1$, and do not depend on r. The unexplored dynamics captured by equation 6.35, which incorporates the effect of spatial disaggregation, can be considered as a distinct system for given values of p and q.

In what follows, it is assumed that the system has converged to the line in 6.32, and therefore the values of p and q are fixed positive constants as given in 6.32. The dynamics are therefore given by the one-dimensional system

$$\dot{r} = -r + \rho_1 q \frac{p(1 - e^{-\beta}) + r(1 + e^{-\beta})}{p(1 + e^{-\beta}) + r(1 - e^{-\beta})}. \tag{6.36}$$

This section proceeds by considering the dynamics of this simplified system, thereby leading to an understanding of how spatial dependency is incorporated into the model, and, specifically, how hostility against the adversary at $\mathbf{y}$ is distributed over the locations $\mathbf{x}_1$ and $\mathbf{x}_2$ for different parameter values.

The system in equation 6.36 is undefined when

$$r = -\left(\frac{1 + e^{-\beta}}{1 - e^{-\beta}}\right) p, \tag{6.37}$$

and so the analysis presented here is restricted to cases in which this condition does not occur. For equality in equation 6.37, r and p must have opposite signs; however, since $d(\mathbf{x}_1, \mathbf{y}) < d(\mathbf{x}_2, \mathbf{y})$, and since distance is hypothesised to have a diminishing effect on the resulting hostility, it may be assumed that $p_1 > p_2$ for $p > 0$ and, therefore, that $r > 0$. Thus, this condition is assumed not to occur in scenarios of interest.

The system in equation 6.36 is stationary when

$$-r + \rho_1 q \frac{p(1 - e^{-\beta}) + r(1 + e^{-\beta})}{p(1 + e^{-\beta}) + r(1 - e^{-\beta})} = 0,$$

the roots of which are solutions to the quadratic equation

$$r^2 + \left(\frac{1 + e^{-\beta}}{1 - e^{-\beta}}\right)(p - \rho_1 q)r - \rho_1 pq = 0. \tag{6.38}$$

There are two real roots to equation 6.38, given by

$$r_{\pm} = -\frac{1}{2}\left(\frac{1+e^{-\beta}}{1-e^{-\beta}}\right)(p-\rho_1 q) \pm \frac{1}{2}\sqrt{\left(\frac{1+e^{-\beta}}{1-e^{-\beta}}\right)^2 (p-\rho_1 q)^2 + 4\rho_1 pq}, \quad (6.39)$$

which implies that there are two equilibria on the line defined by equation 6.32. Since $4\rho_1 pq > 0$, $r_- < 0$ and $r_+ > 0$. The point r_+ is therefore a unique positive equilibrium of equation 6.36.

The stability of this equilibrium can be determined by considering the derivative of $\dot{r}$ with respect to r, at the point r_+. If

$$\left.\frac{d\dot{r}}{dr}\right|_{r_+} < 0, \quad (6.40)$$

then the equilibrium is stable. This condition can be verified by considering small deviations from the equilibrium at $r = r_+$, and determining whether the system will return to the equilibrium value or move away from it. Specifically, if $\epsilon > 0$ is small enough, then, if equation 6.40 holds, the value of $\dot{r}$ at $r = r_+ - \epsilon$ is positive, and so the value of r will increase (since $\dot{r}$ determines the rate at which r changes), and move towards $r = r_+$. Similarly, if equation 6.40 holds, then the value of $\dot{r}$ at $r = r_+ + \epsilon$ will be negative, the value of r will decrease, and again move back towards r_+. The converse also holds: if the derivative of $\dot{r}$ at $r = r_+$ is positive, then the equilibrium is unstable.

Differentiating equation 6.36 obtains

$$\frac{d\dot{r}}{dr} = -1 + \rho_1 pq \frac{(1+e^{-\beta})^2 - (1-e^{-\beta})^2}{(p(1+e^{-\beta}) + r(1-e^{-\beta}))^2}.$$

If $p > r$ as expected, then

$$\begin{aligned} \frac{d\dot{r}}{dr} &< -1 + \rho_1 pq \frac{(1+e^{-\beta})^2 - (1-e^{-\beta})^2}{(p(1+e^{-\beta})^2 + p(1-e^{-\beta})^2)} \\ &= -1 + \frac{\rho_1 q}{p}\left(\frac{(1+e^{-\beta})^2 - (1-e^{-\beta})^2}{((1+e^{-\beta}) + (1-e^{-\beta}))^2}\right). \end{aligned} \quad (6.41)$$

Additionally, substituting the expressions for the equilibrium value of p and q, obtains

$$\begin{aligned} \frac{\rho_1 q}{p} &= \rho_1 \left(\frac{\epsilon_2 + \rho_2 \epsilon_1}{1-\rho_1\rho_2}\right)\left(\frac{1-\rho_1\rho_2}{\epsilon_1 + \rho_1\epsilon_2}\right) \\ &= \frac{\rho_1\epsilon_2 + \rho_1\rho_2\epsilon_1}{\rho_1\epsilon_2 + \epsilon_1} \\ &< 1, \end{aligned}$$

since $\rho_1\rho_2 < 1$. Also,

$$\frac{(1+e^{-\beta})^2-(1-e^{-\beta})^2}{\left((1+e^{-\beta})+(1-e^{-\beta})\right)^2} < \frac{(1+e^{-\beta})^2-(1-e^{-\beta})^2}{((1+e^{-\beta})^2+(1-e^{-\beta})^2)} < 1,$$

and, therefore,

$$\left.\frac{d\dot{r}}{dr}\right|_{r_+} < 0,$$

which holds provided $r < p$ and $r > 0$. Under these conditions the unique positive equilibrium is locally attractive. In addition, since $d\dot{r}/dr$ only changes sign when $r = r_+$ or $r = r_-$, the equilibrium $r = r_+$ is attractive for $r > 0$. Figure 6.4 shows the dynamics of the one-dimensional system for the given set of parameter values. Initial conditions r_0 such that $0 \leq r_0 \leq p$ will always converge to the equilibrium given by r_+, and therefore if $p_1 \geq p_2$, the system in equation 6.31 converges to a single positive equilibrium value.

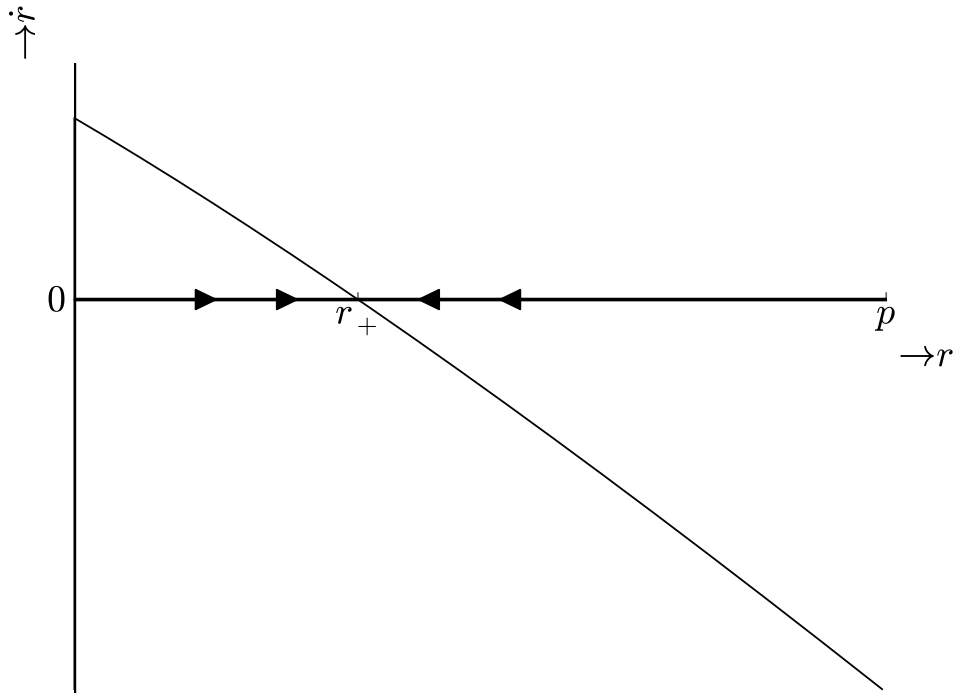

Figure 6.4: **A plot of $\dot{r}$ against r for the one-dimensional system in equation 6.36**. The parameter values used are $\epsilon_1 = \epsilon_2 = 1$, $\rho_1 = \rho_2 = 0.5$ and $\beta = 1$. The arrows show the direction of solution curves $r(t)$ for $t > 0$ along the r-axis.

Under the assumptions of the model, two adversaries engaging in retaliatory

conflict—one of which is distributed over two distinct locations, one nearby to the adversary, and one further away—will approach an equilibrium whereby the respective level of hostile activity at $\mathbf{x}_1$ and $\mathbf{x}_2$ serves to counter the hostility by the adversary at $\mathbf{y}$. If, initially, $p_1 \geq p_2$, which would be anticipated given that $\mathbf{x}_1$ is closer to $\mathbf{y}$ than $\mathbf{x}_2$, and since distance is assumed to play a diminishing role on the retaliatory nature of the conflict, then the resulting distribution of hostility between the locations $\mathbf{x}_1$ and $\mathbf{x}_2$ is determined by the value of r_+, according to equation 6.39. If, for example, $r_+ = 0$, then, at this point, $p_1 = p_2$ and hostility is equally distributed over the locations $\mathbf{x}_1$ and $\mathbf{x}_2$.

Equation 6.39 enables the investigation of how the parameters influence the value of r_+, and therefore influence the resulting spatial distribution of hostility. The parameters ρ_1, ρ_2, ϵ_1 and ϵ_2 have a similar interpretation on the aggregate equilibrium value given in equation 6.32, as in Section 6.2; however, the parameter β does not appear in the original model as it results from the spatial disaggregation.

To investigate how β influences the spatial distribution of the resulting equilibrium, its limiting influence on r_+ is first considered. As $\beta \to 0$,

$$\left(\frac{1+e^{-\beta}}{1-e^{-\beta}}\right) \to \infty,$$

however, the value of r_+ in the limit as $\beta \to 0$ can be found by applying the generalised binomial expansion to the analytical expression of r_+ in equation 6.39, leading to

$$\begin{aligned}
\lim_{\beta\to 0} r_+ = \lim_{\beta\to 0} \Bigg(& -\frac{1}{2}\left(\frac{1+e^{-\beta}}{1-e^{-\beta}}\right)(p-\rho_1 q) + \\
& \frac{1}{2}\left(\frac{1+e^{-\beta}}{1-e^{-\beta}}\right)(p-\rho_1 q)\left(1+\frac{4\rho_1 pq}{\left(\frac{1+e^{-\beta}}{1-e^{-\beta}}\right)^2 (p-\rho_1 q)^2}\right)^{\frac{1}{2}}\Bigg) \\
= \lim_{\beta\to 0} \Bigg(& -\frac{1}{2}\left(\frac{1+e^{-\beta}}{1-e^{-\beta}}\right)(p-\rho_1 q) + \\
& \frac{1}{2}\left(\frac{1+e^{-\beta}}{1-e^{-\beta}}\right)(p-\rho_1 q)\left(1+\frac{1}{2}\frac{4\rho_1 pq}{\left(\frac{1+e^{-\beta}}{1-e^{-\beta}}\right)^2 (p-\rho_1 q)^2}+\ldots\right)\Bigg). \qquad (6.42)
\end{aligned}$$

Higher order terms of equation 6.42 can be neglected since, as $\beta \to 0$, they approach 0 more quickly than the other terms. Consequently,

$$\lim_{\beta\to 0} r_+ = 0.$$

In this case, $p_1 = p_2$, the level of hostility at both $\mathbf{x}_1$ and $\mathbf{x}_2$ is equal, and space plays no role in the model. The condition $\beta > 0$ leads to spatial dependency in the model.

As $\beta \to \infty$,

$$\left(\frac{1+e^{-\beta}}{1-e^{-\beta}}\right) \to 1,$$

and thus

$$\lim_{\beta\to\infty} r_+ = -\frac{1}{2}(p-\rho_1 q) + \frac{1}{2}\sqrt{(p-\rho_1 q)^2 + 4\rho_1 pq},$$

from which, by expanding the squared term inside the square root and then factorising, can be obtained:

$$\lim_{\beta\to\infty} r_+ = \rho_1 q.$$

Therefore, as β increases, the difference in the levels of hostility at $\mathbf{x}_1$ and $\mathbf{x}_2$ approaches the limit $\rho_1 q$. Figure 6.5 plots the value of r_+ given in equation 6.39 for different values of β. The plot produces a monotonically increasing function, which approaches the limit $\rho_1 q$. Therefore, the difference in hostility levels at $\mathbf{x}_1$ and $\mathbf{x}_2$ is at its maximum as $\beta \to \infty$. The parameter β determines the extent to which hostility is distributed over the locations $\mathbf{x}_1$ and $\mathbf{x}_2$, and therefore captures the strength of the spatial dependency in the system. Similar interpretations can also be obtained from the more general system in equation 6.30. As $\beta \to 0$, the system becomes completely aggregated, regardless of the spatial distribution of adversaries, whilst as $\beta \to \infty$, the system becomes increasingly local, with adversaries only being influenced by their immediate neighbours. The value of β determines the strength of spatial dependency and the accessibility of the space, and will require appropriate calibration in the application of the model to conflict scenarios.

6.4.2 A four-dimensional scenario

In this section the complexity of the model is increased by considering a scenario in which each adversary is located over two distinct locations. Suppose that the locations $x_1, x_2, y_1, y_2 \in \mathcal{M}$ are associated with hostility measures $p_1, p_2, q_1, q_2 \in \mathbb{R}$, respectively. For analytic simplicity, the distance metric d is chosen to consist of zeros and ones. In this case, the 2×2 matrix D given by $D_{jl} = d(\mathbf{x}_j, \mathbf{y}_l)$ is defined to be

$$D = \begin{pmatrix} 0 & 1 \\ 1 & 0 \end{pmatrix},$$

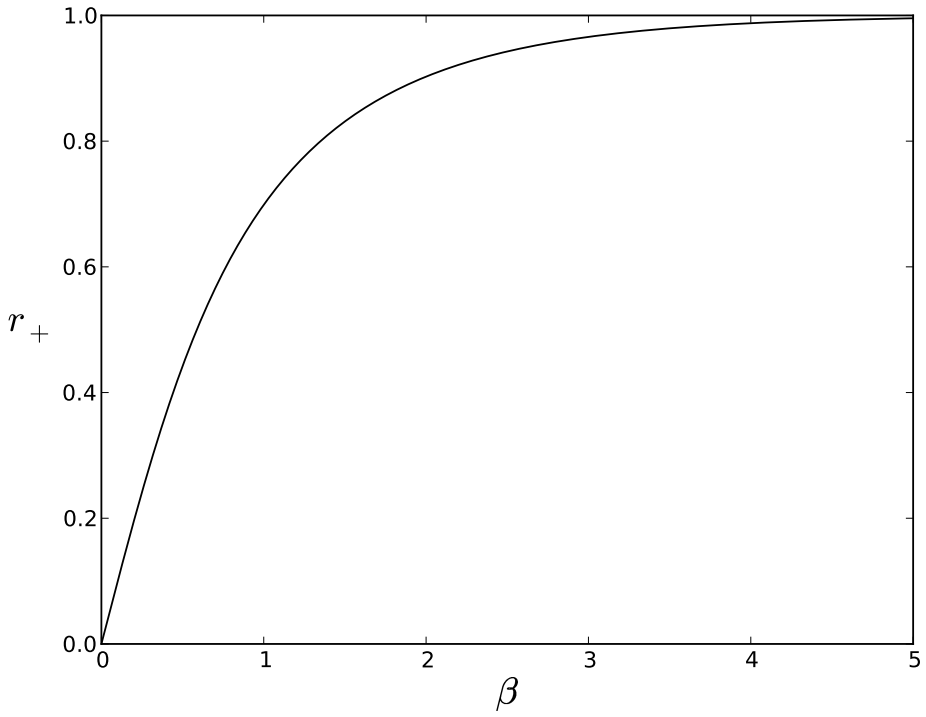

Figure 6.5: **The value of r_+, as given in equation 6.39, for different values of β.** The parameter values used are $\epsilon_1 = \epsilon_2 = 1$, $\rho_1 = \rho_2 = 0.5$ and $\beta = 1$.

so that adversaries are distributed identically on $\mathcal{M}$. The two adversaries can be thought of as being both distributed across two spatial zones. In this scenario, the model in equation 6.30 becomes

$$\begin{aligned}
\dot{p_1} &= -p_1 + \rho_1 \frac{q_1 p_1}{p_1 + p_2 e^{-\beta}} + \rho_1 \frac{q_2 p_1 e^{-\beta}}{p_1 e^{-\beta} + p_2} + \frac{\epsilon_1}{2} \\
\dot{p_2} &= -p_2 + \rho_1 \frac{q_1 p_2 e^{-\beta}}{p_1 + p_2 e^{-\beta}} + \rho_1 \frac{q_2 p_2}{p_1 e^{-\beta} + p_2} + \frac{\epsilon_1}{2} \\
\dot{q_1} &= -q_1 + \rho_2 \frac{p_1 q_1}{q_1 + q_2 e^{-\beta}} + \rho_2 \frac{p_2 q_1 e^{-\beta}}{q_1 e^{-\beta} + q_2} + \frac{\epsilon_2}{2} \\
\dot{q_2} &= -q_2 + \rho_2 \frac{p_1 q_2 e^{-\beta}}{q_1 + q_2 e^{-\beta}} + \rho_2 \frac{p_2 q_2}{q_1 e^{-\beta} + q_2} + \frac{\epsilon_2}{2}.
\end{aligned} \tag{6.43}$$

Similarly to the three dimensional case in section 6.4.1, the dynamics of the original Richardson model can be extracted from this system by a change of variables, leading to a reduced dynamical system to which the system converges for $\rho_1 \rho_2 < 1$. The following parameters are therefore introduced:

$$\begin{aligned}
p &= p_1 + p_2, \qquad & r &= p_1 - p_2, \\
q &= q_1 + q_2, \qquad & s &= q_1 - q_2.
\end{aligned}$$

Substituting these expressions into equation 6.43, and re-writing the system so that it depends only on p, q, r and s, obtains

$$\dot{p} = -p + \rho_1 q + \epsilon_1 \tag{6.44}$$

$$\dot{q} = -q + \rho_2 p + \epsilon_2 \tag{6.45}$$

$$\begin{aligned}
\dot{r} = &-r + \frac{\rho_1}{2}(q+s)\frac{(1-e^{-\beta})p + (1+e^{-\beta})r}{(1+e^{-\beta})p + (1-e^{-\beta})r} \\
&+ \frac{\rho_1}{2}(q-s)\frac{(e^{-\beta}-1)p + (1+e^{-\beta})r}{(1+e^{-\beta})p + (e^{-\beta}-1)r}
\end{aligned} \tag{6.46}$$

$$\begin{aligned}
\dot{s} = &-s + \frac{\rho_2}{2}(p+r)\frac{(1-e^{-\beta})q + (1+e^{-\beta})s}{(1+e^{-\beta})q + (1-e^{-\beta})s} \\
&+ \frac{\rho_2}{2}(p-r)\frac{(e^{-\beta}-1)q + (1+e^{-\beta})s}{(1+e^{-\beta})q + (e^{-\beta}-1)s}.
\end{aligned} \tag{6.47}$$

Equations 6.44 and 6.45 are equivalent to the original Richardson system with $\sigma_1 = \sigma_2 = 1$, whilst equations 6.46 and 6.47 represent the added dynamics and complexity that is due to spatial disaggregation. For $\rho_1 \rho_2 < 1$, the system converges to the plane defined by the equilibrium of the aggregated system, given by

$$p = \frac{\rho_1 \epsilon_2 + \epsilon_1}{1 - \rho_1 \rho_2}, \qquad q = \frac{\rho_2 \epsilon_1 + \epsilon_2}{1 - \epsilon_1 \epsilon_2}. \tag{6.48}$$

For the remainder of the section, it is assumed that $\rho_1\rho_2 < 1$ and that a sufficient amount of time has passed so that the unexplored dynamics of the system are given by equations 6.46 and 6.47, where p and q are constants given in equation 6.48.

The system is undefined when

$$r = \pm\left(\frac{1+e^{-\beta}}{1-e^{-\beta}}\right)p,$$

or when

$$s = \pm\left(\frac{1+e^{-\beta}}{1-e^{-\beta}}\right)q.$$

Consequently, the analysis presented here is restricted to solutions that do not cross this region in phase space. For a value of $\beta > 0$, the lines at which the system is undefined generate a rectangle in rs-space surrounding the origin. Considering possible solutions within this rectangle, it can be observed that the origin is an equilibrium: for $r = 0$ and $s = 0$,

$$\left.\dot{s}\right|_{(r,s)=(0,0)} = \frac{\rho_1 q}{2}\left(\frac{1-e^{-\beta}}{1+e^{-\beta}}\right) + \frac{\rho_1 q}{2}\left(\frac{e^{-\beta}-1}{1+e^{-\beta}}\right) = 0$$
$$\left.\dot{r}\right|_{(r,s)=(0,0)} = \frac{\rho_2 p}{2}\left(\frac{1-e^{-\beta}}{1+e^{-\beta}}\right) + \frac{\rho_2 p}{2}\left(\frac{e^{-\beta}-1}{1+e^{-\beta}}\right) = 0.$$

The origin of the rs-plane represents the point at which $p_1 = p_2$ and $q_1 = q_2$. Thus hostility is equally distributed amongst the different locations in space and the system is perfectly balanced and symmetric.

The stability properties of this equilibrium provide significant insight into the model. On the one hand, if the equilibrium is attractive, then solution curves will converge towards this point and, according to the model, evenly distributed hostility levels in space will be anticipated to arise; however, on the other, if the equilibrium is unstable, then solution curves will be repelled from this point and the model will tend to exhibit more unequal distributions of hostility in space. The stability of the equilibrium point can be determined by considering the planar system in equations 6.46 and 6.47, in which the values of p and q are treated as constants given by equation 6.48, denoted by

$$(\dot{r}, \dot{s}) = \begin{pmatrix} f(r,s) \\ g(r,s) \end{pmatrix},$$

where f and g are given by the right hand sides of equation 6.46 and 6.47, respectively. A Taylor expansion about $(r, s) = (0, 0)$ leads to

$$\begin{pmatrix} f(r,s) \\ g(r,s) \end{pmatrix} = \begin{pmatrix} rf_r(0,0) + sf_s(0,0) + \mathcal{O}(r^2) + \mathcal{O}(s^2) + \mathcal{O}(rs) \\ rg_r(0,0) + sg_s(0,0) + \mathcal{O}(r^2) + \mathcal{O}(s^2) + \mathcal{O}(rs) \end{pmatrix},$$

where the subscript notation represents partial differentiation with respect to the subscripted variable. Using matrix notation, this is equivalent to

$$\begin{pmatrix} \dot{r} \\ \dot{s} \end{pmatrix} = \begin{pmatrix} f_r & f_s \\ g_r & g_s \end{pmatrix} \Bigg|_{(r,s)=(0,0)} \begin{pmatrix} r \\ s \end{pmatrix} + \mathcal{O}(r^2) + \mathcal{O}(s^2) + \mathcal{O}(rs). \tag{6.49}$$

The 2×2 matrix in equation 6.49 is the Jacobian of the function $\mathbf{f} := (f, g)$. Equation 6.49 therefore separates the dynamics of the planar system into a linear component—whose dynamics are given by the Jacobian of $\mathbf{f}$—and a non-linear component, consisting of higher order terms. The Hartman-Grobman theorem states that, for non-linear systems, if the Jacobian matrix evaluated at the equilibrium point is invertible (i.e. has non-zero determinant) then the equilibrium is known as hyperbolic and the behaviour of the system near to the equilibrium point is equivalent to the linear system given by

$$\begin{pmatrix} \dot{r} \\ \dot{s} \end{pmatrix} = \begin{pmatrix} f_r & f_s \\ g_r & g_s \end{pmatrix} \Bigg|_{(r,s)=(0,0)} \begin{pmatrix} r \\ s \end{pmatrix}.$$

More details of this theorem can be found in Guckenheimer and Holmes (1983), for example. Proofs typically consider the relative sizes of the higher order terms in equation 6.49 near to the equilibrium point.

Differentiating, and using the Hartman-Grobman theorem, it can be shown that the behaviour near the equilibrium is equivalent to the linear system given by

$$\begin{pmatrix} \dot{r} \\ \dot{s} \end{pmatrix} = \begin{pmatrix} -1 + \rho_1 \left(1 - \left(\frac{1-e^{-\beta}}{1+e^{-\beta}}\right)^2\right) & \rho_1 \left(\frac{1-e^{-\beta}}{1+e^{-\beta}}\right) \\ \rho_2 \left(\frac{1-e^{-\beta}}{1+e^{-\beta}}\right) & -1 + \rho_2 \left(1 - \left(\frac{1-e^{-\beta}}{1+e^{-\beta}}\right)^2\right) \end{pmatrix} \begin{pmatrix} r \\ s \end{pmatrix}, \tag{6.50}$$

which can be simplified by defining

$$\eta = \left(\frac{1 - e^{-\beta}}{1 + e^{-\beta}}\right), \tag{6.51}$$

which is dependent on $\beta > 0$ in such a way so that $0 < \eta < 1$. Equation 6.50 then becomes

$$\begin{pmatrix} \dot{r} \\ \dot{s} \end{pmatrix} = \begin{pmatrix} -1 + \rho_1(1 - \eta^2) & \rho_1 \eta \\ \rho_2 \eta & -1 + \rho_2(1 - \eta^2) \end{pmatrix} \begin{pmatrix} r \\ s \end{pmatrix}. \tag{6.52}$$

As shown in Section 6.2, the behaviour of a linear system depends exclusively on its eigenvalues and eigenvectors. The eigenvalues are combined in different ways to calculate the trace and determinant, which determine the system's location on the trace-determinant diagram in Figure 6.1, and therefore the qualitative behaviour of the dynamics near the equilibrium. The eigenvalues of the system in equation 6.52 are

$$\lambda_{\pm} = -1 + \frac{1}{2}\left(\rho_1 + \rho_2\right)\left(1 - \eta^2\right) \pm \frac{1}{2}\sqrt{\left(\rho_1 - \rho_2\right)^2\left(1 - \eta^2\right)^2 + 4\eta^2\rho_1\rho_2}. \tag{6.53}$$

For clarity, a simplified scenario in which $\rho_1 = \rho_2 = \rho$ is first considered. This implies that the intensity of the action-reaction dynamics for each adversary is equal. Substituting into equation 6.53, the eigenvalues simplify to

$$\lambda_{\pm} = -1 + \rho(1 - \eta^2 \pm \eta). \tag{6.54}$$

If both eigenvalues are less than zero, then solution curves will converge to the equilibrium value, and it is stable; whereas if at least one eigenvalue is positive, then the magnitude of the dependent variable can grow and almost all initial conditions diverge away from the equilibrium, and it is unstable. Considering first λ_-,

$$\lambda_- = -1 + \rho(1 - \eta^2 - \eta) < -1 + \rho < 0, \tag{6.55}$$

since $\eta > 0$ and $0 < \rho < 1$. Thus one eigenvalue is always negative and the condition for stability depends solely on the eigenvalue λ_+. In particular, the equilibrium is stable when

$$\lambda_+ = -1 + \rho(1 - \eta^2 + \eta) < 0, \tag{6.56}$$

which occurs when

$$\rho < \frac{1}{1 - \eta^2 + \eta}. \tag{6.57}$$

Substituting the expression for η from equation 6.51 into equation 6.57 leads to

$$\rho < \frac{(e^{\beta} + 1)^2}{e^{2\beta} + 4e^{\beta} - 1}. \tag{6.58}$$

Considering the right hand side of equation 6.58,

$$0 < \frac{(e^{\beta} + 1)^2}{e^{2\beta} + 4e^{\beta} - 1} = \frac{e^{2\beta} + 2e^{\beta} + 1}{e^{2\beta} + 4e^{\beta} - 1} < \frac{e^{2\beta} + 2e^{\beta} + 1 + 2(e^{\beta} - 1)}{e^{2\beta} + 4e^{\beta} - 1} = 1, \tag{6.59}$$

and, thus, for $\rho < 1$, it is possible that the equilibrium can be either stable or unstable, depending on the value of ρ in comparison to the value $\bar{\rho}$ given by

$$\bar{\rho}(\beta) = \frac{(e^{\beta} + 1)^2}{e^{2\beta} + 4e^{\beta} - 1}. \tag{6.60}$$

For $\rho < \bar{\rho}$, the equilibrium is stable and all solutions converge towards it, but for $\rho > \bar{\rho}$, the equilibrium is a saddle and almost all solution curves diverge away from it. A bifurcation is said to occur as ρ increases above $\bar{\rho}$, and $\bar{\rho}$ is said to be a bifurcation point.

The dynamics near to the equilibrium, as given by the linear system in equation 6.52, with $\beta = 1$, are shown in Figure 6.6 for both $\rho < \bar{\rho}$ and $\rho > \bar{\rho}$. The directions of the solution curves demonstrate how the equilibrium point qualitatively changes as ρ increases beyond $\bar{\rho}$. This loss of stability implies that a sudden change can occur to the qualitative dynamics as the action-reaction parameter ρ, which might be interpreted as the level of aggression in the system, increases. Moreover, it is possible for this sudden change to occur even before the aggregated system loses stability at $\rho = 1$, after which solution curves diverge away from the plane defined by equation 6.48.

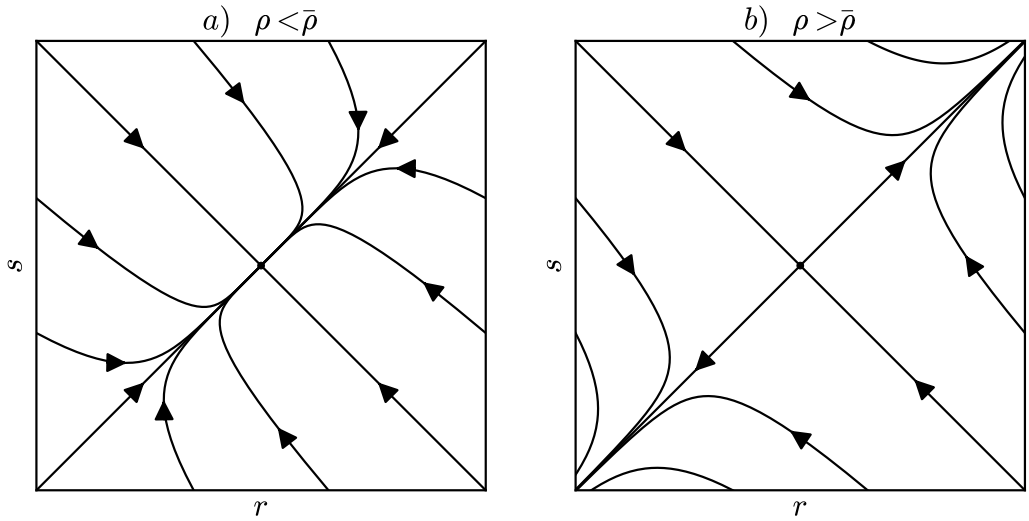

Figure 6.6: **Selected solution curves of the linear system in equation 6.52 for $\rho < \bar{\rho}$ and for $\rho > \bar{\rho}$.** For both figures $\beta = 1$, leading to $\bar{\rho} \approx 0.8$. In a), $\rho = 0.7$ whilst in b), $\rho = 0.9$.

In Figure 6.7, the function $\bar{\rho}(\beta)$ for $\beta > 0$ is shown, in order to demonstrate how the bifurcation point $\bar{\rho}$ varies with the parameter β. In Section 6.4.1, it was shown how the parameter β corresponds to the strength of spatial dependency in the system, with $\beta = 0$ leading to each adversary's location being treated equally regardless of where it is located, and $\beta \to \infty$ leading to more isolated dynamics, in which adversaries

increasingly only respond to those nearby to them. Figure 6.7 shows that for a large range of β, the value of $\bar{\rho}$ is significantly less than one, meaning that bifurcations can occur on the rs-plane by increasing ρ, before the aggregated system loses stability at $\rho = 1$. However, since the value of $\bar{\rho}$ approaches one with increasing β, and since $\bar{\rho}(0) = 1$, bifurcations are only likely to occur when the value of β is of order one, and when the system is balanced between being very isolated (i.e. for large β), and having no spatial dependency (for $\beta = 0$). The minimum of $\bar{\rho}$ can be calculated by differentiating equation 6.60, and occurs at β_{min} such that

$$\left.\frac{d\bar{\rho}}{d\beta}\right|_{\beta=\beta_{\text{min}}} = \frac{2e^{\beta_{\text{min}}}(e^{\beta_{\text{min}}}+1)}{e^{2\beta_{\text{min}}}+4e^{\beta_{\text{min}}}-1} - \frac{2e^{\beta_{\text{min}}}(e^{\beta_{\text{min}}}+2)(e^{\beta_{\text{min}}}+1)^2}{(e^{2\beta_{\text{min}}}+4e^{\beta_{\text{min}}}-1)^2} = 0. \tag{6.61}$$

Calculating the value of β_{min} leads to

$$\beta_{\text{min}} = \ln 3 \approx 1.1, \qquad \bar{\rho}(\beta_{\text{min}}) \approx 0.8. \tag{6.62}$$

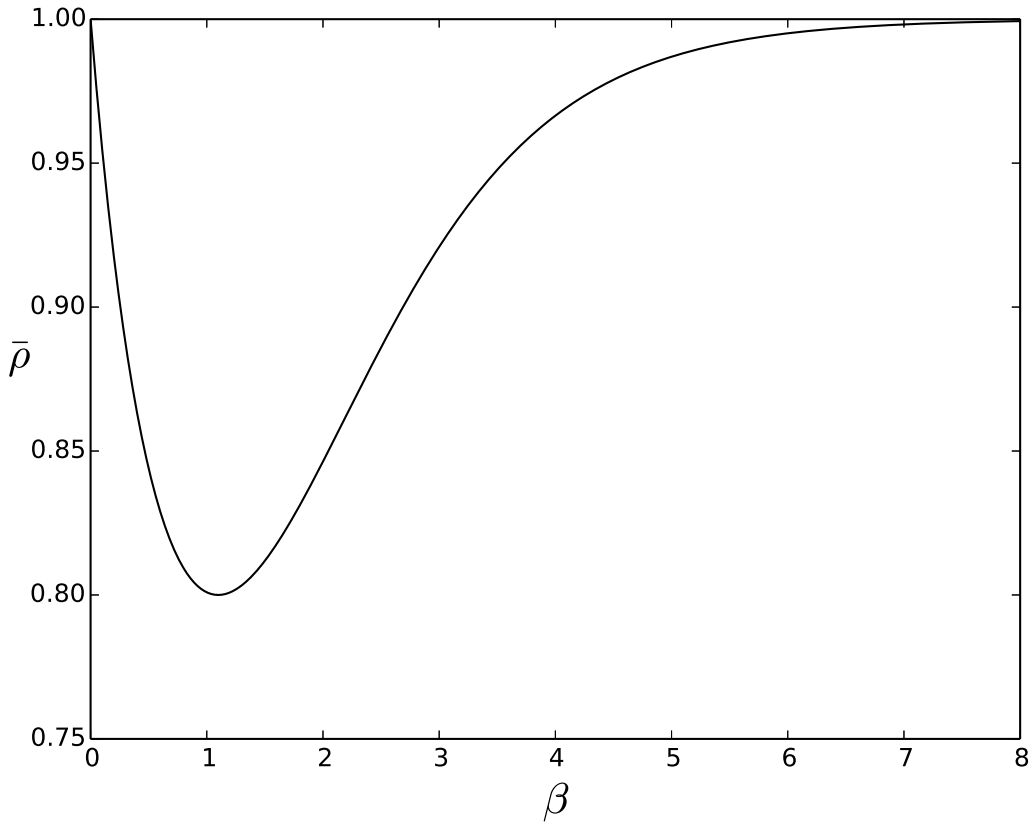

Figure 6.7: **The bifurcation point $\bar{\rho}$ plotted against β according to equation 6.60.**

The existence of the bifurcation has important implications for the model. Given an appropriate value for β, for relatively small values of $\rho < 1$, corresponding to scenar-

ios in which retaliatory dynamics are weak, then hostile activity is likely to be evenly distributed in space. However, if $\rho < 1$ is close to one, corresponding to scenarios with stronger retaliation and therefore higher levels of aggression, then hostile activity is likely to be more unevenly distributed, even if the aggregate system converges to a stable equilibrium.

For $\rho < \bar{\rho}$, the equilibrium at the origin of the rs-plane is locally attractive: initial conditions that begin sufficiently close to this point will converge towards it. For $\rho > \bar{\rho}$, the same equilibrium becomes a saddle. In this case, initial conditions that begin close to this point will almost always diverge away from it. It is natural to consider what might happen to these solution curves. Indeed, if real-world conflicts exhibiting such dynamics were to suddenly lose stability in a similar way, then considering what might happen to the modelled trajectory would be of great importance.

When $\rho = \bar{\rho}$, the matrix in the system in equation 6.52 has a zero eigenvalue, and the matrix is no longer invertible. This implies that the Hartman-Grobman theorem no longer applies and the dynamics near the equilibrium cannot be determined by the linearised system obtained from the Taylor expansion. This is because the higher order terms of the Taylor expansion, which can be neglected for invertible linearised matrices, cannot be neglected when the matrix is not invertible. For this reason, a Taylor expansion is next considered that incorporates more of these higher order terms. The Taylor expansion for a general two-dimensional function $f(x, y)$ about the origin up to third order is given by

$$\begin{aligned} f(x,y) =& f(0,0) + f_x(0,0)x + f_y(0,0)y \\ &+ \frac{1}{2!}\left(f_{xx}(0,0)x^2 + 2f_{xy}(0,0) + f_{yy}(0,0)\right) \\ &+ \frac{1}{3!}\left(f_{xxx}(0,0)x^3 + 3f_{xxy}(0,0)x^2y + 3f_{xyy}(0,0)xy^2 + f_{yyy}(0,0)y^3\right) \\ &+ \mathcal{O}(x^4) + \mathcal{O}(x^3y) + \mathcal{O}(x^2y^2) + \mathcal{O}(xy^3) + \mathcal{O}(y^4), \end{aligned}$$

where, again, subscript notation is used to denote differentiation with respect to the subscripted variable. Evaluating this formula for the planar system given by equations 6.46 and 6.47 leads to

$$\begin{pmatrix} \dot{r} \\ \dot{s} \end{pmatrix} = \begin{pmatrix} (-1+\rho-\rho\eta^2)r + \rho\eta s + \frac{\rho\eta^2}{p^2}(1-\eta^2)r^3 - \frac{\rho\eta}{p^2}(1-\eta^2)r^2 s \\ (-1+\rho-\rho\eta^2)s + \rho\eta r + \frac{\rho\eta^2}{q^2}(1-\eta^2)s^3 - \frac{\rho\eta}{q^2}(1-\eta^2)s^2 r \end{pmatrix}. \quad (6.63)$$

The linearised system in equation 6.52 can be seen as a component within equation 6.63, but there are also additional non-linear terms up to order three which reflect more of the dynamics of the system close to equilibrium. Two phase portraits of the non-linear system in equation 6.63 are shown in Figure 6.8, in which parameter values are chosen to reflect two different values of ρ: one in which $\rho < \bar{\rho}$, and so the equilibrium at the origin of the rs-plane is stable, and one in which $\rho > \bar{\rho}$, after the bifurcation has occurred. For $\rho > \bar{\rho}$, three equilibria exist, two of which appear to stable, and one which is unstable. The figure appears to demonstrate that as ρ increases beyond $\bar{\rho}$, not only does the equilibrium at the origin become unstable, but two new stable equilibria appear. This particular bifurcation is known as a supercritical pitchfork bifurcation.

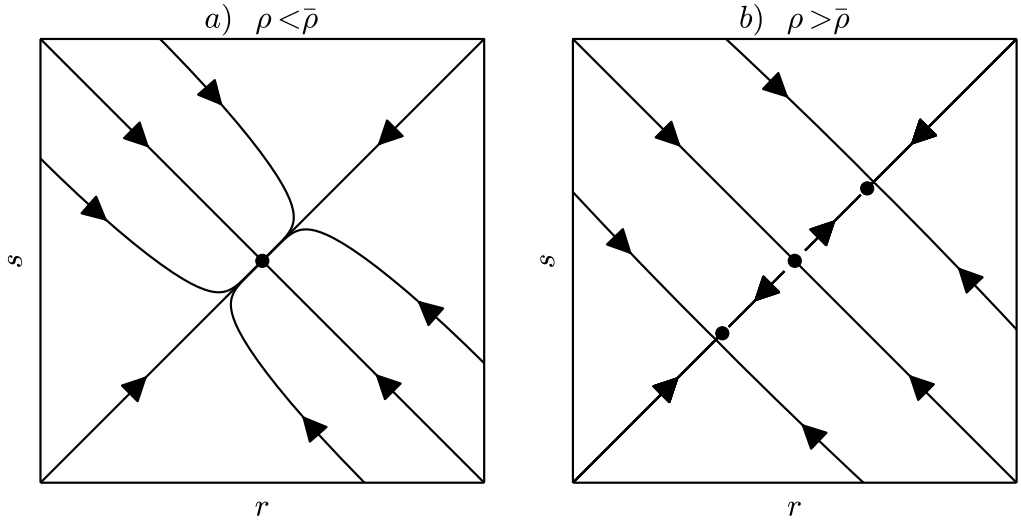

Figure 6.8: **The phase portrait of the system in equation 6.63 for two different values of ρ.** For figure a), $\rho = 0.7$ whilst for figure b), $\rho = 0.803$. All other parameter values are such that $\bar{\rho} = 0.801$.

Suppose now that $r = s$, and that $\epsilon_1 = \epsilon_2$ in equation 6.63. These further simplifying assumptions are employed to investigate analytically the behaviour leading to the supercritical pitchfork bifurcation, and lead to the one-dimensional non-linear system given by

$$\dot{r} = \left(-1 + \rho(1 - \eta^2 + \eta)\right) r + \left(\frac{\rho\eta}{p^2}(1 - \eta^2)(\eta - 1)\right) r^3. \tag{6.64}$$

If $\epsilon_1 = \epsilon_2$, then the system in 6.63 is symmetric and equilibria of the system in 6.64 will correspond to equilibria of the system in 6.63. Equilibria of the system in 6.64 occur

when either $r = 0$ or when

$$r^2 = \frac{1 - \rho(1 - \eta^2 + \eta)}{\frac{\rho\eta}{p^2}(1 - \eta^2)(\eta - 1)}, \tag{6.65}$$

which has solutions only when the right-hand side of equation 6.65 is greater than zero. It can be shown that this occurs when

$$\rho > \frac{1}{1 - \eta^2 + \eta},$$

which is exactly the condition for the loss of stability in the equilibrium at the origin, as identified in equation 6.57. In Figure 6.9, the equilibrium values for the system in 6.64 are shown for different values of ρ. As ρ increases beyond $\bar{\rho}$, two stable equilibria appear, with values given by

$$r_{\pm} = \pm p \left(\frac{1 - \rho(1 - \eta^2 + \eta)}{\rho\eta(1 - \eta^2)(\eta - 1)} \right)^{\frac{1}{2}}. \tag{6.66}$$

A bifurcation of the system in equations 6.46 and 6.47 at the equilibrium of the rs-plane has been shown to exist in the special case when $\rho_1 = \rho_2$. It is important to determine whether the same bifurcation occurs when $\rho_1 \neq \rho_2$. This is because conflict scenarios to which the model may be applied will often be asymmetric: each adversary may adopt different tactics, resulting in different retaliatory mechanisms and therefore result in different action-reaction parameters, as given by ρ_1 and ρ_2. In Figure 6.10 the stability of the origin of the rs-plane is shown for values of ρ_1 and ρ_2 between 0.5 and 1, and for three different values of β. In this figure, green represents stability of the equilibrium, and blue represents instability. The bifurcation can be observed in the transition from stability to instability in each of the three cases considered, across different values for β. This figure confirms that the identified bifurcation is robust to variation of the parameter values. Furthermore, the change in the bifurcation point appears to be smooth with varying parameters: an increase in ρ_1 moves the bifurcation point in the direction of decreasing ρ_2. This suggests that the system requires some total sum of aggression, as determined by a combination of the parameters ρ_1 and ρ_2, before the equilibrium at the origin of the rs-plane becomes unstable.

The four-dimensional model given in equation 6.43 has been shown to exhibit richer behaviour than the three-dimensional case. By investigating the stability of the

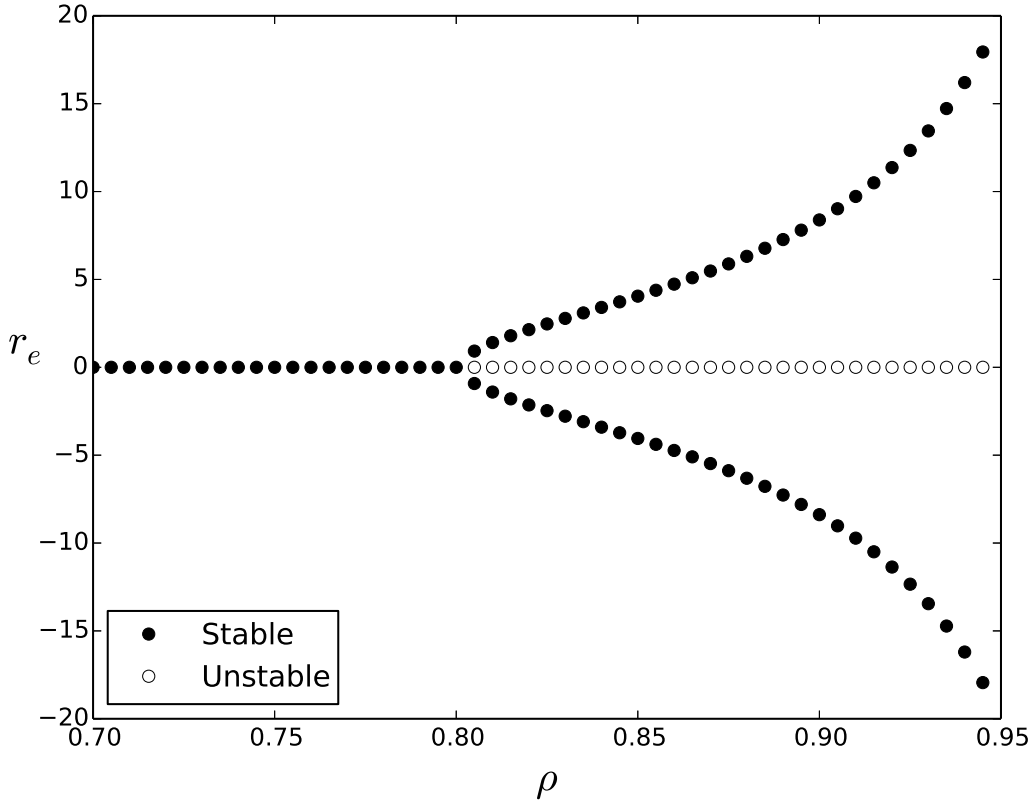

Figure 6.9: **Equilibria of the system in equation 6.64, denoted by r_e, for varying values of ρ.**

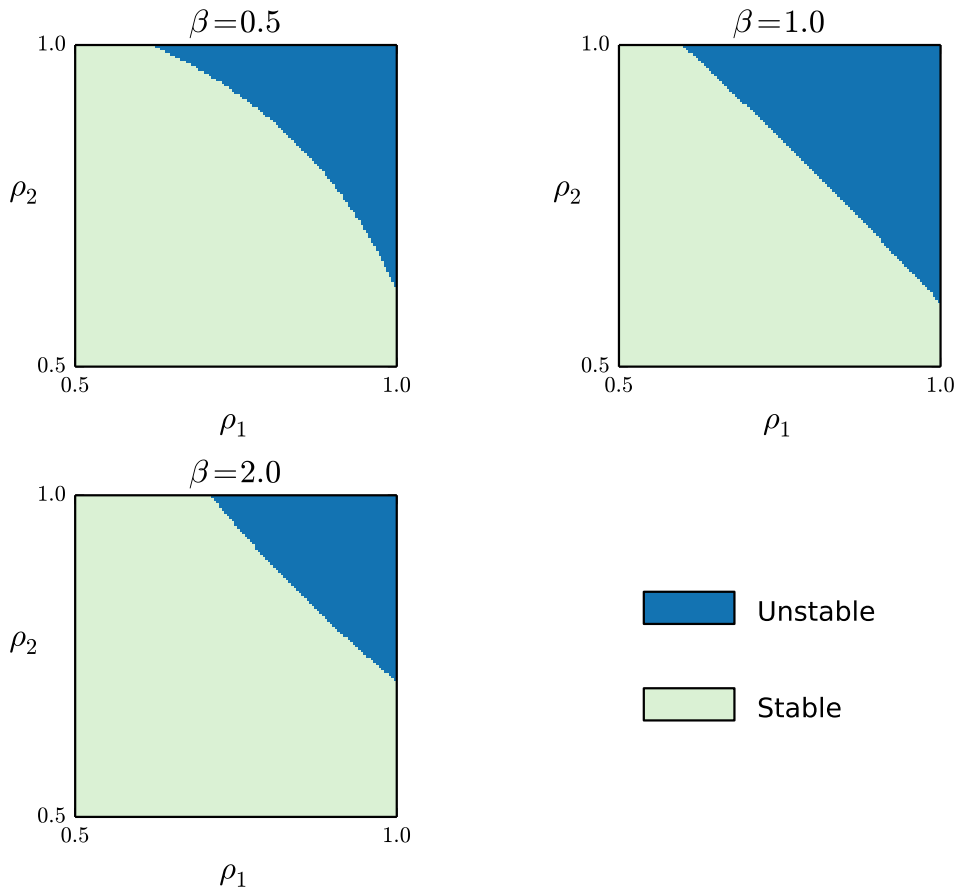

Figure 6.10: **The stability of the equilibrium at the origin of the rs-plane for $\rho_1 \in [0.5, 1)$ and $\rho_2 \in [0.5, 1)$ and for $\beta = 0.5$, $\beta = 1$, and $\beta = 2$.** Blue corresponds to an unstable equilibrium for the given parameter value and green corresponds to a stable equilibrium. The stability of the equilibrium is determined by finding the signs of the eigenvalues whose analytic expressions are given in equation 6.53, for each parameter value. If the real part of both eigenvalues are negative, then the equilibrium is stable; but if either eigenvalue has positive real part then the equilibrium is unstable.

most natural equilibrium point in the system, given by the point at which hostility levels are equally distributed over adversaries, a supercritical pitchfork bifurcation has been identified which can occur within a feasible region of the parameter space. It has been shown that this bifurcation is robust to asymmetric conflicts for scenarios represented by the four-dimensional model. In what follows, further robustness properties of the bifurcation are sought that serve to remove any suspicions of reliance on some of the limiting assumptions employed in this section. In particular, the model is considered with different distance metrics and in higher-dimensional scenarios.

6.4.3 Eight-dimensional scenarios

The supercritical pitchfork bifurcation identified in Section 6.4.2 may have existed as a consequence of the particular form of distance metric employed, or may have even been a result of the number of dimensions included in the model. In this section, an eight-dimensional model with $N = M = 4$ is considered with two distinct distance metrics, and the stability of the most natural equilibrium as system-wide aggression increases is investigated. Doubling the dimension of the model leads to a reduction in analytical tractability. As a consequence, numerical simulation of the model is used to explore the range of potential scenarios in what follows. Numerical simulations are employed using the Runge-Kutta method for temporal discretisation. It was found that step sizes of around 0.1 produced consistent simulation results which were in agreement with the analytical results presented in Sections 6.4.1 and 6.4.2.

The first metric proposed for studying the eight-dimensional system with $N = M = 4$ is a natural extension to the example studied in Section 6.4.2. It is assumed that, instead of adversaries being located across two distinct zones, they are instead located across 4 distinct zones. The metric $d : \mathcal{M} \times \mathcal{M} \to \mathbb{R}$ is defined analogously to Section 6.4.2, so that the distance within the same zone is negligible, whilst any two distinct zones are a significant distance from each other. The 4×4 matrix D given by $D_{jl} = d(\mathbf{x}_j, \mathbf{y}_l)$ is defined to be

$$D = \begin{pmatrix} 0 & 1 & 1 & 1 \\ 1 & 0 & 1 & 1 \\ 1 & 1 & 0 & 1 \\ 1 & 1 & 1 & 0 \end{pmatrix}, \tag{6.67}$$

and a corresponding spatial distribution of adversaries that might correspond to this matrix is shown in Figure 6.11. In Figure 6.11, the spatial arrangement of four distinct locations for each adversary (themselves distinguished by color) are shown, with the corresponding zonal structure that is used in this model. For a given adversary, each location has nearby to it another adversary with whom interaction will be strongest; but they also interact to a lesser extent with adversaries in neighbouring zones, according to the distance metric. Interactions across zones are set to occur with the same strength, regardless of whether zones share a portion of their boundary, or whether they meet in a single point.

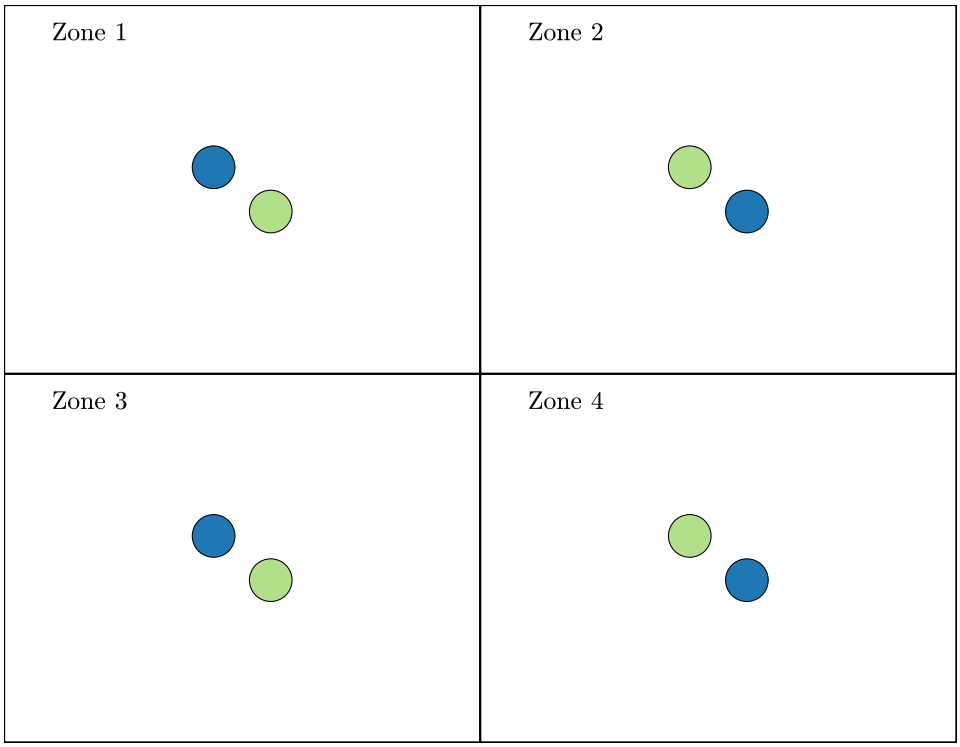

Figure 6.11: **A scenario corresponding to the distance metric as defined in equation 6.67.** Adversaries, who are distinguished by color, interact strongest with the adversary nearest to them in the same zone. Cross-zonal interactions occur with the same strength.

In Figure 6.12, the sum of the two solution curves for each adversary within each zone in Figure 6.11 for two different sets of parameter values are shown. Two sets of parameter values are chosen in order to demonstrate the evolution of the system under two distinct regimes. The first set of parameter values are chosen to correspond to a

scenario in which the level of aggression in the system, governed by the parameters ρ_1 and ρ_2, does not exceed some characteristic level of aggression, denoted by $\hat{\rho}$, which is used to approximate the bifurcation point. In this case, the sum of the solution curves, shown as the solid line, undergoes convergence to an equilibrium in which hostility levels are constant within each zone, and given by

$$p_j = \frac{1}{4}\frac{\rho_1\epsilon_2 + \epsilon_1}{1 - \rho_1\rho_2}, \qquad q_l = \frac{1}{4}\frac{\rho_2\epsilon_2 + \epsilon_2}{1 - \rho_1\rho_2},$$

for $j, l = 1, 2, 3, 4$, which are obtained from the aggregate equilibrium solution together with the finding that the equilibrium is constant across zones.

The second set of parameter values have been chosen so that the magnitude of aggression in the system exceeds this characteristic level of aggression $\hat{\rho}$. In this case, if the bifurcation identified in Section 6.4.2 also exists in higher dimensions, then the evenly distributed equilibrium would be unstable, and solution curves would move elsewhere. This is indeed what is observed: solution curves in zone 1 converge to a larger equilibrium value and solution curves in the other zones decrease to compensate for the increase in zone 1. In performing both numerical simulations, initial conditions in zone 1 were perturbed slightly to ensure the solution curves did not rest on the now unstable equilibrium in equation 6.68. The author believes that it is for this reason why hostility levels increase in zone 1, as opposed to any of the other zones.

Since the scenario defined by the distance metric in equation 6.67 can be thought of as a natural extension to the model investigated in Section 6.4.2, it might be the case that the bifurcation identified in Figure 6.12 arises because of the nature of the distance metric used. Next, a scenario is considered for a different distance metric, which is defined by the 4×4 matrix D where $D_{jl} = d(\mathbf{x}_j, \mathbf{y}_l)$, given by

$$d = \begin{pmatrix} 0 & 1 & 2 & 3 \\ 1 & 0 & 1 & 2 \\ 2 & 1 & 0 & 1 \\ 3 & 2 & 1 & 0 \end{pmatrix}. \tag{6.68}$$

This metric can be thought of as imposing a different spatial structure on the system. Since the distance between zone j and l is determined by $|j - l|$ for $j, l = 1, 2, 3, 4$, consecutive zones can be considered to be near to each other in space, and non-consecutive zones further apart. A scenario which this model may represent is depicted in Figure

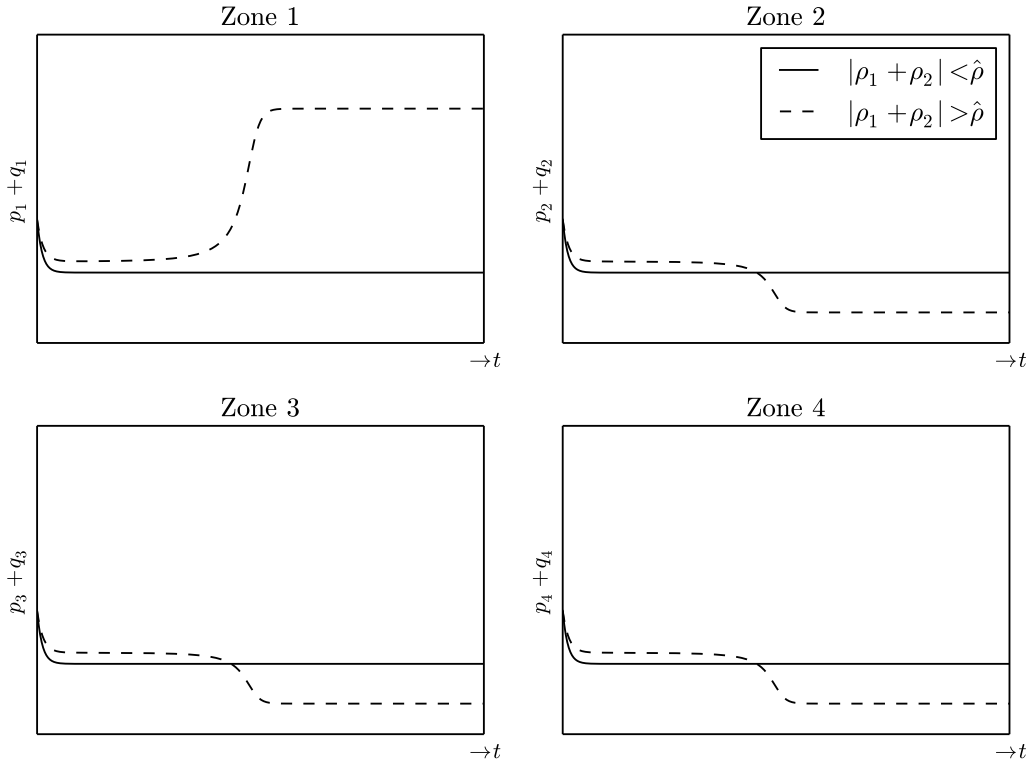

Figure 6.12: **The sum of the two solution curves in each zone for the spatial arrangement of zones as shown in Figure 6.11, for two different sets of parameter values.** The parameter values are chosen so that the magnitude of aggression in the system lies on either side of an approximate bifurcation point, denoted by $\hat{\rho}$. The parameter values used are, in the case of the solid line, $\rho_1 = 0.8$, $\rho_2 = 0.85$, $\epsilon_1 = \epsilon_2 = 0.4$, and $\beta = 1$; and in the case of the dashed line, $\rho_1 = 0.8$, $\rho_2 = 0.9$, $\epsilon_1 = \epsilon_2 = 0.4$ and $\beta = 1$.

6.13. Adversaries are supposed to interact strongest with the adversary located in the same zone, as specified by the zeros on the diagonal of the matrix in equation 6.68. In contrast to the previous example, adversaries in different zones now interact with different strengths. Neighbouring zones interact more strongly than non-neighbouring zones, leading to a more complex spatial structure than previously considered.

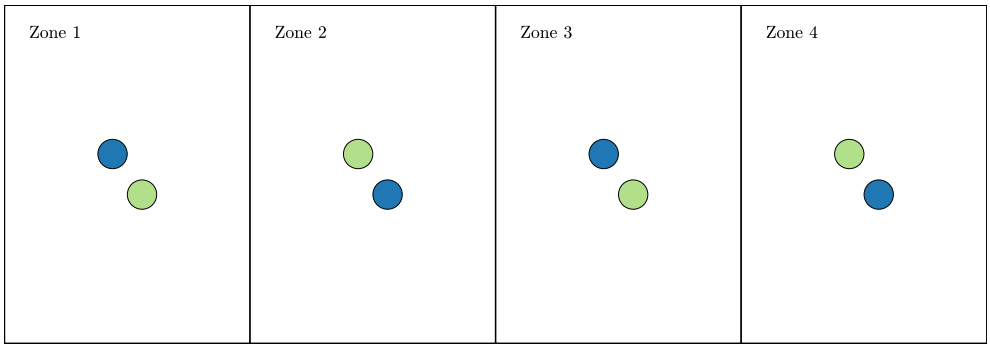

Figure 6.13: **A scenario corresponding to the distance metric as defined in equation 6.68.** Adversaries, who are distinguished by color, interact strongest with the adversary nearest to them in the same zone. Cross-zonal interactions occur according to the relative positions of the zones.

Figure 6.14 shows the sum of the two solution curves in each zone, for each of the four zones in the scenario in Figure 6.13, for two different sets of parameter values. Again, the parameter values have been chosen so that the total amount of aggression in the system, specified by the magnitude of the action-reaction terms ρ_1 and ρ_2, lie on either side of an approximate bifurcation point for this scenario, which is denoted by $\hat{\rho}$. For $|\rho_1 + \rho_2| < \hat{\rho}$, corresponding to the solid line in Figure 6.13, the system appears to converge to a natural equilibrium. According to the numerical solution with these parameter values, this equilibrium is given by

$$\begin{aligned} p_1 &= 0.21, & p_2 &= 0.25, & p_3 &= 0.25, & p_4 &= 0.21, \\ q_1 &= 0.20, & q_2 &= 0.23, & q_3 &= 0.23, & q_4 &= 0.20. \end{aligned}$$

In this case, the hostility levels are not equal across zones, since zones 2 and 3 experience higher levels of hostility. This is because the model is no longer symmetric. Furthermore, the relative values of the equilibrium emphasise the spatial structure of

the system, since zones 2 and 3 are the zones that closest to all other zones, and will therefore experience the greatest amount of interaction with other zones. The equilibrium brought about by the magnitude of aggression in the system being less than $\hat{\rho}$ is not the equilibrium that leads to equality of resulting hostility across zones, but represents a spatially-weighted equilibrium, in which zones that are closest to other zones are naturally assumed to contain higher levels of hostility than zones that are farther away.

The second set of parameter values used to generate the solution curves represented by the dashed curves in Figure 6.14 converge to an asymmetric solution. Since resulting hostility levels in zone 2 are much greater than hostility levels in zone 3, this equilibrium can be considered distinct from the spatially-weighted equilibrium to which the solid curve converges. This provides further support that the bifurcation identified in Section 6.4.2 exists not just in higher dimensions, but also for more general distance metrics and spatial distributions of adversaries. Similarly to the previous example, zone 1 is given perturbed initial conditions to avoid resting on any unstable equilibrium states. However, in this case, rather than zone 1 experiencing a dramatic increase in hostility levels, zone 2 is the one that increases. It is hypothesised that this is due to the more central location of zone 2 in comparison to zone 1.

This section has demonstrated the model's versatility in being applied to a range of potential spatial conflict scenarios. The two eight-dimensional models considered have both been shown to contain bifurcation-type behaviour for feasible parameter values, supporting the hypothesis that the bifurcation identified in Section 6.4.2 exists in higher dimensions, and in more general spaces. The second example used in this section, in which the spatial structure of the system is made asymmetric, has shown that the most natural equilibrium to which the system appears to converge for small values of ρ_1 and ρ_2, is not necessarily an equilibrium with equal hostility levels in each zone, as was the case for the first example. Instead, the model appears to converge to a spatially-weighted equilibrium, for which adversaries located closest to other adversaries have a higher resulting level of hostility. The fact that a spatially-weighted solution is an equilibrium confirms intuition regarding the evolution of spatial conflict: it is those areas nearest to an adversary that are likely to experience greater levels of conflict over long periods of time. The existence of the bifurcation, however, and the somewhat

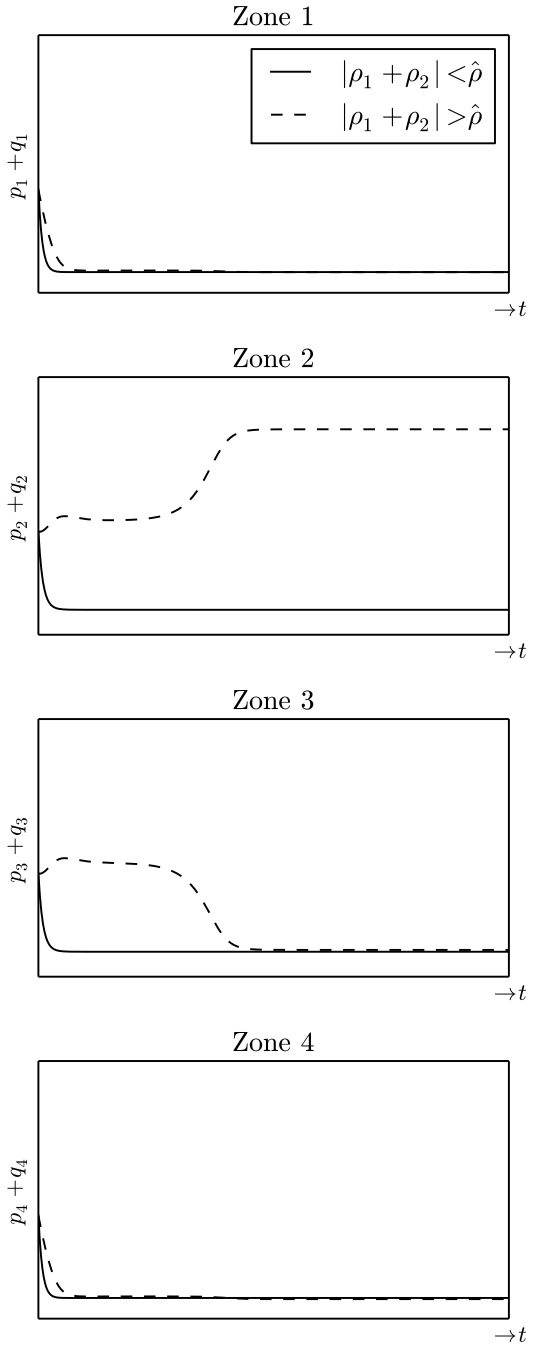

Figure 6.14: **The sum of the two solution curves in each zone for the spatial arrangement of zones as defined in equation 6.68, for two different parameter values.** Similarly to Figure 6.12, $\hat{\rho}$ represents an approximate bifurcation point and parameters are chosen so that the system lies on either side of this parameter value. The parameter values used are, for the solid line, $\rho_1 = 0.6$, $\rho_2 = 0.5$, $\epsilon_1 = \epsilon_2 = 0.4$ and $\beta = 1$; and, for the dashed line, $\rho_1 = 0.8$, $\rho_1 = 0.9$, $\epsilon_1 = \epsilon_2 = 0.4$, $\beta = 1$. The layout of the figures is chosen to reflect the linear spatial arrangement of zones in the model.

unpredictable nature of resulting solution curves after the bifurcation has taken place, is a counter-intuitive finding that is generalised further in the next section.

6.4.4 A randomly-generated large N-dimensional model

Conflicts can occur over large areas and involve a number of participants located in distinct locations. So far in this chapter, only scenarios involving up to four distinct participants on each side of the conflict have been considered. The model is now investigated in higher dimensions. This is done to emphasise that the model may be scaled up to consider conflict occurring over large spatial scales and involving many participants, as well as to determine whether the bifurcation identified in Sections 6.4.2 and 6.4.3 exists in a more general setting, and does not arise as a result of the particular form of the scenarios already considered. To this end, the model proposed in this section contains 100 dimensions, in which $N \neq M$, and in which a Euclidean distance metric is used that is distinct from the zonal approach to defining the metrics used in Section 6.4.3.

To specify the model, first set

$$\mathcal{M} = \left\{(x, y) \in \mathbb{R}^2 | 0 \leq x \leq 1,\, 0 \leq y \leq 1\right\},$$

so that adversaries are located within a unit square and define $d : \mathcal{M} \times \mathcal{M} \to \mathbb{R}$ to be the Euclidean distance metric. One hundred points in $\mathcal{M}$ are uniformly randomly generated and each point is uniformly randomly allocated to either one of two adversaries. Each point is assigned an initial hostility level equal to one.

A scenario is constructed from this random process, which obtains a realisation of a random spatial distribution of adversaries with $N = 46$ and $M = 54$. The parameter space is simplified by setting $\epsilon = \epsilon_1/N = \epsilon_2/M$ and $\rho_1 = \rho_2 = \rho$. In what follows, $\epsilon = 0.1$ and $\beta = 1$.

Solutions of the system in equation 6.30 are numerically solved using the Runge-Kutta method. According to these numerical simulations, for $\rho < 1$ there exists $\bar{t} > 0$ such that

$$|p_j(\bar{t} + \delta t) - p_j(\bar{t})| < 10^{-8}, \qquad |q_l(\bar{t} + \delta t) - q_l(\bar{t})| < 10^{-8}, \tag{6.69}$$

for $j = 1, 2, ..., N$ and $l = 1, 2, ..., M$, where $\delta t = 0.1$. It is therefore assumed that the system converges to an equilibrium in all cases of interest, and that this equilibrium is

given by the values of $p_j(\bar{t})$ and $q_l(\bar{t})$ for $j = 1, 2, ..., N$ and $l = 1, 2, ...M$, where $t = \bar{t}$ is the first value of t for which the condition in equation 6.69 holds.

The equilibria for two different values of ρ are shown in Figure 6.15. These figures depict the conflict scenario by plotting each location of each adversary as it is located on $\mathcal{M}$. The colour of each point is used to distinguish between each adversary, and the size of each point is proportional to the corresponding hostility level of each point at the equilibrium. In Figure 6.15 a), $\rho = 0.8$ and in Figure 6.15 b), $\rho = 0.9$.

Considering first Figure 6.15 a), and comparing the size of the resulting equilibrium near the boundary of $\mathcal{M}$ with those near the middle, it can be seen that the equilibrium is largest for locations towards the centre of the manifold, and therefore for locations that are, on average, closest to the locations of their adversary. This is consistent with the finding in Section 6.4.3, where it was suggested that the system converges to its most natural equilibrium, which is spatially weighted according to the locations of the adversaries.

Figure 6.15 b) shows another equilibrium; however, in this case, the resulting hostility levels of the overall system are largely concentrated within a very small proportion of the possible locations. In particular, the distribution of the equilibrium in Figure 6.15 b) appears to be very different from the spatially weighted equilibrium in Figure 6.15 a), suggesting that the spatially weighted equilibrium in Figure 6.15 a) may have become unstable between $\rho = 0.8$ and $\rho = 0.9$, and, therefore, that the bifurcation identified in Section 6.4.2 also exists in this system. Furthermore, although in Figure 6.15 b), the locations with the highest level of hostility are towards the centre of the manifold, it would be difficult to predict the locations with dramatically concentrated levels of hostility as ρ increases *a priori*, since there are many possible locations that might have experienced a similar increase in hostility. The system with $\rho = 0.9$ might be considered much more unpredictable and potentially dangerous than the system with $\rho = 0.8$, in which the hostility levels are more balanced over the possible locations.

In order to test whether the bifurcation exists for this more complex model, equilibria for different values of ρ are now compared. With increasing ρ, the most natural equilibrium to which the system converges, one which is spatially-weighted according to the locations of adversaries, is anticipated to become unstable for $\rho > \hat{\rho}$ for some value $\hat{\rho} < 1$, denoting the approximate proposed bifurcation point. When $\rho > \hat{\rho}$, the

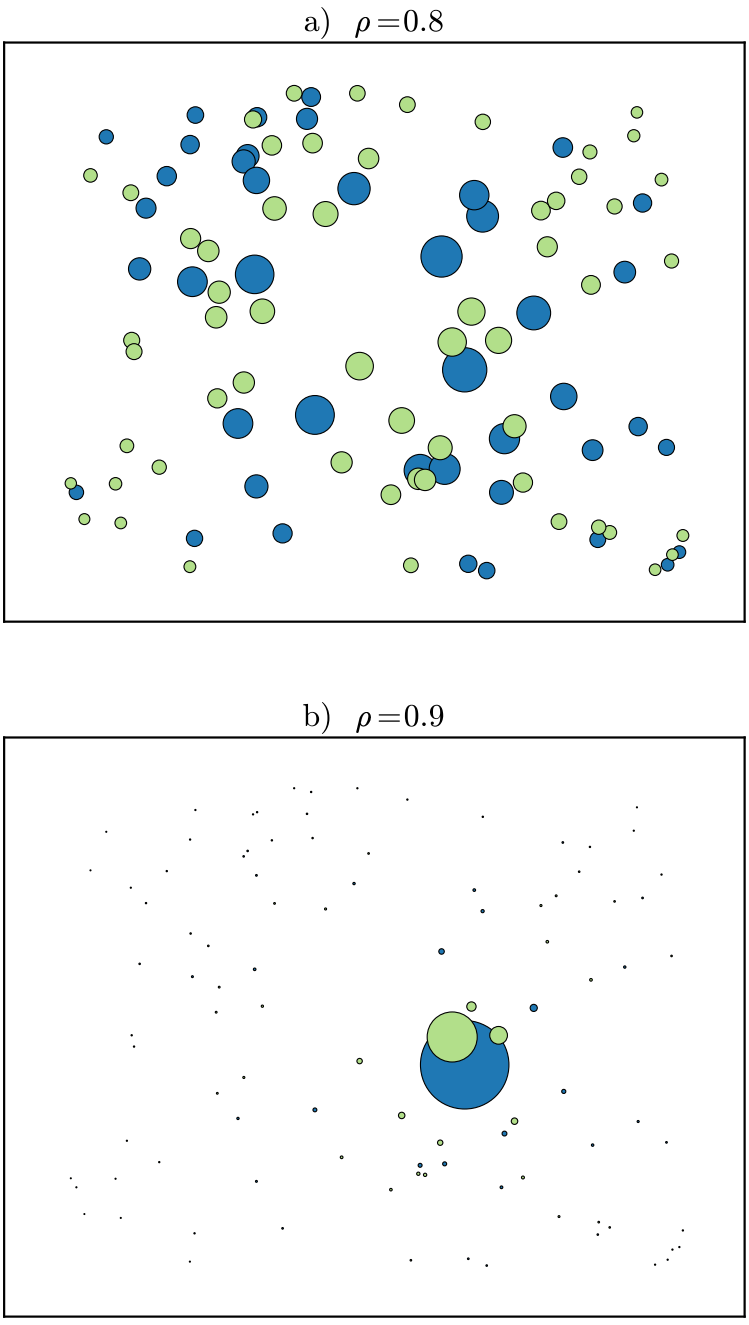

Figure 6.15: **The equilibrium of the system with a) $\rho = 0.8$ and b) $\rho = 0.9$.** The location of each point represents the location of the adversary on $\mathcal{M}$, the colours distinguish between each adversary at each location, and the size of the point is proportional to the corresponding equilibrium value at that point, as defined by the condition in equation 6.69.

system is anticipated to converge to an equilibrium in which the levels of hostility are highly concentrated in a few locations within the system. One way of measuring this is to consider the variance of the resulting hostility levels; however, the variance was found to vary with increasing values of ρ due to the changing equilibrium, and therefore would not have been able to identify the bifurcation.

Instead, for each adversary, the rank of each location according to their equilibrium value is considered. If the equilibrium is considered to be stable and spatially-balanced with increasing ρ, then the rank of each location would be expected to remain fairly consistent. However, if the equilibrium was to suddenly become highly concentrated in a small number of locations, then the ranks of the equilibrium values at each location would be expected to drastically change. This was the case for the scenarios in Section 6.4.3, for which the ranks were different before and after the bifurcation. Changing ranks corresponds to a form of instability in the system, since the dynamical equilibrium is both qualitatively and quantitatively being altered by a potentially small increase in parameter values.

The rank of location $\mathbf{x}_j$ is

$$\mathfrak{R}_j = \sum_{j'=1}^{N} \mathbf{1}\left(\bar{p}_{j'}(\rho) > \bar{p}_j(\rho)\right), \tag{6.70}$$

for $j = 1, 2, ..., N$, where $\bar{p}_j(\rho)$ denotes the value of the equilibrium at location $\mathbf{x}_j$, which is dependent on ρ, and $\mathbf{1}(.)$ is an indicator function, equal to one if the condition inside the brackets is satisfied, and equal to zero otherwise.

To determine the state of the equilibrium, the ranks of the system are compared for different values of ρ. For small values of $\delta\rho$, the function given by

$$f(\rho) = \frac{1}{2}\sum_{j=1}^{N} |\mathfrak{R}_j(\rho + \delta\rho) - \mathfrak{R}_j(\rho)|, \tag{6.71}$$

where $\mathfrak{R}_j(\rho)$ is given in equation 6.70, calculates the number of changes in the ranks of equilibria between ρ and $\rho + \delta\rho$. The resulting value is divided by two since any one permutation in the ranked list of equilibrium points requires swapping the positions of two locations.

Figure 6.16 plots the cumulative version of this function, given by

$$F(\rho) = \int_{\rho'=0}^{\rho} f(\rho')d\rho', \tag{6.72}$$

where $f(\rho')$ is given in equation 6.71, which tracks the number of rank changes in the equilibrium value as ρ increases from 0 to ρ for each value of $\rho < 1$. The plot shows a sudden transition between $\rho = 0.8$ and $\rho = 0.9$ during which a large number of rank changes occur. This value is consistent with previous approximations of the bifurcation point $\hat{\rho}$, and suggests that the bifurcation is indeed present in this high-dimenensional scenario, during which a more evenly distributed equilibrium suddenly loses stability and results in the concentration of hostility over a few distinct locations.

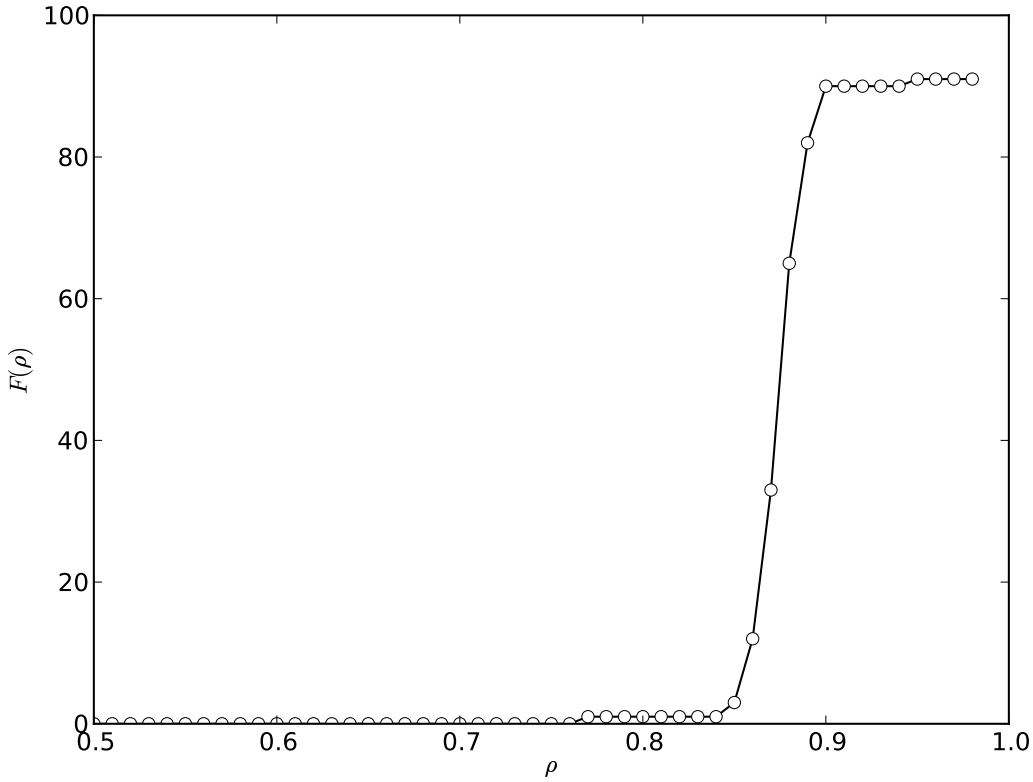

Figure 6.16: **The value of $\mathbf{F}(\boldsymbol{\rho})$, given in equation 6.72 for different values of $\boldsymbol{\rho}$, for the scenario depicted in Figure 6.15.** $F(\rho)$ is the cumulative number of rank changes in the resulting equilibrium values of the model, as ρ increases.

Evidence has been presented that the bifurcation identified in section 6.4.2 is robust to a variety of parameter values, dimensions and distance metrics. This is a significant result brought about by the spatial disaggregation of the system, and highlights the types of insights that can be obtained using non-linear dynamical systems analysis. In particular, according to the model, in spatially dependent systems with increasing aggression, a qualitative change in the spatial distribution of hostility levels would be

anticipated to be observed, before the entire system becomes unstable and an arms race is initiated (according to the original Richardson model). In what follows, the applicability of the model to real-world conflict scenarios, and the types of inferences about those systems that might be made, are discussed.

6.5 Discussion

In this chapter, a novel spatially explicit version of Richardson's conflict model has been derived and analysed using the tools of non-linear dynamical systems analysis. The motivation for introducing the model has been justified by identifying the need to incorporate space in deterministic models of conflict, whilst also noting limitations associated with other spatial models of conflict, many examples of which were described in Chapter 2. The model addresses some of these limitations by being discrete in space, and by providing explicit model assumptions, which are based on the principle of maximum entropy, together with the constraints introduced in equations 6.14, 6.17 and 6.18.

The model has been analysed using concepts of dynamical systems analysis that rely on the evolution of solution curves in phase space. Conditions for convergence to a natural equilibrium have been proposed, and this equilibrium has been described using a range of case studies. In particular, a supercritical pitchfork bifurcation has been identified that occurs as the magnitude of aggression in the system increases. The effect of this bifurcation requires interpretation in the context of real-world conflict scenarios.

Prior to the bifurcation, for low levels of aggression in the system, solution curves are expected to converge naturally to an equilibrium which is spatially weighted according to the relative locations of adversaries. For higher levels of aggression in the system, once the bifurcation has occurred, the spatially weighted equilibrium becomes unstable and the model converges to a new equilibrium in which hostility levels are highly concentrated within a few locations. Increasing the level of aggression in the system further can, as demonstrated in the analysis of Richardson's original model, lead to an unstable escalating arms race. The bifurcation hints at a potential early-warning system for real-world conflicts: with increasing aggression, before the system results in an arms race and hostility increases exponentially, some spatial instability is

expected and particular locations may suddenly experience disproportionate increases in hostility or conflict. If vulnerable locations can be identified prior to such increases in aggression, then policy interventions might seek to reduce tensions in those areas that are likely to experience this initial increase in hostility.

The potential insights that might be obtained from this model are greater than any of the other models considered in this thesis. The model not only enables forecasting of how a conflict might evolve, but also how a change in the intensity of the interactions might influence the resulting stability of the system. This opens up a more sophisticated range of policy applications. For instance, rather than just tracking the intensity with which two adversaries retaliate to one another, tracking the change in intensity might enable analysis of whether or not the system is close to a bifurcation point, such as the one identified in this chapter. Policy interventions might then be targeted at ensuring certain parameters do not vary into undesirable regimes of behaviour.

Any insights are, of course, reliant on the assumptions in the model providing a plausible account of the underlying mechanisms. In the same spirit as Richardson's original model, the model explored here can be used to investigate scenarios in which the actions of participants in the conflict are mechanistic, or if actors "did not stop to think" (Richardson, 1960b). Despite in many cases leading to models far removed from the real-world, deterministic modelling frameworks can demonstrate how complex behaviour might arise and are able to capture the consequences of certain well-defined scenarios.

There are limitations associated with the specific form of the bifurcation identified in the model. Supercritical pitchfork bifurcations are known to be structurally unstable, since a small change in the model specification often leads to a scenario in which there is no bifurcation. The normal form of the supercritical pitchfork bifurcation, together with a perturbed system is shown in Figure 6.17. For many real world systems, only structurally stable results are generally observed, due to underlying noise. Nevertheless, the identification of the bifurcation is an important one. Even when the system has been perturbed, and there is no bifurcation, there is still the introduction of new stationary solutions in the system. In addition, the stationary solution on which the system is located may also drastically change, as shown on the right hand side of Figure 6.17. The bifurcation identified acts as a special case. Given uncertainty surrounding the

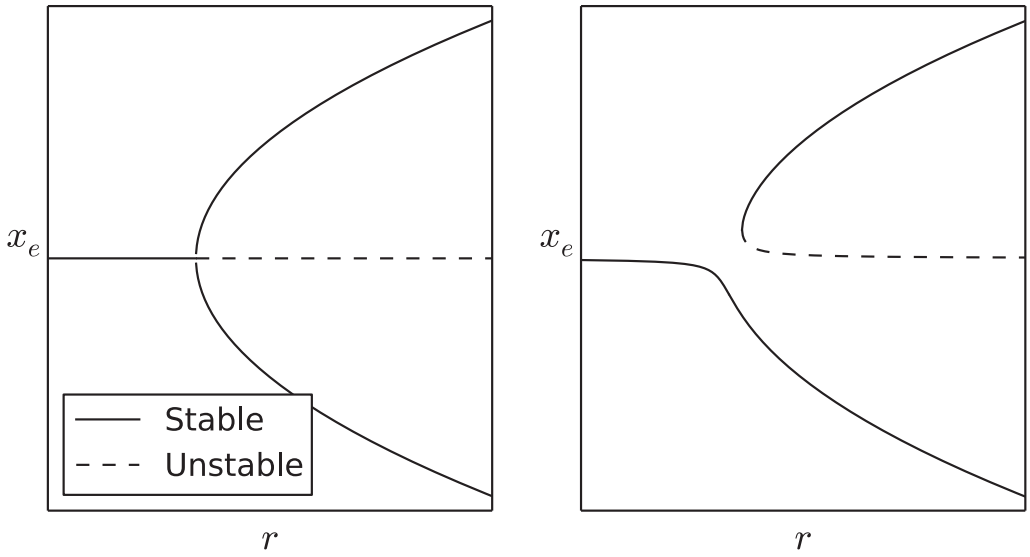

Figure 6.17: **Normal form of the supercritical pitchfork bifurcation (left hand side) and its perturbation (right hand side).** The values of x_e plotted are the equilibria in each case. The parameter r is the bifurcation parameter.

noise providing the perturbation, it is likely to be unclear *a priori* which of the possible resulting solution curves will be the one that the system takes.

Finally, although demonstrating how the inclusion of space in models of civil violence can lead to richer behaviour, the derivation and analysis of the model in this chapter has been approached from a more abstract and general perspective than any of the other models considered in this thesis. This enables the model to be potentially applicable over a wide range of examples. Furthermore, it also demonstrates the mathematical insights that deterministic models can sometimes afford, and emphasises, in particular, the complications that the inclusion of spatial dependencies in such models can sometimes have. As this chapter has highlighted, the insights obtained from deterministic models are sometimes more qualitative than quantitative, and can force the researcher to consider not only what is happening, but what might happen should the underlying mechanisms be altered. This will be discussed further in the conclusion chapter that follows.

Chapter 7

Conclusions and discussion

7.1 Comparison of modelling frameworks

This thesis has employed different frameworks to model civil violence in space and time. Four frameworks have been presented: data-driven approaches that exploit aggregate statistics from the empirical data and combine basic assumptions to construct null models against which the data can be compared; a statistical model of discrete spatial choice, which uses attributes of targets to quantify criminological theory; point process models that explicitly account for event interdependency to obtain some degree of predictive power; and a spatially-explicit differential equation-based model, which extends a well-studied non-spatial model of conflict escalation. Each framework has a different perspective of the real-world phenomenon considered. In this section, these different frameworks are summarised and a comparison is made with respect to the types of insights that can be obtained. It is argued that a plurality of modelling frameworks applied to any given problem can lead to increased trust in the way models are used in a policy setting. Furthermore, a plurality of model frameworks can greatly improve the accuracy of inferences about the real-world.

Data-driven frameworks, such as those presented in Chapter 3, are exploratory since they can be used to gain understanding into the principal features of a dataset. In some cases, sophisticated insights are obtained by constructing null models with relatively high levels of complexity. This was done in Chapter 3 by proposing a null model for the geographic independence of events to explore the localised patterns of diffusion during rioting.

Such approaches can lead to robust findings for a particular dataset but have two principal limitations. The first is concerned with data availability. Although an increasing amount of data on civil violence has become available, particularly of a spatial nature (Gleditsch and Weidmann, 2012), data-driven frameworks require a significant amount of accurate data at an appropriate level of aggregation to produce meaningful insights. In many cases, available data provides only a partial view, or is not supplied at the desired level of accuracy and precision (Weidmann, 2015). A reliance on available empirical data leads to insights that are specific to the particular case study considered. This means, on the one hand, that some insights may not be generalised to other case studies, but, on the other, ensures that the insights are closely related to the scenario of interest and have relatively high levels of confidence. The second limitation associated

with data-driven approaches is that they are typically unable to incorporate mechanisms that may be responsible for the generation of the event data. As a consequence, they are often unsuitable for investigating theories or testing our understanding of a given phenomenon.

The strength of data-driven frameworks is that they can be used to identify prominent features of an empirical dataset, which may lead to further analyses and models. In Chapter 4, insights from the data-driven analysis of the London riots inspired a model of target choice by suggesting that environmental features and contagion were likely to play prominent roles in the decision-making of offenders.

Statistical regression modelling is also specific to the scenario considered. In contrast to data-driven approaches, the objective of statistical regression models is to capture some mechanism in the underlying data-generating process. This is achieved by using sample data to determine whether variables associated with this mechanism covary with the empirical data in the expected direction. This in turn invites insights into the proposed mechanisms corresponding to those variables. Data-driven models might be preferred over statistical regression models if there are no preconceptions or pre-existing theories that might explain the phenomenon. They might also be preferred if statistical regression models produce no significant insights.

In Chapter 4, a discrete choice model was used to investigate rioter target choice with respect to three key theories from the criminological and social science literature. Evidence was provided that all three of those theories can be used to explain at least some of the variance in rioter target choice, and, moreover, that rioter target choice was consistent with arguments based on the bounded rationality of rioters. The proposed mechanisms, which were quantified via this model, were used as the data generating process in a microsimulation model. The model generated simulated riot scenarios, given the location and times at which rioters were known to have offended. Although this model relied on empirical data to inform its initialisation, it was argued that it could form a component in a policy tool by modelling the resulting spatial distribution of the riots and considering how best to formulate police deployment strategies based on this output. In proposing specific and quantifiable mechanisms for the way in which the decision-making of rioters leads to the spatial patterns observed, the model is transformed into a predictive tool that can be considered in the context of different scenarios.

It should be borne in mind, however, that the model is calibrated on data specific to the London riots. Out of sample testing of the model is not performed due to a lack of data on other riot scenarios.

Stochastic point processes consider the timings and, in some cases, the locations of event occurrence. In Chapter 5, a series of such models are applied to the Naxal insurgency. A number of models are proposed and are used to evaluate hypotheses regarding the spatial and temporal distribution of the insurgency. These models are notable in that they depend only on the history of the system and consist of relatively simple proposed mechanisms for how events spread in space and time. Although it is possible to incorporate a range of structural covariates into such models (Zammit-Mangion et al., 2012), it is demonstrated in Chapter 5 how, by incorporating just the history of the process in a mathematically sophisticated but relatively parsimonious model, some predictive power can be obtained in an out of sample test. Point process models are naturally prospective and, as such, can often be usefully employed as predictive models to determine the likely locations and timings of future events (Mohler et al., 2011). Such information would be invaluable in designing targeted interventions aimed at reducing insurgent violence. Since the models are stochastic, they explicitly account for uncertainty, which may lead to more confidence in their output when decisions are to be made in the context of uncertainty.

Insurgencies can change dramatically over their life course. In the case of the models presented in Chapter 5, the performance of the model for Naxal events did not seem to be affected by the long duration of the study period. This was shown by demonstrating that the residual process, containing events that were poorly predicted by the model, was very close to a Poisson process for the entire study period. This may not be the case in other scenarios. If underlying mechanisms were to qualitatively change during an insurgency, then the predictive performance of the model may be diminished. Some studies have attempted to account for a change in the underlying mechanisms of insurgency by altering the model when the empirical data suggest the insurgency may be in a different dynamical regime (Lewis et al., 2011).

Although stochastic models explicitly account for uncertainty, deterministic models may still generate useful insights as a result of their analytical tractability. This is demonstrated by the long history of such models being applied to problems relating to

conflict and violence. For these models, the emphasis is less on the prediction of future events and more on determining the implications of a specific mechanism by which the system is thought to evolve.

In Chapter 6, the Richardson model of conflict escalation is considered. This model specifies a deterministic mechanism in which two actors increase their levels of hostility towards one another but are restrained by internal processes. Policy relevant implications of the hypothesised relationship between the two adversaries can be obtained from the original Richardson model. It was shown, for instance, that an arms race can occur when two nations act in their own self-interest and when their reaction to their adversary outweighs the effect that might be restraining them from more internal processes. Although the policy-relevant insights that can be obtained from simplified models are often confirmation of common sense, it can still be useful to articulate them in a mathematical formulation. Richardson (1960a) eloquently explains why this is the case, emphasising the benefits associated with deterministic models, whilst also providing a word of caution when employing models that are inevitably simplified from the real-world process:

> "To have to translate one's verbal statements into mathematical formulae compels one carefully to scrutinize the ideas therein expressed. Next the possession of formulae makes it much easier to deduce the consequences. In this way absurd implications, which might have passed unnoticed in a verbal statement, are brought clearly into view and stimulate one to amend the formula. An additional advantage of a mathematical mode of expression is its brevity, which greatly diminishes the labour of memorizing the idea expressed. If the statements of an individual become the subject of a controversy, this definiteness and brevity lead to a speeding up of discussions over disputable points, so that obscurities can be cleared away, errors refuted and truth found and expressed more quickly than they could have been, had a more cumbrous method of discussion been pursued. Mathematical expressions have, however, their special tendencies to pervert thought: the definiteness may be spurious, existing in the equations but not in the phenomena to be described; and the brevity may be due to the omission of the more important things, simply because they cannot be

> mathematized. Against these faults we must constantly be on our guard. It will probably be impossible to avoid them entirely, and so they ought to be realized and admitted."

More complex deterministic models can lead to more intricate insights. For instance, in Chapter 6, by constructing a spatially disaggregated version of the model, a bifurcation is identified that indicates a loss of system stability as hostility increases. This occurs prior to the loss of global stability in the aggregated system, suggesting a potential means of detecting the onset of an escalation process. This study emphasises the advantages that analytically tractable deterministic models have over their stochastic counterparts. Their relative mathematical simplicity enables the exploration of the model over a wide range of potential regimes, and not just the regime within which the real-world system is thought to be located. By considering how the system might qualitatively change (for instance, by undergoing a bifurcation), such approaches can lead to high levels of insight. Policy interventions may also be formulated that seek to constrain the system within a viable region of the phase space (a concept explored further in Deffuant and Gilbert (2011)).

Deterministic differential equations rely on the proposed mechanism in the model being the actual mechanism that drives behaviour in the phenomenon of interest. In many cases, the assumptions are highly simplified and there is likely to be noise and uncertainty in translating the implications of the analysis into the real world. As a consequence, the plausibility of such insights are sometimes treated with more skepticism than approaches that rely more on empirical data. The modelling assumptions must be carefully considered when acting on any insights obtained from such models. If communicating the results of such a model to a policy-maker, this means that the articulation of these assumptions becomes a crucial component in how the model might be used to aid policy-making.

The mathematical form of the Hawkes mutually-exciting point process model in equation 5.18 and the linear Richardson in equation 6.1 enables a analytical comparison to be made between the two models. Recall that, for the mutually exciting point process model, whose conditional intensity function is given by

$$\lambda^{(l)} = \mu_l + \sum_{\substack{t_i<t \\ m_i=1}} \alpha_{l1}\omega_l e^{-\omega_l(t-t_i)} + \sum_{\substack{t_i<t \\ m_i=2}} \alpha_{l2}\omega_l e^{-\omega_l(t-t_i)}, \tag{7.1}$$

for different types of event $l = 1, 2$, the long term expected value of the intensity in the case of a stationary process is given by the vector

$$(I_2 - A)^{-1}\boldsymbol{\mu}, \tag{7.2}$$

where I_2 is the 2-dimensional identity matrix, $A = (\alpha_{ll'})_{l,l'=1,2}$ is a matrix composed of the self- and mutual-excitation terms and $\boldsymbol{\mu} = (\mu^{(1)}, \mu^{(2)})$ is a vector consisting of the background rates for each process. Thus, for a long-term stationary process,

$$\begin{aligned} \mathbb{E}\left(\lambda^{(1)}\right) &= \frac{(1-\alpha_{22})\mu_1 + \alpha_{12}\mu_2}{(1-\alpha_{11})(1-\alpha_{22}) - \alpha_{12}\alpha_{21}}, \\ \mathbb{E}\left(\lambda^{(2)}\right) &= \frac{\alpha_{21}\mu_1 + (1-\alpha_{11})\mu_2}{(1-\alpha_{11})(1-\alpha_{22}) - \alpha_{12}\alpha_{21}}. \end{aligned} \tag{7.3}$$

Considering the analysis of the Richardson model in Chapter 6, the equilibrium of the original Richardson model in equation 6.1 in the case $\rho_1\rho_2 \neq \sigma_1\sigma_2$, was shown to be

$$p_e = \frac{\sigma_2\epsilon_1 + \rho_1\epsilon_2}{\sigma_1\sigma_2 - \rho_1\rho_2}, \qquad q_e = \frac{\sigma_1\epsilon_2 + \rho_2\epsilon_1}{\sigma_1\sigma_2 - \rho_1\rho_2}. \tag{7.4}$$

The form of equation 7.3 and equation 7.4 suggests an analytical comparison might be made between the two modelling frameworks. Specifically, assuming that the resulting expected intensity of a stationary point process is equivalent to the equilibrium of the Richardson model, and that the grievance terms in the Richardson model may be interpreted as the background rate in the Hawkes process (so that $\mu_1 = \epsilon_1$ and $\mu_2 = \epsilon_2$), the following relationships can be obtained:

$$\begin{aligned} 1 - \alpha_{11} = \sigma_1, \qquad & 1 - \alpha_{22} = \sigma_2 \\ \alpha_{12} = \rho_1, \qquad & \alpha_{21} = \rho_2. \end{aligned} \tag{7.5}$$

This implies that the self-excitation of a Hawkes process corresponds to one minus the inhibition parameter in the Richardson model, whilst a mutual-excitation is directly equivalent to the action-reaction parameter of the model. This means that the parameter estimates of Model 4 in Chapter 5, corresponding to the system in equation 5.18, can be considered in the context of the Richardson framework. In particular, the point estimates of the Richardson parameter values for the Naxal system are given by

$$\sigma_1 = 0.1296 \qquad \sigma_2 = 0.6192 \tag{7.6}$$

$$\rho_1 = 0.3766 \qquad \rho_2 = 0.0842. \tag{7.7}$$

These values suggest that the Naxal conflict has a stable node in the Richardson system. The value $\rho_1\rho_2/\sigma_1\sigma_2 = 0.3953$ compares the magnitude of aggression in the system against the magnitude of inhibition, and gives some indication of the distance between the estimated system and the bifurcation identified in Chapter 6. In Chapter 6, the bifurcation was observed to occur when values of this ratio were around 0.8. It therefore appears as though the Naxal system is located a significant distance from this bifurcation and is not at risk of the onset of spatial instability.

Comparing the initial data-driven approaches of Chapter 3 with the final model investigated in Chapter 6 emphasises the range of model frameworks that might be employed to investigate civil violence. The spectrum introduced in Chapter 1 is reproduced in Figure 7.1, this time including positions of each framework used in this thesis. In Chapter 3, the models were grounded in reality, leading to a high degree of confidence in their plausibility, but the insights that could be obtained, particularly with regards to mechanisms that might be at play and the predictive nature of the modelling, were limited. In Chapter 6, proposed mechanisms were explored without any empirical data informing the model development, leading to wide-ranging potential insights but, at the same time, leading to complications with respect to how the model might be translated into the real world.

The modelling frameworks explored in Chapter 4 and Chapter 5 can be thought to lie somewhere in between these two extremes since they both investigate the mechanisms of the phenomenon studied but also incorporate empirical data into the modelling process. In Chapter 4, the model tested a range of covariates inspired by theories regarding offender behaviour, whereas in Chapter 5, the models were driven by patterns of spatio-temporal dependency in the empirical data. Although both approaches used empirical data, they did so in different ways. The modelling objective in Chapter 4 was more concerned with the explanation of the phenomenon and its structural covariates, rather than evaluating the level of prediction that can be obtained by explicitly modelling event interdependency, as was the case in Chapter 5. It is interesting to compare the relative levels of success in terms of prediction of the model in Chapter 4, in which it was examined whether a microsimulation model that utilised the results of the regression model was able to reproduce the general patterns in the data, with the predictive ability of the point process in Chapter 5, where only relatively basic theories

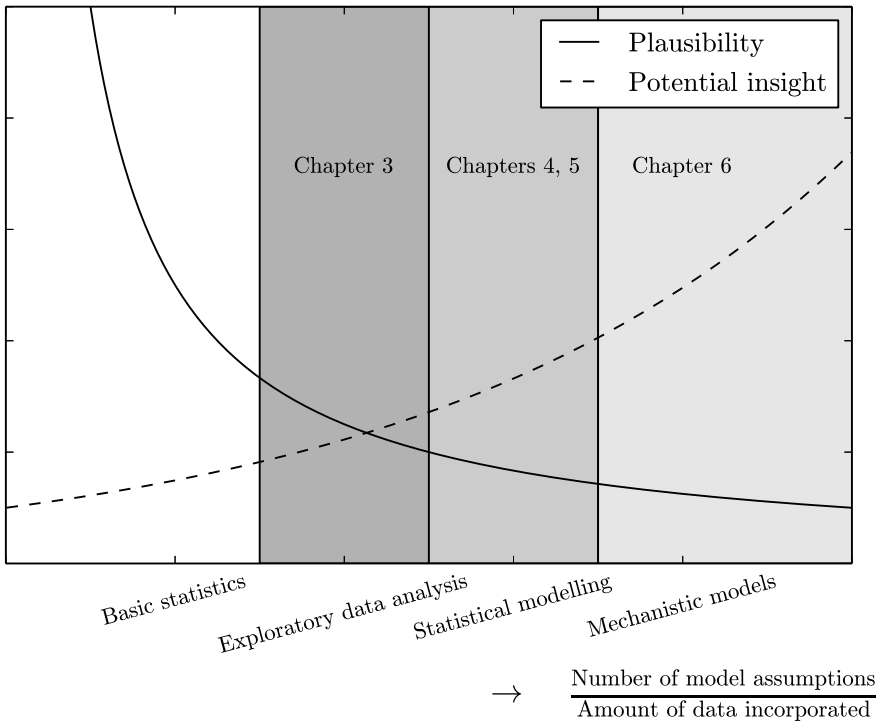

Figure 7.1: **Potential insight and plausibility of different modelling frameworks.** The frameworks considered in this thesis are placed along a spectrum broadly defined by a ratio given by the number of model assumptions that remove each approach from the real world, to the extent to which empirical data forms part of the model development.

concerning the generation of insurgent violence were used to construct models. In particular, although a more extensive amount of structural data was employed, a number of notable discrepancies were found between the model outputs in Chapter 4 and the patterns in the sample data. In contrast, in Chapter 5, a surprising level of predictive ability was obtained with relatively small amounts of data. This raises questions as to the appropriate balance between explanation and prediction in models of civil violence. Understanding the salience of different theories can be extremely useful when developing broader policies, which might seek more longer term strategies for reducing civil violence. Prediction of events might be more useful when designing more targeted interventions.

This serves to highlight that, in any modelling task, an appropriate choice of framework is required. If, on the one hand, the modelling task is specific and well-defined (e.g. to assess a range of proposed policy options) and if there is data available, then more empirical approaches may be preferred. On the other hand, if the objective for modelling is to consider how a range of proposed mechanisms might correspond to the underlying data generating processes, then the appropriate framework may lie towards the right hand side of the spectrum in Figure 7.1.

More generally, this thesis has demonstrated that model frameworks across this spectrum can be usefully employed to gain insights into the spatio-temporal dependencies of civil violence. Furthermore, the range of models and their respective frameworks have an associated range of advantages and disadvantages, which have been discussed in this section. The range of insights that can be obtained from each of them varies with respect to their generality, their accuracy, and their usefulness for aiding the design of policy interventions. Since no single modelling framework can be shown to dominate any of the others with respect to the advantages associated with it, this thesis concludes that each has a part to play, and that a plurality of modelling approaches can be used to gain a more rounded perspective of the phenomena considered.

7.2 Topics for further research

There are a number of opportunities for extensions to the work presented in this thesis. It has been demonstrated that it is important to consider the strengths and limitations of different modelling frameworks when investigating the spatio-temporal dependencies

of civil violence. Furthermore, this thesis has concluded by suggesting that, rather than using a single modelling framework to consider policy questions, a number of frameworks might be used to obtain a more rounded view of the important features of the problem, and to consider the range of mechanisms that might be at play. The same is likely to be true of other problems encountered in policy. A unified approach to identifying suitable modelling frameworks for different types of policy problems would be a valuable guide to applying models in a policy setting. To achieve this, new methods for comparing different modelling approaches, particularly concerning the tradeoff between potential insight against plausibility, as proposed by Figure 7.1, might be required.

In addition, once a range of plausible models have been constructed, each using different frameworks, and each obtaining complementary perspectives, there remains the challenge of how insights can be usefully incorporated into the policy-making process. Conveying model outcomes to policy-makers typically requires relatively short presentations at which the modeller is required to present concise insights with associated levels of uncertainty. At present, consolidating the evidence for policy-making that might be obtained from different model frameworks is a research challenge that is yet to be overcome in many fields (reports from the Intergovernmental Panel on Climate Change is one example where some success has been achieved in this regard (IPCC, 2013)).

Within each of the model frameworks presented in this thesis, there are a number of avenues for future research. Focusing first on exploratory data-driven modelling, as employed in Chapter 3, further research might consider the how the binary approach to geographic diffusion of events presented in this thesis might be used in different scenarios. If the patterns of offending observed during the London riots can also be observed during other outbreaks of rioting, both within the UK and in different countries around the world, then it can be assessed whether or not the patterns correspond to some inherent property of rioting, or whether they are dependent on the underlying geography or the underlying motivation for the riots. Comparing the patterns across different types of civil violence may also yield useful insights.

Extensions to the analysis might consider different patterns of diffusion by changing the geographic neighbourhood of the focal cells into which events may spread. In

addition, further advances might be made by optimising the randomisation procedure that permutes the spatial and temporal units in which events occur. For instance, in the proposed algorithm, Chebyshev's inequality was used for its generality but is known to often provide suboptimal criteria for many underlying distributions. A more nuanced stopping criteria might lead to more computational efficiency. Additionally, the problem of estimating binary contingency tables might also be improved by considering other approaches to this problem, some of which employ Markov Chain Monte Carlo methods (Besag and Clifford, 1989; Bezáková et al., 2007; Verhelst, 2008; Blanchet and Stauffer, 2013).

The discrete choice analysis of target selection during rioting, as presented in Chapter 4, would also benefit by applying the analysis to different examples of civil unrest around the globe. Consistent findings were found in a recent cross-national analysis of target choice by burglars (Townsley et al., 2015) and, in addition, a recent study has compared the consistency of target selection across different crime types (Johnson and Summers, 2015). If the same findings regarding rioter target choice can be found in different examples of civil unrest, then the resulting simulation models that were described in Chapter 4 might be more likely to provide plausible insights.

Although the microsimulation model of rioter target choice in Chapter 4 was able to reproduce the broad patterns of the distribution of rioting, there were discrepancies observed between the model and the empirical data. There was two principal sources of discrepancy which might form the basis of future research. First, the empirical data appeared to be much more spatially clustered than the resulting spatial distribution arising from the microsimulation model. This may have arisen due to the averaging procedure employed to obtain model outputs. Averaging across different realisations of the simulation was required since the model was a result of a series of random choices, and therefore a single realisation would not have led to a fair assessment. Methods to compare the model outputs with the empirical data without the use of this averaging procedure may lead to insights that alleviate this limitation. The second discrepancy was that a number of areas were predicted to have been selected as targets in the model but did not appear as targets in the empirical data. It was observed, for instance, that the risk of rioting in one of these areas may have been increased due to the presence of a high number of schools. Refining the variables used to explain the impact of crime

pattern theory might lead to more successful predictive models of target choice.

The microsimulation model of rioter target choice in Chapter 4 might also be expanded upon. One way of doing this is to consider a mixed logit model of discrete choice in which the selection of model parameters are correlated over decision-makers (Train, 2003). Further theories regarding the underlying mechanisms of the riots might also be incorporated. For example, the Riots Communities and Victims Panel (2011) separated the UK rioters into four different profiles: "Organised criminals", who were first to the scene and who set off a 'chain reaction'; "Violent aggressors", who committed the most serious crimes; "Late night shoppers", who deliberately travelled to different sites for looting; and "Opportunists" who were drawn into riots and encouraged to engage as a result of situational precipitators. Disaggregating a spatial choice model so that each decision-maker is categorised as one of these four types of offender might lead to further insights and a more accurate microsimulation or agent-based model. In addition, the inclusion of a dynamic mechanism of target choice based on the actions of police might open the model up to being used to explore public order policing strategies.

Considering Chapter 5, similar models of stochastic point processes have been shown to produce useful predictions regarding the onset and occurrence of conflict and crime (Zammit-Mangion et al., 2012; Mohler, 2014). Even with a relatively parsimonious model such as the one presented in this thesis, an out of sample test demonstrated some predictive power associated with the model. Further work might consider improving these predictions by incorporating a range of structural covariates that might also be thought to influence the onset of violent events in a similar way to the model of target choice in Chapter 4. These covariates might be informed by a range of spatial regression models that were discussed in Chapter 2 and which have examined the predictive capability of various socio-economic, demographic, and geographical variables associated with insurgent and civil violence.

In Chapter 6, the spatially-explicit deterministic model of conflict was explored within a relatively restricted region of the phase space. Specifically, it was the geographically weighted equilibrium that was stable for low levels of aggression in the system, and the deviation from this equilibrium as the level of aggression in the system increased that was explored. Since the model is nonlinear, a number of other trajec-

tories are possible. The analysis was also not extensive with respect to the range of parameters considered. Further research might do more to comprehensively explore the parameter space.

Another avenue for further research is the application of the model in Chapter 6 to real-world scenarios. Calibrating the model against empirical data might determine where the real-world system lies in the phase space, and therefore might indicate whether the system is near to an undesirable bifurcation. A clue for model calibration that explicitly accounts for some of the uncertainty in the model might come from the relationship between Richardson's model and Hawkes' mutual-exciting point process model, as outlined in section 7.1. Stochastic spatially-explicit models that account for spatial dependencies in the same way as the deterministic model in Chapter 6 might provide useful predictive models, whilst, at the same time, be of a form that can be analytically interrogated in order determine bifurcations and other instabilities that might arise if the system changes. The development of a "best of both worlds" modelling framework, based on stochastic differential equations, might lead to a framework that can be useful in designing policy interventions.

7.3 Concluding remarks

Four modelling frameworks have been utilised to construct models of civil violence. For each of these frameworks, contributions to the literature have been made with regards to how civil violence is modelled in space and time. To conclude, the main contributions of the thesis are now summarised.

A novel data-driven exploratory approach for analysing local patterns of diffusion was proposed and applied to the 2011 London riots. The Monte-Carlo model against which the empirical data is compared against is an extension on the state of the art (Cohen and Tita, 1999; Rey et al., 2011; Schutte and Weidmann, 2011) and enables the exploration of empirical data in which the geographic scope of the violence is of interest, rather than its intensity. This is particularly useful for rioting, which exhibits high levels of spatial and temporal clustering, and distinctive patterns of geographic diffusion in the 2011 London riots were found and discussed.

It was argued how analysis of the geographic diffusion of rioting can be used to consider some of the behaviours of the rioters. Specifically, it was argued that three

types of behaviours were occurring – rioters were influenced by their surroundings, which they utilised for the acquisition of high-value goods; rioters were influenced by those around them, who, by engaging in the riots, prompted, permitted, pressured and provoked those around them to engage similarly; and rioters were influenced by the presence and behaviours of the police.

With a desire to seek out more mechanistic approaches, a discrete spatial choice model of rioter target choice was next proposed, in which, criminological theories were used to construct proposed covariates. Regressing the discrete choice model against these variables led to the evaluation of a series of hypotheses regarding the underlying mechanisms associated with target choice. This is a novel contribution to the literature, since it uses a model not previously employed to study riots to a particular component of rioting that has seen recent calls for further research (Wilkinson, 2009). It was demonstrated how such a model might also be incorporated into a computational tool to plan police resources.

The behaviour of the police was not incorporated into the model of rioter target choice due to a lack of sufficient data on their locations and strategies. Inspired by the need to more closely investigate the interactions of adversaries, the example of the Naxal insurgency was considered, using data that distinguished between actions of insurgents and police. To do this, a modelling framework was employed that has previously been shown to provide significant predictive power (Zammit-Mangion et al., 2012; Mohler, 2014). A series of novel multivariate and, in some cases, nonlinear point process models were proposed for the rate at which events associated with the Naxal insurgency occur. The calibration of these models highlighted certain features of the conflict, such as the strong local influence from prior events, and the ability for self-excitation, rather than mutual excitation, to explain a large amount of the variance in the data. The model was assessed with regards to its predictive power. As others have pointed out, the predictive power of statistical models has had insufficient attention in the literature. In particular, Ward et al. (2010) argue that many statistical models associated with the study of conflict include many covariates that do little to improve predictive performance. The study presented in this thesis provides further support that more sophisticated mathematical models, although somewhat parsimonious with regards to the amount of data used, might be usefully employed in a predictive modelling

framework.

Many traditional models for the interaction between adversaries use deterministic differential equations to articulate proposed mechanisms. From these models, the logical implications of those hypotheses can be deduced. In Chapter 6, an entropy-maximisation approach to spatial disaggregation of the Richardson model of conflict escalation resulted in a novel model that was explored from a nonlinear dynamical systems perspective. A bifurcation was identified that came about as a result of considering space in this way, which may indicate the onset of undesirable escalation processes between two adversaries.

In addition to these specific advances, this thesis has demonstrated that there are a wide range of frameworks that might be employed to model civil violence in space and time. In much prior literature, models are often proposed without due justification of the framework employed. Careful consideration of the type of framework used is crucial if the insights obtained from such models are to be useful in designing successful policy interventions. In addition, the different perspectives obtained from different modelling frameworks might all contribute to a given policy decision and so a plurality of modelling approaches, consolidated in a way in which their insights can be usefully conveyed to a policy-maker, is likely to lead to a more comprehensive view of the problem and its potential solutions.

Bibliography

Abudu, M. J., Raine, W. J., Burbeck, S. L., and Davison, K. K. 1972. Black ghetto violence: A case study inquiry into the spatial pattern of four Los Angeles riot event-types. *Social Problems*, 19(3):408–426.

Abudu Stark, M. J., Raine, W. J., Burbeck, S. L., Keith, K., and Davison, K. K. 1974. Some empirical patterns in a riot process. *American Sociological Review*, 39(6): 865–876.

Agresti, A. and Agresti, B. F. 1978. Statistical analysis of qualitative variation. In Schuessler, K. F., editor, *Sociological Methodology*. Jossey-Bass, San Francisco, CA.

Aguirre, B. E., El-Tawil, S., Best, E., Gill, K. B., and Fedorov, V. 2011. Contributions of social science to agent-based models of building evacuation. *Contemporary Social Science: Journal of the Academy of Social Sciences*, 6(3):415–432.

Ahuja, P. and Ganguly, R. 2007. The fire within: Naxalite insurgency violence in India. *Small Wars and Insurgencies*, 18(2):249–274.

Anselin, L. 1995. Local indicators of spatial association - LISA. *Geographical Analysis*, 27(2):93–115.

Anselin, L., Cohen, J., Cook, D., Gorr, W., and Tita, G. 2000. Spatial analyses of crime. In Duffee, D., editor, *Criminal Justice 2000: Volume 4, Measurement and Analysis of Crime and Justice*, pages 213–262. National Institute of Justice, Washington, DC.

Asal, V., Gill, P., Rethemeyer, R. K., and Horgan, J. 2015. Killing range: Explaining lethality variance within a terrorist organisation. *Journal of Conflict Resolution*, Forthcoming.

Atkinson, M. P., Gutfraind, A., and Kress, M. 2011. When do armed revolts succeed: Lessons from Lanchester theory. *Journal of the Operational Research Society*, 63 (10):1363–1373.

Auyero, J. and Moran, T. P. 2007. The dynamics of collective violence: Dissecting food riots in contemporary Argentina. *Social Forces*, 85(3):1341–1367.

Ball, P. 2012. *Why society is a complex matter: Meeting Twenty-first Century Challenges with a New Kind of Science*. Springer, Berlin.

Ballas, D., Rossiter, D., Thomas, B., Clarke, G., and Dorling, D. 2005. *Geography Matters*. Joseph Rowntree Foundation, York.

Barabási, A.-L. 2005. The origin of bursts and heavy tails in human dynamics. *Nature*, 435:207–211.

Basu, I. 2011. Security and development - are they two sides of the same coin? Investigating India's two-pronged policy towards left wing extremism. *Contemporary South Asia*, 19(4):373–393.

Batty, M. 2013. *The New Science of Cities*. MIT Press, Cambridge, MA.

Batty, M., Desyllas, J., and Duxbury, E. 2003. Safety in numbers? Modelling crowds and designing control for the Notting Hill Carnival. *Urban Studies*, 40(8):1573–1590.

Beck, N., Gleditsch, K. S., and Beardsley, K. 2006. Space is more than geography: Using spatial econometrics in the study of political economy. *International Studies Quarterly*, 50:27–44.

Behlendorf, B., LaFree, G., and Legault, R. 2012. Microcycles of violence: Evidence from terrorist attacks by ETA and the FMLN. *Journal of Quantitative Criminology*, 28:49–75.

Beinhocker, E. 2007. *The origin of wealth: Evolution, complexity and the radical remaking of economics*. Random House Business Books, London.

Bell, B., Jaitman, L., and Machin, S. 2014. Crime deterrence: Evidence from the London 2011 riots. *The Economic Journal*, 124:480–506.

Belur, J. 2010. *Permission to Shoot? Police Use of Deadly Force in Democracies*. Springer, New York, NY.

Bennett, D. 2008. Governments, civilians, and the evolution of insurgency: Modeling the early dynamics of insurgencies. *Journal of Artificial Societies and Social Simulation*, 11(4):7.

Bennett, P. 1987. Beyond game theory - where? In Bennett, P., editor, *Analysing Conflict and its Resolution: Some Mathematical Contributions*, pages 43–69. Clarendon Press, Oxford.

Berestycki, H. and Nadal, J.-P. 2010. Self-organised critical hot spots of criminal activity. *European Journal of Applied Mathematics*, 21(4–5):371–399.

Berk, R. A. 1974. A gaming approach to crowd behavior. *American Sociological Review*, 39(3):355–373.

Berk, R. A. and Aldrich, H. E. 1972. Patterns of vandalism during civil disorders as an indicator of selection of targets. *American Sociological Review*, 37(5):523–47.

Bernasco, W. 2006. Co-offending and the choice of target area in burglary. *Journal of Investigative Psychology and Offender Profiling*, 3:139–155.

Bernasco, W. 2010a. A sentimental journey to crime: Effects of residential history on crime location choice. *Criminology*, 48:389–416.

Bernasco, W. 2010b. Modeling micro-level crime location choice: Application of the discrete choice framework to crime at places. *Journal of Quantitative Criminology*, 26(1):113–138.

Bernasco, W. and Block, R. 2009. Where offenders choose to attack: A discrete choice model of robberies in Chicago. *Criminology*, 47(1):93–130.

Bernasco, W. and Nieuwbeerta, P. 2005. How do residential burglars select target areas? A new approach to the analysis of criminal location choice. *British Journal of Criminology*, 44(3):296–315.

Bernasco, W., Block, R., and Ruiter, S. 2013. Go where the money is: Modeling street robbers location choices. *Journal of Economic Geography*, 13(1):119–143.

Besag, J. and Clifford, P. 1989. Generalized Monte Carlo significance tests. *Biometrika*, 76(4):633–642.

Besag, J. and Diggle, P. J. 1977. Monte Carlo tests for spatial pattern. *Journal of the Royal Statistical Society. Series C (Applied Statistics)*, 26(3):327–333.

Bezáková, I., Bhatnagar, N., and Vigoda, E. 2007. Sampling binary contingency tables with a greedy start. *Random Structures and Algorithms*, 30(1-2):168–205.

Bhavnani, R. and Choi, H. J. 2012. Modeling civil violence in Afghanistan: Ethnic geography, control, and collaboration. *Complexity*, 17(6):42–51.

Bhavnani, R., Donnay, K., Miodownik, D., Mor, M., and Helbing, D. 2014. Group segregation and urban violence. *American Journal of Political Science*, 58(1):226–245.

Birkin, M. and Wu, B. 2012. A review of microsimulation and hybrid agent-based approaches. In Heppenstall, A., Crooks, A., See, L., and Batty, M., editors, *Agent-based models of geographical systems*, pages 51–68. Springer, New York.

Birks, D., Townsley, M., and Stewart, A. 2012. Generative explanations of crime: Using simulation to test criminological theory. *Criminology*, 50(1):221–254.

Blanchet, J. and Stauffer, A. 2013. Characterizing optimal sampling of binary contingency tables via the configuration model. *Random Structures and Algorithms*, 42(2): 159–184.

Blank, L., Enomoto, C. E., Gegax, D., Mcguckin, T., and Simmons, C. 2008. A dynamic model of insurgency: The case of the war in Iraq. *Peace Economics, Peace Science and Public Policy*, 14(2):1–26.

Blundell, C., Heller, K. A., and Beck, J. M. 2012. Modelling reciprocating relationships with Hawkes processes. In Pereira, F., Burges, C., Bottou, L., and Weinberger, K., editors, *Advances in Neural Information Processing Systems 25*, pages 2600–2608. Curran Associates, Inc.

Bohorquez, J. C., Gourley, S., Dixon, A. R., Spagat, M., and Johnson, N. F. 2009. Common ecology quantifies human insurgency. *Nature*, 462(7275):911–4.

Bosse, T. and Gerritsen, C. 2010. Social simulation and analysis of the dynamics of criminal hot spots. *Journal of Artificial Societies and Social Simulation*, 13(2):5.

Bowers, K. J. and Johnson, S. D. 2005. Domestic burglary repeats and space-time clusters: The dimensions of risk. *European Journal of Criminology*, 2(1):67–92.

Bowers, K. J., Johnson, S. D., Guerette, R. T., Summers, L., and Poynton, S. 2011. Spatial displacement and diffusion of benefits among geographically focused policing initiatives: a meta-analytical review. *Journal of Experimental Criminology*, 7(4): 347–374.

Bowsher, C. 2007. Modelling security market events in continuous time: Intensity based, multivariate point process models. *Journal of Econometrics*, 141:876–912.

Braithwaite, A. 2010. Resisting infection: How state capacity conditions conflict contagion. *Journal of Peace Research*, 47(3):311–319.

Braithwaite, A. and Johnson, S. D. 2012. Space-time modeling of insurgency and counterinsurgency in Iraq. *Journal of Quantitative Criminology*, 28:31–48.

Brantingham, P. J. and Brantingham, P. L. 1981. *Environmental Criminology*. Sage Publications, Inc., Thousand Oaks, CA.

Brantingham, P. J. and Brantingham, P. L. 1993. Environment, routine, and situation: Toward a pattern theory of crime. In *Routine Activity and Rational Choice: Advances in Criminological Theory*, volume 5, pages 259–294. Transaction, New Brunswick, NJ.

Brantingham, P. J., Tita, G. E., Short, M. B., and Reid, S. E. 2012. The ecology of gang territorial boundaries. *Criminology*, 50(3):851–885.

Brauer, J. 2002. Survey and review of the defense economics literature on Greece and Turkey: What have we learned? *Defense and Peace Economics*, 13(2):85–107.

Brémaud, P. and Massoulie, L. 1996. Stability of nonlinear Hawkes processes. *The Annals of Probability*, 24(3):1563–1588.

Britton, J. R., Kriegh, R. B., and Rutland, L. W. 1963. *Calculus and Analytic Geometry*. W.H. Freeman and Company, San Francisco, CA.

Buhaug, H. and Gates, S. 2002. The geography of civil war. *Journal of Peace Research*, 39(4):417–433.

Buhaug, H. and Gleditsch, K. S. 2008. Contagion or confusion? Why conflicts cluster in space. *International Studies Quarterly*, 52(2):215–233.

Buhaug, H. and Rød, J. K. 2006. Local determinants of African civil wars. *Political Geography*, 25:315–335.

Buhaug, H., Gleditsch, K. S., Holtermann, H., Østby, G., and Tollefsen, A. F. 2011. It's the local economy, stupid! Geographic wealth dispersion and conflict outbreak location. *Journal of Conflict Resolution*, 55(5):814–840.

Buhuag, H., Gates, S., and Lujala, P. 2009. Geography, rebel capability, and the duration of civil conflict. *Journal of Conflict Resolution*, 53(4):544–569.

Bursik, R. J. 1988. Social disorganization and theories of crime and delinquency: Problems and prospects. *Criminology*, 26:519–552.

Cederman, L.-E. 2003. Modeling the size of wars: From billiard balls to sandpiles. *American Political Science Review*, 97(1):135.

Cederman, L.-E., Weidmann, N. B., and Gleditsch, K. S. 2011. Horizontal inequalities and ethnonationalist civil war: A global comparison. *American Political Science Review*, 105(3):478–495.

Clare, J., Fernandez, J., and Morgan, F. 2009. Formal evaluation of the impact of barriers and connectors on residential burglars' macro-level offending location choices. *Australian and New Zealand Journal of Criminology*, 42(2):139–158.

Clauset, A. and Gleditsch, K. S. 2012. The developmental dynamics of terrorist organisations. *PLoS One*, 7(11):e48633.

Cohen, J. and Tita, G. 1999. Diffusion in homicide: exploring a general method for detecting spatial diffusion processes. *Journal of Quantitative Criminology*, 15(4): 451.

Cohen, L. E. and Felson, M. 1979. Social change and crime rate trends: A routine activity approach. *American Sociological Review*, 44(4):588–608.

Colizza, V., Barrat, A., Barthelemy, M., Valleron, A.-J., and Vespignani, A. 2007. Modeling the worldwide spread of pandemic influenza: Baseline case and containment interventions. *PLoS Medicine*, 4(1):e13.

Collier, P. and Hoeffler, A. 2004. Greed and grievance in civil war. *Oxford Economic Papers*, 56(4):563–595.

Corman, J. C. 1967. The riot commission's report. *Arizona Law Review*, 9:347–359.

Cornish, D. B. and Clarke, R. V. 1986. *The Reasoning Criminal: Rational Choice Perspectives on Offending*. Springer-Verlag, New York, NY.

Cornish, D. B. and Clarke, R. V. 2008. The rational choice perspective. In Wortley, R. and Mazerolle, L., editors, *Environmental Criminology and Crime Analysis*. Willan Pub., Portland OR.

Cox, D. 1955. Some statistical methods connected with series of events. *Journal of the Royal Statistical Society*, 17(2):129–164.

Cox, D. 1972. Regression models and life-tables. *Journal of the Royal Statistical Society. Series B (Methodological)*, 34(2):187–220.

Curtis, J. P. and Smith, F. T. 2008. The dynamics of persuasion. *International Journal of Mathematical Models and Methods in Applied Sciences*, 2(1):115–122.

Daley, D. and Vere-Jones, D. 2003. *An Introduction to the Theory of Point Processes, Volume I: Elementary Theory and Methods*. Springer, New York, 2nd edition.

Davies, T. P., Fry, H. M., Wilson, A. G., and Bishop, S. R. 2013. A mathematical model of the London riots and their policing. *Scientific reports*, 3:1303.

Davis, J. and Goadrich, M. 2006. The relationship between precision-recall and ROC Curves. In *Proceedings of the 23rd International Conference on Machine Learning*, ICML '06, pages 233–240, New York, NY, USA.

De La Barrera, E. 2005. On the sesquicentennial of Fick's laws of diffusion. *Nature Structual and Molecular Biology*, 12(4):280.

Deffuant, G. and Gilbert, N. 2011. *Viability and Resilience of Complex Systems: Concepts, Methods and Case Studies from Ecology and Society*. Springer-Verlag, Berlin.

Deitchman, S. J. 1962. A Lanchester model of guerrilla warfare. *Operations Research*, 10(6):818–827.

Dennett, A. and Stillwell, J. 2008. Population turnover and churn: Enhancing understanding of internal migration in Britain through measures of stability. *Population Trends*, 134:24–41.

Dennett, A. and Wilson, A. G. 2013. A multi-level spatial interaction modelling framework for estimating inter-regional migration in Europe. *Environment and Planning A*, 45:1491–1507.

Diggle, P. J. 2013. *Statistical Analysis of Spatial and Spatio-temporal Point Patterns*. CRC Press, Boca Raton, FL, third edition.

Diggle, P. J., Chetwynd, A., Häggkvist, R., and Morris, S. 1995. Second-order analysis of space-time clustering. *Statistical Methods in Medical Research*, 4:124–136.

Dixon, P. M. 2002. Ripley's K function. In El-Shaarawi, A. H. and Piegorsch, W. W., editors, *Encyclopedia of Environmetrics*, volume 3, pages 1796–1803. John Wiley & Sons, Chichester.

Do, Q.-T. and Iyer, L. 2010. Geography, poverty and conflict in Nepal. *Journal of Peace Research*, 47(6):735–748.

Drury, J. and Stott, C. 2011. Contextualising the crowd in contemporary social science. *Contemporary Social Science: Journal of the Academy of Social Sciences*, 6(3):275–288.

Dunne, P. J. and Smith, R. P. 2007. The econometrics of military arms races. In Sandler, T. and Hartley, K., editors, *Handbook of Defense Economics*, volume 2, chapter 28, pages 913–940. North-Holland, Amsterdam.

Durrett, R. and Levin, S. 1994. The importance of being discrete (and spatial). *Theoretical Population Biology*, 46:363–394.

Egesdal, M., Fathauer, C., Louie, K., and Neuman, J. 2010. Statistical and stochastic modeling of gang rivalries in Los Angeles. *SIAM Undergraduate Research Online*, 3:72–94.

Embrechts, P., Liniger, T., and Lin, L. 2011. Multivariate Hawkes processes: An application to financial data. *New Frontiers in Applied Probability*, 48A:367–378.

Epstein, J. M. 1997. *Nonlinear dynamics, mathematical biology, and social science*. Addison-Wesley, Reading, MA.

Epstein, J. M. 2002. Modeling civil violence: an agent-based computational approach. *Proceedings of the National Academy of Sciences of the United States of America*, 99 Suppl 3(2):7243–7250.

Epstein, J. M. 2008. Why model? *Journal of Artificial Societies and Social Simulation*, 11(4):12.

Epstein, J. M. and Axtell, R. 1996. *Growing Artificial Societies*. MIT Press, Cambridge, MA.

Farmer, J. D. and Foley, D. 2009. The economy needs agent-based modelling. *Nature*, 460:685–686.

Fawcett, T. 2006. An introduction to ROC analysis. *Pattern Recognition Letters*, 27: 861–874.

Fearon, J. D. and Laitin, D. D. 2003. Ethnicity, insurgency, and civil war. *American Political Science Review*, 97(1):75.

Fonoberova, M., Fonoberov, V. A., Mezic, I., Mezic, J., and Brantingham, P. J. 2012. Nonlinear dynamics of crime and violence in urban settings. *Journal of Artificial Societies and Social Simulation*, 15:2.

Fotheringham, A. S. and O'Kelly, M. E. 1989. *Spatial interaction models: Formulations and applications*. Kluwer Academic Publishers, Dordrecht, the Netherlands.

Freud, S. 1921. *Group Psychology and Analysis of Ego*. International Psychoanalytic Press, London.

Fry, H. and Wilson, A. G. 2012. A dynamic global trade model with four sectors: food, natural resources, manufactured goods and labour. *CASA Working Paper*, 178.

Gail, M. H., Lubin, J. H., and Rubinstein, L. V. 1981. Likelihood calculations for matched case-control studies and survival studies with tied death times. *Biometrika*, 68(3):703–707.

Geary, R. 1954. The contiguity ratio and statistical mapping. *The Incorporated Statistician*, 5(3):115–127.

Geller, A. and Alam, S. J. 2010. A socio-political and -cultural model of the war in Afghanistan. *International Studies Review*, 12:8–30.

Getis, A. and Ord, J. 1992. The analysis of spatial association by use of distance statistics. *Geographic Analysis*, 24(3):189–206.

Gilbert, N. 2007. *Agent-based models*. Sage Publications, Inc, Thousand Oaks, CA.

Gillespie, J. V., Zinnes, D. A., Tahim, G., Schrodt, P. A., and Rubison, R. M. 1977. An optimal control model of arms races. *The American Political Science Review*, 71(1): 226–244.

Gleditsch, K. S. and Ward, M. D. 2000. War and peace in space and time: The role of democratization. *International Studies Quarterly*, 44:1–29.

Gleditsch, K. S. and Weidmann, N. B. 2012. Richardson in the information age: Geographic Information Systems and spatial data in International Studies. *Annual Review of Political Science*, 15(1):461–481.

Goldsmith, B. E. 2007. Arms racing in 'space': Spatial modelling of military spending around the world. *Australian Journal of Political Science*, 42(3):419–440.

Goldstone, J. A., Bates, R., Epstein, D., Lustik, M., Marshall, M., Ulfelder, J., and Woodward, M. 2010. A global model for forecasting political instability. *American Journal of Political Science*, 54:190–208.

González, E. and Villena, M. 2011. Spatial Lanchester models. *European Journal of Operational Research*, 210(3):706–715.

Gordon, M., Nadal, J.-P., Phan, D., and Semeshenko, V. 2009. Discrete choices under social influence: Generic properties. *Mathematical Models and Methods in Applied Sciences*, 19(supp01):1441–1481.

Granovetter, M. 1978. Threshold models of collective behavior. *American Journal of Sociology*, 83(6):1420–1443.

Grimm, V., Berger, U., DeAngelis, D. L., Polhill, G. J., Giske, J., and Railsback, S. F. 2010. The ODD protocol: A review and first update. *Ecological Modelling*, 221: 2760–2768.

Gross, M. 2011. Why do people riot? *Current Biology*, 21(18):673–676.

Grubesic, T. H. and Mack, E. A. 2008. Spatio-temporal interaction of urban crime. *Journal of Quantitative Criminology*, 24:285–306.

Guckenheimer, J. and Holmes, P. 1983. *Nonlinear Oscillations, Dynamical Systems, and Bifurcations of Vector Fields*. Springer-Verlag, New York, NY.

Guichaoua, Y. 2010. Processes of violent political mobilisation: An overview of contemporary debates and CRISE findings. Technical report, Centre for Research on Inequality, Human Security and Ethnicity.

Gurr, T. 1970. *Why Men Rebel*. Princeton University Press, Princeton.

Harris, B. and Wilson, A. 1978. Equilibrium values and dynamics of attractiveness terms in production-constrained spatial-interaction models. *Environment and Planning A*, 10:371–388.

Haushofer, J., Biletzki, A., and Kanwisher, N. 2010. Both sides retaliate in the Israeli-Palestinian conflict. *Proceedings of the National Academy of Sciences of the United States of America*, 107(42):17927–17932.

Hawkes, A. G. 1971. Spectra of some self-exciting and mutually exciting point processes. *Biometrika*, 58(1):83–90.

Hawkes, A. G. and Oakes, D. 1974. A cluster process representation of a self-exciting process. *Journal of Applied Probability*, 11(3):493–503.

Hegre, H., Østby, G., and Raleigh, C. 2009. Poverty and civil war events: A disaggregated study of Liberia. *Journal of Conflict Resolution*, 53(4):598–623.

Hegre, H., Karlsen, J., Nygård, M., Strand, H., and Urdal, H. 2013. Predicting armed conflict, 2010–2050. *International Studies Quarterly*, 57:250–270.

Helbing, D., Johansson, A., and Al-Abideen, H. 2007. Dynamics of crowd disasters: An empirical study. *Physical Review E*, 75(4):046109.

Helbing, D., Brockmann, D., Chadefaux, T., Donnay, K., Blanke, U., Woolley-Meza, O., Moussaid, M., Johansson, A., Krause, J., Schutte, S., and Perc, M. 2015. Saving human lives: What complexity science and information systems can contribute. *Journal of Statistical Physics*, 158(3):735–781.

Heppenstall, A., Crooks, A., See, L. M., and Batty, M. 2012. *Agent-based Models of Geographical Systems*. Springer, New York.

Hirsch, M. W., Smale, S., and Devaney, R. L. 2004. *Differential Equations, Dynamical Systems & an Introduction to Chaos*. Elsevier, San Diego, CA, second edition.

HMIC. 2011. The rules of engagement: A review of the August 2011 disorders. Technical report, HMIC.

Holden, R. T. 1986. The contagiousness of aircraft hijacking. *American Journal of Sociology*, 91(4):874–904.

Holtermann, H. 2015. Relative capacity and the spread of rebellion: Insights from Nepal. *Journal of Conflict Resolution*, Forthcoming.

House of Commons. 2011. Policing large scale disorder: Lessons from the disturbances of August 2011. Technical report, House of Commons.

Hsueh, Y.-H., Lee, J., and Beltz, L. 2012. Spatio-temporal patterns of dengue fever cases in Kaoshiung City, Taiwan, 2003–2008. *Applied Geography*, 34:587–594.

Ilachinski, A. 2004. *Artificial War: Multiagent-Based Simulation of Combat*. World Scientific Publishing Co. Pte. Ltd., Singapore.

Intriligator, M. D. and Brito, D. L. 1976. Formal models of arms races. *Conflict Management and Peace Science*, 2(1):77–88.

Intriligator, M. D. and Brito, D. L. 1988. A predator-prey model of guerrilla warfare. *Synthese*, 2:235–244.

IPCC. 2013. Fifth Assessment Report (AR5). Technical report, Intergovernmental Panel on Climate Change, Geneva, Switzerland.

Jackson, S., Russett, B., Snidal, D., and Sylvan, D. 1978. Conflict and coercion in dependent states. *Journal of Conflict Resolution*, 22(4):627–657.

Jacquez, G. M. 1996. A k nearest neighbour test for space-time interaction. *Statistics in Medicine*, 15:1935–1949.

Johnson, D. H. 1996. Point process models of single-neuron discharges. *Journal of Computational Neuroscience*, 3:275–299.

Johnson, N. F., Carran, S., Botner, J., Fontaine, K., Laxague, N., Nuetzel, P., Turnley, J., and Tivnan, B. 2011. Pattern in escalations in insurgent and terrorist activity. *Science*, 333(81):81–84.

Johnson, N. F., Medina, P., Zhao, G., Messinger, D. S., Horgan, J., Gill, P., Bohorquez, J. C., Mattson, W., Gangi, D., Qi, H., Manrique, P., Velasquez, N., Morgenstein, A., Restrepo, E., Johnson, N., Spagat, M., and Zarama, R. 2013. Simple mathematical law benchmarks human confrontations. *Scientific Reports*, 3:3463.

Johnson, S. D. 2008. Repeat burglary victimisation: A tale of two theories. *Journal of Experimental Criminology*, 4(3):215–240.

Johnson, S. D. and Bowers, K. J. 2004. The stability of space-time clusters of burglary. *British Journal of Criminology*, 44(1):55–65.

Johnson, S. D. and Braithwaite, A. 2009. Spatio-temporal distribution of insurgency in Iraq. *Countering Terrorism through SCP, Crime Prevention Studies*, 25:9–32.

Johnson, S. D. and Groff, E. R. 2014. Strengthening theoretical testing in Criminology using agent-based modeling. *Journal of Research in Crime and Delinquency*, 51(4): 509–525.

Johnson, S. D. and Summers, L. 2015. Testing ecological theories of offender spatial decision making using a discrete choice model. *Crime and Delinquency*, Forthcoming.

Jones, S. G. and Kulldorff, M. 2012. Influence of spatial resolution on space-time disease cluster detection. *PLOS One*, 7(10):e48036.

Kalyvas, S. N. 1999. Wanton and senseless?: The logic of massacres in Algeria. *Rationality and Society*, 11(3):243–285.

Karmeshu, M., Jain, V., and Mahajan, A. 1990. A dynamic model of domestic political conflict process. *Journal of Conflict Resolution*, 34(2):252–269.

Keane, T. 2011a. Combat modelling with partial differential equations. *Applied Mathematical Modelling*, 35(6):2723–2735.

Keane, T. 2011b. Partial differential equations versus cellular automata for modeling combat. *The Journal of Defense Modeling and Simulation: Applications, Methodology, Technology*, 8(4):191–204.

Knox, E. G. 1964a. The detection of space-time interactions. *Journal of the Royal Statistical Society, Series C (Applied Statistics)*, 13(1):25–30.

Knox, G. 1964b. Epidemiology of childhood leukaemia in Northumberland and Durham. *British Journal of Preventive and Social Medicine*, 18:17–24.

Kocher, M. A., Pepinsky, T. B., and Kalyvas, S. N. 2011. Aerial bombing and counterinsurgency in the Vietnam war. *American Journal of Political Science*, 55(2): 201–218.

Kress, M. and MacKay, N. J. 2014. Bits or shots in combat? The generalized Deitchman model of guerrilla warfare. *Operations Research Letters*, 42:102–108.

Kubrin, C. E. and Weitzer, R. 2003. New directions in social disorganization theory. *Journal of Research in Crime and Delinquency*, 40(4):374–402.

Kulldorff, M. 1997. A spatial scan statistic. *Communications in Statistics - Theory and Methods*, 26(6):1481–1496.

Kulldorff, M. 2001. Prospective time periodic geographical disease surveillance using a scan statistic. *Journal of the Royal Statistical Society A*, 164(1):61–72.

Kulldorff, M., Heffernan, R., Hartman, J., Assunção, R., and Mostashari, F. 2005. A space-time permutation scan statistic for disease outbreak detection. *PLoS Medicine*, 2(3):e59.

LaFree, G., Dugan, L., and Korte, R. 2009. The impact of British counterterrorist strategies on political violence in Northern Ireland: Comparing deterrence and backlash models. *Criminology*, 47(1):17–45.

LaFree, G., Dugan, L., Xie, M., and Singh, P. 2012. Spatial and temporal patterns of terrorist attacks by ETA 1970 to 2007. *Journal of Quantitative Criminology*, 28(1): 7–29.

Lanchester, F. W. 1916. *Aircraft in Warfare: The Dawn of the Fourth Arm*. Constable and Company Limited, London.

Le Bon, G. 1896; 1960. *The Crowd: A Study of the Popular Mind*. Viking Press, New York.

Lewis, E., Mohler, G., Brantingham, P. J., and Bertozzi, A. L. 2011. Self-exciting point process models of civilian deaths in Iraq. *Security Journal*, 25(3):244–264.

Lewis, P. and Shedler, G. 1979. Simulation of non-homogeneous Poisson processes by thinning. *Naval Research Logistics Quarterly*, 26:403–413.

Liebovitch, L. S., Naudot, V., Vallacher, R., Nowak, A., Bui-Wrzosinska, L., and Coleman, P. 2008. Dynamics of two-actor cooperation-competition conflict models. *Physica A: Statistical Mechanics and its Applications*, 387(25):6360–6378.

Lim, M., Metzler, R., and Bar-Yam, Y. 2007. Global pattern formation and ethnic/cultural violence. *Science*, 317(5844):1540–1544.

Liniger, T. J. 2009. *Multivariate Hawkes Processes*. PhD thesis, Swiss Federal Institute of Technology, Zurich.

Linke, A. M., Witmer, F. D., and O'Loughlin, J. 2012. Space-time Granger analysis of the war in Iraq: A study of coalition and insurgent action-reaction. *International Interactions*, 38(4):402–425.

Lyall, J. 2009. Does indiscriminate violence incite insurgent attacks?: Evidence from Chechnya. *Journal of Conflict Resolution*, 53(3):331–362.

Malchow, H., Petrovskii, S., and Venturino, E. 2008. *Spatiotemporal Patterns in Ecology and Epidemiology*. Chapman and Hall/CRC, Boca Raton, FL.

Malizia, N. 2013. Inaccuracy, uncertainty and the space-time permutation scan statistic. *PLOS One*, 8(2):e52034.

Malleson, N., Heppenstall, A., and See, L. 2010. Crime reduction through simulation: An agent-based model of burglary. *Computers, Environment and Urban Systems*, 34:236–250.

Mantel, N. 1967. The detection of disease clustering and a generalized regression approach. *Cancer Research*, 27:209–220.

Marchione, E. and Johnson, S. D. 2013. Spatial, temporal and spatio-temporal patterns of maritime piracy. *Journal of Research in Crime and Delinquency*, 50(4):504–524.

Martin, A. W., McCarthy, J. D., and McPhail, C. 2009. Why targets matter: Toward a more inclusive model of collective violence. *American Sociological Review*, 74(5): 821–841.

Mason, T. D. 1984. Individual participation in collective racial violence: A rational choice synthesis. *American Political Science Review*, 78(4):1040–1056.

McColl, R. W. 1969. The insurgent state: Territorial bases of revolution. *Annals of the Association of American Geographers*, 59(4):613–631.

McFadden, D. 1974. Conditional logit analysis of qualitative choice behavior. In Zarembka, P., editor, *Frontiers in Econometrics*, volume 1 of *Economic theory and mathematical economics*, chapter 4, pages 105–142. Academic Press.

McFadden, D. 1979. Quantitative methods for analysing travel behaviour of individuals: Some recent developments. In Hensher, D. A. and Stopher, P. R., editors, *Behavioural Travel Modelling*, chapter 13, pages 279–319. Croom Helm, London.

McFadden, D. 2001. Economic choices. *The American Economic Review*, 91(3): 351–378.

McLennan, D., Barnes, H., Noble, M., Davies, J., Garratt, E., and Dibben, C. 2011. *The English Indices of Deprivation 2010*. UK Department of Communities and Local Government, London.

McPhail, C. 1991. *The Myth of the Madding Crowd*. Aldine, New York, NY.

Metropolitan Police Service. 2012. 4 days in August: Strategic review into the disorder of August 2011. Technical report, Metropolitan Police Service.

Midlarsky, M. 1978. Analyzing diffusion and contagion effects: The urban disorders of the 1960s. *The American Political Science Review*, 72(3):996–1008.

Mohler, G. 2013. Modeling and estimation of multi-source clustering in crime and security data. *The Annals of Applied Statistics*, 7(3):1525–1539.

Mohler, G. 2014. Marked point process hotspot maps for homicide and gun crime prediction in Chicago. *International Journal of Forecasting*, 30:491–497.

Mohler, G. O., Short, M. B., Brantingham, P. J., Schoenberg, F. P., and Tita, G. E. 2011. Self-exciting point process modeling of crime. *Journal of the American Statistical Association*, 106(493):100–108.

Moran, P. A. 1950. Notes on continuous stochastic phenomena. *Biometrika*, 37(1/2): 17–23.

Morrell, G., Scott, S., McNeish, D., and Webster, S. 2011. The August riots in England: Understanding the involvement of young people. Technical report, National Centre for Social Research.

Most, B. A. and Starr, H. 1980. Diffusion, reinforcement, geopolitics and the spread of war. *The American Political Science Review*, 74(4):932–946.

Myers, D. J. 1997. Racial rioting in the 1960s: An event history analysis of local conditions. *American Sociological Review*, 62(1):94–112.

Myers, D. J. 2000. The diffusion of collective violence: Infectiousness, susceptibility, and mass media networks. *American Journal of Sociology*, 106(1):173–208.

Myers, D. J. 2010. Violent protest and heterogeneous diffusion processes: The spread of U.S. racial rioting from 1964 to 1971. *Mobilization*, 15(3):289–321.

Nelder, J. and Mead, R. 1965. A simplex method for function minimization. *The Computer Journal*, 7(4):308–313.

Newman, M. 2011. Complex Systems: A survey. *American Journal of Physics*, 79: 800–810.

North, B., Curtis, D., and Sham, P. 2002. A note on the calculation of empirical P values from Monte Carlo procedures. *American Journal of Human Genetics*, 71(2): 496–502.

Ogata, Y. 1981. On Lewis' simulation method for point processes. *IEEE Transactions on Information Theory*, 27(1):23–31.

Ogata, Y. 1988. Statistical models for earthquake occurrences and residual analysis for point processes. *Journal of the American Statistical Association*, 83(401):9–27.

Oléron Evans, T. P. and Bishop, S. R. 2013. Static search games played over graphs and general metric spaces. *European Journal of Operational Research*, 231:667–689.

O'Loughlin, J. and Witmer, F. D. 2010. The localized geographies of violence in the North Caucasus of Russia. *Annals of the Association of American Geographers*, 101 (1):178–201.

O'Loughlin, J. and Witmer, F. D. 2012. The diffusion of violence in the North Caucasus of Russia, 1999–2010. *Environment and Planning A*, 44:2379–2396.

O'Loughlin, J., Witmer, F. D., and Linke, A. M. 2010a. The Afghanistan-Pakistan wars, 2008–2009: Micro-geographies, conflict diffusion and clusters of violence. *Eurasian Geography and Economics*, 51(4):437–471.

O'Loughlin, J., Witmer, F. D., Linke, A. M., and Thorwardson, N. 2010b. Peering into the fog of war: The geography of the Wikileaks Afghanistan war logs, 2004–2009. *Eurasian Geography and Economics*, 51(4):472–495.

O'Loughlin, J., Holland, E. C., and Witmer, F. D. 2011. The changing geography of violence in Russia's North Caucasus, 1999–2011: Regional trends and local dynamics in Dagestan, Ingushetia, and Kabardino-Balkaria. *Eurasian Geography and Economics*, 52(5):596–630.

Olzak, S. and Shanahan, S. 1996. Deprivation and race riots: An extension of Spilerman's analysis. *Social Forces*, 74(3):931–961.

Openshaw, S. 1984. *The Modifiable Areal Unit Problem*. Geo Books, Norwich, Norfolk.

Østby, G. 2008. Polarization, horizontal inequalities and violent civil conflict. *Journal of Peace Research*, 45(2):143–162.

Østby, G., Nordås, R., and Rød, J. K. 2009. Regional inequalities and civil conflict in sub-Saharan Africa. *International Studies Quarterly*, 53:301–324.

Ozaki, T. 1979. Maximum likelihood estimation of Hawkes' self-exciting point processes. *Annals of the Institute of Statistical Mathematics*, 31:145–155.

Peng, R. 2003. Multi-dimensional point process models in R. *Journal of Statistical Software*, 8(16):1–27.

Peng, R. D., Schoenberg, F. P., and Woods, J. A. 2005. A space-time conditional intensity model for evaluating a wildfire hazard index. *Journal of the American Statistical Association*, 100(469):26–35.

Picoli, S., del Castillo-Mussot, M., Ribeiro, H., Lenzi, E., and Mendes, R. 2014. Universal bursty behaviour in human violent conflicts. *Scientific Reports*, 4:4773.

Pitcher, A. B. 2010. Adding police to a mathematical model of burglary. *European Journal of Applied Mathematics*, 21:401–419.

Porter, M. D. and White, G. 2012. Self-exciting hurdle models for terrorist activity. *The Annals of Applied Statistics*, 6(1):106–124.

Qubbaj, M. and Muneepeerakul, R. 2012. Two-actor conflict with time delay: A dynamical model. *Physical Review E*, 86(5):056101.

Radil, S. M., Flint, C., and Tita, G. E. 2010. Spatializing social networks: Using social network analysis to investigate geographies of gang rivalry, territoriality and violence in Los Angeles. *Annals of the Association of American Geographers*, 100 (2):307–326.

Raleigh, C. and Hegre, H. 2009. Population size, concentration, and civil war: A geographically disaggregated analysis. *Political Geography*, 28:224–238.

Ratcliffe, Jerry, H. 2000. Aoristic analysis: The spatial interpretation of unspecific temporal events. *International Journal of Geographical Information Science*, 14: 669–679.

Rey, S. J., Mack, E. A., and Koschinsky, J. 2011. Exploratory space-time analysis of burglary patterns. *Journal of Quantitative Criminology*, 28(3):509–531.

Richardson, L. F. 1951. Could an arms-race end without fighting? *Nature*, 168(4274): 567–8.

Richardson, L. F. 1960a. *Arms and Insecurity*. The Boxwood Press, Pittsburgh, PA.

Richardson, L. F. 1960b. *Statistics of Deadly Quarrels*. The Boxwood Press, Pittsburgh.

Riots Communities and Victims Panel. 2011. 5 days in August: An interim report on the 2011 English riots. Technical report, Riots Communities and Victims Panel.

Rodriguez, N. and Bertozzi, A. 2010. Local existence and uniqueness of solutions to a PDE model for criminal behavior. *Mathematical Models and Methods in Applied Sciences*, 20(supp01):1425.

Rojas-Pacheco, A., Obregón-Quintana, B., Liebovitch, L. S., and Guzmán-Vargas, L. 2013. Time-delay effects on dynamics of a two-actor conflict model. *Physica A: Statistical Mechanics and its Applications*, 392(3):458–467.

Rosenfeld, M. 1997. Celebration, politics, selective looting and riots: A micro level study of the Bulls riot of 1992 in Chicago. *Social Problems*, 44(4):483–501.

Rossmo, K. D. 2000. *Geographic Profiling*. CRC Press LLC, Boca Raton, FL.

Rutherford, A., Harmon, D., Werfel, J., Gard-Murray, A. S., Bar-Yam, S., Gros, A., Xulvi-Brunet, R., and Bar-Yam, Y. 2014. Good fences: The importance of setting boundaries for peaceful coexistence. *PLOS ONE*, 9(5):e95660.

Ryan, A. 2006. About the bears and the bees: Adaptive responses to asymmetric warfare. In Minai, A., Braha, D., and Bar-Yam, Y., editors, *Proceedings of the Sixth International Conference on Complex Systems*, pages 1–9. New England Complex Systems Institute.

Sahni, A. 2007. Andhra Pradesh: The state advances, the Maoists retreat. *South Asia Intelligence Review: Weekly Assessments and Briefings*, 6(10):1.

Salehyan, I. and Gleditsch, K. S. 2006. Refugees and the spread of civil war. *International Organization*, 60(2):335–366.

Sampson, R. J. and Groves, W. B. 1989. Community structure and crime: Testing social-disorganization theory. *American Journal of Sociology*, 94:774–802.

Sampson, R. J., Raudenbush, S. W., and Earls, F. 1997. Neighborhoods and violent crime: A multilevel study of collective efficacy. *Science*, 277:918–924.

Saperstein, A. M. 2007. Chaos in Models of Arms Races and the Initiation of War. *Complexity*, 12(3).

Schelling, T. C. 1971. Dynamic models of segregation. *Journal of Mathematical Sociology*, 1:143–186.

Schoenberg, F. P. 2003. Multidimensional residual analysis of point process models for earthquake occurrences. *Journal of the American Statistical Association*, 98(464): 789–795.

Schrodt, P. A. 2014. Seven deadly sins of contemporary quantitative political analysis. *Journal of Peace Research*, 51(2):287–300.

Schutte, S. and Weidmann, N. B. 2011. Diffusion patterns of violence in civil wars. *Political Geography*, 30(3):143–152.

Shaw, C. R. and McKay, H. D. 1969. *Juvenile Delinquency and Urban Areas*. Behavior research fund monographs. University of Chicago Press, Chicago, IL.

Short, M. B., D'Orsogna, M. R., Pasour, V. B., Tita, G. E., Brantingham, P. J., Bertozzi, A. L., and Chayes, L. B. 2008. A statistical model of criminal behaviour. *Mathematical Models and Methods in Applied Sciences*, 18(supp01):1249–1267.

Short, M. B., Bertozzi, A., and Brantingham, P. 2010a. Nonlinear patterns in urban crime: Hotspots, bifurcations and suppression. *SIAM Journal of Applied Dynamical Systems*, 9(2):462–483.

Short, M. B., Brantingham, P. J., Bertozzi, A. L., and Tita, G. E. 2010b. Dissipation and displacement of hotspots in reaction-diffusion models of crime. *Proceedings of the National Academy of Sciences*, 107(9):3961–3965.

Short, M. B., Mohler, G. O., Brantingham, P. J., and Tita, G. E. 2014. Gang rivalry dynamics via coupled point process networks. *Discrete and Continuous Dynamical Systems - Series B*, 19(5):1459–1477.

Simon, H. A. 1955. A behavioral model of rational choice. *The Quarterly Journal of Economics*, 69(1):99–118.

Smith, L. M., Keegan, M. S., Wittman, T., Mohler, G. O., and Bertozzi, A. L. 2010. Improving density estimation by incorporating spatial information. *EURASIP Journal on Advances in Signal Processing*, 2010:265631.

Snook, B., Cullen, R. M., Mokros, A., and Harbort, S. 2005. Serial murderers' spatial decisions: Factors that influence crime location choice. *Journal of Investigative Psychology and Offender Profiling*, 2:147–164.

Solomos, J. 2011. Race, rumours and riots: Past, present and future. *Sociological Research Online*, 16(4):20.

Spilerman, S. 1970. The causes of racial disturbances: A comparison of alternative explanations. *American Sociological Review*, 35(4):627–649.

Spilerman, S. 1971. The causes of racial disturbances: Tests of an explanation. *American Sociological Review*, 36:427–42.

Spilerman, S. 1976. Structural characteristics of cities and the severity of racial disorders. *American Sociological Review*, 41:771–793.

Starr, H. and Most, B. A. 1983. Contagion and border effects on contemporary African conflict. *Comparative Political Studies*, 16:92–117.

Stolzenberg, L. and D'Alessio, S. J. 2008. Co-offending and the age-crime curve. *Journal of Research in Crime and Delinquency*, 45(1):65–86.

Strogatz, S. H. 1994. *Nonlinear Dynamics and Chaos with Applications to Physics, Biology, Chemistry and Engineering*. Perseus Books, Reading, MA.

Therneau, T. M. 2014. *A Package for Survival Analysis in S*. R package version 2.37-7.

Tita, G., Riley, K., Ridgeway, G., Grammich, C., Abra-hamse, A. F., and Greenwood, P. W. 2003. *Reducing gun violence: Results from an intervention in East Los Angeles*. Rand, Santa Monica, CA.

Tita, G. E. and Radil, S. M. 2011. Spatializing the social networks of gangs to explore patterns of violence. *Journal of Quantitative Criminology*, 27:521–545.

Tobler, W. R. 1970. A computer model simulating urban growth in the Detroit region. *Economic Geography*, 46:234–240.

Toft, M. D. and Zhukov, Y. M. 2012. Denial and punishment in the North Caucasus: Evaluating the effectiveness of coercive counter-insurgency. *Journal of Peace Research*, 49(6):785–800.

Torrens, P. M. and McDaniel, A. W. 2013. Modeling Geographic Behavior in Riotous Crowds. *Annals of the Association of American Geographers*, 103(1):20–46.

Townsley, M. and Sidebottom, A. 2010. All offenders are equal, but some are more equal than others: Variation in journeys to crime between offenders. *Criminology*, 48:897–917.

Townsley, M., Homel, R., and Chaseling, J. 2003. Infectious burglaries: A test of the near repeat hypothesis. *British Journal of Criminology*, 43:615–633.

Townsley, M., Johnson, S. D., and Ratcliffe, J. H. 2008. Space time dynamics of insurgent activity in Iraq. *Security Journal*, 21(3):139–146.

Townsley, M., Birks, D., Bernasco, W., Ruiter, S., Johnson, S. D., White, G., and Baum, S. 2015. Burglar target selection: A cross-national comparison. *Journal of Research in Crime Delinquency*, 52:3–31.

Train, K. 2003. *Discrete Choice Methods With Simulation*. Cambridge University Press, Cambridge.

Vadlamannati, K. C. 2011. Why Indian men rebel? Explaining armed rebellion in the Northeastern states of India, 1970-2007. *Journal of Peace Research*, 48(5):605–619.

Verhelst, N. D. 2008. An efficient MCMC algorithm to sample binary matrices with fixed marginals. *Psychometrika*, 73(4):705–728.

Ward, M. D. and Gleditsch, K. S. 2002. Location, location, location: An MCMC approach to modeling the spatial context of war and peace. *Political Analysis*, 10(3): 244–260.

Ward, M. D., Greenhill, B. D., and Bakke, K. M. 2010. The perils of policy by p-value: Predicting civil conflicts. *Journal of Peace Research*, 47(4):363–375.

Weidmann, N. B. 2015. On the accuracy of media-based conflict event data. *Journal of Conflict Resolution*, Forthcoming.

Weidmann, N. B. and Salehyan, I. 2013. Violence and ethnic segregation: A computational model applied to Baghdad. *International Studies Quarterly*, 57(1):52–64.

Weidmann, N. B. and Ward, M. D. 2010. Predicting conflict in space and time. *Journal of Conflict Resolution*, 54(6):883–901.

Weidmann, N. B. and Zürcher, C. 2013. How wartime violence affects social cohesion: The spatial-temporal gravity model. *Civil Wars*, 15(1):1–18.

Weisburd, D., Bernasco, W., and Bruinsma, G. J. 2009. *Putting Crime in its Place: Units of Analysis in Geographic Criminology*. Springer, New York, NY.

White, G., Porter, M. D., and Mazerolle, L. 2013. Terrorism risk, resilience and volatility: A comparison of terrorism patterns in three Southeast Asian countries. *Journal of Quantitative Criminology*, 29(2):295–320.

Wilcox, A. R. 1973. Indices of qualitative variation and political measurement. *The Western Political Quarterly*, 26:325–343.

Wilkinson, S. I. 2009. Riots. *Annual Review of Political Science*, 12(1):329–343.

Wilson, A. G. 1970. *Entropy in Urban and Regional Modelling*. Pion, London, UK.

Wilson, A. G. 2000. *Complex spatial systems: The modelling foundations of urban and regional analysis*. Prentice Hall, Harlow.

Wilson, A. G. 2006. Ecological and urban systems models: Some explorations of similarities in the context of complexity theory. *Environment and Planning A*, 38: 633–646.

Wilson, A. G. 2008. Boltzmann, Lotka and Volterra and spatial structural evolution: An integrated methodology for some dynamical systems. *Journal of the Royal Society, Interface / the Royal Society*, 5(25):865–71.

Wortley, R. 2008. Situational precipitators of crime. In Wortley, R. and Mazerolle, L., editors, *Environmental Criminology and Crime Analysis*, pages 48–69. Willan Pub., Portland OR.

Wortley, R. and Mazerolle, L. 2008. *Environmental Criminology and Crime Analysis*. Willan Publishing, Portland, OR.

Zammit-Mangion, A., Dewar, M., Kadirkamanathan, V., and Sanguinetti, G. 2012. Point process modelling of the Afghan War Diary. *Proceedings of the National Academy of Sciences of the United States of America*, 109(31):12414–12419.

Zarboutis, N. and Marmaras, N. 2004. Searching efficient plans for emergency rescue through simulation: The case of a metro fire. *Cognition, Technology & Work*, 6(2): 117–126.

Zhukov, Y. M. 2012. Roads and the diffusion of violence: The logistics of conflict in Russia's North Caucasus. *Political Geography*, 31:144–156.

Zinnes, D. A. and Muncaster, R. G. 1984. The dynamics of hostile activity and the prediction of war. *Journal of Conflict Resolution*, 28(2):187–229.

Zipf, G. K. 1949. *Human Behavior and the Principle of Least Effort*. Addison-Wesley, Oxford.